Band 121

Schriften zu Immobilienökonomie und Immobilienrecht

Herausgeber:
IREIBS International Real Estate Business School

Prof. Dr. Sven Bienert
Prof. Dr. Stephan Bone-Winkel
Prof. Dr. Kristof Dascher
Prof. Dr. Dr. Herbert Grziwotz
Prof. Dr. Tobias Just
Prof. Gabriel Lee, Ph. D.
Prof. Dr. Kurt Klein
Prof. Dr. Jürgen Kühling, LL.M.
Prof. Dr. Gerrit Manssen
Prof. Dr. Dr. h.c. Joachim Möller
Prof. Dr. Karl-Werner Schulte HonRICS
Prof. Dr. Wolfgang Schäfers
Prof. Dr. Steffen Sebastian
Prof. Dr. Wolfgang Servatius
Prof. Dr. Frank Stellmann
Prof. Dr. Martin Wentz

Anna Knoppik

Assessing Environmental Risks in Real Estate Markets from an Economic Perspective

IRE|BS
International Real Estate Business School
Universität Regensburg

Anna Knoppik

Assessing Environmental Risks in Real Estate Markets from an Economic Perspective

Die Deutsche Bibliothek – CIP Einheitsaufnahme
Anna Knoppik
Assessing Environmental Risks in Real Estate Markets from an Economic Perspective
Regensburg: Universitätsbibliothek Regensburg 2026
(Schriften zu Immobilienökonomie und Immobilienrecht; Bd. 121)
Zugl.: Regensburg, Univ. Regensburg, Diss., 2026
ISBN 978-3-88246-569 -3

ISBN 978-3-88246-569 -3
© IRE|BS International Real Estate Business School, Universität Regensburg
Verlag: Universitätsbibliothek Regensburg, Regensburg 2026
Zugleich: Dissertation zur Erlangung des Grades eines Doktors der Wirtschaftswissenschaften, eingereicht an der Fakultät für Wirtschaftswissenschaften der Universität Regensburg
Tag der mündlichen Prüfung: 21.10.2026
Berichterstatter: Prof. Dr. Wolfgang Schäfers
Prof. Dr. Stephan Bone-Winkel

Declaration on the Use of Artificial Intelligence (AI)

In the preparation of this dissertation, AI-assisted tools and large language models were used to improve spelling and grammar, and to support the linguistic optimization of my own wording. After using these tools, the content was independently reviewed and, where necessary, revised. I take full responsibility for the content of the submitted academic work. As of the time of writing, no official or specific guidelines of the Faculty of Business, Economics, and Real Estate of the University of Regensburg regarding the use of AI in dissertations have been adopted. Therefore, reference is made to the guidelines of the Faculty of Law of the University of Regensburg, dated May 7, 2025.

Table of Contents

List of Tables ..... **VIII**

List of Figures ..... **X**

1 Introduction **1**

1.1 Motivation and Background 1

1.2 Course of Analysis and Research Questions 4

1.3 Co-Authors, Submissions, and Conference Presentations 8

1.4 References 12

2 The Price of Clean Air - Quantifying Air Pollution Exposure in Real Estate Decisions **15**

2.1 Abstract 15

2.2 Introduction 16

2.3 Data and Methodology 19

2.4 Results 28

2.4.1 Model Validation – PM_{10} 31

2.4.2 Model Validation – NO_2 34

2.5 Conclusion 38

2.6 Appendix 40

2.7 References 41

3 Quantifying the Impact of Urban Heat Islands on Residential Property Prices **45**

3.1 Abstract 45

3.2 Introduction 46

3.3 Related Literature 49

3.4 Data and Methodology 53

3.4.1 Housing Data 53

3.4.2 Urban Heat Island Data 54

3.4.3 Summary Statistics 55

3.5 Research Methodologies 60

3.6 Results 63

3.7 Concluding Remarks 82

3.8 Appendix 84
3.8.1 Appendix I – Descriptive Statistics 84
3.8.2 Appendix II – Formulas for KPI Analysis 87
3.8.3 Appendix III – Robustness Check - Changing the Reference 89
3.8.4 Appendix IV – Robustness Check - Spatial Analysis 90
3.9 References 92

4 The Impact of Energy Policies in Residential Markets: Quantifying Retrofit Incentives and Asset Performance 98

4.1 Abstract 98
4.2 Introduction 99
4.3 Regulatory Background of Energy Efficiency Policy in the European Union 100
4.4 Literature Review 102
4.5 Data 105
4.6 Methodology 109
4.7 Results 112
4.8 Conclusion 119
4.9 Appendix 120
4.9.1 Appendix I – Descriptive Statistics 120
4.9.2 Appendix II – Regression Outputs 121
4.9.3 Appendix III – Energy Performance Certificate in Germany 123
4.10 References 124

5 Resilience through Energy Efficiency? Evidence from Price and Liquidity Dynamics across Market Regimes 129

5.1 Abstract 129
5.2 Introduction 130
5.3 Institutional and Market Background 132
5.4 Related Literature 134
5.5 Data 141
5.6 Methodology 144
5.7 Results 147
5.7.1 Price Effects 147
5.7.2 Liquidity Effects 156

5.7.3 Robustness Check 161
5.8 Conclusion 163
5.9 Appendix 166
5.9.1 Appendix I – Descriptive Statistics 166
5.9.2 Appendix II – Price Analysis 168
5.9.3 Appendix III – Robustness Check 171
5.10 References 174
6 Conclusion 182
6.1 Executive Summary 182
6.2 Final Remarks 190
6.3 References 193

List of Tables

Table 2.1 Descriptive Statistics 22

Table 2.2 RMSE for Interpolation Methods for PM_{10} Values 29

Table 2.3 Goodness-of-Fit Results for Selected Model Options 29

Table 2.4 GAM Regression Output of Model 2018 and 2021 30

Table 3.1 Descriptive Statistics 56

Table 3.2 OLS Results for 4 a.m. UHI Intensity 64

Table 3.3 OLS Results for 1 p.m. UHI intensity 65

Table 3.4 GAM results for 4 a.m. UHI intensity 66

Table 3.5 GAM Results for 1 p.m. UHI Intensity 67

Table 3.6 Model Performance Comparison Metrics 68

Table 3.7 House Price Growth and Risk Return Metrics by UHI Intensity 76

Table 3.8 Variable Description 84

Table 3.9 Correlations of Variables 85

Table 4.1 EPC Nomenclature in Germany 102

Table 4.2 Literature Review of Green Premiums for Prices in Europe 103

Table 4.3 Descriptive Statistics of the Rent Dataset 107

Table 4.4 Descriptive Statistics of the Price Dataset 108

Table 4.5 Model Comparison of OLS and GAM 112

Table 4.6 Average Percentage Change in Rents after Refurbishment 114

Table 4.7 Average Percentage Change in Prices after Refurbishment 114

Table 4.8 Mean Rent-to-Price Ratio Analysis Pre- and Post-Retrofit 117

Table 4.9 Variables in the Model 120

Table 4.10 Regression Output for Model 2 121

Table 4.11 Regression Output for Model 4 122

Table 4.12 Distribution of Energy Performance Values 123

Table 5.1 EPC Nomenclature in Germany 132

Table 5.2 Descriptive Statistics 143

Table 5.3 Model Performance 148

Table 5.4 GAM Results 149
Table 5.5 EPC Class Price Premiums and Discounts over Time 154
Table 5.6 EPC Class Price Premiums and Discounts by Urbanization Levels 156
Table 5.7 Cox Survival Model Results 157
Table 5.8 Pearson Correlation 166
Table 5.9 OLS and GAM Model Results for Prices 168
Table 5.10 TOM Results: Cox and AFT Models 171

List of Figures

Figure 2.1 Sensor Map of 150 Stations in Berlin 20
Figure 2.2 Daily PM Concentrations with Thresholds in 2018 and 2021 21
Figure 2.3 Evaluation of the Particulate Matter Values 24
Figure 2.4 PM_{10} and Rents 2018 32
Figure 2.5 PM_{10} and Rents 2021 32
Figure 2.6 Rent Deviation according to the PM_{10} Concentration in 2018 33
Figure 2.7 Rent Deviation according to the PM_{10} Concentration in 2021 33
Figure 2.8 NO_2 and Rents 2018 35
Figure 2.9 NO_2 and Rents 2021 35
Figure 2.10 Rent Deviation according to the NO_2 Concentration in 2018 36
Figure 2.11 Rent Deviation according to the NO_2 Concentration in 2021 36
Figure 2.12 PM_{10} Distribution in 2018 and 2021 37
Figure 2.13 Scatterplot Matrix of selected Variables for 2021 40
Figure 3.1 Drivers of UHI 47
Figure 3.2 Boxplot of UHI Intensity across the Sample Period 57
Figure 3.3 Maps of the UHI Intensity at 4 a.m. across Berlin over Time 58
Figure 3.4 Maps of the UHI Intensity at 1 p.m. across Berlin over Time 59
Figure 3.5 Price Deviation as a Function of UHI Intensity 69
Figure 3.6 Price as a Function of UHI Intensities and Distance to CBD 71
Figure 3.7 Price as a Function of UHI Intensities and Distance to Park 72
Figure 3.8 Price as a Function of UHI Intensities and Household Income 73
Figure 3.9 Price Trends across UHI Intensities 74
Figure 3.10 Year-on-Year Price Change across UHI Intensities 75
Figure 3.11 Price Effects for Summer Months 78
Figure 3.12 Price Effects for Winter Months 78
Figure 3.13 Alternative Reference Points for UHI Intensity: R1 80
Figure 3.14 Geographically Weighted Regression 81
Figure 3.15 Alternative Reference Points for UHI Intensity: R2 89

Figure 3.16 Geographically Weighted Regression for 2014-16 90
Figure 3.17 Geographically Weighted Regression for 2017-19 91
Figure 4.1 Timeline of Directives/Regulations for the Building Sector 101
Figure 4.2 Mean Rent and Age per EPC 109
Figure 4.3 Mean Price and Age per EPC 109
Figure 4.4 Rents by EPC and Population Density over Time (Pre-Retrofit) 113
Figure 4.5 Prices by EPC and Population Density over Time (Pre-Retrofit) 113
Figure 4.6 Rent-to-Price Ratio Development by Regulations 116
Figure 5.1 Distribution of EPC Classes over Time 142
Figure 5.2 Average TOM by EPC Class and Year 144
Figure 5.3 Relative Price Effects by EPV 151
Figure 5.4 Time-Varying Price Effects by EPV 153
Figure 5.5 Spatial Variation in Price Effects by EPV 155
Figure 5.6 Relative Delisting Hazard by EPV 158
Figure 5.7 Relative Delisting Hazard by EPV over Time 159
Figure 5.8 Relative Delisting Hazard by EPV and Urbanization Levels 161
Figure 5.9 Extended Sample for Year-Specific Price Effects by EPV 162
Figure 5.10 Relative Price Effects by EPC 170
Figure 5.11 Relative TOM by EPV (AFT Specification) 172
Figure 5.12 Relative TOM by EPV and Urbanization Levels (AFT Specification) 172
Figure 5.13 Relative TOM by EPV over Time (AFT Specification) 173

1 Introduction

1.1 Motivation and Background

The acceleration of climate change is placing environmental factors such as heat stress, biodiversity loss, rising greenhouse gas concentrations, and the frequency of extreme weather events at the forefront of global concerns, with growing economic and societal implications (Intergovernmental Panel on Climate Change, 2023; United Nations Environment Programme, 2026). The corresponding climatic risks fall into two categories: physical risks and transition risks. Physical risks arise from direct exposure to acute or chronic environmental and climate hazards such as floods, storms, or persistent overheating in urban areas. Transition risks emerge from the adjustment toward a low-carbon economy, including regulatory changes, technological requirements, retrofitting obligations, evolving financing conditions, and shifting market preferences (United Nations Environment Programme Finance Initiative, 2023). This risk classification is embedded in the broader concept of sustainability. According to the report "Our Common Future", it is the responsibility of society to act both intra- and intergenerationally, ensuring that the needs of present generations are met while preserving the ability of future generations to meet their own needs (World Commission on Environment and Development, 1987). This intergenerational responsibility is particularly evident in sectors characterized by long-term impacts on both human well-being and resource consumption. The real estate and building sector is a key example, as decisions on planning, construction, and use of the built environment shape future living conditions, resource requirements, and ecological impacts (The German Government, 2025).

The building and construction sector is responsible for nearly 50% of global material use, around 28% of global energy consumption, and approximately 37% of global carbon dioxide (CO_2) emissions (United Nations Environment Programme, 2022, 2026). The industry also contributes to other externalities, such as waste generation and pollution (United Nations Environment Programme, 2026). Given its environmental footprint, the sector is one of the most resource-intensive industries and a major contributor to climate change. Concurrently, real estate assets are directly exposed to climate risks due to their fixed location, long economic lifespan, and high capital intensity (Contat et al., 2024; Duca et al., 2021). These risks affect assets through different but interrelated channels. Physical risks primarily determine the building condition, the technical lifespan, operating and maintenance costs, and location quality (Addoum et al., 2024; Albouy et al., 2016; Bernstein et al., 2019; Chay & Greenstone, 2005; Sinha & Cropper, 2013). Transition risks,

by contrast, materialize through regulatory requirements, retrofit and investment needs, financing conditions, and long-term asset performance expectations (Brounen & Kok, 2011; Chegut et al., 2020; Muzio et al., 2025; Lu & Spaenjers, 2025). Both types of risk may ultimately affect values and marketability by increasing expected costs, reducing demand, or impairing future cash flows (Bernstein et al., 2019; Cajias et al., 2019; Chegut et al., 2020; Muzio et al., 2025; Lu & Spaenjers, 2025).

Environmental risks are systemic and extend beyond the scope of individual assets. Addressing them requires coordinated approaches that integrate asset-specific measures with urban planning and regulatory intervention (United Nations Environment Programme Finance Initiative, 2023). In this context, the United Nations Sustainable Development Goals (SDGs) provide a holistic and multidimensional framework for all economic sectors, including the real estate industry, to respond to pressing global challenges (United Nations, 2015). Building on this sustainability agenda, European and national policy frameworks have introduced specific regulatory measures. At the European level, the European Green Deal is a central policy framework for advancing decarbonization, including targets to reduce net greenhouse gas emissions by at least 55% by 2030 and achieve climate neutrality by 2050 (European Commission, 2021). In the building sector, this shift is reflected in the Energy Performance of Buildings Directive (EPBD), which sets out zero-emission standards for new buildings while placing greater emphasis on energy efficiency improvements for the "worst-performing buildings" in the existing building stock (European Parliament & Council of the European Union, 2024). Although these goals are defined at the European level, their implementation depends on national regulations and market structures. A country-specific perspective is therefore essential for assessing how sustainability-oriented policies are implemented and how associated risks materialize in markets. Accordingly, this dissertation focuses on the German residential sector as a coherent and economically relevant market context for evaluating these dynamics.

Germany's position in international sustainability assessments, including its fourth place in the implementation of the SDGs (Sachs et al., 2025), reflects the country's pioneering role in the sustainability policy framework. National objectives likewise emphasize Germany's commitment to climate protection, including the target of achieving climate neutrality by 2045 (Bundesministerium für Wirtschaft und Klimaschutz, 2023). This objective creates transformation pressure in the building sector, given that parts of the existing building stock still exhibit low energy efficiency and renovation rates remain below the level required to meet the decarbonization pathway (Bundesverband energieeffiziente Gebäudehülle, 2026). The German housing market is further characterized by high regulatory density and a strong rental sector (Eurostat, 2026; Mense et al., 2023;

Voigtländer, 2014). These characteristics shape the incentives for sustainable investment among market participants in distinct ways (Galvin, 2023). Collectively, they make the German residential market a particularly relevant case for examining how climate risks are priced and translated into market responses.

Recent market developments have altered the broader economic and financial context in which sustainability-related characteristics are evaluated. The COVID-19 pandemic, rising construction costs, increasing energy costs, inflationary pressure, and variations in interest rates have changed the conditions in which real estate markets operate, as these factors are key determinants of affordability, investment conditions, and transaction activity (Bach & Knautz, 2022; Bernanke, 2018; Duca et al., 2021; Singhal et al., 2026; Wang, 2021). Much of the existing research on sustainability-related real estate characteristics was conducted under more stable market conditions. These studies often reflect a period in which decarbonization targets were less salient and financing conditions were more favorable (Ou et al., 2025). In the current market, environmental risks remain central to real estate analysis, as climate and retrofit targets pose implementation challenges (Bundesverband energieeffiziente Gebäudehülle, 2026; United Nations Environment Programme, 2026). This reinforces the need to embed these risks in a comprehensive framwork that accounts for changing market regimes.

Direct property markets are commonly evaluated through rents and prices, as rents reflect underlying supply and demand conditions, and prices incorporate rental income expectations and capitalization rates (DiPasquale & Wheaton, 1992). However, these indicators provide only a partial perspective on how markets process and reflect sustainability-related information, particularly in the context of transition risks. Unlike physical risks, they typically materialize through regulatory, financial, and market-related channels rather than direct exposure to climate hazards. Assessing these effects requires methodological frameworks that link heterogeneous data sources to capture nonlinear market responses across different contexts (Cajias & Piazolo, 2013; Copiello & Coletto, 2023).

On this basis, this dissertation aims to quantify how climate risks are reflected in the German residential real estate market. It distinguishes between physical environmental exposures, such as air pollution and urban heat stress, and transition-related pressures arising from regulatory requirements, retrofit obligations, and changing market conditions. By incorporating rental values, property prices, investment performance indicators, and liquidity, the dissertation provides a comprehensive assessment of how environmental sustainability is valued across urbanization levels and market regimes.

1.2 Course of Analysis and Research Questions

The following section presents the analytical framework and outlines the objectives and research questions of the papers that constitute this cumulative dissertation. Together, these four papers provide a comprehensive analysis of how climate-related risks shape property market outcomes amid increasing sustainability-related transparency and regulatory attention. While the first and second papers examine the effects of physical risks on property prices and rents, the third and fourth papers investigate transition risks and additionally consider market-related indicators, including rent-to-price ratios and market liquidity. The thematic alignment of these papers provides the foundation for the subsequent research questions.

Paper 1: The Price of Clean Air - Quantifying Air Pollution Exposure in Real Estate Decisions

Paper 1 presents research on the impact of air pollution on the rental market in Berlin, the capital of Germany. Using air pollution values for daily measurements of particulate matter with an aerodynamic diameter of 10 µm or less (PM_{10}) and nitrogen dioxide (NO_2) before and after the onset of the COVID-19 pandemic, the two pollutants are modeled and predicted over time. In addition, 22 hedonic, socioeconomic and spatial variables are incorporated within a generalized additive model (GAM) to estimate rents. The approach of combining geostatistics, geoinformatics, and econometric methods provides a comprehensive framework for examining the relationship between air pollution and economic outcomes. Therefore, the research aims to assess the effect of air quality based on the central research questions:

- Is air pollution a contributing factor to the housing market in Berlin?
- How does the association between air pollution and rents vary according to the pollutant concentrations and pollutant types?
- Are pre- and post-pandemic changes in air pollution reflected in residential rents?

Paper 2: Quantifying the Impact of Urban Heat Islands on Residential Property Prices

Paper 2 extends the analysis to another environmental factor affecting residential properties in Berlin, particularly in the context of urbanization. This article utilizes granular, building-level temperature data to assess the economic impacts of temperature deviations within a single city and its localized effects on prices. Daily temperatures are mapped over the ten-year period from 2014 to 2023 on a 30 m × 30 m grid to estimate Urban Heat Island (UHI) intensity. After merging the UHI variable with the corresponding property dataset, prices are estimated using a GAM regression that includes linear, nonlinear and interaction terms. Additionally, the analysis examines spatial and socioeconomic heterogeneity by incorporating interaction effects related to proximity to the central business district (CBD), distance to urban green spaces, and neighborhood income structures. In accordance with these considerations, the research aims to investigate whether localized temperature differences influence real estate price dynamics based on daily temperature data. The central considerations are therefore as follows:

- To what extent is UHI intensity reflected in residential property prices in Berlin?
- How does the relationship between UHI intensity and prices vary across Berlin's urban structure?

Paper 3: The Impact of Energy Policies in Residential Markets: Quantifying Retrofit Incentives and Asset Performance

Paper 3 examines energy policy measures and their effectiveness in creating incentives for retrofitting residential properties. The analysis focuses on the Munich metropolitan area from April 2014 to August 2023. The period is segmented into four phases based on key regulatory and economic changes. Rents and prices are estimated using a semi-parametric approach under two conditions: before and after a synthetic retrofit. The rent-to-price ratio for both conditions is then used as a market-based indicator to assess asset-level economic performance in response to evolving regulations and their effect on the market. The analysis accounts for spatial and demographic heterogeneity by distinguishing between sparsely and densely populated areas. This research aims to determine whether market and regional conditions shape the implications of policy measures in the residential real estate market. The corresponding research questions are:

- To what extent do rental and investment markets respond to increasing regulatory pressure on energy efficiency standards?
- How do regulatory measures affect buildings across different EPC ratings?
- Which market structures are decisive for the incentivization and take-up of energy-efficient renovations?
- How does the capitalization of energy efficiency vary over time in response to regulatory changes?

Paper 4: Resilience through Energy Efficiency? Evidence from Price and Liquidity Dynamics across Market Regimes

The fourth paper assesses the resilience of green properties in the German residential real estate market from 2017 to 2025, spanning both the expansion phase and the subsequent market downturn. The analysis draws on 29 variables, comprising hedonic, socioeconomic, and location-specific characteristics, as well as liquidity metrics such as time on market (TOM) and listing attention. Given the dual focus on price and liquidity, the research follows a two-step approach. Price effects are estimated using a GAM, allowing for a flexible, nonlinear relationship between energy performance values (EPV) and prices. Liquidity dynamics are analyzed using a Cox proportional hazards model. Both models additionally account for temporal and spatial heterogeneity, including varying degrees of urbanization, to examine whether pricing and marketability vary under changing market regimes and urbanization contexts. Accordingly, the research aims to examine how pricing and demand patterns for energy-efficient properties change across shifting market conditions by addressing the following research questions:

- How do green premiums and brown discounts evolve over time under changing market regimes?
- How does energy efficiency influence market liquidity in different market environments?
- Are price and liquidity adjustments synchronized across energy efficiency levels under adverse economic conditions?

1.3 Co-Authors, Submissions, and Conference Presentations

This section provides an overview of co-authors, journal submissions, publication status and conference presentations.

Paper 1: The Price of Clean Air - Quantifying Air Pollution Exposure in Real Estate Decisions

Authors:

Rebecca Restle, Marcelo Cajias, Anna Knoppik

Submission Details:

Journal: Journal of Property Investment & Finance

Status: Published: January 30, 2024

Conference Presentations:

This paper was presented at:

- the 40th Annual Conference of the American Real Estate Society (ARES) in Orlando, USA (2024)

Awards:

This paper was awarded the "2024 Manuscript Prize for Sustainable Real Estate" at the 40th Annual Conference of the American Real Estate Society.

Paper 2: Quantifying the Impact of Urban Heat Islands on Residential Property Prices

Authors:

Anna Knoppik, Marcelo Cajias, Felix Weinel, Sebastian Leutner, Wolfgang Schäfers

Submission Details:

Journal: Journal of Real Estate Research

Status: Major Revision: May 20, 2026

Conference Presentations:

This paper was presented at:

- the 31st Annual Conference of the European Real Estate Society (ERES) in Athens, Greece (2025)
- the 32nd Annual Conference of the Pacific Rim Real Estate Society (PRRES) in Adelaide, Australia (2026)
- the 5th Annual Conference of the European Commercial Real Estate Data Alliance (E-CREDA) in London, United Kingdom (2026)

Paper 3: The Impact of Energy Policies in Residential Markets: Quantifying Retrofit Incentives and Asset Performance

Authors:

Anna Knoppik, Marcelo Cajias, Wolfgang Schäfers

Submission Details:

Journal: Journal of Property Research

Status: Under Review: December 08, 2025

Conference Presentations:

This paper was presented at:

- the 30th Annual Conference of the European Real Estate Society (ERES) in Gdansk, Poland (2024)
- the 41st Annual Conference of the American Real Estate Society (ARES) in Tucson, USA (2025)

Paper 4: Resilience through Energy Efficiency? Evidence from Price and Liquidity Dynamics across Market Regimes

Authors:

Julius Kerker, Anna Knoppik, Sven Bienert

Submission Details:

Journal: Journal of Real Estate Research

Status: Under Review: May 25, 2026

Conference Presentations:

This paper was presented at:

- the 31st Annual Conference of the European Real Estate Society (ERES) in Athens, Greece (2025)
- the 42nd Annual Conference of the American Real Estate Society (ARES) in Sandestin, USA (2026)

This paper will be presented at:

- the 32nd Annual Conference of the European Real Estate Society (ERES) in Vienna, Austria (2026)

1.4 References

Addoum, J. M., Eichholtz, P., Steiner, E., & Yönder, E. (2024). Climate change and commercial real estate: Evidence from hurricane Sandy. *Real Estate Economics*, 52(3), 687–713.

Albouy, D., Graf, W., Kellogg, R., & Wolff, H. (2016). Climate amenities, climate change, and American quality of life. *Journal of the Association of Environmental and Resource Economists*, 3(1), 205–246.

Bach, S., & Knautz, J. (2022). Hohe Energiepreise: Ärmere Haushalte werden trotz Entlastungspaketen stärker belastet als reichere Haushalte. *DIW Wochenbericht*, 89(17), 244–251.

Bernanke, B. S. (2018). The real effects of disrupted credit: Evidence from the global financial crisis. *Brookings Papers on Economic Activity*, 49(2), 251–322.

Bernstein, A., Gustafson, M. T., & Lewis, R. (2019). Disaster on the horizon: The price effect of sea level rise. *Journal of Financial Economics*, 134(2), 253–272.

Brounen, D., & Kok, N. (2011). On the economics of energy labels in the housing market. *Journal of Environmental Economics and Management*, 62(2), 166–179.

Bundesverband energieeffiziente Gebäudehülle. (2026). *Sanierungsquote*. Accessed: 2026-05-16. URL: https://buveg.de/sanierungsquote/

Bundesministerium für Wirtschaft und Klimaschutz. (2023). *Klimaschutzplan 2050 Klimaschutzpolitische Grundsätze und Ziele der Bundesregierung*. Bundesministerium für Wirtschaft und Klimaschutz.

Cajias, M., Fuerst, F., & Bienert, S. (2019). Tearing down the information barrier: The price impacts of energy efficiency ratings for buildings in the German rental market. *Energy Research & Social Science*, 47, 177–191.

Cajias, M., & Piazolo, D. (2013). Green performs better: Energy efficiency and financial return on buildings. *Journal of Corporate Real Estate*, 15(1), 53–72.

Chay, K. Y., & Greenstone, M. (2005). Does air quality matter? Evidence from the housing market. *Journal of Political Economy*, 113(2), 376–424.

Chegut, A., Eichholtz, P., Holtermans, R., & Palacios, J. (2020). Energy efficiency information and valuation practices in rental housing. *Journal of Real Estate Finance and Economics*, 60, 181–204.

Contat, J., Hopkins, C., Mejia, L., & Suandi, M. (2024). When climate meets real estate: A survey of the literature. *Real Estate Economics*, 52(3), 618–659.

Copiello, S., & Coletto, S. (2023). The price premium in green buildings: A spatial autoregressive model and a multi-criteria optimization approach. *Buildings*, 13(2), 276.

DiPasquale, D., & Wheaton, W. C. (1992). The markets for real estate assets and space: A conceptual framework. *Real Estate Economics*, 20(2), 181–198.

Duca, J. V., Muellbauer, J., & Murphy, A. (2021). What drives house price cycles? International experience and policy issues. *Journal of Economic Literature*, 59(3), 773–864.

European Commission. (2021). *Fit for 55: delivering the EU's 2030 climate target on the way to climate neutrality (COM/2021/550)* [Communication].

European Parliament & Council of the European Union. (2024). *Directive (EU) 2024/1275 of the European Parliament and of the Council of 24 April 2024 on the energy performance of buildings (recast)* [Directive]. Official Journal of the European Union, L 2024/1275.

Eurostat. (2026). *Distribution of population by tenure status, type of household and income group—EU SILC survey*. Eurostat. Accessed: 2026-05-15. URL: https://ec.europa.eu/eurostat/databrowser/view/ILC_LVHO02__custom_3553007/bookmark/table?lang=en&bookmarkId=2457e44e-df35-4995-aacc-e79684402691

The German Government. (2025). *Shaping transformation fairly together German Sustainable Development Strategy Update 2025*.

Galvin, R. (2023). Do housing rental and sales markets incentivise energy-efficient retrofitting of western Germany's post-war apartments? Challenges for property owners, tenants, and policymakers. *Energy Efficiency*, 16(4), 25.

Intergovernmental Panel on Climate Change. (2023). *Climate change 2023: Synthesis report. Contribution of Working Groups I, II and III to the Sixth Assessment Report of the Intergovernmental Panel on Climate Change* (H. Lee & J. Romero, Eds.).

Lu, X., & Spaenjers, C. (2025). Energy labels, misreporting, and heuristic hedonic models. *Real Estate Economics*, 53(6), 1200–1222.

Mense, A., Michelsen, C., & Kholodilin, K. A. (2023). Rent control, market segmentation, and misallocation: Causal evidence from a large-scale policy intervention. *Journal of Urban Economics,* 134, 103513.

Muzio, M. J., Niu, D., Steil, J., & Zheng, S. (2025). Understanding housing market responses to stringent energy codes. *Real Estate Economics,* 53(4), 676–700.

United Nations. (2015). *Transforming our World: The 2030 Agenda for Sustainable Development* (Resolution A/RES/70/1).

United Nations Environment Programme. (2022). *2022 global status report for buildings and construction: Towards a zero-emission, efficient and resilient buildings and construction sector*.

United Nations Environment Programme. (2026). *Global status report for buildings and construction 2025–2026: As climate risks rise and cities grow, we must rethink how we build to create better lives for all.*

United Nations Environment Programme Finance Initiative. (2023). *Climate Risks in the Real Estate Sector*.

Ou, Y., Bailey, N., McArthur, D. P., & Zhao, Q. (2025). The price premium of residential energy performance certificates: A scoping review of the European literature. *Energy & Buildings*, 332, 115377.

Sachs, J.D., Lafortune, G., Fuller, G., & Iablonovski, G. (2025). *Sustainable development report 2025: Financing sustainable development to 2030 and mid-century*. Sustainable Development Solutions Network.

Sinha, P., & Cropper, M. L. (2013). *The value of climate amenities: Evidence from US migration decisions* (Working Paper No. 18756). National Bureau of Economic Research.

Singhal, P., Kaestner, K., Schwarz, A., & Pahle, M. (2026). How do households react to a real cost shock? Evidence from the energy price crisis in Germany. *Energy Economics*, 155, 109142.

Wang, B. (2021). How does COVID-19 affect house prices? A cross-city analysis. *Journal of Risk and Financial Management*, 14(2), 47.

Voigtländer, M. (2014). The stability of the German housing market. *Journal of Housing and the Built Environment,* 29(4), 583–594.

Wood, S. N. (2017). Generalized additive models. An introduction with R (2nd ed.). CRC Press.

World Commission on Environment and Development. (1987). *Our common future: Report of the world commission on environment and development.* Oxford University Press.

2 The Price of Clean Air - Quantifying Air Pollution Exposure in Real Estate Decisions

2.1 Abstract

Purpose – The purpose of this paper is to explore the significant impact of air quality as a contributing factor on residential property rents by applying geoinformatics to economic issues. Since air pollution poses a severe health threat, city residents should have the right to know about the (invisible) hazards they are exposed to.

Design/methodology/approach – Within spatial-temporal modeling of air pollutants in Berlin, Germany, three interpolation techniques are tested. The most suitable one is selected to create seasonal maps for 2018 and 2021 with pollution concentrations for particulate matter values and nitrogen dioxide for each 1,000 m^2 cell within the administrative boundaries. Based on the evaluated pollution particulate matter values, which are used as additional variables for semi-parametric regressions, the impact of the air quality on rents is estimated.

Findings – The findings reveal a compelling association between air quality and the economic aspect of the residential real estate market, with noteworthy implications for both tenants and property investors. The relationship between air pollution variables and rents is statistically significant. However, there is only a "willingness to pay" for low particulate matter values, but not for nitrogen dioxide concentrations. With good air quality, residents in Berlin are willing to pay a higher rent (3%).

Practical implications – These results suggest that a "marginal willingness to pay" occurs in a German city. The research underscores the multifaceted impact of air quality on the residential rental market in Berlin. The evidence supports the notion that a cleaner environment not only benefits human health and the planet but also contributes significantly to the economic bottom line of property investors.

Originality – The paper has a unique data engineering approach. It collects spatiotemporal data from a network of state-certified measuring sites to create an index of air pollution. This spatial information is merged with residential listings. Afterward, nonlinear regression models are estimated.

Keywords: Residential Real Estate, Air Pollution, Particulate Matter Concentrations, Empirical Bayesian Kriging, Rents, Generalized Additive Model, Machine Learning

2.2 Introduction

Air pollution is one of the most significant threats worldwide, causing substantial environmental and social problems, particularly in megacities where its impacts are most acutely felt. The European Environment Agency (2022) published that in the European Union (EU), an estimated 327,000 premature deaths were a result of the pervasive problem of air pollution concentrations in 2021. For particulates, the resulting health risks can be caused by the dust itself, as it can damage the organs depending on the size. The bigger the particle, the more likely it is for the dust to be exhaled or stay in the nose. The smaller the particle, the more dangerous, as they can penetrate deeper organs, e.g., lungs and bronchial tubes. In addition, heavy metals can adhere to the surface of the particles, which would produce toxic air. Short-term studies showed higher risks of hypertension and heart rhythm variability for high concentrations (Simoni et al., 2015).

It is important to note that even if most epidemiological studies found significant relationships between certain diseases and air pollution, the causality is not always conclusively evident (Schraufnagel et al., 2019). It is not always possible to understand the harmfulness of each component, as there is exposure to a combination of substances (Brook et al., 2010). The majority of pollutants come from the combustion of fuels via transportation and industrial processes. Fine particulates often consist of black carbon and trace metals, for instance lead or arsenic, and are referred to as fine particulate matter ($PM_{2.5}$) or nitrogen dioxide (NO_2). Particulates with a higher diameter, so-called coarse particles, are referred to as PM_{10} and come from agricultural erosion and road dust from transportation, among others (Umweltbundesamt, 2022).

Air pollutants can negatively impact the environment as well. While the greenhouse gas, CO_2, is a prominent contributor to climate change, NO_2 or SO_2 cause effects on the ecosystem through acid rain (United States Environmental Protection Agency, 2016). NO_2 presence in the atmosphere arises from the oxidation of nitrogen monoxide. Another major pollutant that affects the climate is black carbon, a component of $PM_{2.5}$, methane (CH_4), and ground-level ozone (O_3).

Moreover, the emission sources and the interaction between individual pollutants are of crucial significance as well. The combustion of fuels primarily leads to the release of PM_{10} and NO_2, while chemical reactions between oxygen and ambient nitrogen gases contribute to this issue. With the rise of the electric-powered car or other alternatives, traffic will have a smaller share in air pollution in the next few years (Eichlseder et al., 2021). Various factors play a significant role in mitigating air pollution. These include natural elements such as vegetation, altitude, and wind speed, which are responsible for pollution concentrations.

Conversely, high pollution levels can often be attributed to the nature of emission sources or their proximity to heavily trafficked roads. More precisely, meteorological characteristics affect the concentration and distribution of pollution. Wind speed can have a strong influence, followed by air pressure, humidity, and temperature, and their impact also varies with the seasons (Yang et al., 2020). Thereby, the impact is pollutant-specific. Humidity negatively correlates with PM_{10} levels since the particles become heavier as they absorb water and therefore reduce their distribution range (Rumaling et al., 2022). Conversely, the finer particle size is less affected by humidity, which is the case with $PM_{2.5}$ (Munir et al., 2017).

Governments recognize the severe impacts of air pollution, prompting the setting of threshold values by EU members to mitigate its effects. Nevertheless, in contrast to other regions of the world (Chen & Lee, 2020; Kumar & Dash, 2018; Zhang et al., 2016), Europe still has comparatively low levels of air pollution. Berlin's air quality is moderate when compared to several other cities, especially in Eastern Europe and Italy, although Berlin has the worst air quality among German cities (European Environmental Agency, 2023).

Like many large cities, Berlin is subject to constant dynamics[1]. Recent years have shown that the city is experiencing a renaissance. A dynamic rental market can be observed with accompanying price increases and high migration flows. This metropolitan area, with nearly 3.8 million residents spread across approximately 890 km^2, is synonymous with heavy traffic and industrial zones, contributing to it being a nexus for air pollution (Amt für Statistik Berlin-Brandenburg, 2022).

The motivation behind dealing with air pollution in economic studies can be traced back to environmental economics. In theory, externalities describe the positive/negative impact economic decisions have on uninvolved parties. Widely used in environmental economics is the concept of negative externalities: Air pollution is a concern for everyone, but its effects are not compensated for, and the originator is not required to cover the costs. Several methods have been developed to determine these – mostly theoretical – costs. The "Revealed Preference" method is used to investigate air pollution. This method determines the value consumers place on environmental quality by analyzing their purchasing behavior for goods that are either directly or indirectly related to environmental quality (Kahn, 1995). This theoretical framework has been directly applied through hedonic regression. The discipline of using hedonic regression to estimate the effect of air pollution concentrations on residential property values was implemented by Ridker and Henning

[1] The Berlin rental ceiling, a law intended to freeze rents in Berlin for five years, was not directly dependent on prevailing rent levels. The law set upper limits for rents in Berlin based on several factors. These limits were set independently of the actual rents at the time the law came into force and does not harm the study, therefore.

(1967). Most studies following their approach find a significant, negative relationship between air pollution and real estate prices. As a low pollution concentration imply high prices, vice versa (Borja-Urbano et al., 2021; Le Boennec & Salladarré, 2017; Ridker & Henning, 1967). The studies before 2000 lack implications for further applications, as they only study the relationship and then lose interest in applying the results (Smith & Huang, 1993).

Even though the issue has received little attention in the European context, the relationship between real estate and air quality is examined in other parts of the world. For the Asian and American continents, a willingness to pay for good air, confirmed by findings of negative correlations between pollution levels and housing prices, is observed (Borja-Urbano et al., 2021; Sun & Yang, 2020).

In Quito, Ecuador, Borja-Urbano et al. (2021) find a significant negative relationship between housing prices and air pollutants like CO_2, $PM_{2.5}$, and NO_2 values. Based on their results, an increase of 1% of $PM_{2.5}$ leads to a reduction of 15 US \$/m^2 ceteris paribus.

Sun and Yang (2020) analyze the effect of $PM_{2.5}$ on housing prices in several Chinese cities. They combine geographically weighted quantile regression to highlight spatial non-stationarity and conclude that there is a negative relationship between $PM_{2.5}$ and housing prices and that cities with rapid growth and increased industrial activity experience a real estate boom. The differentiation between housing price quantiles allows them to increase the information content: the adverse effect is more substantial in regions with high industrial standards, especially in the upper quantiles of price levels. This leads them to conclude that cities with rapid growth and increased industrial activity experience a real estate boom. In these areas, residents seem to have a marginal willingness to pay for clean air. The origin of their $PM_{2.5}$ data is not self-interpolated, but external raster data with a depth of detail of 1 km^2 is used.

Reasons for the differences between the studies might be attributed to cultural characteristics. The US is known for its urban sprawl. Most central business districts become less significant in terms of residential living. The migration away from dense urban centers to extensive open space might explain the relationship between high air pollution levels and low housing prices.

One of the only known European studies is conducted in France by Le Boennec and Salladarré (2017). The hedonic regression reveals that in the city of Nantes, noise has a significant negative impact on rent prices, air pollution does not. Pollution values are derived from an atmospheric dispersion modeling system.

To contribute to the discourse on air quality, this research aims to formalize the assessment of air quality in Germany. Simultaneously, it advocates for greater diversity in pollutant sensor coverage, an initiative that open data measurement projects could support. This research utilizes three distinct spatial interpolation techniques within a geographical information system (GIS) to meticulously generate maps illustrating the dispersion of air pollutants. By combining geostatistics, geoinformatics, and econometric methods, air quality is "valued" to create incentives for the corresponding real estate sector in order to evaluate if Berlin's housing market considers air pollution after accounting for hedonic, socioeconomic, and spatial control variables. While this topic remains relatively underexplored in Europe, its significance is undeniable.

This paper is organized as follows. Firstly, the current study is embedded in the existing literature, providing some background on the evaluation of air pollutants and considering the generalized additive model (GAM) regression as an essential element to evaluate the impact on rents. The following sections then describe the research approach and econometric models. This is followed by a comprehensive analysis of the collected data and the presentation of empirical results by offering insights into the multifaceted interactions between environmental air quality and the residential rental market. Finally, the discussion of the implications paves the way for the formulation of informed policy recommendations.

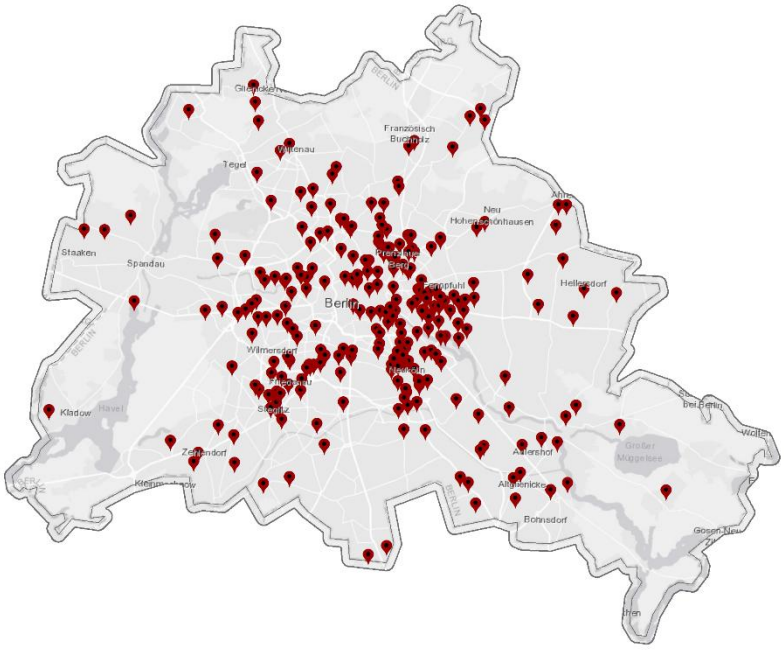
2.3 Data and Methodology

Although Berlin, like every other city in Germany, has a network of state-certified measuring sites (17 stations in total) for all kinds of outdoor pollutants, these stations can hardly represent a reflection of reality, as the obtained data is also influenced by external factors such as the height of the measurements, proximity to water or traffic axes. Regarding the lack of official measuring stations, this research makes use of a publicly available sensor network of low-cost sensors, which measure particulate matter concentrations in European cities. These low-cost sensors serve as a valuable open-data source to examine the relationship between air quality and property data, even though they encounter lower performance under special conditions such as high humidity (Budde et al., 2018). One initiator of a citizen science project that seeks to build a global air pollution network with currently 14,000 working low-cost sensors (for about 50€) is the "Sensor Community" (formerly luftdaten.info). The data utilized in this research for PM_{10} and nitrogen dioxide (NO_2) were retrieved from this open data hub and subsequently

processed in RStudio. Dealing with a limited number of air pollutants does not produce a proper index. For this reason, not only are interpolations for particulate matter distribution conducted, but also for NO_2.

By choosing 2018 as a pre-pandemic year with high data availability in Berlin and a more recent year (2021), the potential influencing factor of changing external conditions due to the pandemic is omitted. Nevertheless, the resulting dataset consists of approximately 150 stations, as Figure 2.1 indicates, that continuously transmit data.

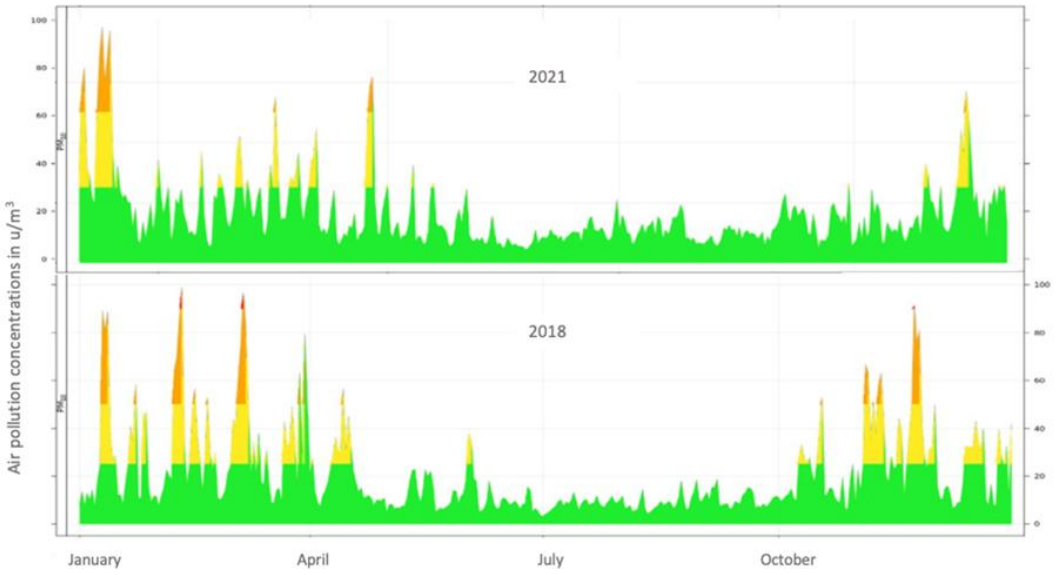
Figure 2.1 Sensor Map of 150 Stations in Berlin



Note: This figure illustrates the distribution of 150 stations utilized for conducting a spatial analysis of particulate matter (PM_{10}) concentrations across Berlin. The map provides insights into the geographical spread and density of the stations, facilitating an understanding of how PM_{10} levels vary across different urban areas. This spatial arrangement serves as a foundational element for the subsequent analysis and interpretation of PM_{10} data.

An initial data exploration phase is shown in Figure 2.2, as differences in summer and winter are visible, besides some anomalies around June. The short-term threshold values are regularly exceeded in the autumn/winter months in both years. The daily measurements are then aggregated to heating (October–April) and non-heating (May–September) season averages in line with the semi-official heating period in Germany. A slight underprediction of low-cost sensors should be considered since the occurrence of low-cost sensors varies in terms of quantity, altitude, or site conditions.

Figure 2.2 Daily PM Concentrations with Thresholds in 2018 and 2021



Note: The figure shows the initial data exploration phase, which indicates a timeline of particulate matter concentrations (PM_{10}) of the depicted years and additionally visualizes European threshold values for daily particulate matter concentrations by color. This graph illustrates the seasonal variations and shows clear differences between summer and winter, except for certain deviations in June. The short-term thresholds were consistently exceeded in the fall and winter months in both years observed.

It can be assumed that the data is spatially non-stationary; the amount of data points and the automatic estimation of the variogram assist in interpolating the best variability in this respect, in contrast to NO_2, where a strong spatial simplification can be expected. Furthermore, Moran's I index[2] with a spatial weight matrix reveals significant but medium spatial autocorrelation between individual PM_{10} sensor points, indicating concentrations are not randomly distributed. Implicitly, the index values of 0.504 for 2018 and 0.487 for 2021 further affirm this observation. This provided an appropriate baseline for each of the interpolation techniques computed with the geostatistical analyst. The basic environment settings are the same for all. Air pollution values are interpolated with a resolution of 100 meters in a projected coordinate reference system (UTM 33N)[3] with the processing extent of the administrative boundaries of Berlin.

The data in this analysis originates from two distinct sources – on the one hand, the air pollution dataset and on the other hand, the property data. The latter is obtained from "empirica AG", a German research and consulting institute that uses a machine learning method that analyzes, processes, and verifies real estate listings from more than 100 sources. The database includes continuous and categorical variables: Rents, hedonic

[2] The formula for Moran's I involves comparing the difference between each data point and the mean of all data points with the differences between the data point and the values of neighboring points, weighted by a spatial weight matrix.
[3] Anisotropy implicit the directional dependence of air pollution. In this context, the distribution and concentration of air pollution are influenced by the direction of the wind.

features such as availability of bathtubs or kitchens, quality, and age of the building, or energy consumption. The database is also enriched with information about the purchasing power in the respective ZIP code area and distance data to the city center, the closest café or supermarket. The further processing of the data includes data reduction to only relevant variables and choosing listings in Berlin since 2018. The descriptive statistics in Table 2.1 demonstrate the variables and the distribution of the rent dataset. The initial dataset consists of 80,000 observations, with a concentration of the highest rents per m^2 (>20 €/m^2) in the map´s center.

Table 2.1 Descriptive Statistics

Variable	Unit	Mean 2018	Mean 2021
Rent	€/p.m.	788.41	788.31
Size	m^2	70.88	66.31
Rent m^2	€/m^2/p.m.	10.94	11.68
Age	Relative to 2017	63.6	57.77
Bathtub	Binary	0.59	0.48
Refurbished	Binary	0.18	0.13
Built-in kitchen	Binary	0.51	0.48
Balcony	Binary	0.63	0.63
Parking	Binary	0.22	0.21
Elevator	Binary	0.40	0.49
Terrace	Binary	0.13	0.12
Purchasing Power	€/HH/zip	36,200	38,200
PM_{10}	µm/m^3	17.35	14.32
NO_2	µm/m^3	25.00	16.37
City center distance	km	7.90	7.6
Bus stop distance	km	0.19	0.19
Post box distance	km	0.21	0.19
Bar distance	km	0.48	0.53
School distance	km	0.32	0.33
Fast food distance	km	0.31	0.31
Park distance	km	0.27	0.27
Restaurant distance	km	0.23	0.25
Café distance	km	0.37	0.39
Playground distance	km	0.19	0.18
Supermarket distance	km	0.28	0.29
ATM distance	km	0.54	0.55

Note: The table reports the summary statistics comprising data as of 2018 and 2021. Age is calculated as the difference of the building age to the year 2017. All distance variables are calculated as the Euclidean distance to the specific dwelling in kilometers. Binary variables report whether the dwelling includes a certain characteristic (1) or not (0). Rent is presented as Euro (€) per month. Information on households (HH) is reported on zip level.

Two fundamental approaches exist for assessing air pollution distributions. The first one uses physical and chemical processes to calculate the distribution starting from the pollution source (Knote et al., 2015). The second one, which is considered in this paper, estimates values by applying geoinformatics and geostatistical interpolation methods on the measurement network through the city (Deligiorgi & Philippopoulos, 2011).

The land use regression (LUR) framework is widely used for modeling air pollution (Chen et al., 2012; Habermann et al., 2015; Wolf et al., 2017). It incorporates potentially

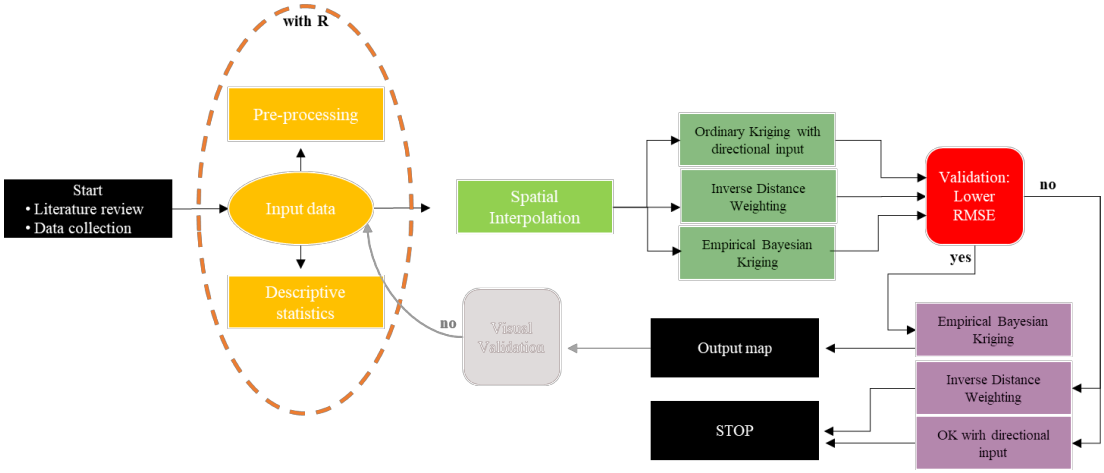
determining characteristics such as building density, proximity to emitters such as high-traffic roads or industry, and vegetation. The regression model further predicts concentration values at sites without measurements. This can be done by either using rasterized or vectorized datasets (Beelen et al., 2013).

Tobler's first law of geography states, "everything is related to everything else, but near things are more related than distant things" (Tobler, 1970). This fundamental principle underlies spatial interpolation, embodying the concept of leveraging known data points to estimate or infer values at unfamiliar or unknown locations. Deterministic interpolation methods, such as inverse distance weighting (IDW), and interpolation methods based on a statistical model that additionally produces a prediction error map, like Kriging, are used to apply this.

A lot of studies try to compare different techniques to find the best model. LUR, Kriging, IDW and other modeling techniques are tested. When interpolating measurement networks, a lot of the time, Kriging methods show superiority (Anselin & Lozano-Gracia, 2008; Beelen et al., 2009). However, there is evidence that a hybrid approach (LUR and Kriging) leads to high model performance, especially in the case of sparse monitoring (Wu et al., 2018). As this paper is based on measurements instead of estimates, the LUR is not applied. In general, the LUR would include information on road proximity and traffic density in the model, while other methods might use more detailed climate indicators to produce results.

Therefore, the following three interpolation methods are tested: IDW, ordinary Kriging accounting for anisotropy (OK-wind), and empirical Bayesian Kriging (EBK), which produce continuous surfaces with PM_{10} and NO_2 concentrations. After cross-validation, the model with the highest performance is chosen for further analysis. Seasonal variations in air pollution concentrations are considered by including seasonal and yearly values. Figure 2.3 summarizes the process visually.

Figure 2.3 Evaluation of the Particulate Matter Values



Note: The figure provides an overview of the research design utilized to assess the final particulate matter values, outlining the essential software tools employed in the process, including ArcGIS and RStudio. The applied methodologies encompass empirical Bayesian Kriging, ordinary Kriging with directional input, and inverse distance weighting. Subsequently, the outcomes derived from these methodologies are meticulously evaluated and further integrated into the research.

One of the more straightforward methods is IDW, as each measured point is influenced locally. The general interpolation equation corresponds to:

$$\hat{X}(s_0) = \sum_{i=1}^{N} \lambda_i X(s_i) \tag{2.1}$$

The predicted position in location $s_0$is indicated by $\hat{X}$. Whereby N is the number of measured values and $X(s_i)$ is the observed value for location i, with λ_i as an unknown weight. The weighting is solely dependent on the distance to the predicted location, and the output is a surface raster with weighted averages. As more weight λ_i is given to points closer than those located further away, this is known as the IDW. The distance exponent, represented by the power parameter, is set to 2 – a lower power results in a stronger influence from distant points. Also, the standard search neighborhood parameter is chosen.

As air pollution is influenced by wind[4] (Yang et al., 2020), the second method is based on an approach suggested by ESRI, a software company for geoinformation systems (GIS), for ozone distribution. The wind in Berlin usually originates from a southwestern direction. A grid with monthly wind directions for the years 2011 and 2012 with a resolution of 1 km^2 from the German weather service is used to obtain average seasonal wind directions[5]. Using this information, the directional influence or anisotropy is mapped with the

[4] Winter months: 220°; Summer 233°
[5] ArcGIS is GIS software developed by ESRI, used for creating, managing, and analyzing geographic data and maps (ESRI 2022).

geostatistical wizard. This allows manual adjustment of different parameter settings and is helpful in fitting the semi-variogram to the dataset.

The final approach is based on the concept of Kriging, which assumes that the variability of natural phenomena is based on spatial autocorrelation and, therefore, can be modeled statistically (Deligiorgi & Philippopoulos, 2011). Its weighting process of measured values is conducted by a statistical analysis, modeling of the semi-variogram and thereby the prediction of the surface. The semi-variogram computes the variance of the sample values over distances. In simplified terms, Kriging can be described by the following base formula.

$$\hat{X}(s_i) = \mu(s_i) + \varepsilon(s_i) \tag{2.2}$$

Where $\hat{X}(s_i)$ is the estimated variable of interest, $\mu(s_i)$ is the deterministic trend and $\varepsilon(s_i)$represents the error term. s_i is the indicator for the geographic location, such as longitude and latitude coordinates.

A modified form of Kriging is a relatively automated process in a GIS software[6] "that accounts for the error in estimating the underlying semi-variogram through repeated simulations" (ESRI 2022). In other words, the method finds the best-fitted semi-variogram by calculating the most suitable one for each subset of sample points. Due to the automatization, manual parameter adjustments are seldom required, except for fundamental environmental settings. Various parameters are set to facilitate the research process. For the search neighborhood, a standard circular parameter is chosen, consisting of a maximum of 15 and a minimum of 10 neighbors. Additional model specifications include a maximum of 100 points in each local model, with a baseline of 20 points, and a local model area overlap factor set at 1. A total of 100 semi-variograms are simulated, with a baseline number established at 30.

In comparison, the juxtaposition of the methods shows that IDW is known for its simplicity and deterministic nature, which makes it an efficient method for interpolating spatial data. Nevertheless, it assumes that the influence of the variable of interest decreases with distance, which is not always consistent with the spatial behavior of environmental variables. Compared to this, OK-wind introduces a directional component that considers the influence of prevailing winds on pollutant dispersion. This increases the complexity and potential accuracy of the interpolation, but at the same time requires robust wind field data and can lead to errors if the wind patterns are not consistent. The EBK method

[6] The Universal Transverse Mercator (UTM) is a system of map projection based on a horizontal spatial representation that is used to assign coordinates to geographic positions on the Earth's surface.

possesses several benefits compared to alternative techniques. It is highly automated, making the process more efficient. Even though the available data is limited, this method can produce significant and reliable results. It is particularly effective in handling data that shows reasonable variability or fluctuation, allowing for accurate predictions (ESRI, 2022). One of the notable features of this method is the ability to provide diverse output formats, including a geostatistical layer and a prediction error map, which enhances the consistency and comprehensiveness of the approach. Nevertheless, EBK can be computationally intensive and can produce results that are difficult to interpret without a sound statistical background.

Negative externalities are assessed by several methods, primarily focusing on the theoretical costs associated with adverse outcomes or impacts. The revealed-preference method is particularly noteworthy in this context. It deduces the value consumers place on environmental quality by observing their market purchases related to environmental quality. This theoretical framework corresponds directly to the hedonic regression, which is a price calculation method to evaluate rents based on influencing hedonic characteristics (Rosen, 1974). The basic regression term can be expressed by:

$$R_h = f_h(S_h, N_h, L_h, T_h, X_h) \tag{2.3}$$

The Rent R_h of an apartment or house is estimated by its structural attributes S_h(size, number of bedrooms and others) and characteristics of the neighborhood N_h (amenities, crime rates). L_h represents the location itself (geocoordinates), and T_h the time of the transaction. Depending on the underlying research question, additional hedonic attributes are included. In the field of environmental economics, the respective ecological characteristics of the locality are represented by X_h.

An ordinary multiple linear regression model might not be the right choice for answering the underlying hypothesis. Since the relationship between the response and explanatory variables is consistently not linear, a flexible model is used. The scatterplot matrix of selected variables for 2021, which can be found in the Appendix, provides a visual representation of the relationships between variables. Therefore, the GAM is a suitable solution to account for nonlinearity while still using an interpretable model with transparent relationships between predictors and the response variable. The semi-parametric regression allows the combination of linear, nonlinear, and interacting factors influencing the dependent variable (Wood, 2017). The outcome encompasses not only linear coefficients but also incorporates complex, adaptable smooth functions, known as splines. In addition, the interactions between variables are taken into account, which

overall improves the ability to explain the unique aspects of correlation, the so-called "wiggliness".

The GAM is defined for each timespan t ($t \in \{2018, 2021\}$) by the following set of equations:

$$y_{i,t} = cost_{i,t} \underset{ind.}{\sim} \pi(\mu_{i,t}, \theta) \tag{2.4}$$

$$log(\mu_{i,t}) = log\left(E\left(cost_{i,t}\right)\right) \tag{2.5}$$

$$= \alpha + \sum_{p=1}^{P} s_p\left(log\left(X_{p,i,t}\right)\right) + \sum_{b=1}^{B} \beta_b \cdot X_{b,i,t} + \sum_{m=1}^{M} s_m\left(log\left(X_{m,i,t}\right)\right) + \sum_{d=1}^{D} s_d\left(log\left(X_{d,i,t}\right)\right) + \sum_{l=1}^{L} s_l\left(X_{l,i,t}\right) + f\left(X_{lon,i,t}, X_{lat,i,t}\right)$$

with:

- $y_{i,t}$: Asking rent (in €/m²/p.m.) for asset i at time t
- π: Distribution function of the dependent (Gaussian distribution)
- $s_j(.)$:1-dimensional smoothing/spline functions to capture nonlinearities in the data (thin plate regression splines)
- $f\left(x_{lon,i,t}, x_{lat,i,t}\right)$: 2-dimensional smoothing function to capture the dependency of the location variables X_{lon} (longitude) and X_{lat} (latitude) (tensor product/Gaussian process smoother)
- X_p: Interpolated pollutant variables (PM_{10}, NO_2) (logarithmized)
- X_b: Binary hedonic asset characteristics (such as the availability of a balcony, built-in kitchen, elevator, etc.)
- X_m: Metric hedonic asset characteristics (number of rooms and living area, the latter logarithmized)
- X_d: Distances to geographic centers and relevant amenities in km (distance to the ZIP code center, the NUTS-3 center, the nearest ATM, bus stop, supermarket, restaurant, park, etc.) (logarithmized)
- X_l: Location-based variables (number of households and purchasing power per household in ZIP code area) (logarithmized)

In order to identify the optimal combinations of variables, several GAMs are created for different years, seasons and rental scenarios, each of which is subjected to a generalization process. Each model is evaluated and those with the lowest generalized cross-validation

(GCV), the lowest root mean squared error (RMSE) and the highest goodness of fit parameter (R^2) are utilized in the final model.

2.4 Results

The final models for the evaluation of particulate matter values are chosen to incorporate a year-based differentiation with the utilization of average values for each pollutant (Figure 2.3). Studies showed a significant difference between pollution values in the heating and non-heating period (Cichowicz et al., 2017). The results of the interpolations conducted here confirm these assumptions about seasonal variations. Nonetheless, it does not apply to the quantification of air pollution and the housing market. The testing of various simulations reveals no significant superiority of seasonal models, which is why the regression is conducted using annual averages.

The validation process involved a visual comparison between the average particulate matter values obtained from both official monitoring stations and private sensors. Sensors located in spatially similar areas exhibit only slight variations. To quantify these differences, Table 2.2 presents the RMSE values. Despite the minor differences, especially between EBK and OK-wind sensors, the data derived from the EBK sensors are selected for further analysis. The EBK approach is highly effective in predicting particulate matter levels, as it has the lowest error values compared to other methods, confirming its robustness and reliability in the analysis of pollution concentrations in the atmosphere. Furthermore, a consistent application of the EBK is obtained by extending its use to NO_2 concentrations, thus ensuring methodological consistency. A detailed review of the collected data from 2018 to 2021 underscored the remarkable precision of the EBK method in accurately modeling aggregate annual mean concentrations of pollutants. This is evident in the substantial reductions observed in the pollutant levels: the average PM_{10} concentrations receded from 17.35 µg/m³ in 2018 to 13.89 µg/m³ in 2021, and a parallel decline is witnessed in the average NO_2 levels, from 25 µg/m³ in 2018 to 21.54 µg/m³ in 2021. These empirical results illustrate the ability of the EBK method to correctly capture temporal variations in pollutant concentrations, supporting its applicability and value for improved air pollutant modeling and assessment.

Table 2.2 RMSE for Interpolation Methods for PM_{10} Values

		2018		2021	
		Winter	Summer	Winter	Summer
		PM_{10}	PM_{10}	PM_{10}	PM_{10}
EBK	RMSE	7.79	3.16	8.85	8.85
OK-wind	RMSE	7.99	3.20	13.32	9.41
IDW	RMSE	8.49	3.36	13.85	9.25

Note: Root mean squared error (RMSE) values are presented for various approaches, focusing on their performance in modeling particulate matter values within a seasonal context. The approaches that achieve the lowest, and thus, desirable error values are highlighted. For consistency, the terms "winter" and "summer" are utilized in lieu of "heating" and "non-heating period" to facilitate a more straightforward and uniform understanding of the seasonal variations discussed in the analysis.

For the GAM regression model, it is tested whether a log-transformation is needed for rents. The model's goodness of fit is much better when all metric variables are log-transformed by the natural logarithm, as Table 2.3 indicates. The only key performance indicator, namely R^2, scored slightly less in the log-model. Although the more optimized error value (0.207) is observed in the log model, the performance of R^2 is slightly lower. Other than that, both models explain more than 80% of the rental price variations.

Table 2.3 Goodness-of-Fit Results for Selected Model Options

	Rents			
	log		non-log	
	2018	2021	2018	2021
Observations	50,223	30,800	50,223	30,800
Adjusted R^2	0.829	0.767	0.846	0.783
RMSE	0.207	0.275	0.246	0.434
GCV	0.043	0.076	37,922	70,116

Note: The table includes observations, adjusted R-squared (R^2) values, root mean squared error (RMSE) statistics, and the Generalized Cross-Validation (GCV) scores for both log-transformed and non-log-transformed data. These metrics are critical for evaluating the quality of the models and their ability to accurately capture rental data. The results provide insight into the performance and suitability of various model specifications for analyzing rental trends over the specified years.

The regression outputs of the final models can be found in Table 2.4. Referring to the most relevant factors, the air pollution variables are included as a smooth term for the logarithm of the average PM_{10} and NO_2 levels. The variables are highly significant in both years, suggesting nonlinear effects on the dependent variable. In summary, the GAM regression output indicates that both the linear and nonlinear terms included in the model have significant effects on the rent for both years. The model appears to be robust, given the high R^2 and deviance explained, and the noteworthy significance of the smooth terms indicates that the nonlinear relationships captured by the GAM are essential for understanding the behavior of the dependent variable.

Table 2.4 GAM Regression Output of Model 2018 and 2021

2018					2021				
Parametric coefficients					**Parametric coefficients**				
	Est.	**SE**	**p-value**			**Est.**	**SE**	**p-value**	
(Intercept)	6.431	0.002	<0.0005	***	*(Intercept)*	6.326	0.004	<0.0005	***
Newly built	0.172	0.003	<0.0005	***	*Newly built*	0.271	0.005	<0.0005	***
Parking lot	0.042	0.003	<0.0005	***	*Parking lot*	0.075	0.004	<0.0005	***
Terrace	0.048	0.003	<0.0005	***	*Terrace*	0.085	0.005	<0.0005	***
Balcony	-0.001	0.002	0.715		*Balcony*	-0.007	0.004	0.0343	*
Refurbished	-0.014	0.002	<0.0005	***	*Refurbished*	-0.022	0.005	<0.0005	***
BI Kitchen	0.111	0.002	<0.0005	***	*BI Kitchen*	0.214	0.004	<0.0005	***
Elevator	0.015	0.002	<0.0005	***	*Elevator*	0.029	0.004	<0.0005	***
Approximate significance of smooth terms					**Approximate significance of smooth terms**				
	edf	**Ref.edf**	**p-value**			**edf**	**Ref.edf**	**p-value**	
s(log(avg PM_{10}))	4.241	5.369	<0.0005	***	*s(log(avg PM10))*	6.988	7.918	<0.0005	***
s(log(avg NO_2))	8.876	8.993	<0.0005	***	*s(log(avg NO2))*	5.459	6.571	<0.0005	***
s(log(rooms)	3.910	3.994	<0.0005	***	*s(log(rooms)*	3.938	3.996	<0.0005	***
s(log(living area)	8.701	8.969	<0.0005	***	*s(log(living area)*	7.803	8.624	<0.0005	***
s(households per zip)	8.993	9.000	<0.0005	***	*s(households per zip)*	4.335	5.346	<0.0005	***
s(purchasing power per household)	8.174	8.804	<0.0005	***	*s(purchasing power per household)*	8.530	8.925	<0.0005	***
s(*log(Centroid zip distance)*	7.639	8.515	<0.0005	***	*s(log(Centroid zip distance)*	8.568	8.943	<0.0005	***
s(*log(Centroid NUTS distance)*	8.425	8.848	<0.0005	***	*s(log(Centroid NUTS distance)*	8.663	8.942	<0.0005	***
s(log(Bus stop distance)	8.117	8.786	<0.0005	***	*s(log(Bus stop distance)*	3.822	4.816	<0.0005	***
s(log(Post box distance)	8.516	8.897	<0.0005	***	*s(log(Post box distance)*	5.058	6.249	<0.0005	***
s(log(Bar distance	7.548	8.444	<0.0005	***	*s(log(Bar distance*	3.671	4.610	<0.0005	***
s(log(School distance)	7.207	8.164	<0.0005	***	*s(log(School distance)*	8.850	8.988	<0.0005	***
s(log(Fast food distance)	6.579	7.724	0.103		*s(log(Fast food distance)*	7.470	8.421	0.103	
s(log(Park distance)	7.694	8.518	<0.0005	***	*s(log(Park distance)*	8.195	8.814	<0.0005	***
s(log(Restau-rant distance)	7.737	8.603	<0.0005	***	*s(log(Restau-rant distance)*	7.905	8.688	<0.0005	***
s(log(Café distance)	6.222	7.396	<0.0005	***	*s(log(Café distance)*	5.505	6.684	<0.0005	***
s(log(Play-ground distance)	4.408	5.537	<0.0005	***	*s(log(Play-ground distance)*	7.601	8.630	<0.0005	***
s(log(Super-market distance)	8.479	8.906	<0.0005	***	*s(log(Super-market distance)*	8.835	8.986	<0.0005	***
s(log(ATM distance)	3.279	4.198	<0.0005	***	*s(log(ATM distance)*	5.507	6.690	<0.0005	***
te(longitude, latitude)	23.795	23.957	<0.0005	***	*te(longitude, latitude)*	22.054	22.660	<0.0005	***
Adj. R^2			0.829		Adj. R^2			0.767	
Deviance explained			83.0%		Deviance explained			76.8%	
n			50,223		n			30,800	

Note: Significance levels; "***" p<0.005, "**" p<0.001, "*" p<0.01, "." p<0.1

The regression results of the GAM models for 2018 and 2021 are summarized in Table 2.4, showing both linear and smooth variables. The estimates (Est.) and standard errors (SE) quantify the magnitude and precision of the impact of each predictor on the log-transformed dependent variable, with the transformation allowing for a percentage-based interpretation of the effects. P-values are provided to assess the statistical significance of each predictor, with lower values indicating stronger rejection of the null hypothesis and, therefore, a significant impact on the dependent variable. The R^2 values provide a quantitative assessment of the explanatory power of the models. Such results contribute to a nuanced understanding of the factors affecting rent trends within the specified time frame.

For the observation years, each pollutant is illustrated in the following maps, which reveal annual and spatial differences.

2.4.1 Model Validation – PM_{10}

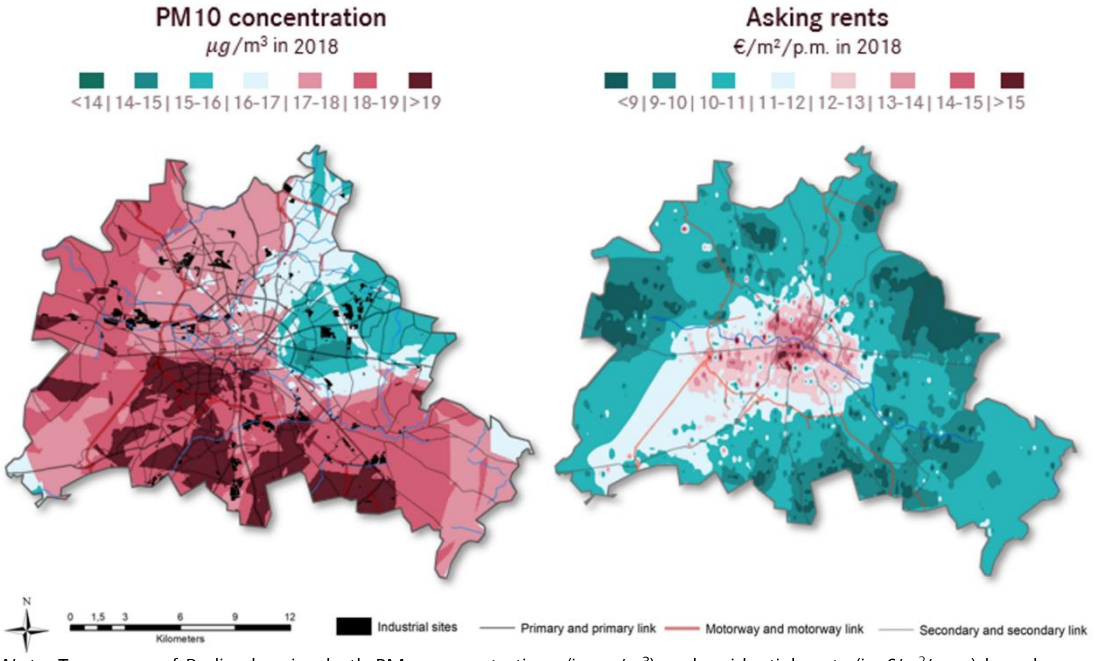
Figure 2.4 shows maps of PM_{10} distribution in the reference year 2018, while Figure 2.5 illustrates the corresponding maps for 2021. Notably, there is a difference in concentration patterns between these two years. In 2018, the highest values (> 19 µg/m^3) were found in the south of Berlin, whereas in 2021, this area shows the lower values of < 15 µg/m^3. Conversely, lower concentrations are more widespread in 2021, displaying a distinct separation between these minimal levels and the higher concentrations predominantly located in the north-west regions of Berlin. Concentrations are generally lower in 2018, but the distribution pattern is different. In general, the range of values is narrower in 2018.

When assessing asking rents, it is evident that the highest rents are concentrated within the central business district and gradually decrease with increasing distance from the central business district. A visual comparison between 2018 and 2021 highlights the rising rents over this period and the expansion of areas with higher rents in Berlin.

Furthermore, Figure 2.6 provides a representation of rent deviation in 2018. Apartments located in areas with lower pollution levels boast rental incomes that are 2% higher than the market average. Conversely, properties situated in highly polluted areas are offered at a discount ranging from -2% to 6% compared to the market average.

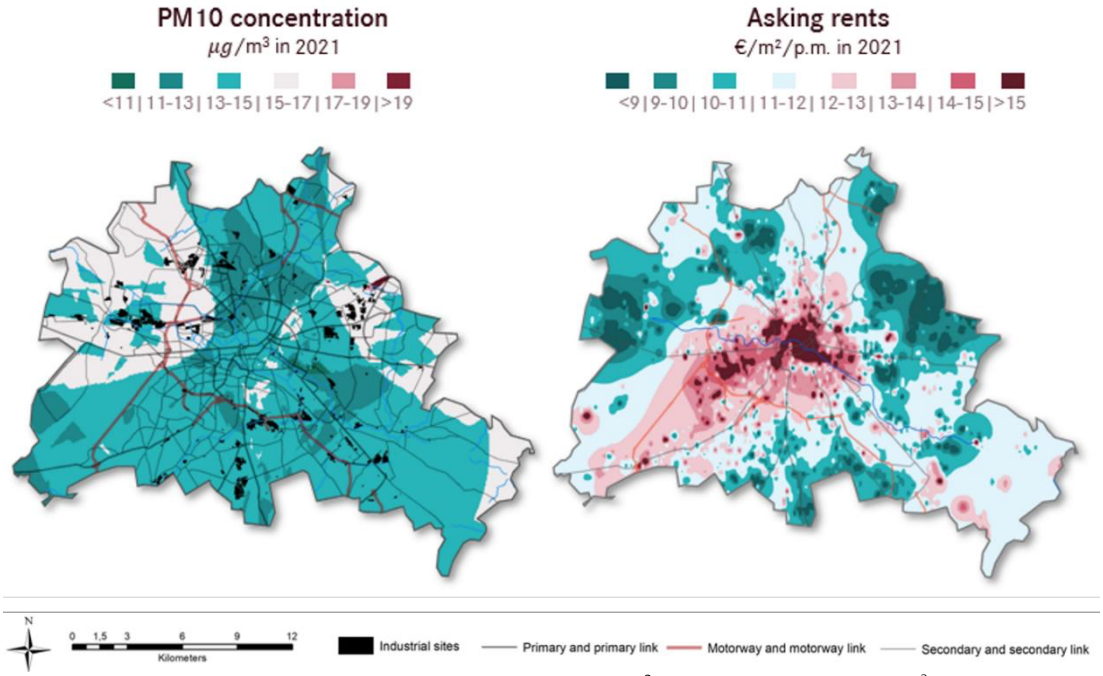
Figure 2.7, on the other hand, offers insights into the year 2021. This year, assets situated in areas with low pollution levels are either priced at market average rates or command a premium of up to 6% over the average market rates. In contrast, properties in highly polluted areas in 2021 are generally traded at a discount, ranging from -4% to -8%.

Figure 2.4 PM_{10} and Rents 2018



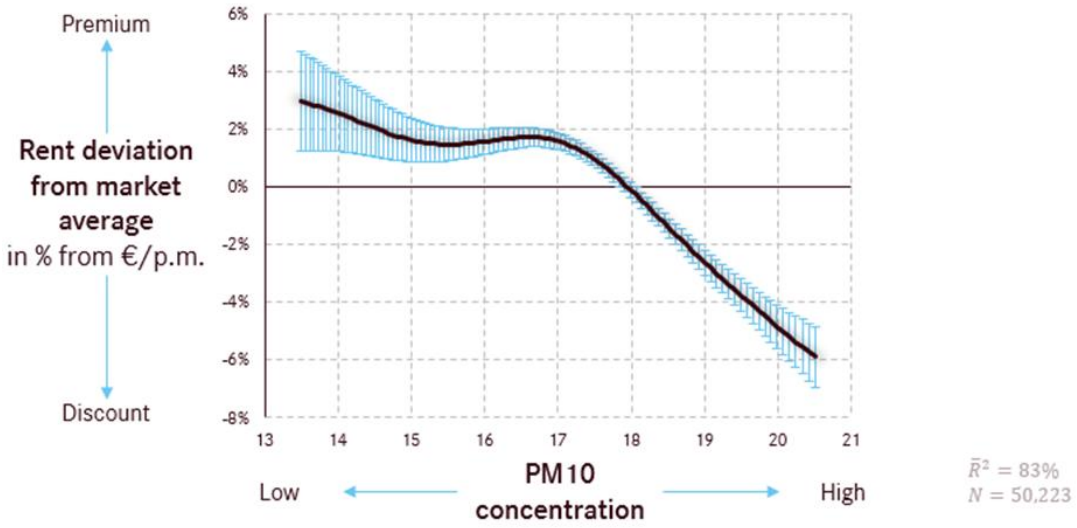
Note: Two maps of Berlin showing both PM_{10} concentrations (in µg/m³) and residential rents (in €/m²/p.m.) based on an annual observation. Color coding was used to effectively visualize and distinguish patterns in different areas within the maps and provides a detailed representation of PM_{10} concentrations and corresponding rent values in different parts of the city. In this color-coded representation, red represents high values while green represents lower values, allowing for a more intuitive and comprehensive interpretation of the data.

Figure 2.5 PM_{10} and Rents 2021



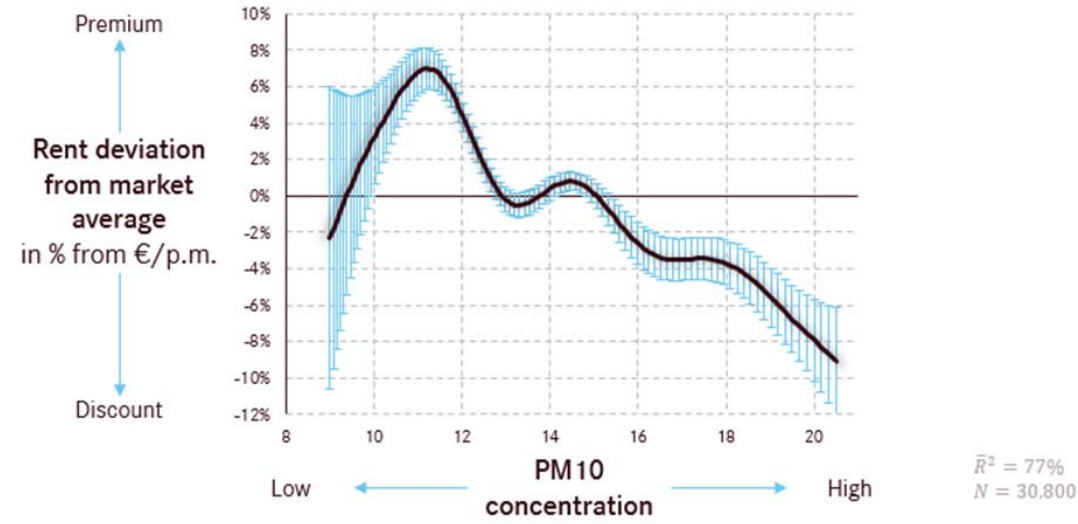
Note: Two maps of Berlin showing both PM_{10} concentrations (in µg/m³) and residential rents (in €/m²/p.m.) based on an annual observation. Color coding was used to effectively visualize and distinguish patterns in different areas within the maps and provides a detailed representation of PM_{10} concentrations and corresponding rent values in different parts of the city. In this color-coded representation, red represents high values while green represents lower values, allowing for a more intuitive and comprehensive interpretation of the data.

Figure 2.6 Rent Deviation according to the PM_{10} Concentration in 2018



Note: This figure illustrates the relationship between rent deviation and PM_{10} concentration in the year 2018. The rental values are derived from a generalized additive model (GAM) regression with a goodness-of-fit value of 83%, based on an extensive dataset comprising 50,223 observations. On the y-axis, the PM_{10} distribution is represented, while the x-axis displays the rental distribution in percentage terms. The figure provides insights into how changes in PM_{10} concentration correspond to variations in rental prices, underscoring the influence of air quality on the rental market dynamics.

Figure 2.7 Rent Deviation according to the PM_{10} Concentration in 2021



Note: This figure illustrates the relationship between rent deviation and PM_{10} concentration in the year 2021. The rental values are derived from a generalized additive model (GAM) regression with a goodness-of-fit value of 77%, based on an extensive dataset comprising 30,800 observations. On the y-axis, the PM_{10} distribution is represented, while the x-axis displays the rental distribution in percentage terms. The figure provides insights into how changes in PM_{10} concentration correspond to variations in rental prices, underscoring the influence of air quality on the rental market dynamics.

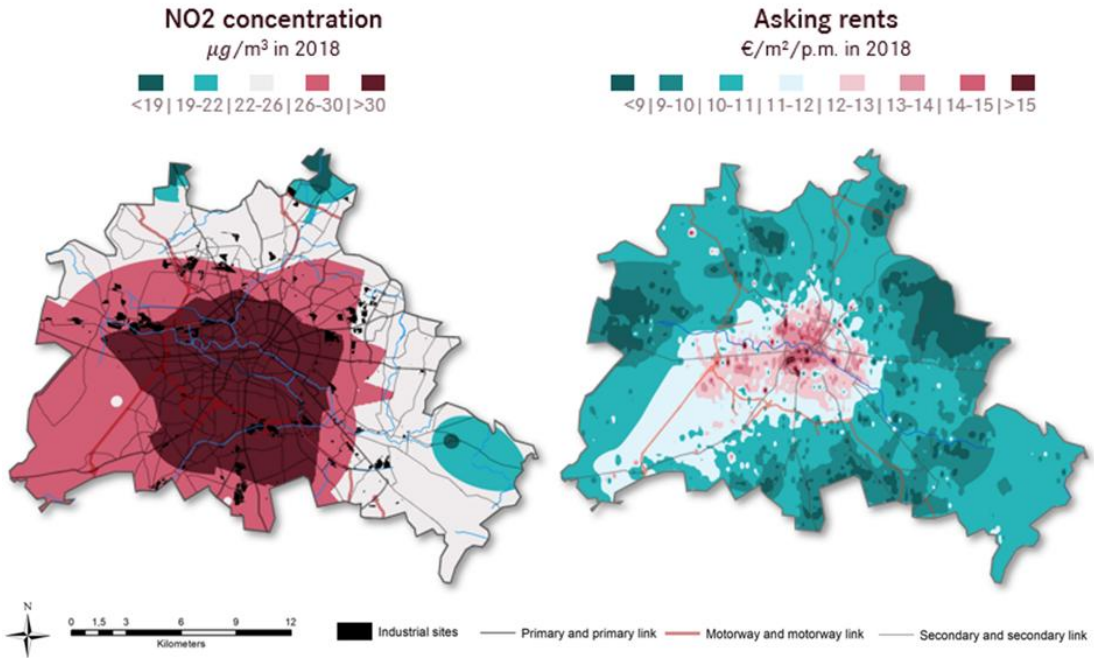
2.4.2 Model Validation – NO_2

The concentration of NO_2 in Berlin exhibits a pattern similar to the PM_{10} distribution. In 2018 (Figure 2.8), the distribution appears more extensive and wide-ranging compared to 2021 (Figure 2.9). The changes observed are an indication of a significant environmental change within the city. This trend can be attributed to a variety of factors, including behavioral changes as a result of the pandemic. The strict lockdowns, social distancing measures and remote working have led to a decrease in vehicle traffic, which is a major source of NO_2 emissions. The more limited and less widespread distribution of NO_2 in 2021 may therefore reflect the decline in commuting and industrial activity during this period. Nevertheless, the city center consistently registered the highest levels of nitrogen dioxide in both years. The distribution pattern remains consistent across the two years, characterized by lower NO_2 values in the northern regions and elevated concentrations within a corridor running from the north-east to the south-west. It is worth highlighting that the northern areas consistently exhibit superior air quality with respect to NO_2 pollution throughout the observed time periods.

In accordance with the previous literature, a willingness to pay for good air might be expected. According to the GAM plots, this should mean a negative sign. However, for NO_2, this effect is not present; in fact, there is a positive effect. In other words, higher concentrations mean higher rental prices. Specifically, Figure 2.10 reveals that apartments situated in areas characterized by low traffic and minimal combustion from motor vehicles exhibited a pricing discount, ranging from -2% to -6% in comparison to the prevailing market average. Conversely, properties located in regions with elevated levels of nitrogen dioxide enjoy a premium, albeit one less than 8%, relative to the established market average rates. Insufficient measuring stations and the associated errors in the interpolation may lead to this result. Moreover, the range of pollutant concentrations is not high.

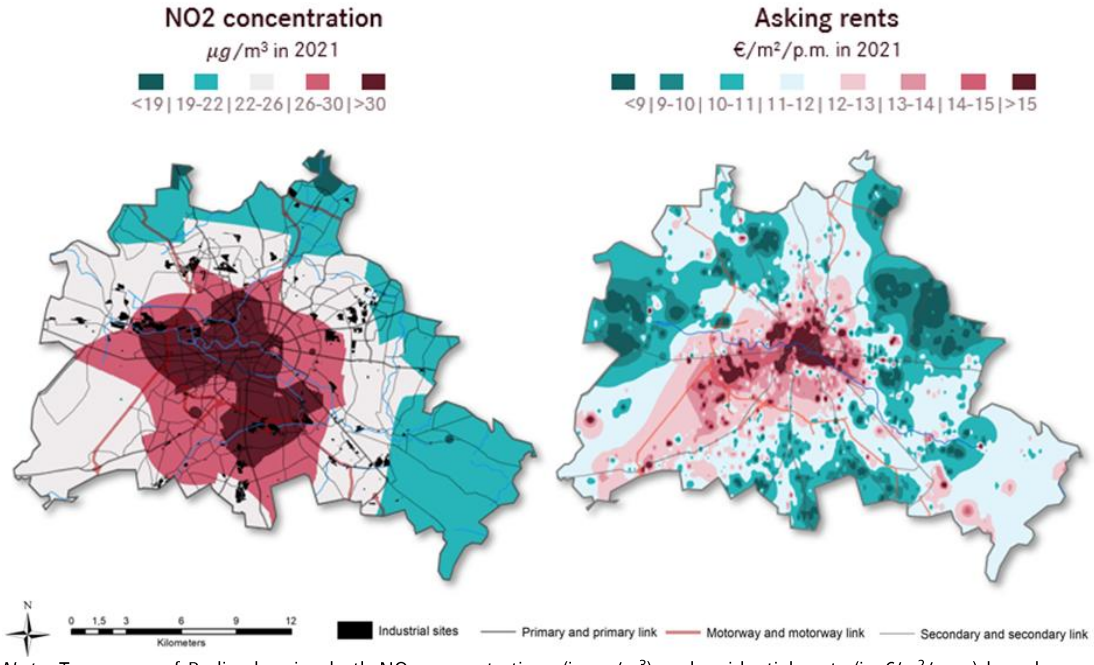
Figure 2.11 illustrates the scenario of 2021 in which low traffic areas with limited vehicle combustion command premiums that can be as much as 14% above the market average. This illustrates a notable market correction, highlighted by a discernible change in pricing dynamics under the influence of air quality considerations.

Figure 2.8 NO_2 and Rents 2018



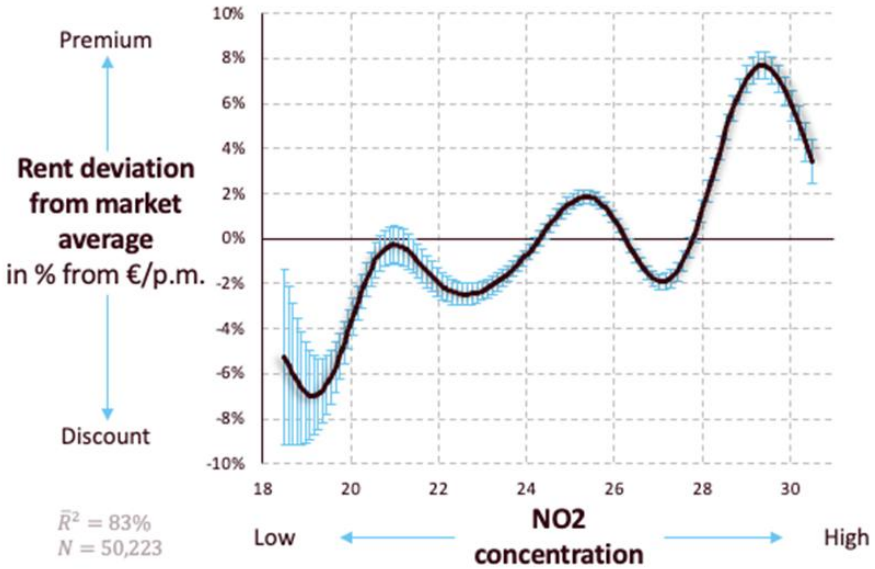
Note: Two maps of Berlin showing both NO_2 concentrations (in µg/m³) and residential rents (in €/m²/p.m.) based on an annual observation. Color coding was used to effectively visualize and distinguish patterns in different areas within the maps, and provides a detailed representation of NO_2 concentrations and corresponding rent values in different parts of the city. In this color-coded representation, red represents high values while green represents lower values, allowing for a more intuitive and comprehensive interpretation of the data.

Figure 2.9 NO_2 and Rents 2021



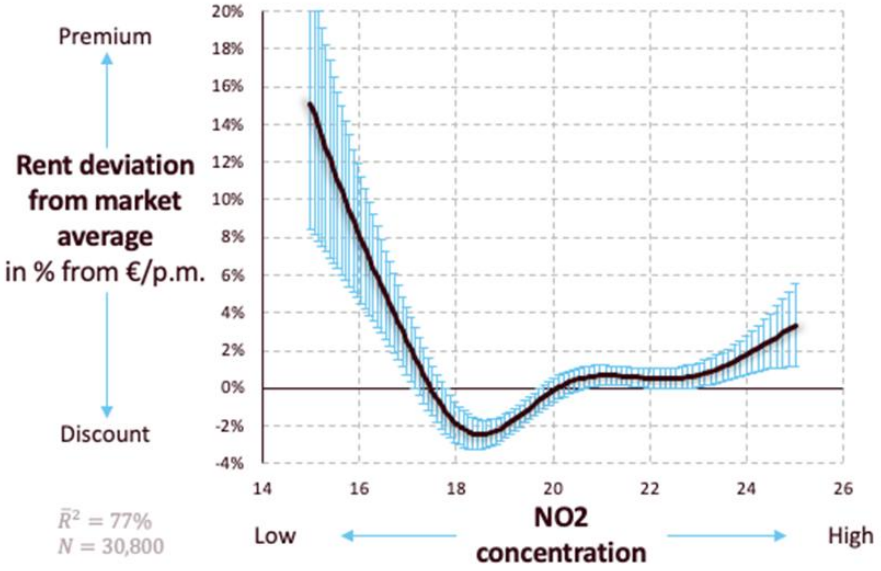
Note: Two maps of Berlin showing both NO_2 concentrations (in µg/m³) and residential rents (in €/m²/p.m.) based on an annual observation. Color coding was used to effectively visualize and distinguish patterns in different areas within the maps, and provides a detailed representation of NO_2 concentrations and corresponding rent values in different parts of the city. In this color-coded representation, red represents high values while green represents lower values, allowing for a more intuitive and comprehensive interpretation of the data.

Figure 2.10 Rent Deviation according to the NO_2 Concentration in 2018



Note: This figure illustrates the relationship between rent deviation and NO_2 concentration in the year 2018. The rental values are derived from a generalized additive model (GAM) regression with a goodness-of-fit value of 83%, based on an extensive dataset comprising 50,223 observations. On the y-axis, the NO_2 distribution is represented, while the x-axis displays the rental distribution in percentage terms. The figure provides insights into how changes in NO_2 concentration correspond to variations in rental prices, underscoring the influence of air quality on the rental market dynamics.

Figure 2.11 Rent Deviation according to the NO_2 Concentration in 2021

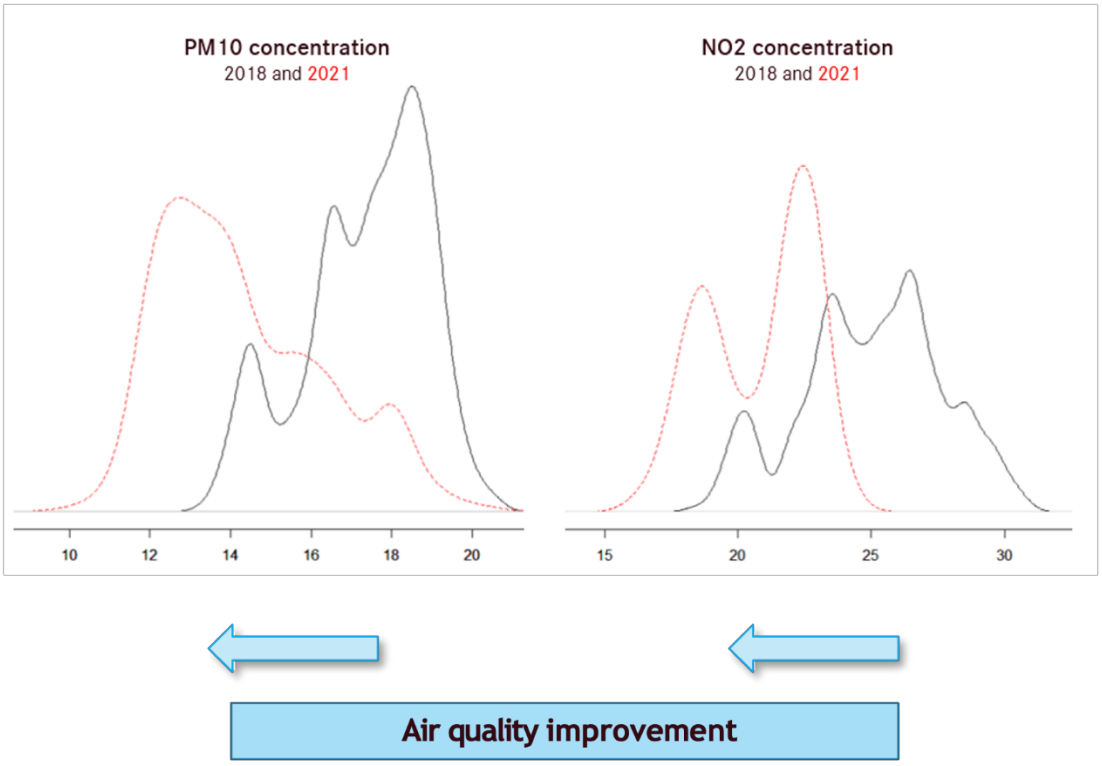


Note: This figure illustrates the relationship between rent deviation and NO_2 concentration in the year 2021. The rental values are derived from a generalized additive model (GAM) regression with a goodness-of-fit value of 77% based on an extensive dataset comprising 30,800 observations. On the y-axis, the NO_2 distribution is represented, while the x-axis displays the rental distribution in percentage terms. The figure provides insights into how changes in NO_2 concentration correspond to variations in rental prices, underscoring the influence of air quality on the rental market dynamics.

The data suggest that individuals seeking apartments exhibit a willingness to pay a premium for residences with lower PM_{10} concentrations. This willingness could be attributed to the pronounced importance and perceptibility of the pollutant levels associated with PM_{10} particles. Unlike NO_2, PM_{10} particles have a larger diameter (10 µm), making them more conspicuous and visible. This visibility of PM_{10} particles might matter in the decision-making process when looking for housing and contributes to reducing information bias among prospective tenants.

Generally, the research reveals that air quality in Berlin has shown notable improvements since 2018 (Figure 2.12). This positive trend signals a shift in human behavior and mobility patterns, perhaps influenced by a growing awareness of environmental issues and government policies aimed at reducing pollution. This change in air quality dynamics holds promise for both the well-being of Berlin's residents and its property market.

Figure 2.12 PM_{10} Distribution in 2018 and 2021



Note: This figure visually represents the distribution of particulate matter for both PM_{10} and NO_2 in the years 2018 and 2021. The graphs illustrate the concentration of particulate matter in micrograms per cubic meter (µm/m^3) on the y-axis, emphasizing the distribution of these concentrations. In each graph, the black line corresponds to the data for 2018, while the red line represents the data for 2021.

2.5 Conclusion

It is well-established that poor air quality is linked to various health problems, including respiratory diseases, cardiovascular issues, and a diminished overall quality of life. In this context, the results shed light on the critical role of air quality in optimizing a rental property portfolio. They highlights that, even with limited monitoring, machine learning techniques can effectively predict pollution levels. When sufficient monitoring is available, interpolation techniques, particularly Kriging, prove superior.

In accordance with the previous literature, the valuation of air pollution in the residential sector includes air pollution as a hedonic variable embedded in various regression techniques. The application of nonlinear regression models reveals that air quality significantly influences rental rates, underscoring the economic relevance of environmental considerations and emphasizing the need to account for negative externalities associated with poor air quality in the real estate market.

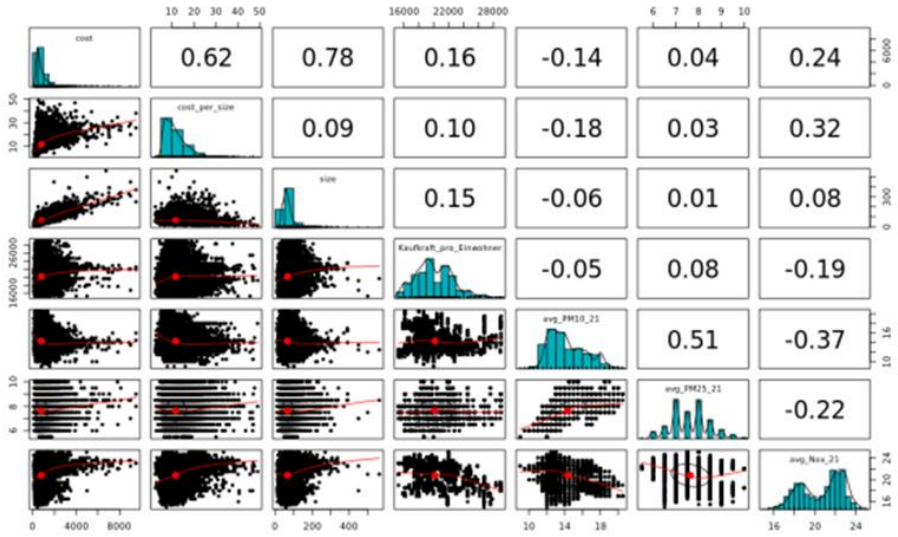
A marginal willingness to pay in a German city, namely its capital, Berlin, is only partially supported. The significant effect of air pollution on rents is revealed for particulate matter concentrations. After considering socioeconomic, spatial, and hedonic control variables, a marginal willingness to pay is determined for Berlin in 2018 and 2021 for low PM_{10} values and good air quality conditions. More specifically, this translates to a rent premium of approximately 3% above the average rent price for good air quality with a bandwidth of 70 basis points. However, this is not consistently observed for NO_2 concentrations, as areas with higher NO_2 levels surprisingly registered higher rental prices, indicating a complex relationship between air quality and rental values. This finding, alongside noticeable pricing dynamics in 2021, suggests a shifting influence of air quality on the Berlin rental property market, possibly influenced by the perceptibility of PM_{10} particles. Nevertheless, a consistent spatial pattern in NO_2 concentration over the years 2018 and 2021 is observed, with the city center consistently registering the highest levels and the northern regions maintaining better air quality.

Since this work cannot cover the entire scope, some suggestions for future research are given. To begin with, just two out of a large range of pollutants are analyzed. Expanding the analysis to include a wider variety of pollutants would offer a more comprehensive and nuanced understanding of the research topic. Another possibility could be to investigate the conscious preference for good air when looking for housing. This might be answered through a survey to provide insight into information bias. Nevertheless, air pollution values and rent levels differ from region to region. Thus, the results cannot be transferred entirely, but it is possible to replicate the methodology for other European cities.

The link between air pollution and rent levels presents opportunities for the real estate industry to implement changes. Strategies such as air filters, clean heating technologies, and greening measures can be adopted to enhance living environments. A standardized network of pollution sensors can increase transparency and drive future research.

2.6 Appendix

Figure 2.13 Scatterplot Matrix of selected Variables for 2021



Note: In these scatterplots, red lines depict the linearity of relationships. For instance, the relationship between cost and size is evidently linear, as indicated by the straight red line. Nevertheless, for most other variables, the relationships are not as clearly linear. This observation is pivotal in determining the appropriate model for the analysis.

2.7 References

Amt für Statistik Berlin-Brandenburg. (2022). *Überblick Bevölkerung*, Accessed: 2023-10-24. URL: https://www.statistik-berlin-brandenburg.de/bevoelkerung

Anselin, L., & Lozano-Gracia, N. (2008). Errors in variables and spatial effects in hedonic house price models of ambient air quality. *Empirical Economics*, 34(1), 5–34.

Beelen, R., Hoek, G., Pebesma, E., Vienneau, D., Hoogh, K. D., & Briggs, D. J. (2009). Mapping of background air pollution at a fine spatial scale across the European Union. *Science of The Total Environment*, 407(6), 1852–1867.

Beelen, R., Hoek, G., Vienneau, D., Eeftens, M., Dimakopoulou, K., Pedeli, X., Tsai, M., Künzli, N., Schikowski, T., Marcon, A., Eriksen, K. T., Raaschou-Nielsen, O., Stephanou, E., Patelarou, E., Lanki, T., Yli-Tuomi, T., Declercq, C., Falq, G., Stempfelet, M., Birk, M., Cyrys, J., von Klot, S., Nádor, G., Varró, M. J., Dėdelė, A., Gražulevičienė, R., Mölter, A., Lindley, S., Madsen, C., Cesaroni, G., Ranzi, A., Badaloni, C., Hoffmann, B., Nonnemacher, M., Krämer, U., Kuhlbusch, T., Cirach, M., de Nazelle, A., Nieuwenhuijsen, M., Bellander, T., Korek, M., Olsson, D., Strömgren, M., Dons, E., Jerrett, M., Fischer, P., Wang, M., Brunekreef, B., & Hoogh, K. D. (2013). Development of NO_2 and NO_x land use regression models for estimating air pollution exposure in 36 study areas in Europe – The ESCAPE project. *Atmospheric Environment,* 72, 10–23.

Borja-Urbano, S., Rodríguez-Espinosa, F., Luna-Ludeña, M., & Toulkeridis, T. (2021). Valuing the impact of air pollution in urban residence using hedonic pricing and geospatial analysis, evidence from Quito, Ecuador. *Air, Soil and Water Research*, 14, 117862212110532.

Brook, R. D., Rajagopalan, S., Pope, C. A., Brook, J. R., Bhatnagar, A., Diez-Roux, A. V., Holguin, F., Hong, Y., Luepker, R. V., Mittleman, M. A., Peters, A., Siscovick, D., Smith, S. C., Whitsel, L., & Kaufman, J. D. (2010). Particulate matter air pollution and cardiovascular disease: An update to the scientific statement from the American Heart Association. *Circulation*, 121(21), 2331–2378.

Budde, M., Schwarz, A. D., Müller, T., Laquai, B., Streibl, N., Schindler, G., Köpke, M., Riedel, T., Dittler, A., & Beigl, M. (2018). Potential and limitations of the low-cost SDS011 particle sensor for monitoring urban air quality. In *ProScience: Proceedings of the 3rd International Conference on Atmospheric Dust* (DUST2018) (Vol. 5, pp. 6–12).

Chay, K. Y., & Greenstone, M. (2005). Does air quality matter? Evidence from the housing market. *Journal of Political Economy*, 113(2), 376–424.

Chen, L., Wang, Y., Li, P., Ji, Y., Kong, S., Li, Z., & Bai, Z. (2012). A land use regression model incorporating data on industrial point source pollution. *Journal of Environmental Sciences*, 24(7), 1251–1258.

Chen, Y., & Lee, C.-C. (2020). The impact of real estate investment on air quality: Evidence from China. *Environmental Science and Pollution Research*, 27(18), 22989–23001.

Cichowicz, R., Wielgosiński, G., & Fetter, W. (2017). Dispersion of atmospheric air pollution in summer and winter season. *Environmental Monitoring and Assessment*, 189(12), 1–10.

Dall'O', G., Galante, A., & Pasetti, G. (2012). A methodology for evaluating the potential energy savings of retrofitting residential building stocks. *Sustainable Cities and Society*, 4, 2–21.

Deligiorgi, D., & Philippopoulos, K. (2011). Spatial interpolation methodologies in urban air pollution modeling: Application for the greater area of metropolitan Athens, Greece. In: F. Nejadkoorki (Ed.), *Advanced Air Pollution* (pp. 341-362). InTech.

European Environment Agency. (2023). *European city air quality viewer*, Accessed: 2023-10-15. URL: https://www.eea.europa.eu/themes/air/urban-air-quality/european-city-air-quality-viewer

Eichlseder, H., Hausberger, S., Beidl, C., & Steinhaus, T. (2021). Zero impact – Objective and significance for vehicle powertrains and air quality. In: J. Liebl, C. Beidl, and W. Maus (Eds.), *Internationaler Motorenkongress 2021* (pp. 437–451), Springer.

Habermann, M., Billger, M., & Haeger-Eugensson, M. (2015). Land use regression as method to model air pollution. Previous results for Gothenburg/Sweden. *Procedia Engineering*, 115, 21–28.

Kahn, M. E. (1995). A revealed preference approach to ranking city quality of life. *Journal of Urban Economics*, 38(2), 221–235.

Knote, C., Tuccella, P., Curci, G., Emmons, L., Orlando, J. J., Madronich, S., Baró, R., Jiménez-Guerrero, P., Luecken, D., Hogrefe, C., Forkel, R., Werhahn, J., Hirtl, M., Pérez, J. L., San José, R., Giordano, L., Brunner, D., Yahya, K., & Zhang, Y. (2015). Influence of the choice of gas-phase mechanism on predictions of key gaseous pollutants during the AQMEII phase-2 intercomparison. *Atmospheric Environment*, 115, 553–568.

Kumar, S. D., & Dash, A. (2018). Seasonal variation of air quality index and assessment. *Global Journal of Environmental Science and Management*, 4(4), 483–492.

Le Boennec, R., & Salladarré, F. (2017). The impact of air pollution and noise on the real estate market. The case of the 2013 European Green Capital: Nantes, France. *Ecological Economics*, 138, 82–89.

Munir, S., Habeebullah, T. M., Mohammed, A. M. F., Morsy, E. A., Rehan, M., & Ali, K. (2017). Analysing $PM_{2.5}$ and its association with PM_{10} and meteorology in the arid climate of Makkah, Saudi Arabia. *Aerosol and Air Quality Research*, 17(2), 453–464.

Ohlwein, S., Kappeler, R., Joss, M. K., Künzli, N., & Hoffmann, B. (2019). Health effects of ultrafine particles: A systematic literature review update of epidemiological evidence. *International Journal of Public Health*, 64(4), 547–559.

Parida, V., & Wincent, J. (2019). Why and how to compete through sustainability: A review and outline of trends influencing firm and network-level transformation. *International Entrepreneurship and Management Journal*, 15(1), 1–19.

Ridker, R. G., & Henning, J. A. (1967). The determinants of residential property values with special reference to air pollution. *The Review of Economics and Statistics*, 49(2), 246–257.

Rosen, S. (1974). Hedonic prices and implicit markets: Product differentiation in pure competition. *Journal of Political Economy*, 82(1), 34–55.

Rumaling, M. I., Chee, F. P., Chang, H. W. J., Payus, C. M., Kong, S. K., Dayou, J., & Sentian, J. (2022). Forecasting particulate matter concentration using nonlinear autoregression with exogenous input model. *Global Journal of Environmental Science and Management*, 8(1), 27–44.

Serafeim, G. (2020). Public sentiment and the price of corporate sustainability. *Financial Analysts Journal*, 76(2), 26–46.

Schraufnagel, D. E., Balmes, J. R., Cowl, C. T., de Matteis, S., Jung, S.-H., Mortimer, K., Perez-Padilla, R., Rice, M. B., Riojas-Rodriguez, H., Sood, A., Thurston, G. D., To, T., Vanker, A., & Wuebbles, D. J. (2019). Air pollution and noncommunicable disease. A review by the forum of international respiratory societies' environmental committee, part 2: Air pollution and organ systems. *Chest*, 155(2), 409–416.

Simoni, M., Baldacci, S., Maio, S., Cerrai, S., Sarno, G., & Viegi, G. (2015). Adverse effects of outdoor pollution in the elderly. *Journal of Thoracic Disease*, 7(1), 34–45.

Smith, V. K., & Huang, J. C. (1993). Hedonic models and air pollution: Twenty-five years and counting. *Environmental and Resource Economics*, 3(4), 381–394.

Sun, B., & Yang, S. (2020). Asymmetric and spatial non-stationary effects of particulate air pollution on urban housing prices in Chinese cities. *International Journal of Environmental Research and Public Health*, 17(20), 7443.

Tobler, W. (1970). A computer movie simulating urban growth in the Detroit region. *Economic Geography*, 46(1), 234–240.

Tschöke, H. (2021). Von der Emission zur Immission. In W. Siebenpfeiffer (Ed.), *Mobilität der Zukunft: Intermodale Verkehrskonzepte* (pp. 227–248), Springer.

Umweltbundesamt. (2022). *Natürliche Quellen der Luftschadstoffe*. Accessed: 2023-09-04. URL: https://www.uba.de/n94500de

United States Environmental Protection Agency. (2016). *What is acid rain?* Accessed: 2023-09-01. URL: https://www.epa.gov/acidrain/what-acid-rain

Wolf, K., Cyrys, J., Harciníková, T., Gu, J., Kusch, T., Hampel, R., Schneider, A., & Peters, A. (2017). Land use regression modeling of ultrafine particles, ozone, nitrogen oxides and markers of particulate matter pollution in Augsburg, Germany. *The Science of the Total Environment*, 579(1), 1531–1540.

Wood, S. N. (2017). Generalized additive models. An introduction with R (2nd ed.). CRC Press.

Wu, C.-D., Zeng, Y.-T. & Lung, S.-C. C. (2018). A hybrid kriging/land-use regression model to assess $PM_{2.5}$ spatial-temporal variability. *The Science of the Total Environment,* 645, 1456–1464.

Zhang, H., Wang, Z., & Zhang, W. (2016). Exploring spatiotemporal patterns of $PM_{2.5}$ in China based on ground-level observations for 190 cities. *Environmental Pollution*, 216, 559–567.

3 Quantifying the Impact of Urban Heat Islands on Residential Property Prices

3.1 Abstract

Frequent and persistent heat effects in urban environments, particularly urban heat islands (UHIs), pose an increasing risk to cities. However, their economic impact on housing markets remains underexplored. This study employs a semi-parametric approach to examine the relationship between UHI intensity and residential property prices, drawing on a unique building-level dataset with temperature measurements taken twice daily at 1 p.m. and 4 a.m. We find a strong, persistent negative relationship, with nighttime UHI intensity showing the most pronounced and lasting effect on housing prices. Spatial analysis reveals significant variation, with differing patterns of heat exposure and resilience between central and peripheral areas. Socioeconomic disparities worsen the issue. Lower-income neighborhoods experience higher UHI exposure, underscoring climate-related spatial inequalities. Our results suggest that property prices reflect thermal risks and neighborhood microclimates. This study provides the first building-level evidence of the economic impact of UHIs, offering critical insights for investors, policymakers and urban planners aiming to strengthen heat resilience and promote equitable mitigation in housing markets.

Keywords: Urban Heat Island, Residential Property Prices, Housing Market, Physical Climate Risk, Temperature

3.2 Introduction

Research indicates that climate-related risks have a significant impact on global real estate markets.[7] Among these, increasingly frequent and intense heat extremes in urban environments pose a particular threat to the built environment and its inhabitants (Intergovernmental Panel on Climate Change, 2023). In fact, heat-related hazards often account for the majority of fatalities from natural disasters (Gabriel & Endlicher, 2011). By 2100, an estimated 75% of the global population could be at heightened risk of heat-related excess mortality, based largely on evidence from mid-latitude cities in North America and Europe (Mora et al., 2017). This risk is further intensified by the urban heat island (UHI) effect (Heaviside et al., 2016).

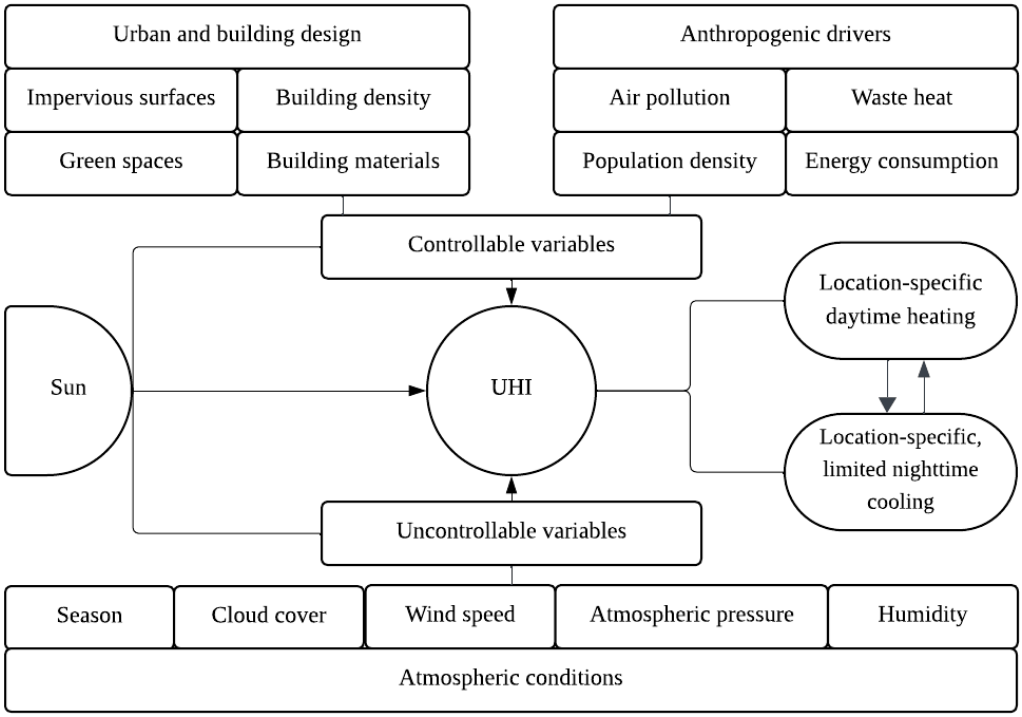
The UHI effect describes the phenomenon in which urban temperatures are significantly higher than those in surrounding suburban or rural areas (Oke, 1982). UHI intensity also varies within cities owing to factors such as building density, building materials, and urban design, resulting in temperature differences between neighborhoods and even individual buildings. Areas with high-density development, extensive impervious surfaces, and heat-absorbing building materials are especially vulnerable. Interactions with other environmental factors, such as air pollution, can further amplify UHI effects (Li et al., 2018a). Urban areas therefore both cause and suffer from UHIs. While UHIs typically result in relative average temperature increases of 4 to 6 degrees Celsius (°C) (7.2 to 10.8 degrees Fahrenheit (°F)) compared to rural areas, localized hotspots can reach up to 10°C (18°F) above the rural baseline (Iodice et al., 2024). The complex drivers of UHIs, ranging from controllable urban factors to uncontrollable environmental conditions, are illustrated in Figure 3.1.

A critical aspect of UHI exposure is its unequal distribution across socioeconomic groups. Higher-income households are more likely to live in cooler neighborhoods with favorable microclimates, reflecting their greater financial flexibility and willingness to pay for climate-related amenities (Borsky et al., 2024). In contrast, lower-income residents are often concentrated in hotter areas characterized by high building density, limited green infrastructure, and reduced adaptive capacity. This climate-driven residential sorting deepens existing socioeconomic inequalities and further reduces the appeal and demand of already disadvantaged urban neighborhoods. As with other climate-related risks, the most vulnerable populations bear the greatest burden (Contat et al., 2024).

[7] See Contat et al. (2024) for a comprehensive overview of climate-related risks and definitions.

Beyond its human, social, and spatial implications, excessive heat also undermines the functionality of buildings and urban infrastructure, imposing significant financial costs on owners and users. Across all building types, changing climatic conditions degrade thermal performance, increase the risk of overheating, and raise cooling demand (Dodoo & Gustavsson, 2016). Rising energy consumption, already a major primary cost driver, is further compounded by pronounced peaks in electricity demand, which can disproportionately inflate operating expenses (Dirks et al., 2015). These peak load requirements also influence the selection and sizing of HVAC systems. Consequently, UHIs raise ongoing operational costs and drive capital expenditures for building design and system upgrades necessary to maintain indoor thermal comfort.

Figure 3.1 Drivers of UHI



Note: This figure illustrates how anthropogenic and environmental factors interact to shape UHI effects. Controllable variables, such as urban form, building design, and anthropogenic drivers, directly influence UHIs, whereas uncontrollable variables, such as atmospheric conditions and solar radiation, do not. The diagram also differentiates between daytime UHI effects (heat exposure) and nighttime UHI effects (heat retention). Source: Author's illustration based on Rizwan et al. (2008).

While UHI price effects are harder to quantify than direct property damage from acute climate risks such as floods, hurricanes, and wildfires, the loss of climate-related amenities represents a significant share of total climate-related damages (Sinha & Cropper, 2013). Risks associated with UHIs, such as deteriorating air quality, overburdened electricity and water infrastructure, and poor indoor climate conditions, can significantly affect housing prices at both the neighborhood and individual property levels.

Despite the far-reaching effects of UHIs, their economic impact on real estate markets remains underexplored. As Contat et al. (2024) emphasized, research on chronic climate risks such as UHIs is increasingly important given projected increases in extreme temperatures. The authors highlighted an urgent need for more granular data and analysis to understand how real estate markets respond to rising temperatures and shifting spatial patterns. Most existing studies focus on national- or state-level temperature effects, while city-level research remains limited. Studies that use cross-city comparisons or coarse spatial data often face difficulties in assessing UHI-related economic impacts at the neighborhood or individual property level.

This study addresses this critical research gap by estimating the effect of temperature deviations on local residential property prices using a generalized additive model (GAM). To our knowledge, this is the first study to apply granular, building-level temperature data to assess the economic impacts of UHIs within a single city. We incorporate temperatures at two times of the day: 4 a.m. to capture overnight heat retention (reduced cooling potential) and 1 p.m. to reflect daytime heat exposure. This allows us to analyze spatial heterogeneity based on proximity to the central business district (CBD) and urban green spaces, as well as temporal dynamics by tracking how UHI intensity evolves and influences return and risk parameters. We also account for socioeconomic conditions that shape neighborhood-level sensitivity to heat. This multidimensional approach offers a comprehensive understanding of how localized UHI effects influence urban housing markets.

Our results show that UHI intensity, measured twice daily at 4 a.m. and 1 p.m., has a negative effect on residential property prices. While the magnitude of the effect differs between daytime and nighttime measurements, the general pattern remains consistent. Cooler-than-average locations tend to command price premiums, whereas above-average UHI exposure results in price discounts. The effects vary spatially and are influenced by urban structure and amenities. Differences in heat resilience and exposure reveal varying market sensitivities between central and peripheral locations. Proximity to green spaces is a critical factor, shaping how thermal stress is reflected in property values. Similarly, household income correlates with differing sensitivity to UHI exposure, underscoring socioeconomic disparities in climate adaptation. Nighttime UHI intensity has the strongest and most persistent impact on long-term price appreciation and risk-adjusted returns, confirming the importance of overnight cooling for urban climate resilience. Overall, our findings suggest that the market prices UHI exposure as a property-specific climate risk, reflecting both its spatial variation and financial relevance.

The remainder of this paper is structured as follows. The next section reviews the relevant literature and situates our research within it. This is followed by a description of the data, variables, and summary statistics, as well as an outline of our research methodology. We then present the empirical results and robustness tests. The final section provides our conclusions.

3.3 Related Literature

As a bricks-and-mortar asset class, real estate is highly exposed to physical climate risks, some more visible than others. These risks fall into two broad categories: acute and chronic. Acute risks, such as floods or wildfires, have immediate and clearly visible impacts on real estate markets. Chronic risks, such as abnormal temperature effects, are typically less apparent and harder to quantify owing to data and measurement limitations.

This study builds on the existing literature examining the relationship between regional climate risk factors and housing markets. It contributes not only to a relatively underdeveloped strand of the literature on chronic risks, as noted by Contat et al. (2024), but, to the best of our knowledge, is also the first study in the field of heat-related hazards to rely on daily, property-level temperature data. This approach allows for more precise estimation and helps address potential heterogeneity concerns that may exist in earlier studies.

In addition, research on physical risks finds that price responses are shaped by general public beliefs and perceptions, which vary across regions, rather than capturing property-specific risk exposure (Sirmans et al., 2025). The data used in this study allow for a more precise investigation of localized risk exposure by disentangling it from broader regional climate or temperature perceptions. This, in turn, enables an assessment of whether heterogeneity in property values may be driven by actual exposure to high-temperature effects and, consequently, affect property-level financial outcomes, such as higher operating costs due to increased cooling demand.

The existing literature on physical climate risks has primarily focused on flood risks linked to natural disasters, such as hurricanes and climate-induced sea-level rise. Harrison et al. (2001) showed that residential properties in Florida experienced price discounts when located within 100-year floodplains, with these discounts increasing after the National Flood Insurance Reform Act of 1994. Similarly, Addoum et al. (2024) and Ortega and Taşpınar (2018) found that Hurricane Sandy led to a persistent decline in property values, both commercial and residential, in New York, even in areas largely unaffected by the

storm. More recently, Contat et al. (2025) confirmed this pattern for Hurricane Ian in Florida. This suggests that natural disasters can amplify perceived climate risk beyond directly impacted zones. After Hurricane Katrina, McKenzie and Levendis (2010) reported a significant price premium for New Orleans homes located in less flood-prone areas. Likewise, Tyndall (2023), using a sample of residential properties on Long Island, found that homes exposed to future sea-level rise face a 1% appreciation discount compared to non-exposed properties while also triggering demand spillover effects. Supporting this trend, Bernstein et al. (2019) estimated that flood-affected properties sell at a 7% discount. In addition to price effects, flood risk also affects the liquidity of residential properties. Using search theory, Turnbull et al. (2013) argued that focusing solely on values and prices may underestimate actual flood risk and emphasize the need to account for liquidity constraints in residential transactions. Beyond the equity side, where lower values, prices, and liquidity are observed, flood exposure also affects loan terms. Nguyen et al. (2022) found that lenders incorporate long-term sea-level rise risk into mortgage pricing, independent of short-term natural hazards or borrower characteristics at loan origination. Similarly, Duanmu et al. (2022) reported stronger risk pricing in counties with greater exposure to natural disasters, where lenders exhibit higher climate risk awareness. Despite this growing awareness in both equity and debt markets, Gourevitch et al. (2023) estimated, using a multivariate repeat-sales model, that US residential properties exposed to flood risk remain overvalued by approximately US$121–US$237 billion, with coastal properties and low-income households disproportionately affected.

Wildfires have gained greater attention in the climate risk literature owing to their rising frequency and severity in recent decades. Loomis (2004) was among the first to show that residential property values in areas spared by a significant wildfire declined by up to 15%, driven by both the loss of green space, which reduces amenity values, and heightened awareness of natural hazards. In areas affected by repeated wildfires, price declines can be even more severe, reaching up to 23% (Mueller et al., 2009). Using a difference-in-differences estimation, Götz et al. (2024) showed that banks apply a mortgage interest margin premium for properties near wildfire events, averaging 13 basis points and reaching up to 22 basis points for low-income borrowers. Rising awareness of wildfire risk also shifts homebuyers' preferences toward fire-resistant materials (Donovan et al., 2007). Baylis and Boomhower (2019) reported that most US federal and state wildfire mitigation funding goes toward protecting private homes, but noted that housing subsidies aimed at affordability can inadvertently encourage development in high-risk areas, undermining wildfire risk reduction efforts.

Sinha and Cropper (2013) suggested that climate-related risks extend beyond natural hazards that cause direct physical damage to buildings. Specifically, physical climate risks that affect climate amenities account for a substantial share of total climate-related damage in real estate markets. A prominent body of research demonstrates a positive relationship between amenity value and property prices, especially in relation to air quality (Chay & Greenstone, 2005; Choi et al., 2023; Cvijanović et al., 2024; Feng et al., 2024; Ridker & Henning, 1967; Zheng et al., 2014; Zhou et al., 2024). However, air quality is shaped not only by climatic factors, such as air pressure, humidity, solar radiation, temperature, and wind speed, but also by anthropogenic influences, including building energy use, industrial activity, and traffic. This interplay complicates efforts to isolate the portion of air quality effects directly attributable to climate change. Roback (1982) was among the first to show that climatic factors alone, such as cloud cover, heating degree days, or snowfall, can influence house prices.

Research increasingly suggests that abnormal temperatures, particularly extreme heat, pose risks to society and the economy comparable in magnitude to the more visible climate hazards highlighted in housing market studies, such as floods, hurricanes, or wildfires. Dell et al. (2012) and Dell et al. (2014) showed that temperature shocks influence a range of national-level socioeconomic factors, including conflict, political stability, and public health, as well as key macroeconomic indicators such as economic growth, industrial output, and labor productivity. Focusing on income effects, Dell et al. (2009) found that the negative relationship between temperature and economic performance holds across countries, within countries, and even at the state level. Beyond macroeconomic effects, Bansal et al. (2016) showed that systematic risk increases with long-term temperature variations, with the temperature-related risk premium for US equities nearly doubling over the past 80 years.

Despite this evidence, the literature linking temperature exposure to real estate outcomes remains relatively limited (Contat et al., 2024). Existing studies typically rely on cross-country or cross-regional comparisons conducted at coarse spatial units, such as metropolitan statistical areas (MSAs), counties, or census regions, and employ temporally aggregated temperature measures. Albouy et al. (2016) found that US households prefer an average temperature of 65°F (18.3°C) at the MSA level and are willing to pay higher housing costs for climate comfort, showing a stronger aversion to excessive heat than to extreme cold. These preferences vary depending on a region's adaptive capacity. While such approaches are well-suited to identifying differences in willingness to pay across broadly warmer or colder geographies, they provide only limited insight into localized temperature risks.

Analyzing temperature effects at the property level is therefore crucial. As highlighted in the literature (e.g., Oke, 1973, 1982; Stewart & Oke, 2012) and corroborated by the data used in this study, temperature effects vary substantially within cities owing to differences in land cover, building density, materials, and microclimatic conditions. Property-level temperature data allow researchers to distinguish between regional climate trends and localized high-temperature risks, improving identification and enabling a more accurate assessment of economic outcomes. Hence, asset-level estimates based on spatially or temporally coarse temperature data may mask economically meaningful heterogeneity across buildings.

Within the commercial real estate literature, Chiang et al. (2022) constructed quarterly temperature risk measures at the Core-Based Statistical Area level and documented a negative relationship between abnormal temperatures and commercial real estate (CRE) returns, attributing the effect primarily to increased environmental risk awareness rather than location-specific exposure. Using temperature data on 4km × 4km grids covering the continental US, Cvijanović and Van de Minne (2024) found a similar relationship. CRE asset-level returns are lower for properties located in extreme-temperature areas. Their results were primarily driven by the impact of extreme temperatures on sale prices and demand channels. At the firm level, Feng et al. (2025) showed that Real Estate Investment Trusts (REITs) with greater exposure to abnormal temperature changes at the county level experience declines in cash flows, firm value, and stock returns.

Related evidence also exists for the residential housing market. However, similar to the CRE literature, temperature exposure is typically measured at relatively coarse spatial scales. Klaiber et al. (2017) used 4km resolution temperature data for Phoenix, AZ, to estimate a hedonic price function and found that temperature mitigation efforts are capitalized into housing prices. They estimated a significant marginal willingness to pay $72 per month for each one-degree (F) reduction in outdoor temperatures. Li et al. (2018b) documented that higher temperatures reduce housing prices in Hong Kong, with stronger effects in highly urbanized areas. Using weather station data near major cities worldwide, Semenenko and Yoo (2019) identified an inverse relationship between residential real estate returns and daily temperature volatility. Ma and Yildirim (2023), combining weather station data with ZIP code level information, found that exposure to local heat shocks significantly reduces house prices but has no effect on rents, suggesting that price discounts reflect long-horizon climate risk beliefs. Using city-level monthly data for China, Chen et al. (2025) showed that heatwaves adversely affect macroeconomic conditions, leading to demand-side effects on housing prices.

3.4 Data and Methodology

3.4.1 Housing Data

To investigate UHI exposure at a highly granular level, this study focuses on Berlin (at the NUTS-3 level), Germany's capital, which provides an ideal housing market for examining UHI impacts relevant to other mid-latitude cities worldwide. With a population of 3.89 million, it is among the most densely populated areas in Europe. Several factors make Berlin particularly suited to this study, including its heat-absorbing building stock (Dugord et al., 2014), 70% land coverage (Umweltbundesamt, 2024), limited green space, and high levels of air pollution (European Environment Agency, 2024). Berlin also illustrates that even cities with a continental climate, typically associated with lower average temperatures, can experience significant UHI effects.

To capture long-term trends in both the residential property market and temperature development, the observation period spans 40 quarters from January 2014 to December 2023. The housing dataset is compiled from multiple data sources, including spatial data from OpenStreetMap[8], socioeconomic data from GfK[9] and real estate data from VALUE market data[10]. VALUE market data aggregates building-level data from over 100 listing platforms across Germany, enabling the collection of both continuous and categorical data, including prices and key hedonic characteristics. To ensure consistency in housing supply and demand perspectives, and to obtain a homogeneous sample, this study focuses exclusively on apartments, with valuation based on asking prices. In the German property market, especially in densely populated areas, asking prices generally align with final transaction prices, as negotiations are uncommon (Ahlfeldt et al., 2023; Kolbe et al., 2021).

The original dataset contains over 140 variables, including hedonic property characteristics, geographical points of interest (POI), and precise spatial coordinates (latitude and longitude). During data cleaning, observations with missing key variables were excluded, and extreme values were removed using upper-tail truncation at the 98th percentile across selected continuous variables (Huber, 1981). The final sample consists of 168,921 observations and 28 variables, enabling each property to be identified through a combination of hedonic and geographic attributes. Demographic data at the postal code level are also included to capture housing demand dynamics, as higher population density correlates with stronger demand (Glaeser & Gottlieb, 2006) and greater traffic intensity (Li

[8] See OpenStreetMap. (https://www.openstreetmap.org).
[9] See Growth from Knowledge (GfK). (https://www.gfk.com/home).
[10] See VALUE market data. (https://www.value-marktdaten.de).

et al., 2018a). Specific POI variables, such as proximity to the nearest park, are incorporated to assess the impact of green space on property values. Each property is georeferenced using longitude and latitude coordinates, allowing subsequent spatial matching to temperature data.

3.4.2 Urban Heat Island Data

The UHI effect describes the tendency of built-up areas to exhibit higher near-surface air temperatures than their rural surroundings (Oke, 1973). For the empirical implementation of this definition, temperature data is obtained from Meteoblue[11], offering citywide coverage of Berlin on a 30 m × 30 m grid from 2014 to 2023 and yielding more than 10 billion observations. The series measures near-surface air temperature (2 meters above ground).[12] Because near-surface air temperature better reflects human-perceived heat exposure, it is more relevant for assessing impacts on property prices.

This study follows the framework of Oke (1982) to capture both day- and nighttime heat dynamics. As summarized in Figure 3.1, direct solar radiation and the differential warming of surface materials generate sizeable daytime temperature differences - a direct measure of heat exposure. At night, these same factors cause buildings to retain stored heat and cool less efficiently than their surroundings. To capture these temperature differences and the resulting spatial UHI effects, air temperatures (°C) were recorded twice daily at 4 a.m. and 1 p.m. The selection of these two time points is based on existing literature (see, e.g., Arnfield, 2003; Oke, 2002; Voogt & Oke,2003).

Traditionally, UHI intensity is measured as the temperature difference between an urban site and a rural reference point outside the city (Oke, 1973). Within our analysis, UHI intensity is calculated as the relative difference between the local temperature for an asset i and the citywide minimum at time t.[13] Therefore, the Berlin-wide minimum temperature serves as the reference value for each timestamp (4 a.m. and 1 p.m.).

$$UHI_{it} = Temp_{it} - \min(Temp_t) \tag{3.1}$$

Two factors motivate our use of a within-city reference. First, the exceptionally high spatial resolution allows for a more localized and less biased estimation of UHI effects. Second,

[11] See Meteoblue. (https://content.meteoblue.com/de).
[12] Throughout this study, UHI intensity refers specifically to atmospheric UHI intensity, which captures near-surface air temperature differences relevant to human-perceived heat exposure.
[13] As a robustness check, we re-estimate our main specification using the traditional UHI definition following Oke (1973), which is based on rural reference locations. The resulting estimates are reported in the Robustness Check and in Appendix III.

relying on a single rural reference point can introduce selection bias: wind can carry urban heat into nearby rural areas, making the urban-rural transition gradual rather than abrupt (Oke, 1982). In addition, no aggregated rural temperature series with sufficient temporal resolution (4 a.m. and 1 p.m.) is available at the state or regional level, further justifying our approach.

After evaluating the UHI values, each temperature grid cell is spatially matched to the exact longitude and latitude coordinates of the property observations. This ensures that each property is assigned to its corresponding grid cell. In this way, high-resolution temperature data can be linked to each price observation, providing fine spatial granularity and enabling a more accurate representation than in previous studies.

3.4.3 Summary Statistics

Table 3.1 reports descriptive statistics for all variables used in the models,[14] covering observations from the entire year, including both winter and summer months. To reduce distortions caused by outliers and right-skewed distributions, the variables price, apartment size, and household income are log-transformed. Temperature variables at 4 a.m. and 1 p.m. are included to capture UHI intensity: UHI 4 a.m. and UHI 1 p.m.

UHI intensity ranges from 0.19°C (0.34°F) to 6.07°C (10.93°F) at night (4 a.m.) and from 0.29°C (0.52°F) to 6.75°C (12.15°F) during the day (1 p.m.). These distributions indicate that daytime urban heating is generally stronger and more spatially variable across neighborhoods. Nighttime UHI effects are also pronounced, with some hotspots remaining up to 6.07°C (10.93°F) warmer than the coolest area.

On average, UHI intensity measures 2.32°C (4.18°F) at 4 a.m. and intensifies to 2.87°C (5.17°F) at 1 p.m. These values correspond to mean absolute temperatures of 8.87°C (47.97°F) (4 a.m.) and 14.45°C (58.01°F) (1 p.m.), a pattern consistent with previous studies (Iodice et al., 2024). The contrast in minimum daily temperatures further reflects this dynamic, with -14.13°C (6.57°F) recorded at night compared to -10.91°C (12.36°F) during the day.

[14] A legend for the variable descriptions is provided in Appendix I, Table 3.8.

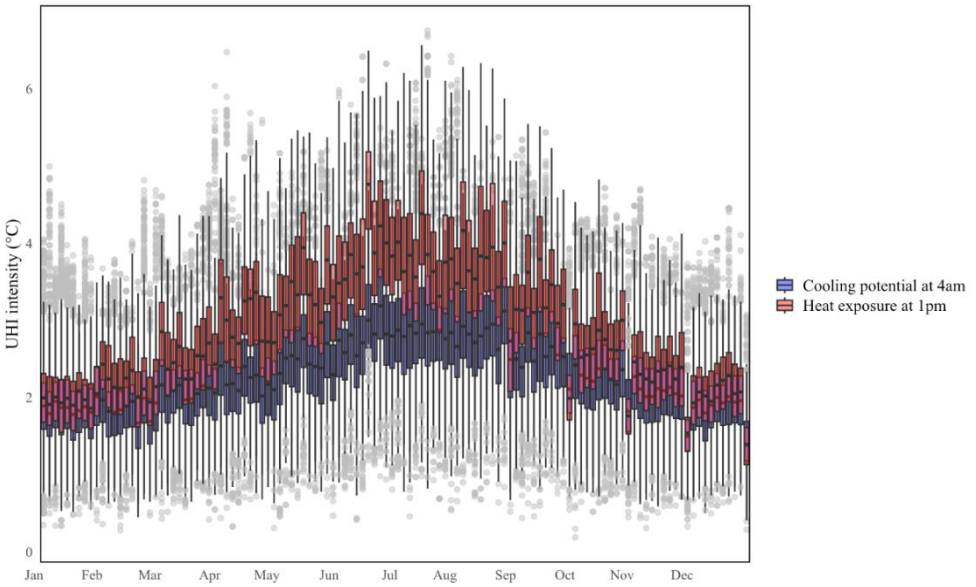
Table 3.1 Descriptive Statistics

Variable	Mean	Std. Dev.	Min	Q5	Median	Q95	Max
Price	358,917.73	243,891.17	16,500.00	95,000.00	292,000.00	869,000.00	1,440,000.00
Log price	12.58	0.66	9.71	11.46	12.59	13.68	14.18
Size	79.78	34.90	8.22	36.00	71.30	150.00	210.00
Log size	4.29	0.43	2.11	3.58	4.27	5.01	5.35
Rooms	2.66	1.08	1.00	1.00	2.50	5.00	6.00
Age	70.54	44.52	0.00	5.00	68.00	124.00	124.00
Floors	2.31	2.02	-1.00	0.00	2.00	5.00	48.00
Retrofitted	0.42	0.49	0.00	0.00	0.00	1.00	1.00
Kitchen	0.43	0.50	0.00	0.00	0.00	1.00	1.00
Parking	0.34	0.47	0.00	0.00	0.00	1.00	1.00
Balcony/ Terrace	0.78	0.41	0.00	0.00	1.00	1.00	1.00
First occupancy	0.24	0.43	0.00	0.00	0.00	1.00	1.00
School distance	0.30	0.19	0.00	0.07	0.26	0.69	1.20
Kindergarten distance	0.21	0.15	0.00	0.05	0.17	0.54	1.26
Restaurant distance	0.20	0.16	0.00	0.03	0.15	0.54	0.95
Supermarket distance	0.27	0.18	0.00	0.05	0.24	0.62	1.23
Kiosk distance	0.51	0.53	0.00	0.07	0.34	1.51	5.01
Park distance	0.27	0.17	0.00	0.07	0.24	0.58	1.38
Playground distance	0.20	0.14	0.00	0.05	0.17	0.49	0.80
CBD distance	7.41	4.23	0.02	1.87	6.85	14.98	26.45
Bus distance	0.18	0.11	0.00	0.03	0.15	0.39	0.65
Hospital distance	1.50	0.95	0.01	0.35	1.33	3.39	7.44
Longitude	13.38	0.09	13.09	13.24	13.37	13.54	13.67
Latitude	52.50	0.05	52.37	52.42	52.50	52.58	52.67
Income per household	37,372.91	5,884.88	26,473.78	29,547.39	36,268.72	48,586.89	70,799.97
Log income per household	10.52	0.15	10.18	10.29	10.50	10.79	11.17
Temp 4 a.m.	8.87	6.56	-14.13	-1.46	9.11	19.13	25.46
Temp 1 p.m.	14.45	8.51	-10.91	1.47	14.28	28.24	38.62
UHI 4 a.m.	2.32	0.70	0.19	1.26	2.27	3.55	6.07
UHI 1 p.m.	2.87	0.97	0.29	1.46	2.75	4.62	6.75

Note: This table summarizes descriptive statistics for the variables used in this analysis, covering the entire observation period. For each variable, the mean, standard deviation (Std.Dev.), minimum (Min.), 5th percentile (Q5), median, 95th percentile (Q95), and maximum (Max.) are reported. To reduce the influence of extreme values, outliers are removed by truncating the upper tail at the 98th percentile for the selected continuous variables.

Figure 3.2 shows the development of the UHI effect across the observation period at monthly intervals. Consistent and systematic differences between daytime and nighttime temperatures are evident, highlighting the seasonality of the UHI effect. UHI intensity increases during warmer months, as indicated by higher quartile values and greater variance in temperature differences. These results align with Xi et al. (2024), who reported that both the distributions and intensities of UHI effects peak in summer. Quantile distributions also show a broader spread of temperatures at 1 p.m. compared to 4 a.m. during these months. Seasonal fluctuations are reflected in the average UHI intensity, with the difference between 1 p.m. and 4 a.m. being larger in summer than in winter. The cooling potential of locations is more pronounced in summer, particularly in areas less affected by UHI dynamics. In contrast, UHI effects are lower in winter across all statistical measures (quantiles, means, and variances), indicating more uniform and stable urban temperature patterns.

Figure 3.2 Boxplot of UHI Intensity across the Sample Period



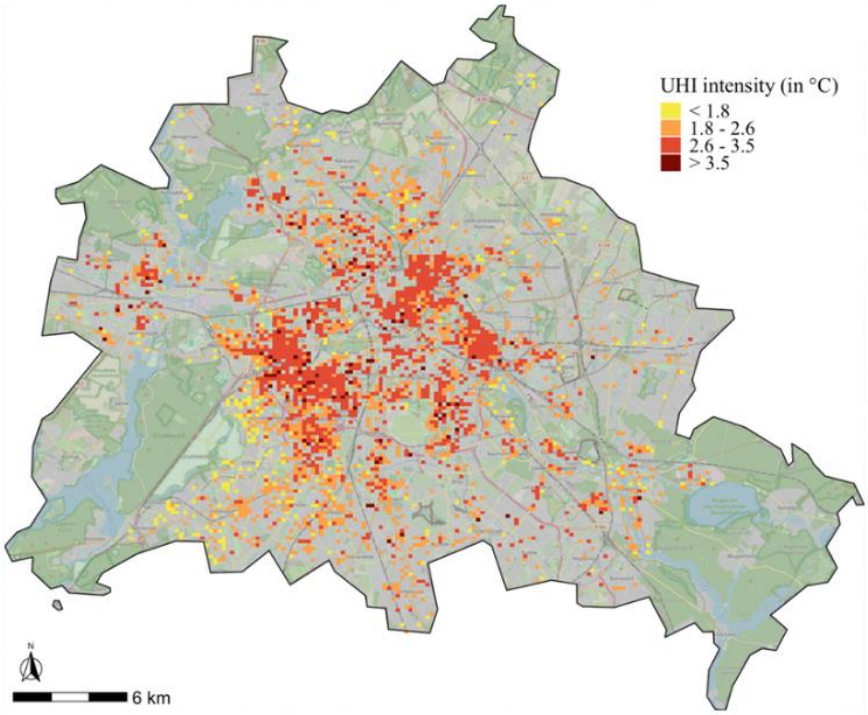
Note: This figure illustrates the distribution of UHI intensity measured at 4 a.m. and 1 p.m. across monthly intervals from 2014 to 2023. The boxplots show temperature differences relative to the minimum temperature for each timeframe, with red representing 1 p.m. (daytime) values and blue representing 4 a.m. (nighttime) values. Grey dots indicate statistical outliers. All temperatures are reported in degrees Celsius (°C).

Figures 3.3 and 3.4 show the temporal and spatial distribution of temperature deviations during the summer months (April–September) of 2014–2016 and 2020–2023. Pronounced UHI effects are evident: intensities peak in the inner city, while suburban and rural zones remain comparatively cooler, consistent with the urban-rural heat gradient described by Oke (1982). Beyond differences between urban and non-urban areas, the figures reveal substantial intra-city variations. These localized temperature differences reflect Berlin's

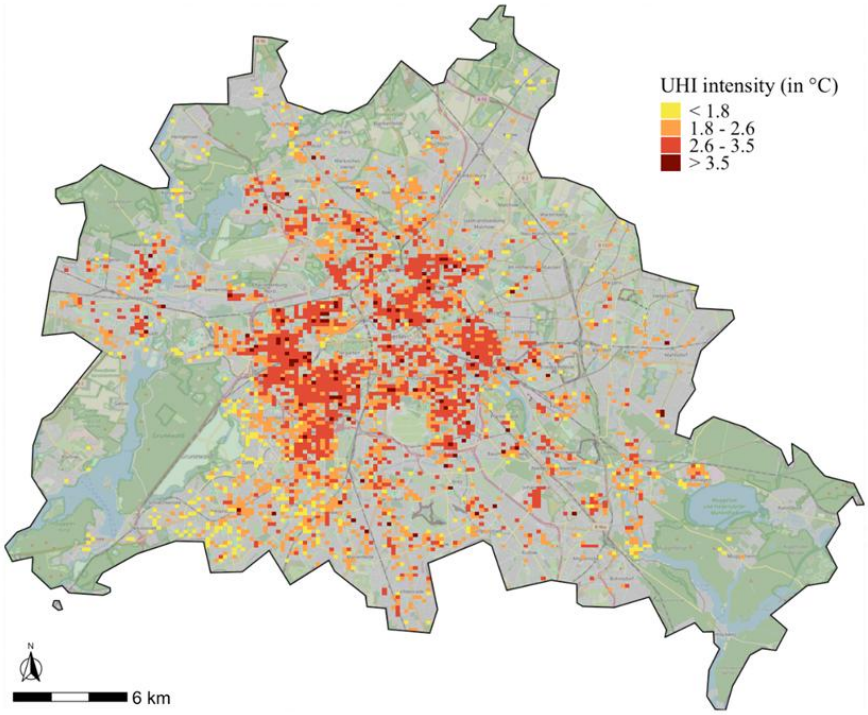
polycentric structure and variations in heat accumulation at both district and individual building levels.

Figure 3.3 Maps of the UHI Intensity at 4 a.m. across Berlin over Time

(a) 2014-2016



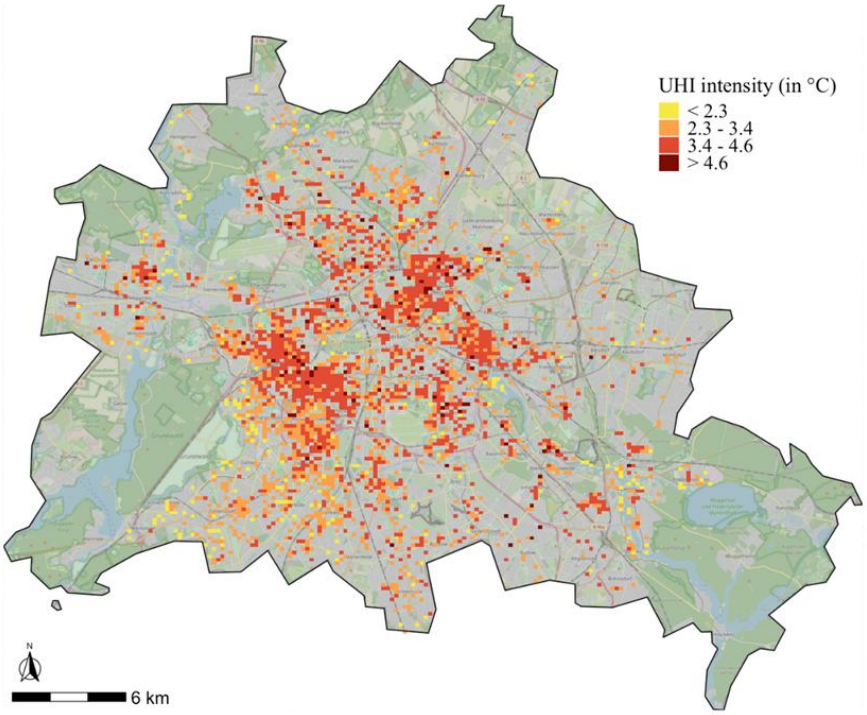
(b) 2020-2023



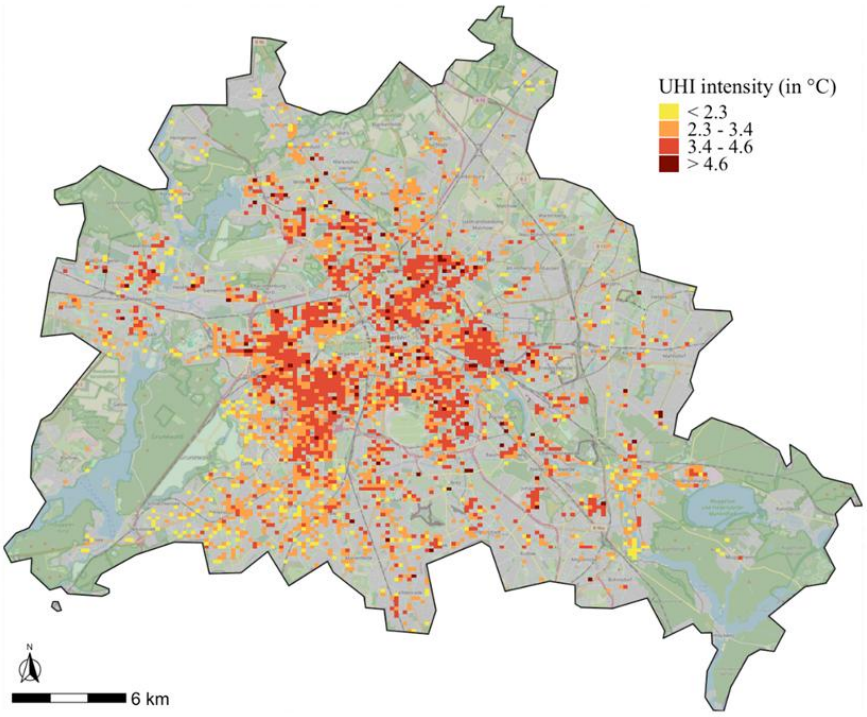
Note: These figures illustrate the spatial distribution of UHI intensity at 4 a.m., with Figure (a) covering 2014–2016 and Figure (b) covering 2020–2023. Each grid cell represents temperature differences (°C) relative to the minimum observed temperature. The legend shows values in degrees Celsius, ranging from 1.2 °C to 4.2 °C, with colors transitioning from yellow (lower differences) through orange (medium) to red (higher differences).

Figure 3.4 Maps of the UHI Intensity at 1 p.m. across Berlin over Time

(a) 2014-2016



(b) 2020-2023



Note: These figures illustrate the spatial distribution of UHI intensity at 1 p.m., with Figure (a) covering 2014–2016 and Figure (b) covering 2020–2023. Each grid cell represents temperature differences (°C) relative to the minimum observed temperature. The legend shows values in degrees Celsius, ranging from 1.6°C to 5.3°C, with colors transitioning from yellow (lower differences) through orange (medium) to red (higher differences).

At 4 a.m., the spatial distribution of temperatures shows UHI effects of up to 4°C (7.2°F), particularly in central districts and densely built-up areas. The city center retains considerable heat owing to extensive sealed surfaces, resulting in a pronounced nighttime cooling gradient, with suburban areas benefiting most from lower nighttime temperatures.

During the day, UHI intensity increases across the city, reaching up to 5°C (9.0°F) in the inner city. Suburban and rural areas continue to experience lower heat intensity, while densely urbanized zones show persistent, highly concentrated hotspots extending outward from central Berlin. These broader daytime spatial extents are driven by direct solar radiation and anthropogenic heat emissions. The historical comparison also indicates an increase in UHI intensity over time, highlighting the growing importance of urban climate effects in assessing microclimatic location qualities.

3.5 Research Methodologies

As a first step, we establish a benchmark model using Ordinary Least Squares (OLS) regression, a common approach in studies of climate risks and real estate prices (Harrison et al., 2001; Li et al., 2018b; Loomis, 2004; Ortega & Taşpınar, 2018). Despite its widespread use, prior research indicates that the relationship between dependent and independent variables should not be universally assumed to be linear (Conroy & Milosch, 2011; McKenzie & Levendis, 2010). OLS can fail to capture the complex, nonlinear relationships characteristic of climate-related risk. Specifically, the assumption of constant marginal effects implies that temperature changes are assumed to affect outcomes uniformly across all exposure levels, thereby obscuring potential threshold effects or nonlinear sensitivities (Schlenker & Roberts, 2008). Furthermore, Cragg and Kahn (1997) suggested that traditional hedonic pricing models may underestimate the value households place on climate stability and reduced annual temperature variability. This flexibility is particularly relevant in the context of UHI effects, as the relationship between climatic factors and real estate prices is unlikely to be linear, and may exhibit thresholds where price reductions increase disproportionately at higher heat intensities.

Introduced by Hastie and Tibshirani (1986), the generalized additive model (GAM) is a semi-parametric approach that incorporates penalized smooth terms, allowing covariates to follow flexible nonlinear functional forms. By relaxing the linearity assumption, GAMs can improve model fit and predictive performance and identify nonlinear sensitivities and threshold effects that are masked by OLS specifications. GAMs have become increasingly

popular in real estate price forecasting (Bin, 2004). These models combine parametric linear components with nonparametric smooth functions: some covariate effects enter linearly, implying constant marginal effects interpretable in an OLS framework, while nonlinear effects are captured by smooth functions whose marginal effects vary with the covariate level. Accordingly, interpretation is inherently functional and relies on smooth effect plots rather than single point estimates.

$$log(P_{ijt}) = X_{ijt}\beta + Z_{jt}\delta + \mu_t\theta + f(\widetilde{UHI}_{it}) + f(\tilde{X}_{ijt}) + \varepsilon_{ijt} \quad (3.2)$$

Equation (3.2) estimates the property price P for an asset i at time t. Determinants are structured as follows: location-specific covariates Z_{jt} capture spatial effects and help mitigate unobserved serial error, with j indexing the postal code. Time fixed effects are included via monthly dummies (μ_t) for the listing period. Property attributes, including both continuous and binary hedonic characteristics, are represented by the matrix X_{ijt}. Nonlinear effects enter via splines $f(\tilde{X}_{ijt})$, allowing associations between structural characteristics, such as floor area, number of rooms, building age, and price. Nonlinear transformations of POIs further allow spatial effects to vary flexibly with proximity, and spatial heterogeneity is additionally captured by a bivariate smoothing term $s(longitude, latitude)$, which accounts for residual effects and reduces distortions from unobserved neighborhood characteristics and spatial autocorrelation[15] . The error term ε_{ijt} captures unexplained variation, and β, δ, and θ denote the vectors of estimated coefficients. The UHI variable $f(\widetilde{UHI}_{it})$ enters the model as a nonlinear component, allowing the relationship between heat stress and property prices to vary across the distribution of temperature differences rather than assuming a constant marginal effect. To assess diurnal variations in UHI effects, two distinct specifications are estimated: one capturing nighttime heat retention ($UHI\ 4\ a.m.$) and one capturing daytime heat exposure ($UHI\ 1\ p.m.$). Both specifications include the same covariates, nonlinear terms, and spatial controls, differing only in the temperature regressor $\widetilde{UHI}_{it}$.

Thin plate regression splines are used to model nonlinear relationships flexibly without requiring explicit knot placement. For interpretation, the effective degrees of freedom (EDF) summarize the structural complexity of each smooth term after penalization: an EDF near one indicates an approximately linear relationship, while higher EDF values indicate more flexible, nonlinear functions. The F-statistics tests the null hypothesis that a smooth

[15] The GAM framework captures spatial heterogeneity through smooth location functions while simultaneously allowing nonlinear covariate effects, unlike spatial lag or spatial error models that explicitly model dependence through spatial weight matrices.

term does not explain variation in the response beyond a constant effect, evaluating whether the predictor contributes meaningfully to the model once penalization is accounted for.[16]

Building on this specification, additional models extend the baseline GAM regression by introducing interaction terms of the form $f\left(\widetilde{UHI}_{it} x\, Z_{ij,t}\right)$ to assess spatial, socioeconomic, and temporal price sensitivities.[17] Models 2 and 3 incorporate spatial variables, with $Z_{ij,t}$ defined as $CBD\ distance$ and $park\ distance$, respectively. This captures price sensitivities to heat stress across central, medium, and peripheral locations, serving as proxies for urban morphology and density, while also evaluating potential mitigating or amplifying effects of green infrastructure. Tensor product splines are used to flexibly model interactions between variables on different scales, such as temperature and distance, allowing marginal temperature effects to vary spatially without imposing restrictive linear interaction structures and capturing complex, context-dependent response patterns. Model 4 focuses on socioeconomic heterogeneity by defining $Z_{ij,t}$ as $household\ income$ terciles. Estimating income-specific sensitivities highlights how variation in adaptability, housing quality, and neighborhood characteristics leads to heterogeneous price responses to temperature fluctuations. Because the interacting variables are categorical, and the specification includes quantile groups and monthly effects, these groups are modeled as discrete segments with price effects estimated independently. Model 5 defines $Z_{ij,t}$ as a vector of $monthly\ dummies$ to capture seasonal heterogeneity, reflecting differences in thermal comfort throughout the year. The resulting interaction between UHI intensity and monthly indicators is used to identify and quantify time-varying price effects associated with temperature dynamics. To evaluate the economic implications of UHI intensity, we compute several Key Performance Indicators (KPIs) based on Model 5.[18] These include total and average price growth through the cumulative growth rate (G_{cum}) and average annual year-on-year (YoY) growth (μ_g), short-term volatility as a market risk indicator (σ_g), long-term annualized growth via the compound annual growth rate ($CAGR$), and risk-adjusted performance through the return-to-risk ratio (R_g) This framework enables consistent comparisons of return and risk profiles across UHI intensity levels using standard measures.

All model specifications and subsequent effect calculations are estimated separately for the 4 a.m. and 1 p.m. temperature measures. This allows a direct comparison of nighttime

[16] Higher F-values indicate stronger evidence that the smooth term is relevant, whereas low values suggest limited explanatory power after penalization.
[17] Seasonal effects are tested in a robustness check by re-estimating Model 1 using filtered datasets for summer and winter months.
[18] Further methodological details are provided in Appendix II.

and daytime UHI pricing effects while holding other factors constant. Separate estimation is necessary because the two measures are strongly collinear.

3.6 Results

Following the methodology, the OLS models initially serve as a reference and plausibility check. Tables 3.2 and 3.3 show significant relationships between UHI intensity and property prices. With an adjusted R^2 of 0.851, the linear specifications demonstrate solid estimation accuracy. However, GAM estimates are then employed to capture nonlinear structures more flexibly. Tables 3.4 and 3.5 present the corresponding GAM results for 4 a.m. and 1 p.m., respectively. The base model (Model 1) already achieves an adjusted R^2 of 0.888. Extended specifications with added interaction terms show similar adjusted R^2 values, indicating stable model quality. The interaction terms are therefore intended to identify heterogeneous effects rather than improve overall model fit. This is further supported by the comparison of error measures, which are similar across models and reflect comparable predictive performance (see Tables 3.6(a) and 6(b)). The tables also contrast OLS and GAM specifications, highlighting the added value of the semi-parametric approach: GAM models not only achieve higher estimation accuracy but also lower error values.

Table 3.2 OLS Results for 4 a.m. UHI Intensity

Variable	Model 1		Model 2		Model 3		Model 4		Model 5	
	Est.	**SE**	**Est.**	**SE**	**Est.**	**SE**	**Est.**	**SE**	**Est.**	**SE**
(Intercept)	514.996***	98.259	10.947	99.298	518.873***	98.352	766.651***	98.370	522.749***	98.379
Log size	1.154***	0.003	1.152***	0.003	1.154***	0.003	1.156***	0.003	1.154***	0.003
Rooms	-0.016***	0.001	-0.015***	0.001	-0.016***	0.001	-0.016***	0.001	-0.016***	0.001
Age	-0.000***	0.000	-0.000***	0.000	-0.000***	0.000	-0.000***	0.000	-0.000***	0.000
Floors	0.014***	0.000	0.014***	0.000	0.014***	0.000	0.014***	0.000	0.014***	0.000
Kitchen	0.061***	0.001	0.061***	0.001	0.061***	0.001	0.061***	0.001	0.061***	0.001
Balcony/Terrace	0.025***	0.002	0.025***	0.002	0.025***	0.002	0.026***	0.002	0.024***	0.002
Parking	0.044***	0.002	0.044***	0.002	0.044***	0.002	0.045***	0.002	0.044***	0.002
Retrofitted	0.016***	0.001	0.015***	0.001	0.016***	0.001	0.016***	0.001	0.016***	0.001
First occupancy	0.351***	0.002	0.352***	0.002	0.351***	0.002	0.349***	0.002	0.350***	0.002
School distance	0.006	0.004	0.005	0.004	0.006	0.004	0.004	0.004	0.006	0.004
Kindergarten distance	0.005	0.005	0.000	0.005	0.005	0.005	0.019***	0.005	0.005	0.005
Restaurant distance	-0.270***	0.005	-0.272***	0.005	-0.270***	0.005	-0.272***	0.005	-0.269***	0.005
Supermarket distance	0.029***	0.004	0.023***	0.004	0.029***	0.004	0.025***	0.004	0.030***	0.004
Kiosk distance	-0.032***	0.002	-0.031***	0.002	-0.032***	0.002	-0.031***	0.002	-0.032***	0.002
Park distance	-0.072***	0.004	-0.072***	0.004	-0.082***	0.012	-0.076***	0.004	-0.072***	0.004
Playground distance	0.038***	0.005	0.031***	0.005	0.038***	0.005	0.061***	0.005	0.039***	0.005
CBD distance	-0.042***	0.000	-0.027***	0.001	-0.042***	0.000	-0.041***	0.000	-0.042***	0.000
Bus distance	0.073***	0.006	0.072***	0.006	0.073***	0.006	0.080***	0.006	0.073***	0.006
Hospital distance	-0.013***	0.001	-0.014***	0.001	-0.013***	0.001	-0.010***	0.001	-0.013***	0.001
Latitude	-9.587***	1.872	0.013	1.892	-9.661***	1.874	-14.283***	1.874	-9.736***	1.874
Longitude	-32.555***	7.357	5.118	7.434	-32.846***	7.364	-51.210***	7.366	-33.157***	7.366
Latitude × Longitude	0.606***	0.140	-0.111	0.142	0.612***	0.140	0.962***	0.140	0.618***	0.140
Log income per HH	0.525***	0.006	0.513***	0.006	0.525***	0.006			0.528***	0.006
UHI 4 a.m.	0.011***	0.001	0.062***	0.002	0.010***	0.002	0.029***	0.002	0.025*	0.010
Month/Year FE	yes		yes		yes		yes		yes	
UHI 4am × CBD dist.			yes							
UHI 4am × Park dist.					yes					
UHI 4am × HH income							yes			
UHI 4am × Month									yes	
Adj. R^2	0.851		0.852		0.851		0.851		0.851	
Deviance explained (%)	85.1		85.2		85.1		85.1		85.1	
AIC	17,220.3		16,249.6		17,221.4		17,547.7		17,103.4	
N	168,921		168,921		168,921		168,921		168,921	

Note: This table reports results from linear regression models across five alternative specifications. The top panel presents coefficient estimates (Est.), standard errors (SE), and corresponding p-values. All models include monthly fixed effects and spatial controls based on latitude and longitude. Interaction rows indicate whether the respective interaction term is included, showing "Yes" when applicable. Model 1 is the baseline with s(UHI 4 a.m.); Model 2 includes te(UHI 4 a.m., CBD distance); Model 3 includes the tensor product te(UHI 4 a.m., Park distance); Model 4 adds UHI × Household income quantile; and Model 5 adds the parametric interaction UHI × Month. The bottom panel reports goodness-of-fit measures, including adjusted R^2, deviance explained (in %), Akaike Information Criterion (AIC), and sample size N . Statistical significance is denoted as *** $p < 0.001$, ** $p < 0.01$, * $p < 0.05$, and . $p < 0.1$. Variance inflation factors (VIFs) were examined for all covariates, indicating no evidence of critical multicollinearity.

Table 3.3 OLS Results for 1 p.m. UHI intensity

Variable	Model 1		Model 2		Model 3		Model 4		Model 5	
	Est.	**SE**	**Est.**	**SE**	**Est.**	**SE**	**Est.**	**SE**	**Est.**	**SE**
(Intercept)	408.012***	97.991	36.705	98.776	410.278***	98.062	707.852***	98.099	415.734***	98.158
Log size	1.154***	0.003	1.153***	0.003	1.154***	0.003	1.157***	0.003	1.154***	0.003
Rooms	-0.016***	0.001	-0.015***	0.001	-0.016***	0.001	-0.016***	0.001	-0.016***	0.001
Age	-0.000***	0.000	-0.000***	0.000	-0.000***	0.000	-0.000***	0.000	-0.000***	0.000
Floors	0.014***	0.000	0.014***	0.000	0.014***	0.000	0.014***	0.000	0.014***	0.000
Kitchen	0.061***	0.001	0.061***	0.001	0.061***	0.001	0.061***	0.001	0.061***	0.001
Balcony/Terrace	0.024***	0.002	0.025***	0.002	0.024***	0.002	0.026***	0.002	0.024***	0.002
Parking	0.044***	0.002	0.044***	0.002	0.044***	0.002	0.045***	0.002	0.044***	0.002
Retrofitted	0.015***	0.001	0.015***	0.001	0.015***	0.001	0.016***	0.001	0.016***	0.001
First occupancy	0.351***	0.002	0.352***	0.002	0.351***	0.002	0.350***	0.002	0.351***	0.002
School distance	0.004	0.004	0.004	0.004	0.004	0.004	0.002	0.004	0.004	0.004
Kindergarten distance	0.006	0.005	0.003	0.005	0.007	0.005	0.021***	0.005	0.006	0.005
Restaurant distance	-0.276***	0.005	-0.277***	0.005	-0.276***	0.005	-0.278***	0.005	-0.275***	0.005
Supermarket distance	0.022***	0.004	0.019***	0.004	0.022***	0.004	0.018***	0.004	0.023***	0.004
Kiosk distance	-0.033***	0.002	-0.033***	0.002	-0.033***	0.002	-0.032***	0.002	-0.033***	0.002
Park distance	-0.068***	0.004	-0.067***	0.004	-0.074***	0.011	-0.072***	0.004	-0.068***	0.004
Playground distance	0.037***	0.005	0.033***	0.005	0.037***	0.005	0.061***	0.005	0.037***	0.005
CBD distance	-0.043***	0.000	-0.031***	0.000	-0.043***	0.000	-0.041***	0.000	-0.043***	0.000
Bus distance	0.071***	0.006	0.069***	0.006	0.071***	0.006	0.077***	0.006	0.071***	0.006
Hospital distance	-0.013***	0.001	-0.013***	0.001	-0.013***	0.001	-0.010***	0.001	-0.013***	0.001
Latitude	-7.546***	1.867	-0.474	1.882	-7.589***	1.868	-13.160***	1.869	-7.695***	1.870
Longitude	-24.515***	7.336	3.245	7.395	-24.685***	7.342	-46.809***	7.345	-25.111***	7.349
Latitude × Longitude	0.453**	0.140	-0.076	0.141	0.456**	0.140	0.878***	0.140	0.464***	0.140
Log income per HH	0.521***	0.006	0.515***	0.006	0.521***	0.006			0.523***	0.006
UHI 1 p.m.	-0.001	0.001	0.030***	0.002	-0.002	0.001	0.007***	0.001	0.014	0.010
Month/Year FE	yes		yes		yes		yes		yes	
UHI 1pm × CBD dist.			yes							
UHI 1pm × Park dist.					yes					
UHI 1pm × HH income							yes			
UHI 1pm × Month									yes	
Adj. R^2		0.851		0.851		0.851		0.850		0.851
Deviance explained (%)		85.1		85.1		85.1		85.0		85.1
AIC		17,302.0		16,596.1		17,303.7		17,883.5		17,182.8
N		168,921		168,921		168,921		168,921		168,921

Note: This table reports results from linear regression models across five alternative specifications. The top panel presents coefficient estimates (Est.), standard errors (SE), and corresponding p-values. All models include monthly fixed effects and spatial controls based on latitude and longitude. Interaction rows indicate whether the respective interaction term is included, showing "Yes" when applicable. Model 1 is the baseline with s(UHI 1 p.m.); Model 2 includes te(UHI 1 p.m., CBD distance); Model 3 includes the tensor product te(UHI 1 p.m., Park distance); Model 4 adds UHI × Household income quantile; and Model 5 adds the parametric interaction UHI × Month. The bottom panel reports goodness-of-fit measures, including adjusted R^2, deviance explained (in %), Akaike Information Criterion (AIC), and sample size N . Statistical significance is denoted as *** $p < 0.001$, ** $p < 0.01$, * $p < 0.05$, and . $p < 0.1$. Variance inflation factors (VIFs) were examined for all covariates, indicating no evidence of critical multicollinearity.

Table 3.4 GAM results for 4 a.m. UHI intensity

Variable	Model 1		Model 2		Model 3		Model 4		Model 5	
	Est.	**SE**	**Est.**	**SE**	**Est.**	**SE**	**Est.**	**SE**	**Est.**	**S**
midrule (Intercept)	11.948***	0.005	11.948***	0.005	11.948***	0.005	4.676***	0.003	11.404***	0.017
Floors	0.013***	0.000	0.013***	0.000	0.013***	0.000	0.013***	0.000	0.013***	0.000
Kitchen	0.063***	0.001	0.063***	0.001	0.063***	0.001	0.063***	0.001	0.063***	0.001
Balcony/Terrace	0.050***	0.001	0.050***	0.001	0.050***	0.001	0.050***	0.001	0.050***	0.001
Parking	0.045***	0.001	0.045***	0.001	0.045***	0.001	0.044***	0.001	0.044***	0.001
Retrofitted	0.064***	0.001	0.064***	0.001	0.064***	0.001	0.065***	0.001	0.064***	0.001
First occupancy	0.199***	0.002	0.199***	0.002	0.199***	0.002	0.198***	0.002	0.199***	0.002
Month/Year FE	yes		yes		yes		yes		yes	
Smooth terms	**edf**	**F-stat.**	**edf**	**F-stat.**	**edf**	**F-stat.**	**edf**	**F-stat.**	**edf**	**F-stat.**
Log size	8.593***	18416.005	8.602***	18395.004	8.582***	18406.786	8.531***	18392.490	8.608***	18373.765
Rooms	8.926***	56.096	8.929***	55.792	8.956***	56.014	8.935***	55.802	8.935***	56.125
Age	8.912***	1932.648	8.922***	1927.479	8.922***	1934.830	8.921***	1940.057	8.925***	1928.939
School distance	8.912***	29.653	8.917***	28.347	8.919***	29.970	8.933***	33.544	8.921***	28.901
Kindergarten distance	8.794***	30.224	8.804***	30.410	8.777***	29.954	8.789***	30.914	8.810***	29.747
Restaurant distance	8.695***	42.882	8.665***	42.771	8.666***	42.759	8.706***	48.390	8.672***	41.776
Supermarket distance	8.753***	21.579	8.731***	20.770	8.773***	21.942	8.735***	23.209	8.794***	21.221
Kiosk distance	7.739***	15.802	7.880***	16.463	7.438***	16.086	8.038***	14.492	8.032***	14.701
Park distance	8.751***	25.605	8.659***	24.174	8.650***	11.976	8.702***	26.550	8.752***	24.377
Playground distance	8.952***	16.172	8.843***	14.530	8.944***	16.827	8.849***	18.520	8.944***	15.898
CBD distance	8.901***	99.417	9.000***	64.022	8.912***	100.184	8.913***	105.352	8.911***	97.103
Bus distance	8.712***	11.617	8.655***	12.640	8.657***	11.408	8.730***	13.024	8.747***	11.422
Hospital distance	8.952***	20.350	8.952***	20.044	8.961***	20.469	8.959***	22.528	8.961***	21.418
Latitude, Longitude	28.954***	1258.936	28.840***	1223.671	28.965***	1254.561	28.996***	1249.582	28.957***	1248.592
Log income per HH	8.684***	108.467	8.625***	110.954	8.708***	109.781			8.706***	115.678
UHI 4 a.m.	6.688***	7.308	6.269†	1.954	5.731	0.904	5.769***	433429.118	7.422***	4131.084
UHI 4am, CBD dist.			8.602***	18395.004						
UHI 4am, Park dist.					8.582***	18406.786				
UHI 4am × HH income							yes			
UHI 4am × YYYYMM									yes	
Model fit										
Adj. R^2		0.888		0.888		0.888		0.888		0.888
Deviance explained (%)		88.8		88.8		88.8		88.8		88.9
N		168,921		168,921		168,921		168,921		168,921

Note: This table reports GAM estimates for log (Price) across five alternative model specifications. The top panel lists parametric terms with coefficients (Est.), standard errors (SE), and p-values (p). The middle panel reports smooth terms, showing effective degrees of freedom (EDF), the approximate F-statistic, and p-values for joint nonlinearity tests. A two–dimensional spatial surface s(Latitude, Longitude) captures unobserved spatial variation, while distances to amenities (POIs) enter as smooths to allow for nonlinear effects. Monthly dummies (YYYYMM) capture time-fixed effects. Interaction rows are ordered to mirror the model sequence and indicate "yes" when the term is included. Model 1 is the baseline with s(UHI 4 a.m.); Model 2 adds te(UHI 4 a.m., CBD distance); Model 3 includes te(UHI 4 a.m., Park distance); Model 4 adds UHI × Household income quantile; and Model 5 adds the parametric interaction UHI × Month. The bottom panel summarizes fit measures: adjusted R2, deviance explained (in %), Akaike Information Criterion (AIC), and sample size N . Significance levels are: *** p < 0.001, ** p < 0.01, * p < 0.05, . p < 0.1. Concurvity diagnostics were assessed for all models. Although high values are mechanically expected with flexible spatial smooths, the key coefficients and functional forms remained stable, indicating no substantive concurvity concerns. Sensitivity analyses excluding either the spatial smooth or CBD distance confirmed the robustness of the findings.

Table 3.5 GAM Results for 1 p.m. UHI Intensity

Variable	Model 1		Model 2		Model 3		Model 4		Model 5	
	Est.	**SE**	**Est.**	**SE**	**Est.**	**SE**	**Est.**	**SE**	**Est.**	**SE**
midrule (Intercept)	11.944***	0.005	11.944***	0.005	11.944***	0.005	3.853***	0.002	11.149***	0.017
Floors	0.013***	0.000	0.013***	0.000	0.013***	0.000	0.013***	0.000	0.013***	0.000
Kitchen	0.063***	0.001	0.063***	0.001	0.063***	0.001	0.063***	0.001	0.063***	0.001
Balcony/Terrace	0.050***	0.001	0.050***	0.001	0.050***	0.001	0.050***	0.001	0.050***	0.001
Parking	0.045***	0.001	0.045***	0.001	0.045***	0.001	0.044***	0.001	0.044***	0.001
Retrofitted	0.064***	0.001	0.064***	0.001	0.065***	0.001	0.065***	0.001	0.064***	0.001
First occupancy	0.199***	0.002	0.199***	0.002	0.199***	0.002	0.198***	0.002	0.199***	0.002
Month/Year FE	yes		yes		yes		yes		yes	
Smooth terms	**edf**	**F-stat.**	**edf**	**F-stat.**	**edf**	**F-stat.**	**edf**	**F-stat.**	**edf**	**F-stat.**
Log size	8.591***	18420.752	8.601***	18398.576	8.593***	18402.529	8.573***	18380.670	8.622***	18392.327
Rooms	8.939***	56.214	8.925***	55.976	8.933***	56.052	8.930***	55.954	8.936***	56.661
Age	8.928***	1932.334	8.913***	1927.019	8.920***	1934.933	8.927***	1939.612	8.926***	1926.527
School distance	8.925***	29.388	8.913***	27.882	8.915***	29.703	8.926***	33.180	8.921***	28.728
Kindergarten distance	8.802***	30.116	8.797***	30.209	8.787***	29.492	8.769***	30.691	8.783***	28.611
Restaurant distance	8.693***	42.658	8.673***	42.852	8.684***	42.450	8.696***	47.864	8.697***	42.190
Supermarket distance	8.783***	21.617	8.737***	20.841	8.760***	21.585	8.725***	22.915	8.781***	21.315
Kiosk distance	7.628***	15.881	7.845***	16.509	7.478***	15.929	8.059***	14.722	7.690***	15.155
Park distance	8.768***	25.597	8.675***	23.904	8.999***	18.090	8.690***	26.978	8.765***	24.330
Playground distance	8.945***	16.355	8.845***	14.805	8.828***	17.022	8.816***	18.666	8.944***	15.855
CBD distance	8.917***	100.237	9.000***	64.550	8.905***	100.421	8.917***	106.515	8.909***	99.377
Bus distance	8.720***	11.615	8.645***	12.896	8.678***	11.812	8.731***	13.156	8.729***	11.293
Hospital distance	8.964***	20.699	8.952***	20.253	8.959***	20.814	8.991***	22.947	8.963***	21.397
Latitude, Longitude	28.965***	1261.967	28.882***	1241.486	28.966***	1248.960	28.997***	1256.281	28.958***	1245.861
Log income per HH	8.696***	108.369	8.639***	110.823	8.691***	108.730			8.691***	111.746
UHI 1 p.m.	3.262***	16.676	4.111	0.418	1.000***	13.655	2.812***	1112753.086	4.563***	9854.763
UHI 1pm, CBD dist.			8.601***	18398.576						
UHI 1pm, Park dist.					8.593***	18402.529				
UHI 1pm × HH income							yes			
UHI 1pm × YYYYMM									yes	
Model fit										
Adj. R^2		0.888		0.888		0.888		0.888		0.888
Deviance explained (%)		88.8		88.8		88.8		88.8		88.9
N		168,921		168,921		168,921		168,921		168,921

Note: This table reports GAM estimates for log (Price) across five alternative model specifications. The top panel lists parametric terms with coefficients (Est.), standard errors (SE), and p-values (p). The middle panel reports smooth terms, showing effective degrees of freedom (EDF), the approximate F-statistic, and p-values for joint nonlinearity tests. A two–dimensional spatial surface s(Latitude, Longitude) captures unobserved spatial variation, while distances to amenities (POIs) enter as smooths to allow nonlinear effects. Monthly dummies (YYYYMM) capture time-fixed effects. Interaction rows are ordered to mirror the model sequence and indicate "yes" when a term is included. Model 1 is the baseline with s(UHI 1 p.m.); Model 2 adds te(UHI 1 p.m., CBD distance); Model 3 includes te(UHI 1 p.m., Park distance); Model 4 adds UHI × Household income quantile; and Model 5 adds the parametric interaction UHI × Month. The bottom panel summarizes fit measures: adjusted R2, deviance explained (in %), Akaike Information Criterion (AIC), and sample size N . Significance levels are: *** p < 0.001, ** p < 0.01, * p < 0.05, . p < 0.1, .p < 0.10. Concurvity diagnostics were assessed for all models. Although high values are mechanically expected with flexible spatial smooths, the key coefficients and functional forms remained stable, indicating no substantive concurvity concerns. Sensitivity analyses excluding either the spatial smooth or CBD distance confirmed the robustness of the findings.

Table 3.6 Model Performance Comparison Metrics

(a) 4 a.m.

	Model 1		Model 2		Model 3		Model 4		Model 5	
Metric	**OLS**	**GAM**	**OLS**	**GAM**	**OLS**	**GAM**	**OLS**	**GAM**	**OLS**	**GAM**
Adj. R^2	0.851	0.888	0.852	0.888	0.851	0.888	0.851	0.888	0.851	0.889
MAE	68,496.100	59.347.380	68,379.490	59,330.920	68,494.430	59,334.330	68,751.040	59,440.970	68,421.050	59,262.200
MAPE (%)	20.330	17.410	20.260	17.400	20.330	17.410	20.380	17.440	20.300	17.390
MdAPE (%)	16.020	13.490	15.970	13.500	16.020	13.470	16.110	13.510	15.990	13.460
RMSE	106,095.970	93,455.950	106,032.590	93,438.730	106,091.880	93,434.330	106,351.890	93,526.360	105,963.760	93,299.900
RRSE	0.435	0.383	0.435	0.383	0.435	0.383	0.436	0.383	0.434	0.383

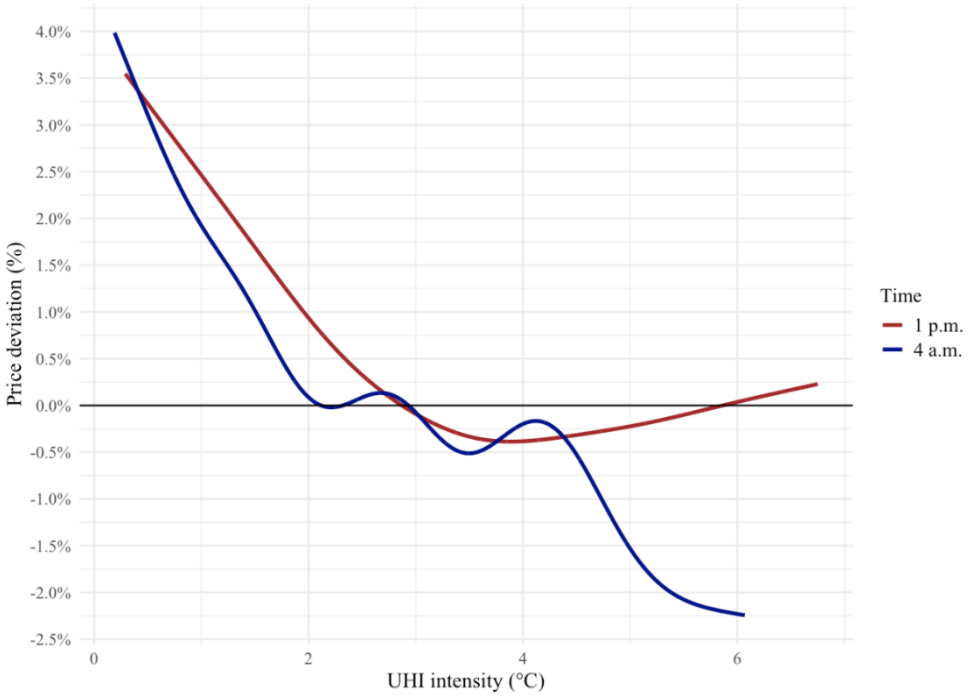
(b) 1 p.m.

	Model 1		Model 2		Model 3		Model 4		Model 5	
Metric	**OLS**	**GAM**	**OLS**	**GAM**	**OLS**	**GAM**	**OLS**	**GAM**	**OLS**	**GAM**
Adj. R^2	0.851	0.888	0.851	0.888	0.851	0.888	0.850	0.888	0.851	0.889
MAE	68,497.320	59,338.330	68,387.570	59,323.410	68,496.650	59,330.380	68,793.550	59,434.220	68,414.910	59,249.330
MAPE (%)	20.330	17.410	20.290	17.400	20.330	17.410	20.400	17.440	20.310	17.390
MdAPE (%)	16.010	13.480	15.980	13.500	16.010	13.490	16.130	13.520	16.000	13.460
RMSE	106,076.310	93,441.740	105,981.210	93,413.630	106,074.110	93,430.330	106,422.690	93,525.540	105,931.110	93,284.610
RRSE	0.435	0.383	0.435	0.383	0.435	0.383	0.436	0.383	0.434	0.382

Note: This table reports error metrics for the five OLS models and the corresponding GAM specifications, each estimated for nighttime and daytime UHI measurements. The adjusted R^2 values are also reported in Tables 3.2, 3.3, 3.4, and 3.5. All error metrics are calculated on the original property price scale. The Mean Absolute Error (MAE) captures the average magnitude of prediction errors, while the Mean Absolute Percentage Error (MAPE) and Median Absolute Percentage Error (MdAPE) express errors in relative terms. The Root Mean Squared Error (RMSE) reflects the quadratic mean of residuals, emphasizing larger deviations, and the Relative Root Squared Error (RRSE) normalizes model performance against a naive benchmark.

Figure 3.5 visualizes how localized thermal exposure affects property prices. It shows percentage price deviations as a function of local UHI intensity, calculated relative to the Berlin-wide mean UHI intensity at each timestamp (mean UHI values of 2.32°C at 4 a.m. and 2.87°C at 1 p.m. serve as benchmarks). At night (4 a.m.), the effects are pronounced at both extremes of the distribution: properties in cooler microclimates (below-average temperatures) show premiums of up to 4.00%, whereas above-average UHI exposure leads to increasing discounts, reaching up to –2.25%. For locations with average UHI intensity of 2.32°C (4.18°F), price deviations are minor, and the curve is relatively flat, suggesting a thermal tolerance zone within which variations have limited impact on property prices.

Figure 3.5 Price Deviation as a Function of UHI Intensity



Note: This figure shows the estimated property price deviation (%) as a function of UHI intensity (°C), measured at 1 p.m. (red line) and 4 a.m. (blue line). The x-axis represents UHI intensity in degrees Celsius, calculated as the deviation from the minimum observed temperature. The y-axis shows the predicted percentage change in property prices. The reference point for price effects is the average UHI intensity, corresponding to 2.32 °C at 1 p.m. and 2.78 °C at 4 a.m., indicated by the zero line on the y-axis. Estimates are derived from the semi-parametric GAM Model 1, with smooth functions fitted separately for daytime and nighttime observations.

For daytime heat exposure (1 p.m.), the price response is more continuous and gradual. Properties in cooler-than-average locations (UHI < 2.87°C; 5.17°F) earn consistent price premiums, reaching up to 3.5% at the lowest UHI levels. This pattern aligns with Klaiber et al. (2017), who showed that even a (1.0°F) change in ambient temperature can significantly affect housing demand and marginal willingness to pay. Conversely, above-average daytime UHI values are associated with modest price discounts that widen to around –0.5% at the upper end of the temperature spectrum. This flat-sloping curve

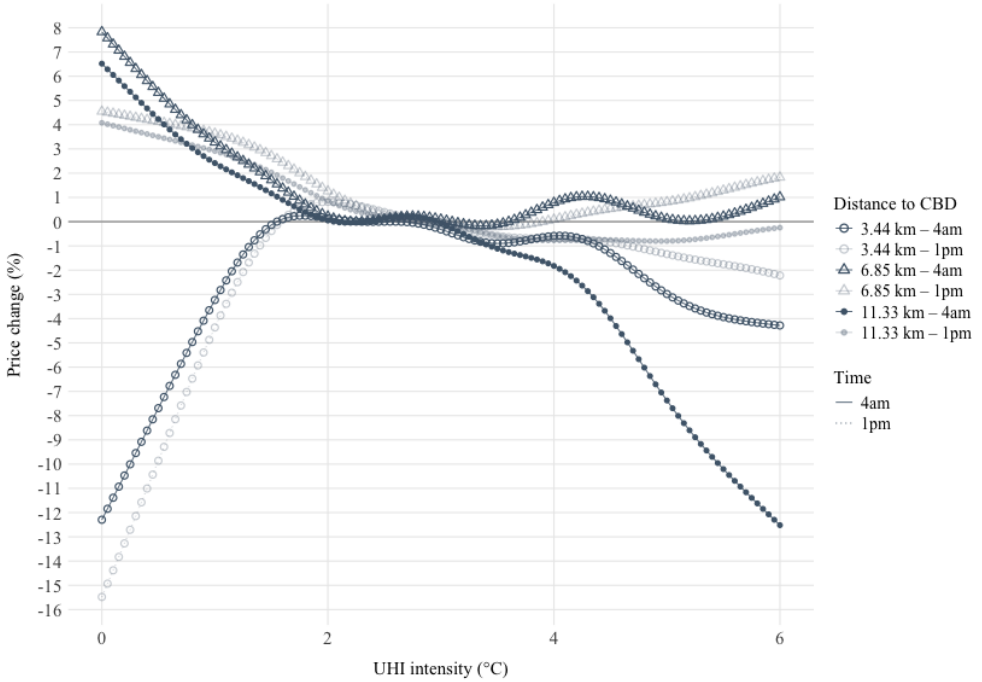
suggests a relatively linear and predictable market response to daytime UHI intensity and the associated thermal discomfort. Consistent with this pattern, daytime effects remain weaker than nighttime effects, reflecting higher occupancy of residential properties during the night and thus greater exposure to heat.

To capture the relationship between spatial effects and pricing for UHI exposure, the baseline specification is extended to model the relationship between UHI intensity and distance to the CBD and the nearest park. At a descriptive level, distance from the CBD has one of the strongest correlations with both UHI measures (-0.30 at 4 a.m. and -0.23 at 1 p.m.), highlighting the role of dense, impervious urban development in generating localized UHI hotspots.[19] The findings align with prior research (Li et al., 2018a). Centrally located, high-demand neighborhoods (often characterized by high-rise structures and limited green infrastructure) absorb and retain more heat during the day and cool more slowly at night. This pattern is central to Berlin's distinct UHI dynamics.

Figure 3.6 shows the varying price sensitivities as a function of UHI intensity and distance to the CBD. At lower UHI intensities, central locations (3.44 km) show price discounts, while midrange (6.85 km) and peripheral (11.33 km) locations command price premiums. As UHI intensity increases, price sensitivity in central locations and those within 7 km of the CBD remains relatively stable, shifting toward neutral or slightly positive values. In contrast, peripheral locations experience substantial price reductions at higher nighttime UHI levels, indicating that elevated temperatures are priced as a significantly negative factor. The flatter gradient observed for central locations suggests greater urban resilience. Dense development patterns, more robust technical infrastructure (including building cooling, insulation and construction quality) and a diverse land-use mix help mitigate price losses as UHI exposure rises. Compared with nighttime patterns, prices are less sensitive to temperature deviations during the day. Properties close to the CBD display a temporary resilience phase (around 2°C to 3°C) in which heat exposure is perceived but not yet penalized. Peripheral areas exhibit only moderate daytime price sensitivity. These patterns suggest that daytime heat is perceived as less disadvantageous in peripheral locations, where it is either less intense or more manageable through individual adaptation. Overall, the market values cooling effects more strongly at night than during the day.

[19] Further details on the correlation are provided in Appendix I.

Figure 3.6 Price as a Function of UHI Intensities and Distance to CBD

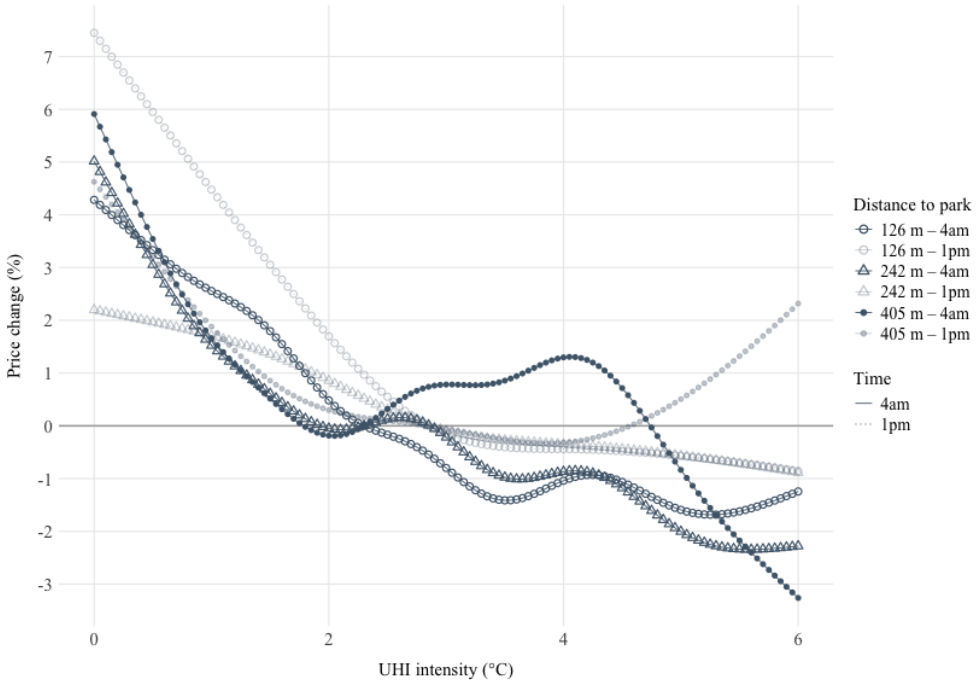


Note: This figure illustrates the relationship between UHI intensity and estimated changes in property prices. Darker lines represent results for 4 a.m., while lighter lines correspond to 1 p.m. UHI intensity (°C) is measured relative to the minimum observed temperature. Price effects are estimated using Model 2, which includes an interaction term between UHI intensity and distance to the CBD. Distances to the CBD are grouped into quantile-based categories with thresholds at 3.44 km, 6.85 km, and 11.33 km.

Since green space is a critical cooling factor in UHI dynamics (Bowler et al., 2010), park proximity is also considered a relevant determinant of price sensitivity. Figure 3.7 shows that properties located very close or moderately close to parks experience positive price responses at lower UHI levels. In particular, locations with below-average UHI intensity (below approximately 2.3°C) exhibit price increases. At higher UHI levels (> 4°C), all distance groups show pronounced price discounts, especially at night. This underscores the importance of park proximity as a key determinant of nighttime cooling potential in overheated urban areas. The nonlinear effects reflect complex trade-offs between local disamenities (such as noise, pollution, and urban density) and the cooling benefits provided by green space. Daytime patterns, however, are more heterogeneous. Properties adjacent to parks show steeper price declines as UHI intensity rises, whereas more peripheral locations display smoother response functions, with stable or slightly positive price effects when UHI exceeds 4.5°C (40.10°F). Daytime cooling benefits appear to be spatially localized, most relevant to buildings directly bordering parks. While parks reduce UHI intensity at night through cooling effects, they moderate daytime temperatures through shade and evapotranspiration. More broadly, although green spaces can regulate neighborhood-scale temperatures, localized UHI intensity is more strongly influenced by micro-level factors, such as building materials and the spatial configuration of nearby structures. This aligns with Chen et al. (2022), who showed that Berlin´s inner city,

dominated by commercial activity, impermeable grey surfaces, including concrete and densely clustered buildings, elevates surface temperatures more than green or blue surfaces.

Figure 3.7 Price as a Function of UHI Intensities and Distance to Park



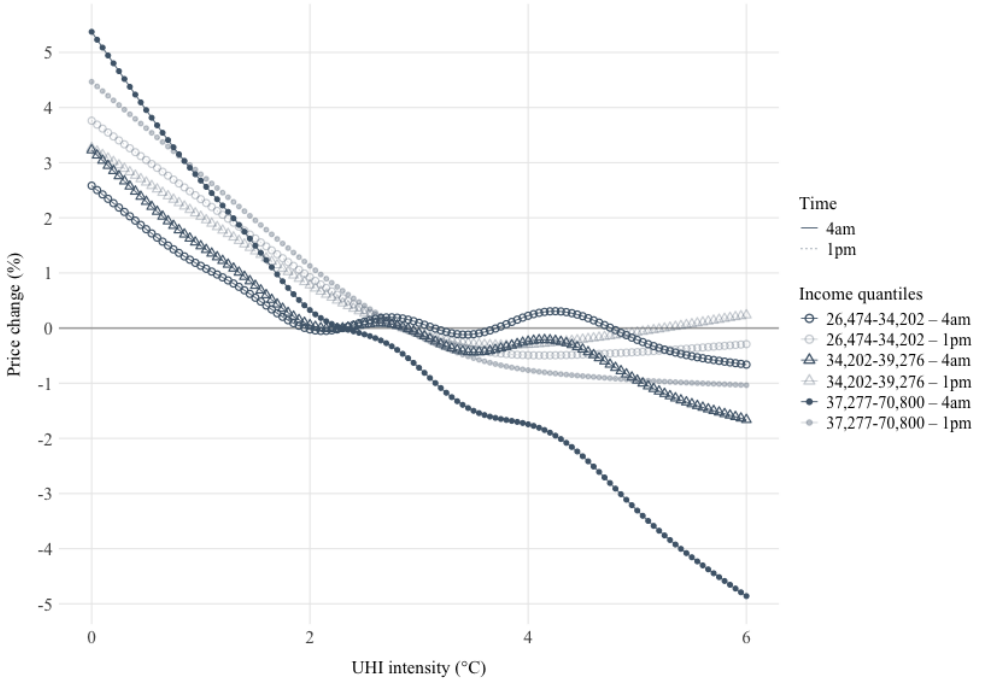
Note: This figure illustrates the relationship between UHI intensity and estimated changes in property prices. Darker lines represent results for 4 a.m., while lighter lines correspond to 1 p.m. UHI intensity (°C) is measured relative to the minimum observed temperature. Price effects are estimated using Model 3, which includes an interaction term between UHI intensity and distance to the nearest park. Distances to the nearest park are grouped into quantile-based categories with thresholds at 126 m, 242 m, and 405 m.

Figure 3.8 plots price premiums by household-income groups as a function of UHI intensity. The highest-income group (represented by the dark dots) shows the steepest slope and correspondingly larger effects, while lower-income groups have flatter curves and weaker sensitivity. These disparities likely reflect uneven urban planning and differential access to cooling infrastructure and resources. Collectively, these patterns corroborate findings in the existing literature, which identify a significant link between household affluence and neighborhood thermal conditions (Borsky et al., 2024; Dell et al., 2009). Higher-income households tend to have greater flexibility in residential decision-making, supported by a higher marginal willingness to pay for cooler microclimates and the financial capacity to prioritize climate-related amenities in housing choices. Consequently, affluent populations are more likely to relocate to rural, suburban, or specific urban zones within Berlin with lower UHI exposure.

Overall, the findings support the notion that physical climate risks in real estate markets increasingly manifest through persistent shifts in thermal comfort. As Sinha and Cropper (2013) noted, climate risks often appear as declining amenity values, especially in cities

where localized heat stress becomes a structural component of housing quality. The income–heat gradient reinforces temperature as a critical, unevenly distributed determinant of amenity value and highlights UHI effects as both a physical risk and a mechanism that can perpetuate social inequality.

Figure 3.8 Price as a Function of UHI Intensities and Household Income

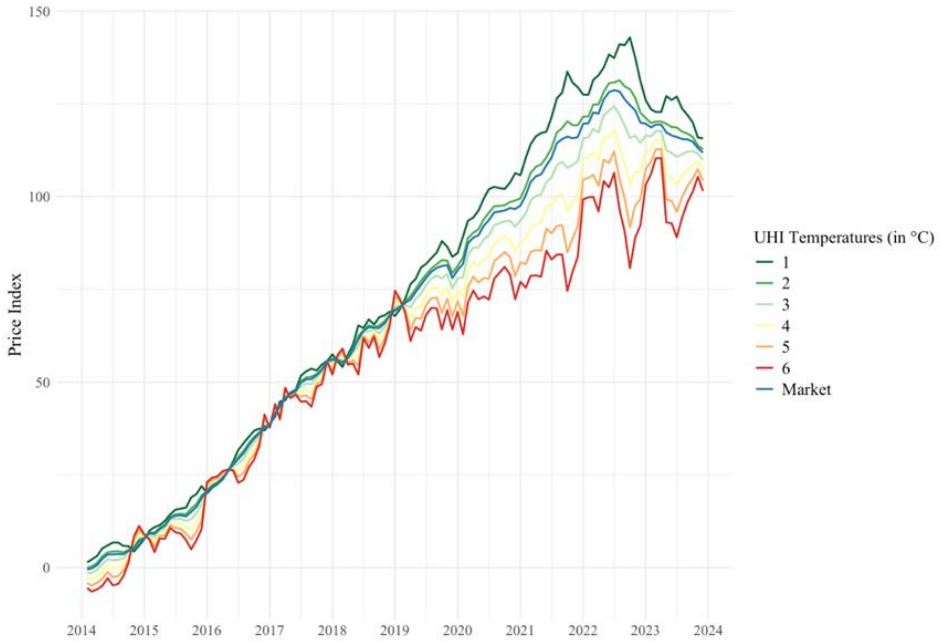


Note: This figure illustrates the relationship between UHI intensity and estimated changes in property prices. Darker lines represent results for 4 a.m., while lighter lines correspond to 1 p.m. UHI intensity (°C) is measured relative to the minimum observed temperature. Price effects are estimated using Model 4, which includes an interaction term between UHI intensity and household income terciles. The reference point for the price effect is the average UHI intensity, expressed as the mean deviation from the minimum temperature. All values are given in degrees Celsius (°C). Household incomes are grouped into quantile-based categories, with thresholds at €26,474–34,202, €34,202–39,276, and €39,277–70,800, representing low, medium, and high-income levels.

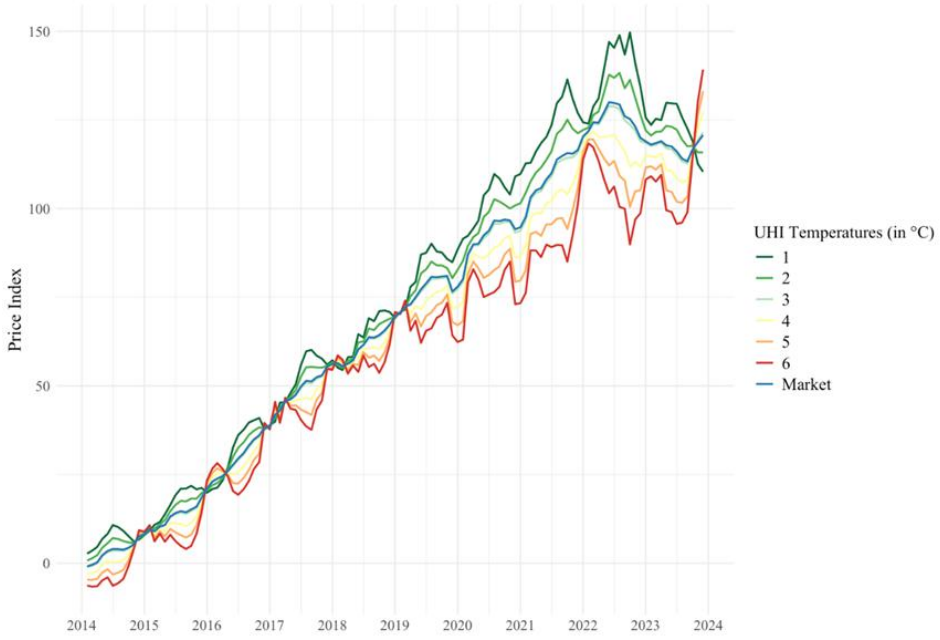
From an investor's perspective, UHI intensity, as a localized measure of heat exposure, is central. The smoothed price trends (3-month averages) in Figures 3.9(a) and (b) reveal clear divergence across UHI intensity groups. In both models, which account for heat exposure (1 p.m.) and cooling potential (4 a.m.), properties located in cooler microclimates (UHI intensity of 1–3°C) consistently outperform those in warmer areas (4–6°C). Over the long term, cooler locations exhibit particularly strong price growth, especially after 2020. The COVID-19 downturn beginning in 2020 is most pronounced in cooler locations, after which the recovery phase leads to a renewed and widening performance gap. Since 2022, amid rising interest rates and high inflation, the spread between UHI groups has widened further. Seasonal comparisons suggest additional dynamics, particularly in Figure 3.9(a): spreads widen in summer and reconverge in winter, indicating higher volatility and a stronger price response to heat stress during summer compared with winter.

Figure 3.9 Price Trends across UHI Intensities

(a) 4 a.m.



(b) 1 p.m.

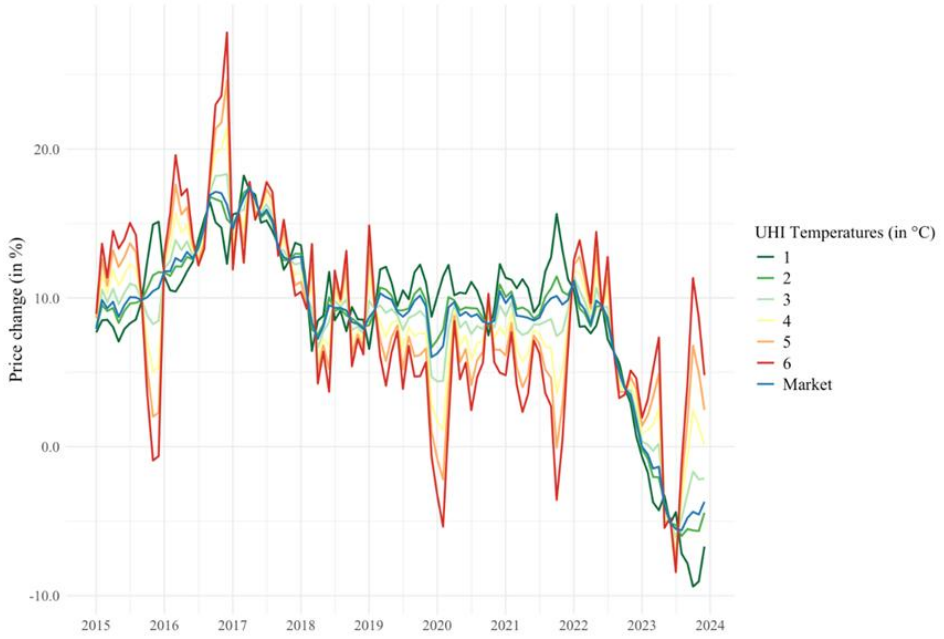


Note: These figures show the indexed long-term trend in estimated property price effects across different UHI intensity levels. Figure (a) presents results for 4 a.m., and Figure (b) for 1 p.m. Colored lines indicate distinct UHI intensity levels in degrees Celsius (°C), using a green-to-red scale from lower to higher intensities. The blue line represents the overall market average. Price effects are estimated using Model 1, the baseline GAM without interaction terms. The index is based on January 2014 and calculated with a three-month moving average. The x-axis represents the observation period from 2014 to 2023.

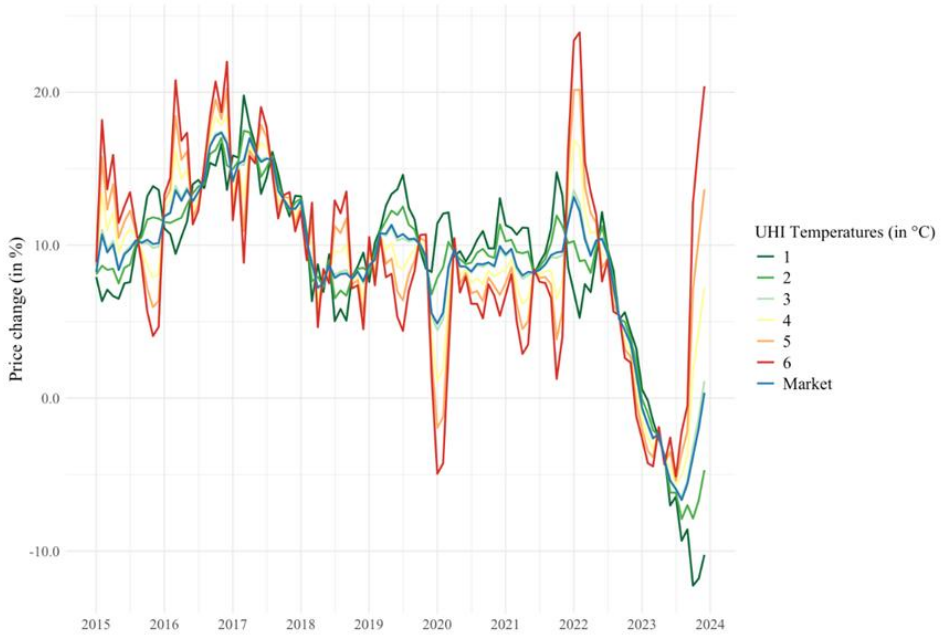
Annual price growth based on smoothed 3-month averages confirms long-term differences between cooler and warmer locations (Figures 3.10(a) and (b)).

Figure 3.10 Year-on-Year Price Change across UHI Intensities

(a) 4 a.m.



(b) 1 p.m.



Note: These figures illustrate the YoY variation in estimated property price effects across different UHI intensity levels. Figure (a) presents results for 4 a.m., and Figure (b) for 1 p.m. Colored lines indicate UHI intensity levels in degrees Celsius (°C), using a green-to-red palette from lower to higher intensities. The blue line represents the overall market average. Price effects are estimated using Model 1, the baseline GAM without interaction terms. YoY changes are computed from a three-month moving average. The x-axis represents the observation period from 2014 to 2023.

From 2014 to 2019, all temperature groups moved largely in parallel, with YoY growth between 6% and 16%. A slight divergence begins to emerge in 2021. While cooler groups (1–3°C) remain relatively steady, warmer locations (4–6°C) lose momentum and exhibit temporarily lower YoY growth rates. The sharpest break occurs in 2022-2023, when all groups turn negative. Since 2023, however, the warmest groups even outperform the cooler ones, indicating that in central locations with high demand or speculative dynamics, climatic impacts may be temporarily counteracted. In particular, the daytime series (1 p.m.) shows no consistent penalty for warmer UHI locations, suggesting that heat exposure during the day poses less of a risk than nighttime heat retention and reduced overnight cooling.

The calculated KPIs confirm this pattern. Tables 3.7(a) and (b) show that reduced nighttime cooling (4 a.m.) acts as a price-depressing risk factor, while daytime heat exposure (1 p.m.) is generally viewed by the market as neutral to slightly positive. Table 3.7(a) indicates that, at night, properties in the cooler UHI groups (1–3°C) outperform across all indicators. They exhibit higher average growth, lower volatility, and a more favorable return-to-risk ratio, indicating greater resilience to market cycles.

Table 3.7 House Price Growth and Risk Return Metrics by UHI Intensity

(a) 4 a.m.						
UHI Intensity (°C)	**1**	**2**	**3**	**4**	**5**	**6**
Cum. Growth (%)	966.60	950.50	936.50	924.70	915.00	907.30
Av. Growth (%)	8.90	8.80	8.70	8.60	8.50	8.40
Risk Ratio (%)	5.90	5.30	5.10	5.20	5.70	6.50
Return-to-Risk Ratio	1.51	1.65	1.70	1.63	1.48	1.30
Compound Average Growth Rate (%)	6.10	5.90	5.70	5.50	5.30	5.10
(b) 1 p.m.						
UHI Intensity (°C)	**1**	**2**	**3**	**4**	**5**	**6**
Cum. Growth (%)	948.20	949.10	952.40	958.30	966.60	977.40
Av. Growth (%)	8.78	8.79	8.82	8.87	8.95	9.05
Risk Ratio (%)	6.30	5.60	5.24	5.30	5.78	6.62
Return-to-Risk Ratio	1.39	1.57	1.68	1.68	1.55	1.37
Compound Average Growth Rate (%)	5.82	6.00	6.19	6.37	6.56	6.74

Note: The tables report KPIs for UHI intensity groups at 4 a.m. and 1 p.m., respectively. All values are derived from YoY estimates based on Model 1; formulas are provided in the Research Methodology section. The KPIs include: Cumulative Growth (%), which captures total long-term price change within each UHI intensity group; Average Growth (%), the mean annual YoY increase; Risk (%), measured as the standard deviation of YoY growth; Return-to-Risk Ratio, a normalized performance metric accounting for risk exposure; and Compound Annual Growth Rate (%), which expresses the smoothed annualized growth rate. Together, these KPIs provide a comprehensive performance profile across UHI groups and enable comparisons between nighttime (4 a.m.) and daytime (1 p.m.) conditions.

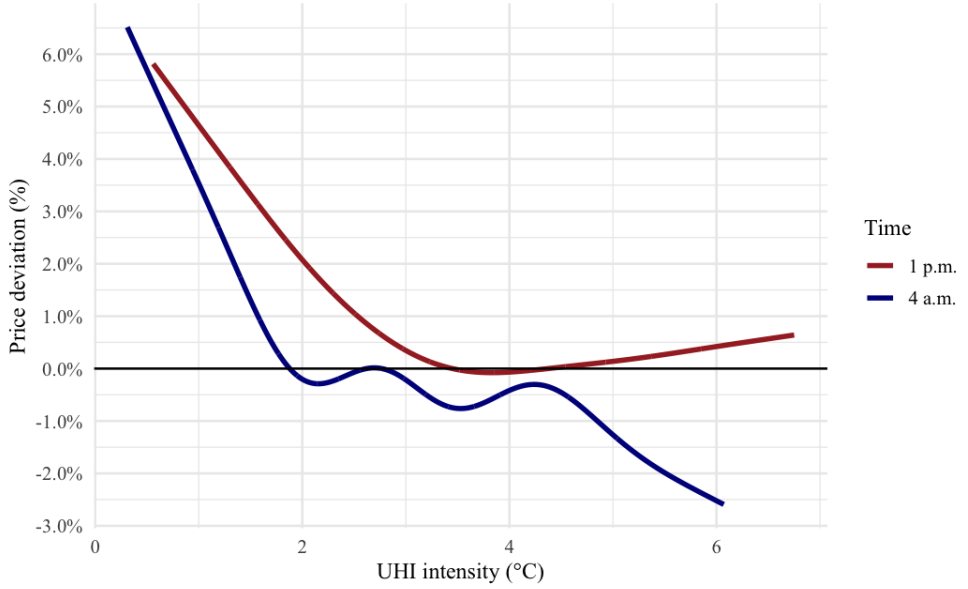
During the day, warmer locations show slightly higher risk, but this is offset by above-average cumulative and average returns (see Table 3.7(b)). Warmer groups (4–6°C), in particular, display a positive relationship between return and risk (e.g., 1.57 for 5°C). This suggests that daytime heat is perceived as less harmful in central locations with good infrastructure or can be mitigated more effectively through urban planning and technical measures.

Robustness Check

Accounting for Summer and Winter Effects

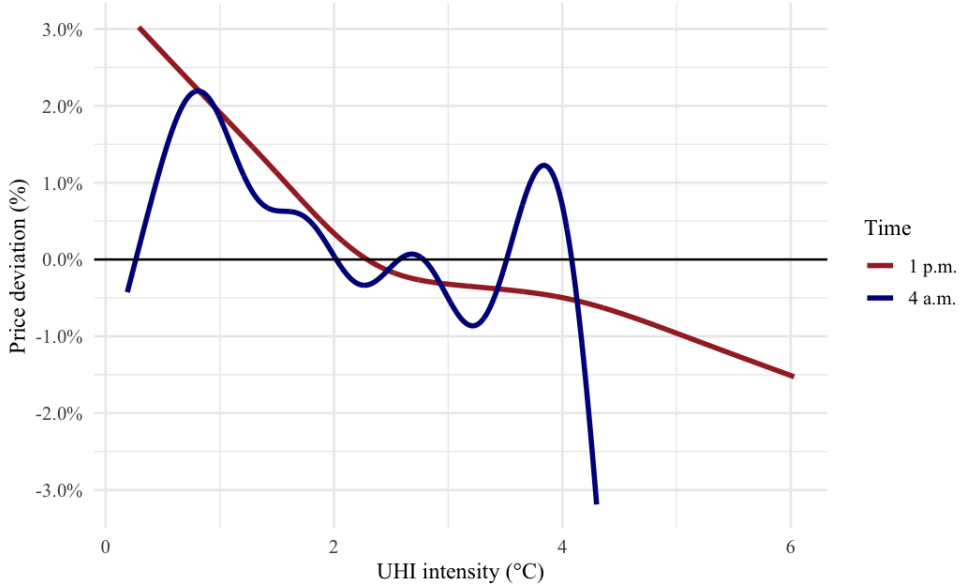
We perform several robustness checks to validate our findings, focusing on the price effects derived from the base model. First, we estimate the baseline specification on seasonally filtered subsamples to account for potential differential trends in housing price appreciation between warmer and colder periods. Specifically, we re-estimate the baseline specification separately for seasonal subsamples (summer: April–September; winter: October–March). The results, shown in Figures 3.11 and 3.12, reveal pronounced nonlinearity and indicate that our key findings remain robust under this more stringent specification, with an even larger estimated effect in the summer months. Consistent with the descriptive statistics, both the level and dispersion of UHI intensities are higher in summer than in transitional and winter months. During summer, prices decline by up to 2.5% in locations with pronounced nighttime overheating. Locations with below-average UHI exposure show price premiums of approximately 6–7% at night (4 a.m.) and around 5–6% during the day (1 p.m.). Winter specifications, however, show lower intensities overall and greater symmetry around the mean, indicating smaller and less systematic price responses. Nevertheless, even in winter, the effects remain more pronounced at night, as urban heat storage is particularly evident during nighttime, while daytime values are more strongly influenced by temporary weather conditions. The larger effects in summer are attributable to increased UHI intensities during warm months, which cause actual heat stress and therefore have a greater impact on living quality, directly affecting prices.

Figure 3.11 Price Effects for Summer Months



Note: This figure illustrates the estimated property price deviation (%) as a function of UHI intensity (°C), measured at 1 p.m. (red line) and 4 a.m. (blue line) for the summer months (April-September). The x-axis represents UHI intensity in degrees Celsius, calculated as the deviation from the minimum observed temperature. The y-axis shows the predicted percentage change in property prices. The reference point for the price effect is the average UHI intensity, corresponding to 3.45°C at 1 p.m. and 2.62°C at 4 a.m., indicated by the zero line on the y-axis. Estimates are derived from the semi-parametric GAM Model 1, with smooth functions fitted separately for daytime and nighttime observations.

Figure 3.12 Price Effects for Winter Months



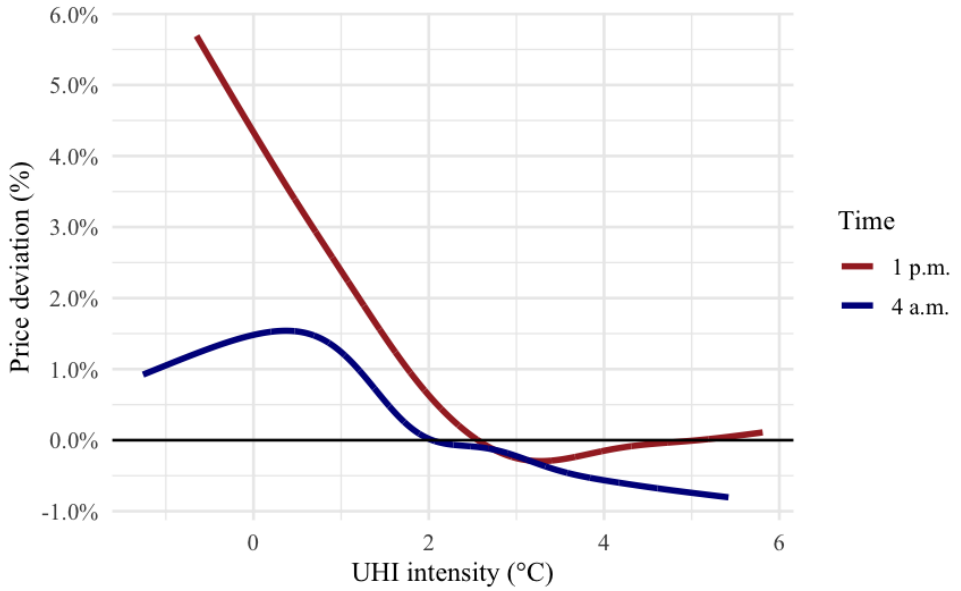
Note: This figure illustrates the estimated property price deviation (%) as a function of UHI intensity (°C), measured at 1 p.m. (red line) and 4 a.m. (blue line) for the winter months (October-March). The x-axis represents UHI intensity in degrees Celsius, calculated as the deviation from the minimum observed temperature. The y-axis shows the predicted percentage change in property prices. The reference point for the price effect is the average UHI intensity, corresponding to 2.29°C at 1 p.m. and 2.02°C at 4 a.m., indicated by the zero line on the y-axis. In winter, nighttime UHI intensity is lower than in summer, resulting in a smaller range of observed values. These seasonal differences in temperature are also reflected in the descriptives. Accordingly, nighttime UHI values are truncated at the 99.9th percentile. Estimates are derived from the semi-parametric GAM Model 1, with smooth functions fitted separately for daytime and nighttime observations.

Adjustment of Reference Points for UHI Measurement

Second, we augment our analysis with a revised reference point to estimate UHI intensities. To do this, the temperature dataset is first restricted to stations located outside the Berlin city boundaries (Stewart & Oke, 2012). From this subset, only grid cells within 1 km^2 population raster cells with fewer than 100 inhabitants are retained, following Gabriel and Endlicher (2011). Within this sub-sample, rural reference locations are randomly selected and labeled R1 and R2. Consistent with our main analysis, UHI intensity is calculated as the difference between the location-specific temperature and the corresponding (rural) reference temperature, measured at 4 a.m. and 1 p.m. The resulting estimates[20], shown in Figure 3.13, indicate that the central structure of the qualitative pattern of price responses remains consistent. However, when UHI intensity is calculated using rural reference locations, the price response during the day is stronger than at night. In locations with below-average UHI intensity, price premiums reach nearly 6%, whereas nighttime premiums are lower, around 1.6%. In areas with higher UHI intensity, negative price reactions persist, particularly at night, and increase further with higher temperatures. Comparing the reference locations also shows that the economic relevance of daytime and nighttime temperatures differs, although the qualitative interpretation of the main results remains unchanged. This difference reflects the sensitivity of daily temperature measurements to the choice of reference location. Daytime heat exposure is particularly price-relevant for reference points in rural regions, where cooler locations are associated with the largest price premiums. In contrast, UHI estimates based on minimum temperatures emphasize nighttime heat stress, when cooling potential is more limited and economically relevant. This finding aligns with established literature, as nighttime minimum temperatures are an important indicator of limited cooling potential, the thermal inertia of buildings, and chronic heat stress (Arnfield, 2003; Oke, 1982; Voogt and Oke, 2003).

[20] Appendix III shows the results for the second rural reference location (R2). The estimated price effects closely mirror those obtained for R1, confirming the robustness of the qualitative response pattern across alternative rural benchmarks.

Figure 3.13 Alternative Reference Points for UHI Intensity: R1



Note: This figure shows the estimated property price deviation (%) as a function of UHI intensity (°C), measured at 1 p.m. (red line) and 4 a.m. (blue line). The x-axis represents UHI intensity in degrees Celsius, defined as the difference between the object-specific temperature and an externally anchored rural reference temperature. The y-axis indicates the predicted percentage change in property prices. The reference point for the price effect is the average UHI intensity, corresponding to 2.56°C at 1 p.m. and 2.04°C at 4 a.m., which is represented by the zero line on the y-axis. Estimates are based on semi-parametric GAM Model 1, with smooth functions fitted separately for daytime and nighttime observations.

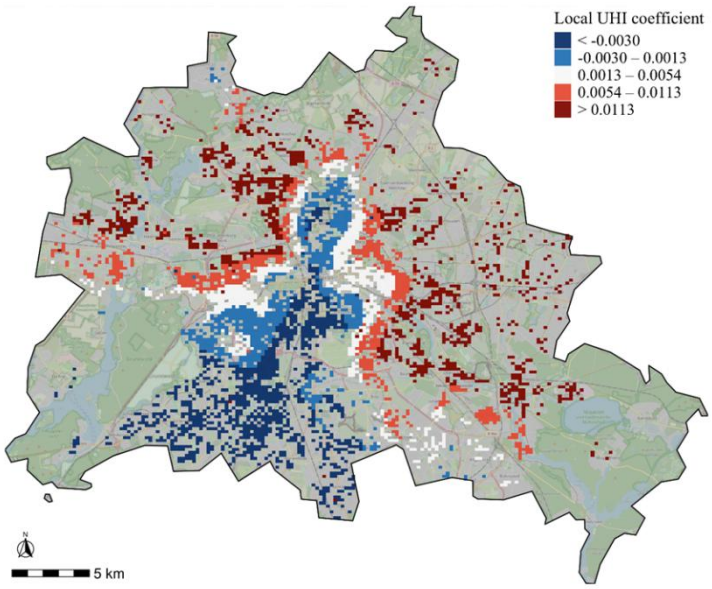
Spatial decomposition of the UHI effect

To capture the spatial heterogeneity of price associations, a geographically weighted regression (GWR) is applied. This approach extends the assumptions of the linear regression model by estimating relationships at the local level and allowing coefficients to vary across space (Fotheringham et al., 2002). Local-specific parameters are estimated for each observation location, with nearby observations receiving greater weight than those farther away. This provides additional evidence of spatial differentiation in price–UHI relationships and allows a clear distinction between functional nonlinearities and spatial heterogeneity. The resulting surface structures are analyzed using spatial parameters that identify patterns in the direction and strength of associations with prices. The results reveal pronounced inner-city differences and temporal heterogeneity. Figures 3.14(a) and (b) show that daytime measurements (1 p.m.) highlight hotspots with predominantly positive coefficients. These areas are concentrated in central, densely built-up locations with high economic demand, where UHI intensity is strongly influenced by local conditions, land use densities, and adaptation behaviors, and varies considerably within the city. In contrast, nighttime UHI effects (4 a.m.) appear more spatially homogeneous, with smaller extremes and less dispersion of coefficients, suggesting a more consistent representation of nighttime heat stress. Notably, GWR primarily maps spatial parameter heterogeneity, showing which sub-areas exhibit stronger or weaker interactions. It does not estimate marginal effects for causal interpretation, limiting conclusions about the relative strength

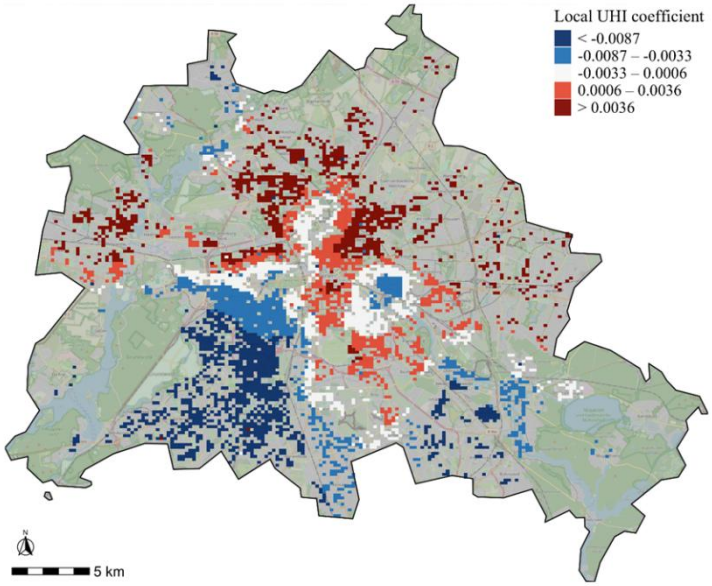
of UHI effects. Nevertheless, GWR supports the conclusion that UHI-related price effects are localized and context-dependent rather than spatially homogeneous across the city.

Figure 3.14 Geographically Weighted Regression

(a) 4 a.m.



(b) 1 p.m.



Note: These figures show the spatially varying coefficients of the UHI effect, estimated using GWR, for the period 2020–2023 at 4 a.m. (a) and 1 p.m. (b). The color scales represent the local regression coefficients, indicating positive or negative relationships between UHI intensity and property prices - higher UHI intensity is associated with higher or lower prices in the respective locations. Corresponding maps for 2014–2016 and 2017–2019 are provided in the appendix.

3.7 Concluding Remarks

This study applies a semi-parametric framework to assess the impact of UHI intensity on residential property prices in Berlin between 2014 and 2023. Using high-resolution temperature data at a 30 meter-grid level, we identify average UHI intensities ranging from approximately 2.32°C to 2.87°C, with localized urban hotspots exceeding 6.5°C. Above-average UHI intensity is associated with price discounts of up to 2.5%, while below-average intensity corresponds to premiums of up to 4%. Risk-adjusted return metrics reinforce this pattern. Nighttime UHI intensity, reflecting reduced cooling potential, has a larger and more persistent impact on property values than daytime UHI intensity, which reflects peak heat exposure.

Accounting for spatial effects, negative price impacts intensify with distance from the CBD and are more pronounced for properties adjacent to parks, where other locational trade-offs offset localized cooling. In contrast, within the immediate CBD, central-location advantages outweigh heat-stress penalties.

Distinct differences emerge across income groups. Price penalties for higher UHI intensities are largest in high-income segments, indicating that wealthier households are more heat-averse and better able to avoid or mitigate heat stress. This pattern aligns with existing evidence on climate-driven residential sorting and uneven adaptive capacity, amplifying socioeconomic inequalities as lower-income groups bear a disproportionate burden of climate risks.

Our findings suggest that market participants assess microclimatic conditions at both the building and neighborhood levels and capitalize these into property values. The inverse relationship between UHI intensity and prices indicates that markets recognize the tangible costs of heat-impaired building and infrastructure performance. Concurrently, deteriorating building performance under escalating heat reduces thermal comfort and degrades air quality, eroding climate amenities and diminishing location appeal. Although UHIs differ from acute hazards such as floods or wildfires, their financial materiality is comparable.

For policymakers and city planners, these results highlight the importance of integrating UHI resilience into urban planning measures. This includes preserving ventilation corridors, expanding green infrastructure, targeting greening of thermal hotspots, and prioritizing vulnerable neighborhoods for mitigation and adaptation interventions.

For real estate decision-makers, UHI exposure represents a material financial risk. Nighttime UHI intensity, in particular, warrants explicit consideration to avoid value losses

and identify climate-resilient locations. Cost-effective measures (such as reflective or high-albedo materials, cool roofs, shading, and reduced surface sealing) can mitigate UHI effects at modest cost while conferring competitive advantages.

Finally, our results confirm the need for future research at the intersection of real estate markets and chronic atmospheric hazards, addressing the research gap identified at the outset of this study.

3.8 Appendix

3.8.1 Appendix I – Descriptive Statistics

Table 3.8 Variable Description

Variable	Source	Scale	Unit	Description
Price	A	Numeric	Euro	Price of the asset
Size	A	Numeric	m^2	Saleable floor area of the apartment
Rooms	A	Numeric	Count	Number of rooms
Age	A	Numeric	Years	Relative to year 2023. Properties built before 1900 are grouped under the construction year of 1900.
Floor	A	Numeric		Indication of the floor of the dwelling. The accessibility of apartments is assumed to be equivalent, whether on the first floor or an upper level.
Retrofitted	A	Binary	1 = yes	"Retrofitting" has taken place once the dwelling has had some improvement measures in terms of renovation or refurbishment.
Kitchen	A	Binary	1 = yes	With kitchen included. In Germany, residential properties are commonly marketed without fitted kitchens, generating variation in this attribute.
First occupancy	A	Binary	1 = yes	Newly built and first occupied
Parking	A	Binary	1 = yes	With parking included
Balcony/Terrace	A	Binary	1 = yes	With a balcony and/or terrace included
School distance	B	Numeric	km	Distance to closest school
Kindergarten distance	B	Numeric	km	Distance to closest kindergarten
Restaurant distance	B	Numeric	km	Distance to closest restaurant
Supermarket distance	B	Numeric	km	Distance to closest supermarket
Kiosk distance	B	Numeric	km	Distance to closest kiosk
Park distance	B	Numeric	km	Distance to closest park
Playground distance	B	Numeric	km	Distance to closest playground
CBD distance	B	Numeric	km	Distance to "Alexanderplatz" as the reference point, accounting for metropolitan centrality and spatial fixed effects.
Bus stop distance	B	Numeric	km	Distance to closest bus stop
Hospital distance	B	Numeric	km	Distance to closest hospital
Longitude	A	Numeric		Longitude coordinate
Latitude	A	Numeric		Latitude coordinate
Income per household	A	Numeric	Euro	Average income per household by postal code
Month/Year fixed effects	A	Factor	60 levels	Monthly time dummies for the date of disclosure from April to September, included to assess seasonal patterns.
UHI 4 a.m.	D	Numeric	°C	Temperature deviation at 4 a.m. from Berlin's temperature minimum
UHI 1 p.m.	D	Numeric	°C	Temperature deviation at 1 p.m. from Berlin's temperature minimum

Note: The table presents a detailed overview of the variables used in this analysis. These include numerical measurements such as the property's list price (in Euros), floor area (in square meters), and the age relative to the year 2023. Proximity to local amenities is captured through distances to the nearest bus stops, schools, and restaurants. Additional binary variables denote specific features, including kitchens, balconies or terraces, parking spaces, and elevators. Environmental exposure is measured using temperature readings recorded at 4 a.m. and 1 p.m. on the day the property was listed. A binary variable indicates whether the property has been retrofitted, capturing refurbishment or energy-efficient improvements. Population density at the postal code level is included to reflect local demographic conditions, while monthly time dummies control for seasonal and temporal variation in property listings.
Sources: A = VALUE market data, B = OpenStreetMap, C = GfK, D = Meteoblue.

Table 3.9 Correlations of Variables

	Price	Log price	Size	Log size	Rooms	Age	Floors	Retrofitted	Kitchen	Parking	Balcony / Terrace	First occupancy	School distance	Kindergarten distance	Restaurant distance
Price	1.00														
Log price	0.92	1.00													
Size	0.75	0.73	1.00												
Log size	0.72	0.74	0.96	1.00											
Rooms	0.59	0.61	0.83	0.84	1.00										
Age	-0.12	-0.12	-0.02	-0.04	-0.07	1.00									
Floors	0.16	0.15	0.07	0.06	0.03	-0.07	1.00								
Retrofitted	-0.05	-0.04	-0.06	-0.06	-0.06	0.41	-0.02	1.00							
Kitchen	0.00	0.00	-0.04	-0.04	-0.05	0.00	0.00	0.15	1.00						
Parking	0.15	0.17	0.14	0.15	0.12	-0.54	0.02	-0.20	0.04	1.00					
Balcony / Terrace	0.16	0.19	0.17	0.20	0.17	-0.23	0.04	-0.07	0.01	0.19	1.00				
First occupancy	0.27	0.30	0.15	0.15	0.14	-0.48	0.06	-0.16	-0.25	0.30	0.15	1.00			
School distance	-0.05	-0.06	0.01	0.02	0.02	-0.15	-0.04	-0.06	0.03	0.13	0.06	0.04	1.00		
Kindergarten distance	-0.04	-0.06	0.01	0.02	0.02	-0.20	-0.06	-0.06	0.05	0.16	0.07	0.05	0.42	1.00	
Restaurant distance	-0.15	-0.18	-0.03	-0.01	0.02	-0.22	-0.12	-0.07	0.05	0.16	0.08	0.02	0.32	0.38	1.00
Supermarket distance	-0.04	-0.05	0.02	0.03	0.03	-0.16	-0.10	-0.06	0.06	0.14	0.06	0.03	0.28	0.38	0.48
Kiosk distance	-0.12	-0.14	-0.01	0.01	0.03	-0.24	-0.10	-0.09	0.04	0.19	0.08	0.05	0.28	0.29	0.43
Park distance	-0.11	-0.14	-0.01	0.00	0.02	-0.10	-0.06	-0.04	0.02	0.08	0.04	0.01	0.28	0.27	0.29
Playground distance	-0.02	-0.04	0.05	0.06	0.04	-0.14	-0.06	-0.06	0.04	0.14	0.05	0.03	0.34	0.36	0.24
CBD distance	-0.17	-0.19	-0.01	0.01	0.04	-0.14	-0.18	-0.05	0.08	0.14	0.08	-0.06	0.31	0.32	0.42
Bus distance	-0.01	-0.01	0.00	0.00	0.00	-0.01	-0.03	0.00	0.00	0.01	0.01	0.02	-0.04	0.01	0.17
Hospital distance	-0.11	-0.12	-0.06	-0.04	-0.01	-0.09	-0.05	-0.03	0.01	0.03	0.01	0.01	0.13	0.08	0.16
Longitude	-0.04	-0.02	-0.04	-0.03	-0.01	-0.11	0.03	-0.02	-0.07	0.01	0.00	0.11	-0.03	-0.01	0.01
Latitude	0.01	0.01	-0.02	-0.02	-0.01	0.00	0.07	-0.01	-0.04	-0.03	-0.04	0.06	-0.11	-0.14	-0.12
Income per Household	0.21	0.24	0.05	0.06	0.06	-0.13	-0.11	-0.03	0.13	0.12	0.08	-0.04	0.17	0.21	0.16
Log income per household	0.22	0.25	0.05	0.06	0.06	-0.13	-0.10	-0.02	0.13	0.12	0.08	-0.04	0.17	0.21	0.14
Temp 4 a.m.	0.02	0.02	-0.01	-0.01	-0.01	0.01	0.01	0.01	0.00	-0.02	-0.01	-0.01	-0.02	-0.01	-0.03
Temp 1 p.m.	0.02	0.02	-0.01	-0.01	-0.01	0.01	0.01	0.01	0.00	-0.02	0.00	-0.01	-0.01	-0.01	-0.03
UHI 4 a.m.	0.05	0.06	-0.02	-0.03	-0.04	0.12	0.09	0.03	-0.04	-0.11	-0.05	0.00	-0.17	-0.17	-0.30
UHI 1 p.m.	0.02	0.03	-0.02	-0.03	-0.03	0.09	0.06	0.03	-0.03	-0.08	-0.04	0.00	-0.13	-0.13	-0.21

continued on next page

Table 3.9 Correlations of Variables – **continued**

	Supermarket distance	*Kiosk distance*	*Park distance*	*Playground distance*	*CBD distance*	*Bus distance*	*Hospital distance*	*Longitude*	*Latitude*	*Income per Household*	*Log income per household*	*Temp 4 a.m.*	*Temp 1 p.m.*	*UHI 4 a.m.*	*UHI 1 p.m.*
Price															
Log price															
Size															
Log size															
Rooms															
Age															
Floors															
Retrofitted															
Kitchen															
Parking															
Balcony / Terrace															
First occupancy															
School distance															
Kindergarten distance															
Restaurant distance															
Supermarket distance	1.00														
Kiosk distance	0.29	1.00													
Park distance	0.14	0.32	1.00												
Playground distance	0.25	0.26	0.36	1.00											
CBD distance	0.35	0.40	0.30	0.30	1.00										
Bus distance	0.10	0.06	0.01	-0.03	-0.02	1.00									
Hospital distance	0.04	0.27	0.16	0.06	0.21	0.02	1.00								
Longitude	-0.14	0.03	0.03	-0.04	-0.35	0.07	0.31	1.00							
Latitude	-0.15	0.06	-0.11	-0.18	-0.43	0.04	-0.09	0.01	1.00						
Income per Household	0.19	0.25	0.09	0.21	0.39	0.01	0.11	-0.12	-0.15	1.00					
Log income per household	0.18	0.25	0.08	0.21	0.39	0.00	0.10	-0.12	-0.16	0.99	1.00				
Temp 4 a.m.	-0.03	-0.03	-0.02	-0.01	-0.02	-0.01	-0.01	0.00	0.00	-0.01	0.00	1.00			
Temp 1 p.m.	-0.03	-0.03	-0.01	-0.01	-0.02	-0.01	0.00	0.00	0.00	0.01	0.01	0.89	1.00		
UHI 4 a.m.	-0.30	-0.25	-0.07	-0.14	-0.30	-0.08	-0.06	0.06	0.08	-0.18	-0.18	0.52	0.56	1.00	
UHI 1 p.m.	-0.23	-0.18	-0.04	-0.11	-0.23	-0.05	-0.04	0.07	0.08	-0.15	-0.15	0.61	0.77	0.77	1.00

contTaNote: This table reports pairwise Pearson correlation coefficients for all variables included in the analysis. Distances are measured in kilometers. All variables are defined as described in Appendix A. Temperatures are recorded at 4 a.m. and 1 p.m. UHI is defined as the local temperature minus the citywide minimum at the respective time.

3.8.2 Appendix II – Formulas for KPI Analysis

This appendix summarizes the definitions and formulas of the KPIs used to quantify price growth dynamics, market risk, and risk-adjusted performance across different UHI exposure levels.

Real estate price dynamics adjust only gradually and tend to reflect underlying market conditions over longer horizons rather than short-term fluctuations. To account for this adjustment process and to stabilize short-term price movements, a three-month moving average of observed prices is used:

$$\tilde{P}_t = \frac{P_t + P_{t+1} + P_{t+2}}{3}. \tag{3.3}$$

To capture the price change over the full observation window, we compute the smoothed end-to-end trend growth based on the three-month moving average:

$$P_{trend,T} = \frac{\tilde{P}_T}{\tilde{P}_{t_0}} - 1. \tag{3.4}$$

Cumulative Growth Rate

Based on the smoothed time series, the year-on-year (YoY) growth rates are computed as follows. YoY growth rates remove seasonal patterns and enable consistent comparisons of price dynamics over time:

$$g_t = \frac{\tilde{P}_t}{\tilde{P}_{t-12}} - 1. \tag{3.5}$$

The cumulative growth rate captures the total long-term price change over the observation period from the starting month t_0 to the end of the sample T, reflecting the overall appreciation or depreciation within the respective UHI intensity levels:

$$G_{cum} = \sum_{t \epsilon \tau} g_t. \tag{3.6}$$

Average Annual Growth

To quantify average growth dynamics, the arithmetic mean of all YoY growth rates is computed, summarizing mean annual price changes and reflecting short-term cyclical growth behavior across UHI exposure groups:

Average Annual Growth - continued

$$\mu_g = \frac{1}{M}\sum_{t\epsilon\tau} g_t. \tag{3.7}$$

Risk Indicator

The associated price risk is measured by the standard deviation of YoY growth rates. Higher values indicate stronger short-term price fluctuations and thus higher market risk:

$$\sigma_g = \sqrt{\frac{1}{M-1}\sum_{t\epsilon\tau}\left(g_t - \mu_g\right)^2}. \tag{3.8}$$

Return-to-Risk Ratio

Risk-adjusted performance is assessed using the return-to-risk ratio. This indicator captures the average price increase per unit of price volatility and enables a consistent comparison of risk-adjusted performance across UHI exposure levels:

$$R_g = \frac{\mu_g}{\sigma_g}. \tag{3.9}$$

Compound Annual Growth Rate (CAGR)

To summarize long-term growth over the entire observation period in annualized terms, the compound annual growth rate (CAGR) is calculated. In contrast to the average annual growth μ_g, which reflects short-term fluctuations, the CAGR captures structural long-term growth and enables long-run comparisons across UHI exposure categories. The number of years covered by the sample is:

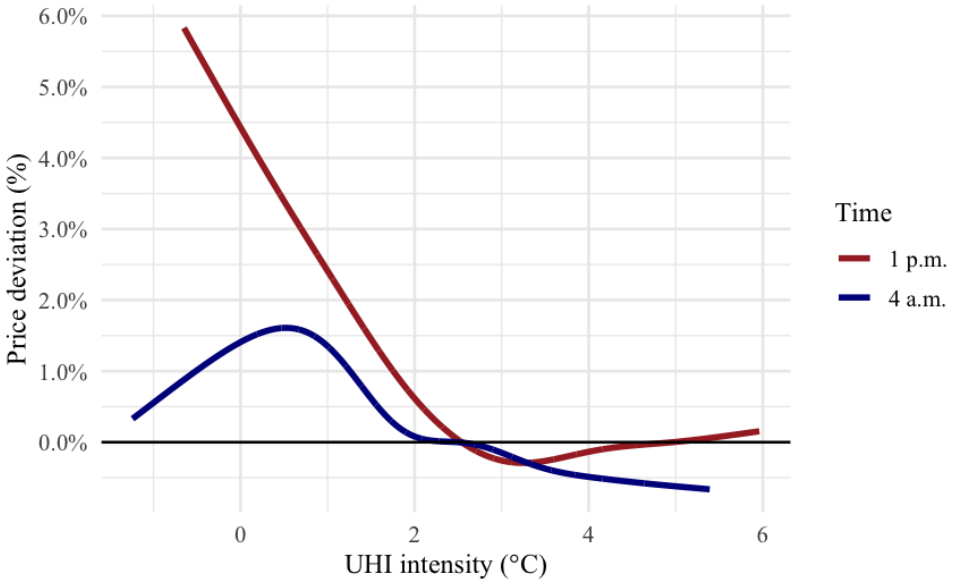
$$Y = \frac{T - t_0}{12}. \tag{3.10}$$

Based on this, the CAGR is defined as:

$$CAGR = \left(\frac{\tilde{P}_T}{\tilde{P}_{t_0}}\right)^{1/Y} - 1. \tag{3.11}$$

3.8.3 Appendix III – Robustness Check - Changing the Reference

Figure 3.15 Alternative Reference Points for UHI Intensity: R2

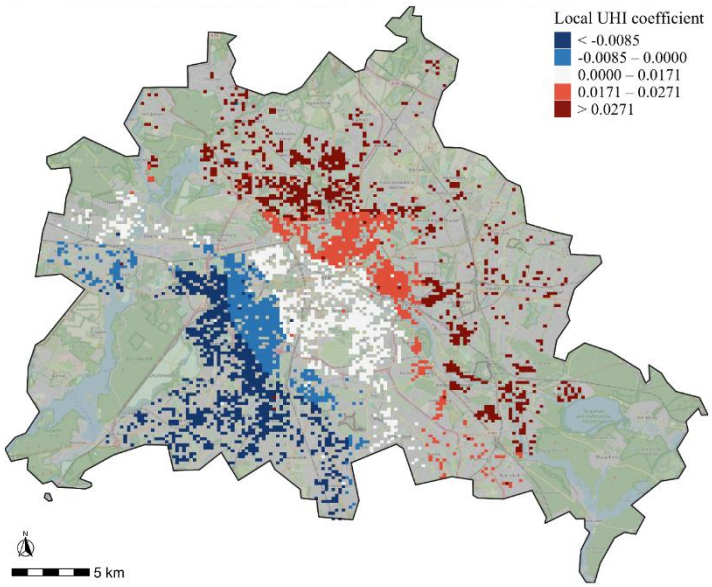


Note: The figure illustrates the estimated property price deviation (%) as a function of UHI intensity (°C), measured at 1 p.m. (red line) and 4 a.m. (blue line). The x-axis represents UHI intensity in degrees Celsius, defined as the temperature difference between the object-specific temperature and an externally anchored rural reference temperature. The y-axis shows the predicted percentage change in property prices. The reference point for the price effect is the average UHI intensity, which corresponds to 2.56°C at 1 p.m. and 2.04°C at 4 a.m., indicated by the zero line on the y-axis. Estimates are derived from the semi-parametric GAM model 1, with smooth functions fitted separately for daytime and nighttime observations.

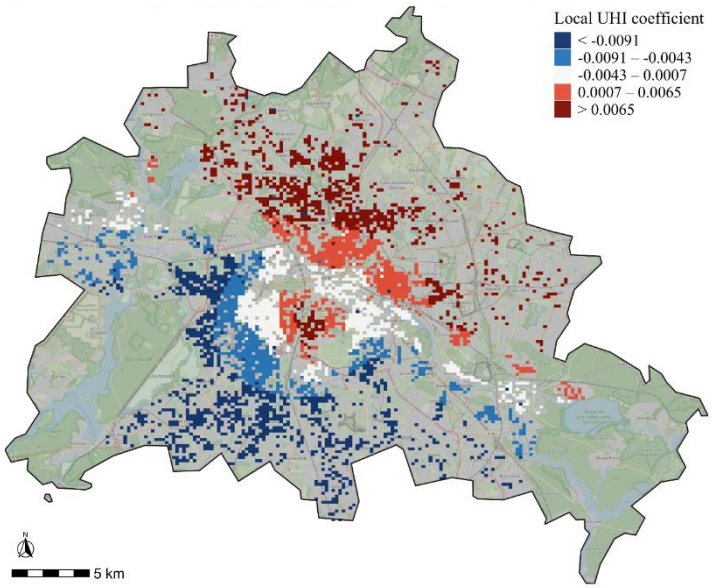
3.8.4 Appendix IV – Robustness Check - Spatial Analysis

Figure 3.16 Geographically Weighted Regression for 2014-16

(a) 4 a.m.



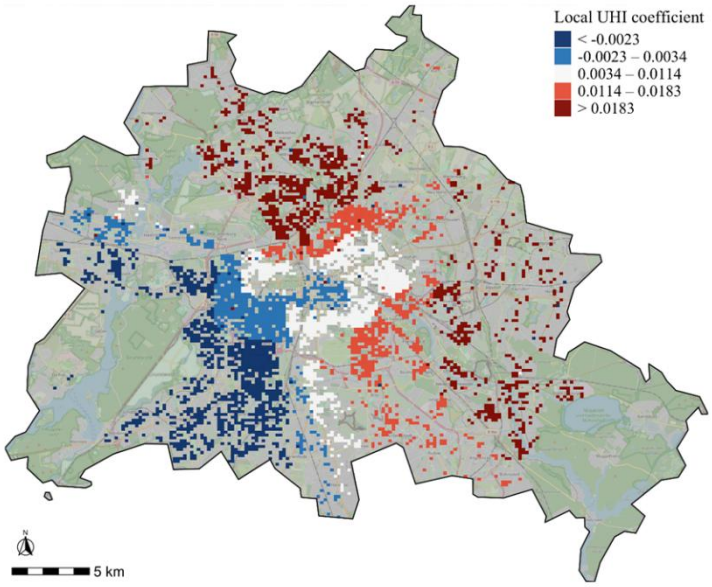
(b) 1 p.m.



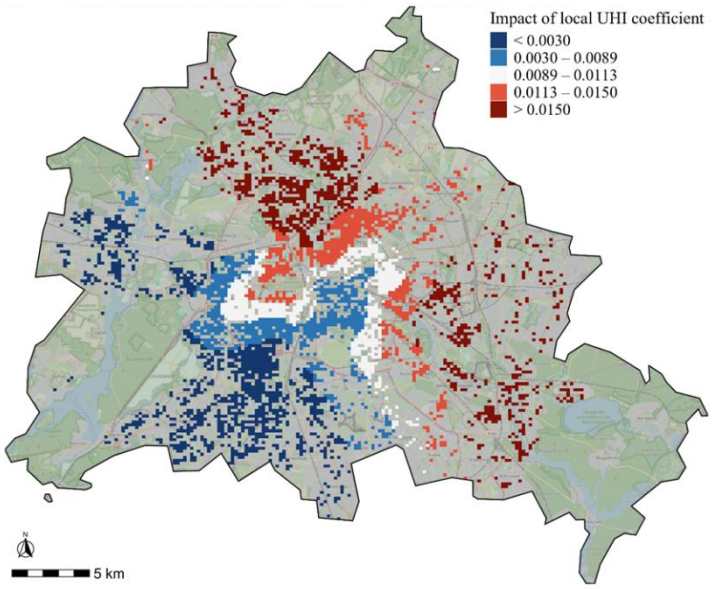
Note: The figures show the spatially varying coefficients of the UHI effect on property prices, determined using GWR, for the period 2014–2016. The color scales indicate the local regression coefficients, where positive (negative) values indicate a positive (negative) effect of UHI intensity on real estate prices, meaning that a higher UHI intensity is associated with higher (lower) property prices in the respective location.

Figure 3.17 Geographically Weighted Regression for 2017-19

(a) 4 a.m.



(b) 1 p.m.



Note: The figures show the spatially varying coefficients of the UHI effect on property prices, determined using GWR, for the period 2017–2019. The color scales indicate the local regression coefficients, where positive (negative) values indicate a positive (negative) effect of UHI intensity on real estate prices, meaning that a higher UHI intensity is associated with higher (lower) property prices in the respective location.

3.9 References

Addoum, J. M., Eichholtz, P., Steiner, E., & Yönder, E. (2024). Climate change and commercial real estate: Evidence from hurricane Sandy. *Real Estate Economics*, 52(3), 687–713.

Ahlfeldt, G. M., Heblich, S., & Seidel, T. (2023). Micro-geographic property price and rent indices. *Regional Science and Urban Economics*, 98, 103836.

Albouy, D., Graf, W., Kellogg, R., & Wolff, H. (2016). Climate amenities, climate change, and American quality of life. *Journal of the Association of Environmental and Resource Economists*, 3(1), 205–246.

Arnfield, A. J. (2003). Two decades of urban climate research: A review of turbulence, exchanges of energy and water, and the urban heat island. *International Journal of Climatology: A Journal of the Royal Meteorological Society*, 23(1), 1–26.

Bansal, R., Kiku, D., & Ochoa, M. (2016). *Price of long-run temperature shifts in capital markets* (Working Paper No. 22529). National Bureau of Economic Research.

Baylis, P., & Boomhower, J. (2019). *Moral hazard, wildfires, and the economic incidence of natural disasters* (Working Paper No. 26550). National Bureau of Economic Research.

Bernstein, A., Gustafson, M. T., & Lewis, R. (2019). Disaster on the horizon: The price effect of sea level rise. *Journal of Financial Economics*, 134(2), 253–272.

Bin, O. (2004). A prediction comparison of housing sales prices by parametric versus semi-parametric regressions. *Journal of Housing Economics*, 13(1), 68–84.

Borsky, S., Fesselmeyer, E., & Vogelsang, L. (2024). Urban heat and within-city residential sorting. *Journal of Environmental Economics and Management*, 127, 103014.

Bowler, D. E., Buyung-Ali, L., Knight, T. M., & Pullin, A. S. (2010). Urban greening to cool towns and cities: A systematic review of the empirical evidence. *Landscape and Urban Planning*, 97(3), 147–155.

Chay, K. Y., & Greenstone, M. (2005). Does air quality matter? Evidence from the housing market. *Journal of Political Economy*, 113(2), 376–424.

Chen, F., Zhang, J., & Chen, Z. (2025). Heat waves and housing markets: Assessing the effects on real estate prices in China. *Environmental and Resource Economics*, 88(6), 1541–1579.

Chen, S., Haase, D., Qureshi, S., & Firozjaei, M. K. (2022). Integrated land use and urban function impacts on land surface temperature: Implications on urban heat mitigation in Berlin with eight-type spaces. *Sustainable Cities and Society*, 83, 103944.

Chiang, C.-C., Feng, Z., & Harrison, D. (2022). *Heat stress and commercial real estate returns.* SSRN.

Choi, A., Kim, P., & Park, A. (2023). The effects of air quality on housing prices: Evidence from the Aliso Canyon gas leak. *Journal of Housing Economics*, 62, 101966.

Conroy, S. J., & Milosch, J. L. (2011). An estimation of the coastal premium for residential housing prices in San Diego County. *The Journal of Real Estate Finance and Economics*, 42(2), 211–228.

Contat, J., Hopkins, C., Mejia, L., & Suandi, M. (2024). When climate meets real estate: A survey of the literature. *Real Estate Economics*, 52(3), 618–659.

Contat, J. C., Doerner, W. M., Renner, R. N., & Rogers, M. J. (2025). Measuring price effects from disasters using public data: A case study of hurricane Ian. *Journal of Real Estate Research*, 47(2), 170–217.

Cragg, M., & Kahn, M. (1997). New estimates of climate demand: evidence from location choice. *Journal of Urban Economics*, 42(2), 261–284.

Cvijanović, D., Rolheiser, L., & Van de Minne, A. (2024). Commercial real estate and air pollution. *Real Estate Economics*, 52(3), 951–989.

Cvijanović, D., & Van de Minne, A. (2024). *Temperature extremes and commercial real estate*. SSRN.

Dell, M., Jones, B. F., & Olken, B. A. (2009). Temperature and income: Reconciling new cross-sectional and panel estimates. *American Economic Review*, 99(2), 198–204.

Dell, M., Jones, B. F., & Olken, B. A. (2012). Temperature shocks and economic growth: Evidence from the last half century. *American Economic Journal: Macroeconomics*, 4(3), 66–95.

Dell, M., Jones, B. F., & Olken, B. A. (2014). What do we learn from the weather? The new climate-economy literature. *Journal of Economic Literature*, 52(3), 740–798.

Dirks, J. A., Gorrissen, W. J., Hathaway, J. H., Skorski, D. C., Scott, M. J., Pulsipher, T. C., & Rice, J. S. (2015). Impacts of climate change on energy consumption and peak demand in buildings: A detailed regional approach. *Energy*, 79, 20–32.

Dodoo, A., & Gustavsson, L. (2016). Energy use and overheating risk of Swedish multi-storey residential buildings under different climate scenarios. *Energy*, 97, 534–548.

Donovan, G. H., Champ, P. A., & Butry, D. T. (2007). Wildfire risk and housing prices: a case study from Colorado Springs. *Land Economics*, 83(2), 217–233.

Duanmu, J., Li, Y., Lin, M., & Tahsin, S. (2022). Natural disaster risk and residential mortgage lending standards. *Journal of Real Estate Research*, 44(1), 106–130.

Dugord, P.-A., Lauf, S., Schuster, C., & Kleinschmit, B. (2014). Land use patterns, temperature distribution, and potential heat stress risk–the case study Berlin, Germany. *Computers, Environment and Urban Systems*, 48, 86–98.

European Environment Agency. (2024). *Europe's air quality status 2024*. Accessed: 2025-02-13. URL: https:// www.eea.europa.eu/publications/europes-air-quality-status-2024

Feng, P., Zhou, Z., Cohen, J. P., & Yasar, M. (2024). Air pollution and the effects on house prices: A push for sustainability. *Journal of Real Estate Research*, 46(3), 336–359.

Feng, Z., Lu-Andrews, R., & Wu, Z. (2025). Commercial real estate in the face of climate risk: Insights from REITs. *Journal of Real Estate Research*, 47(4), 435–463.

Fotheringham, A. S., Brunsdon, C., & Charlton, M. (2002). *Geographically weighted regression: The analysis of spatially varying relationships*. John Wiley & Sons.

Gabriel, K. M. A., & Endlicher, W. R. (2011). Urban and rural mortality rates during heat waves in Berlin and Brandenburg, Germany. *Environmental Pollution*, 159(8-9), 2044–2050.

Glaeser, E. L., & Gottlieb, J. D. (2006). Urban resurgence and the consumer city. *Urban studies*, 43(8), 1275–1299.

Götz, L., Mager, F., & Zietz, J. (2024). The effect of wildfires on mortgage pricing: Evidence from Portugal. *The Journal of Real Estate Finance and Economics*. Advance online publication.

Gourevitch, J. D., Kousky, C., Liao, Y., Nolte, C., Pollack, A. B., Porter, J. R., & Weill, J. A. (2023). Unpriced climate risk and the potential consequences of overvaluation in US housing markets. *Nature Climate Change*, 13(3), 250–257.

Harrison, D., Smersh, G. T., & Schwartz, A. (2001). Environmental determinants of housing prices: The impact of flood zone status. *Journal of Real Estate Research*, 21(1-2), 3–20.

Hastie, T., & Tibshirani, R. (1986). Generalized additive models. *Statistical Science*, 1(3), 297–310.

Heaviside, C., Vardoulakis, S., & Cai, X.-M. (2016). Attribution of mortality to the urban heat island during heatwaves in the West Midlands, UK. *Environmental Health*, 15, S27.

Huber, P. J. (1981). *Robust statistics*. John Wiley & Sons.

Iodice, S., Arbau, L., Maistrali, A., Marando, F., Melchiorri, M., Proietti, P., Sulis, P., Tainguy, O., & Vandecasteele, I. (2024). *EU cities and heat extremes* (Policy Brief No. JRC137891). European Commission.

Intergovernmental Panel on Climate Change. (2023). *Climate change 2023: Synthesis report. Contribution of Working Groups I, II and III to the Sixth Assessment Report of the Intergovernmental Panel on Climate Change* (H. Lee & J. Romero, Eds.).

Klaiber, H. A., Abbott, J. K., & Smith, V. K. (2017). Some like it (less) hot: extracting trade-off measures for physically coupled amenities. *Journal of the Association of Environmental and Resource Economists*, 4(4), 1053–1079.

Kolbe, J., Schulz, R., Wersing, M., & Werwatz, A. (2021). Real estate listings and their usefulness for hedonic regressions. *Empirical Economics*, 61, 3239–3269.

Li, H., Meier, F., Lee, X., Chakraborty, T., Liu, J., Schaap, M., & Sodoudi, S. (2018a). Interaction between urban heat island and urban pollution island during summer in Berlin. *Science of the Total Environment*, 636, 818–828.

Li, R. Y. M., Cheng, K. Y., & Shoaib, M. (2018b). Walled buildings, sustainability, and housing prices: An artificial neural network approach. *Sustainability*, 10(4), 1298.

Loomis, J. (2004). Do nearby forest fires cause a reduction in residential property values? *Journal of Forest Economics*, 10(3), 149–157.

Ma, L., & Yildirim, Y. (2023). High temperature, climate change and real estate prices. In *Proceedings of the EUROFIDAI-ESSEC Paris December Finance Meeting*.

McKenzie, R., & Levendis, J. (2010). Flood hazards and urban housing markets: The effects of Katrina on New Orleans. *The Journal of Real Estate Finance and Economics*, 40(1), 62–76.

Mora, C., Dousset, B., Caldwell, I. R., Powell, F. E., Geronimo, R. C., Bielecki, C. R., Counsell, C. W. W., Dietrich, B. S., Johnston, E. T., Louis, L. V., Lucas, M. P., McKenzie, M. M., Shea, A. G., Tseng, H., Giambelluca, T. W., Leon, L. R., Hawkins, E., & Trauernicht, C. (2017). Global risk of deadly heat. *Nature Climate Change*, 7(7), 501–506.

Mueller, J., Loomis, J., & González-Cabán, A. (2009). Do repeated wildfires change homebuyers' demand for homes in high-risk areas? A hedonic analysis of the short and long-term effects of repeated wildfires on house prices in Southern California. *The Journal of Real Estate Finance and Economics*, 38(2), 155–172.

Nguyen, D. D., Ongena, S., Qi, S., & Sila, V. (2022). Climate change risk and the cost of mortgage credit. *Review of Finance*, 26(6), 1509–1549.

Oke, T. R. (1973). City size and the urban heat island. *Atmospheric Environment (1967)*, 7(8), 769–779.

Oke, T. R. (1982). The energetic basis of the urban heat island. *Quarterly Journal of the Royal Meteorological Society*, 108(455), 1–24.

Oke, T. R. (2002). *Boundary layer climates*. Routledge.

Ortega, F., & Taşpınar, S. (2018). Rising sea levels and sinking property values: Hurricane Sandy and New York's housing market. *Journal of Urban Economics*, 106, 81–100.

Ridker, R. G., & Henning, J. A. (1967). The determinants of residential property values with special reference to air pollution. *The Review of Economics and Statistics*, 49(2), 246–257.

Rizwan, A. M., Dennis, L. Y., & Liu, C. H., (2008). A review on the generation, determination and mitigation of urban heat island. *Journal of Environmental Sciences*, 20(1), 120–128.

Roback, J. (1982). Wages, rents, and the quality of life. *Journal of Political Economy*, 90(6), 1257–1278.

Schlenker, W., & Roberts, M. J. (2008). *Estimating the impact of climate change on crop yields: The importance of nonlinear temperature effects* (Working Paper No. 13799). National Bureau of Economic Research.

Semenenko, I., & Yoo, J. (2019). Climate change and real estate prices. *International Journal of Economics and Finance*, 11(11), 1–11.

Sinha, P., & Cropper, M. L. (2013). *The value of climate amenities: Evidence from US migration decisions* (Working Paper No. 18756). National Bureau of Economic Research.

Sirmans, C. S., Sirmans, G. S., Smersh, G. T., & Winkler, D. T. (2025). Opinions on climate change, disaster risk, and single-family housing price growth. *Journal of Real Estate Research.* Advance online publication.

Stewart, I. D., & Oke, T. R. (2012). Local climate zones for urban temperature studies. *Bulletin of the American Meteorological Society*, 93(12), 1879–1900.

Turnbull, G. K., Zahirovic-Herbert, V., & Mothorpe, C. (2013). Flooding and liquidity on the bayou: The capitalization of flood risk into house value and ease-of-sale. *Real Estate Economics*, 41(1), 103–129.

Tyndall, J. (2023). Sea level rise and home prices: Evidence from Long Island. *The Journal of Real Estate Finance and Economics*, 67(4), 579–605.

Umweltbundesamt. (2024). *Bodenversiegelung*. Accessed: 2025-02-13. URL: https://www.umweltbundesamt.de/daten/flaeche-boden-land-oekosysteme/boden/bodenversiegelung#was ist bodenversiegelung

Voogt, J. A., & Oke, T. R. (2003). Thermal remote sensing of urban climates. *Remote Sensing of Environment*, 86(3), 370–384.

Xi, Y., Wang, S., Zou, Y., Zhou, X., & Zhang, Y. (2024). Seasonal surface urban heat island analysis based on local climate zones. *Ecological Indicators*, 159, 111669.

Zheng, S., Cao, J., Kahn, M. E., & Sun, C. (2014). Real estate valuation and cross-boundary air pollution externalities: evidence from Chinese cities. *The Journal of Real Estate Finance and Economics*, 48(3), 398–414.

Zhou, L., Fan, J., & Lin, Z. (2024). The value of clean air: Evidence from Chinese housing markets. *Journal of Real Estate Research*, 46(3), 360–388.

4 The Impact of Energy Policies in Residential Markets: Quantifying Retrofit Incentives and Asset Performance

4.1 Abstract

This paper quantifies the effectiveness of energy policy measures in creating investment incentives to improve the energy efficiency of residential buildings. Using the rent-to-price ratio as a market-based indicator of investment profitability, the study examines dynamics across property conditions, geographical differences, and time periods. The results confirm that energy retrofits of residential apartments yield both higher rental income and increased capital value. However, the effects vary over time and region, particularly in response to changing macroeconomic conditions and regulatory environments. Especially in markets with declining transaction activity and heightened uncertainty, policy measures fail to generate sufficient investment incentives for improving energy efficiency across market players. This underscores the need for a more targeted policy framework that incorporates market dynamics and spatial factors. The findings also emphasize the importance of market timing in investments related to energy efficiency measures.

Keywords: Residential Real Estate, Energy Performance Certificate, Stranded Assets, Generalized Additive Model

4.2 Introduction

It is estimated that 85-95% of today's buildings in Europe will still be in use by 2050, and around 75% of these are currently not considered energy-efficient (European Commission, 2020). Consequently, real estate owners face a long-term, future-oriented challenge: the need to become more sustainable, as the industry accounts for 37% of global carbon dioxide emissions (United Nations Environment Programme, 2024). To enhance energy efficiency, policymakers regard retrofits as a critical strategy for reducing energy consumption and its associated greenhouse gas emissions. Retrofits represent a crucial vehicle for achieving climate policy targets. Nevertheless, the retrofit rate in 2024 reached only 0.69%, indicating a pronounced need for enhancements (Bundesverband energieeffiziente Gebäudehülle, 2024). To incentivize the implementation of retrofit measures and achieve energy efficiency improvements, several regulatory measures have been implemented in the EU over the years.

This paper provides an understanding of the effectiveness of energy policy measures in evaluating whether they create economic incentives for retrofitting and improving the energy efficiency levels of residential properties. The analysis focuses on the rental and investment markets in Greater Munich over the past decade, a period shaped by fluctuating economic conditions. In addition to temporal developments, differing property conditions and spatial characteristics are considered to identify how market environments and regional disparities influence both investment behavior and the transmission of policy signals. Therefore, the study aims to offer a market-based perspective on how energy policy measures influence investor decisions and capital allocation.

Previous studies have demonstrated that energy efficiency influences the rents and prices of residential properties. Higher energy efficiency is linked to increased property valuation through higher rents and prices, and vice versa (Cajias et al., 2019; Cajias & Piazolo, 2013; Kholodilin et al., 2017; Olaussen et al., 2017; Petrov & Ryan, 2021; Pommeranz & Steininger, 2021; Taruttis & Weber, 2022; Taltavull De La Paz et al., 2019; Taltavull et al., 2017).

To precisely evaluate the impact of retrofitting, we compare rents and prices before and after a synthetic energy efficiency improvement using various semi-parametric regression models. The methodological approach accounts for the property's energy efficiency conditions and spatial factors as critical inputs in estimating rents and prices. The resulting rent-to-price ratio serves as a market-based indicator of investment viability.

The results show that property performance, as influenced by energy efficiency, depends heavily on market conditions. The financial benefit of improved energy efficiency is shaped not only by regional and socioeconomic factors but also by broader macroeconomic trends. In weak markets marked by declining prices, regulatory incentives often fall short, so retrofitting energy-inefficient properties becomes financially infeasible. In these cases, policy efforts have only partly achieved their objectives of encouraging market investment in the "worst-performing buildings". By contrast, retrofits are more viable in strong markets, such as those with rising prices and growing demand. Under such conditions, energy efficiency improvements become financially attractive. Additionally, energy policy measures appear more effective in less populated regions, while showing a lower impact in dense urban areas. Since retrofits lead to a greater change in the rent-to-price ratio in sparsely populated areas, the effects of policy measures vary across market structures. This highlights the need to account for both time and location when assessing energy policy effectiveness and its influence on investment decisions.

The paper is structured as follows: We begin with an overview of the relevant energy policies and prior research, then present the economic model. The following section outlines the dataset and descriptive statistics, providing the basis for the empirical analysis in Chapter 5. We conclude with a summary and directions for future research.

4.3 Regulatory Background of Energy Efficiency Policy in the European Union

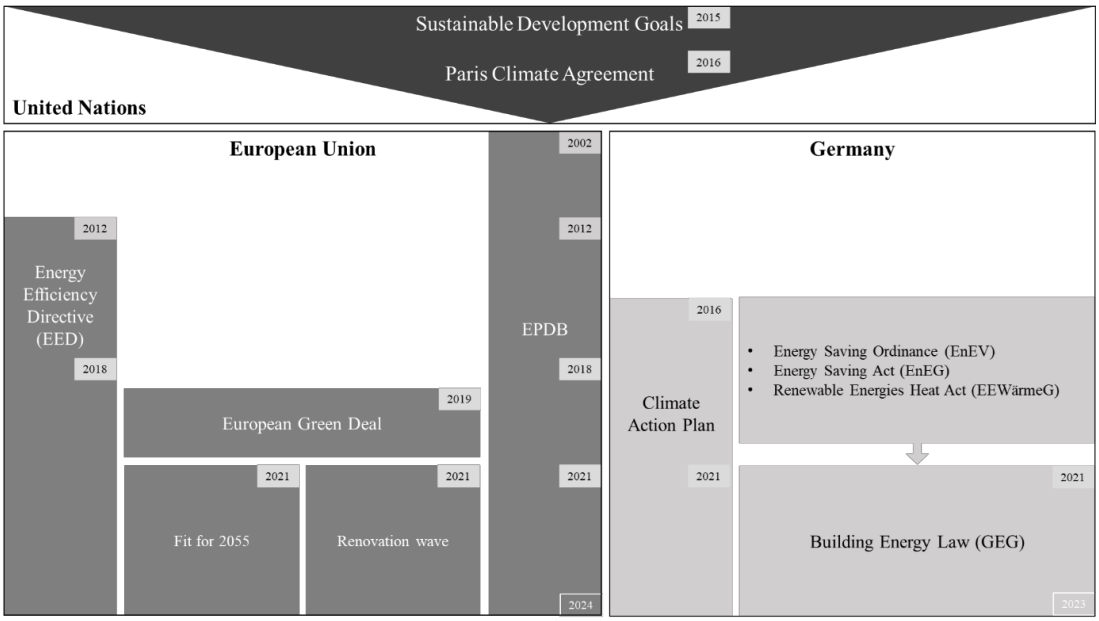
Various laws and regulations have been enacted to define climate targets and incentivize market players to reduce emissions through retrofitting and related measures. These policies aim to establish minimum energy efficiency standards for buildings in the highly heterogeneous real estate market. In this context, the regulatory framework focuses on "worst-performing buildings", as their renovation offers the greatest potential for meeting climate protection goals (Deutsche Energie-Agentur, 2021).

At the European level, the Energy Performance of Buildings Directive (EPBD) and the European Green Deal are the central directives for the building sector. With the recast of the EPBD in 2024, the European Union (EU) has introduced additional measures aligned with minimum energy performance standards to curb emissions. These measures aim to reduce average energy consumption in residential buildings by 16% by 2030 and 20–22% by 2035, relative to 2020. By 2050, all buildings are to become emission-free (European Parliament & Council of the European Union, 2024).

However, implementation varies across Europe, depending on political and legal frameworks and local housing market conditions. For example, the European Green Deal targets greenhouse gas neutrality by 2050 (European Commission, 2021) and Germany's Climate Action Plan sets a target for 2045 (Bundesklimaschutzgesetz [KSG], 2021).

Figure 4.1 outlines the critical directives and energy policies affecting the building sector in Europe and Germany, which are crucial for reaching the 2050 goal. Several laws have been enacted in Germany, some more detailed and restrictive than those in other European countries.

Figure 4.1 Timeline of Directives/Regulations for the Building Sector



Note: The figure illustrates the regulatory landscape of the building sector at three levels: global, European Union, and Germany. The upper section highlights global initiatives, such as the United Nations Sustainable Development Goals (SDGs) and the Paris Climate Agreement, which have spurred multiple directives in Europe and Germany. European directives are presented on the left-hand side of the figure, while German regulations are detailed on the right-hand side. The figure includes specific timelines for the enactment and subsequent amendments of these regulations, highlighting the interrelated impacts. The most recent amendment is the recast of the Energy Performance of Buildings Directive (EPBD) within the European Union.

Translating these goals into concrete retrofitting strategies requires the creation of an effective and comparable framework for assessing the energy efficiency of buildings. In the EU, energy performance certificates (EPCs) serve as the predominant framework. However, assessment methods vary across member states. In the United Kingdom (UK), the rating scale ranges from A to G (Government UK, 2023), whereas in Germany, it spans from AA to H (see Table 4.1) (Gebäudeenergiegesetz [GEG]). Due to the regional differences in energy efficiency - driven by geography and climate - a targeted analysis is required to assess the feasibility of retrofitting at the national or regional level (Himmelberg et al., 2005).

Table 4.1 EPC Nomenclature in Germany

EPC	AA	A	B	C	D	E	F	G	H
Energy performance values (EPV) in kWh/m²/year	0–30	31–50	51–75	76–100	101–130	131–160	161–200	201–250	> 250

Note: The EPC nomenclature is based on the GEG, §80 and outlines the classification of buildings' energy characteristics. The energy efficiency classes are categorized from AA to H, with continuous energy performance values expressed in kWh/m²/year.

4.4 Literature Review

Historically, one of the earliest research papers to apply a hedonic pricing model to energy efficiency and house purchase prices examined fuel savings and their effect on sales prices in Des Moines, Iowa (Dinan & Miranowski, 1989). Since then, numerous studies have been conducted globally. Europe shows a relatively low green premium compared to other continents (Cespedes-Lopez et al., 2019). Due to the regional variation in energy efficiency, depending on geography and climate, a targeted analysis is needed to assess retrofitting feasibility at a national or regional level (Himmelberg et al., 2005).

Within the EU, the study by Brounen and Kok (2011) was among the first to demonstrate that higher EPC ratings, especially when paired with quality labels, have a significant impact on transaction prices. Subsequent studies have built on these findings. Table 4.2 summarizes the most relevant studies on the European market.

Despite variability in the size of green premiums[21] and brown discounts[22], EPCs remain useful indicators for valuation. However, McCord et al. (2020) and Lu and Spanjers (2025) show that the influence of EPCs varies significantly by region and market transparency due to differing levels of understanding and trust among market participants.

Since tenants and owners have distinct perspectives on value development, incorporating both is essential for a comprehensive understanding. This is particularly relevant in Germany, Europe's second-largest rental market, where approximately 50.5% of all households are renters (Eurostat, 2023). The German rental market remains stable by international standards, especially in its resilience to inflationary and speculative pressures (Chinloy et al., 2018). Within this context, Cajias & Piazolo (2013) examine a positive relationship between rents and energy efficiency, with returns improving as energy consumption decreases. However, the short observation window between 2008 and 2010

[21] The green premium refers to the additional value attributed to environmental features in houses or property conditions. This premium directly influences housing prices and rents, as buyers have a higher willingness to pay (WTP) for sustainable amenities.
[22] The brown discount reflects the implicit price reductions associated with from a lower energy efficiency, serving as the inverse of the green premium (Marmolejo-Duarte & Chen, 2019).

limits the relevance of their findings in light of subsequent regulatory and macroeconomic developments. Extending the analysis, Cajias et al. (2019) highlight the nonlinear nature of this relationship, with notable differences between urban and rural areas. In densely populated urban markets with high demand, energy efficiency tends to be less impactful than location-specific factors (Petrov & Ryan, 2021).

Table 4.2 Literature Review of Green Premiums for Prices in Europe

Citation	Location	Property type	Method	Variable type	Price Premium
Kholodilin et al. (2017).	Germany	Single-family houses	Hedonic regression	Continuous (EPV)	> 0.05% per m² for every 1 kWh/m²/year decrease in energy consumption
Olaussen et al. (2017).	Norway	Range of residential types	Hedonic regression	Categorical (EPC)	Houses with better EPC sold for a higher price, with no significant price premium associated with EPC
Taltavull et al. (2017).	Romania	Dwellings	Hedonic regression	Continuous (EPV)	> 2.2% to 6.5% per m²for every 1 kWh/m²/year decrease in energy consumption
Taltavull de La Paz et al. (2019).	Spain	Multi-family houses	Hedonic regression	Continuous (EPV)	> 3% per m² for every 1 kWh/m²/year decrease in energy consumption
Fuerst et al. (2015).	United Kingdom	Dwellings	Hedonic regression	Continuous (EPV)	> 6% B/C compared to D > -10 - 11% for F/G compared to D
Chegut et al. (2016).	Nether-lands	Dwellings	Hedonic regression	Categorical (EPC)	All premiums are based on the reference EPC C > 6.3% for EPC A > 2.0% for EPC B > -0.7% for EPC D > -1.6% for EPC E > -1.7% for EPC F > -1.3% for EPC G
Taruttis & Weber (2022).	Germany	Single-family houses	Hedonic regression	Continuous (EPV)	Per m² if energy consumption decreases by 1 kWh/m²/year > 0.04% in large cities > 0.06% in urban areas > 0.09% in densely populated rural areas > 0.10% in sparsely populated rural areas
de Ayala et al. (2016).	Spain	Dwellings	Hedonic regression	Categorical (EPC)	> 9.8% for A-C compared to D-G

Note: This table compares the impact of energy efficiency on real estate prices across various countries as investigated in several academic publications. Each entry in the table includes a literature citation, the geographical location, the category of property studied, the statistical method used, the type of variable (either categorical or continuous with respect to energy efficiency), and the observed price premium or change in property value. The studies span from 2015 to 2023 and cover a range of regional areas in Europe. The table provides insight into the effect of energy efficiency on property prices under different market conditions and varying energy efficiency standards.

Nevertheless, growing environmental awareness and rising energy costs have increased the importance of energy efficiency in rental pricing. Pommeranz and Steininger (2021) find that energy-inefficient dwellings are increasingly subject to rental discounts. These findings are supported by international studies that report rental green premiums in markets beyond Germany (Brändle et al., 2025; Hyland et al., 2013; McCord et al., 2024). Energy-efficient assets thus serve as a hedge against future regulatory and cost-related risks (Cajias et al., 2019). Cajias et al. (2019) analyze green premiums on the rental market up to 2017. However, since their dataset predates major energy policy measures, such as the EU Taxonomy and the revised Building Energy Act (GEG), as well as the COVID-19 pandemic, potential shifts in market behavior remain unexplored.

Previous research has already highlighted the importance of market dynamics and investment perspectives in the commercial market. For example, Ghosh and Petrova (2024) demonstrate that the green premium in commercial real estate markets is sensitive to broader economic conditions. Therefore, it seems reasonable to assume that evolving market conditions influence the impact of refurbishments on rents and prices in the residential market.

Several studies address barriers to energy retrofit investments in the housing market. These include information deficits, capital constraints and limited short-term profitability, particularly for low-income households, even in the presence of subsidies (Schuetz, 2024). Caloia and Mastrogiacomo (2022) show that renovations are only economically viable when supported by strong regulatory frameworks. Muzio et al. (2025) find that while the impact of command-and-control regulations, such as stricter energy standards, increases willingness to pay, they also suppress construction activity, leading to long-term supply shortages. As a result, market capitalization tends to become insufficient and delayed. Similarly, Deng et al. (2024) argue that policy tools like credit restrictions or transaction taxes may help stabilize prices in overheated markets but can also trigger unintended volatility and distortions in submarkets. Additionally, André et al. (2017) demonstrate that economic uncertainty increases price volatility and limits investment activity. In such periods, existing barriers to investment become more pronounced, reinforcing the need for targeted policy measures.

Cajias (2019) uses the rent-to-price ratio to quantify investment risk within this context. Expanding on this, Gilbukh et al. (2022) emphasize the value of the ratio as an early warning signal for real estate markets, especially under fluctuating market conditions.

The previous studies confirm the existence of green premiums and how they vary by region and property condition. However, the regulatory and market context in which they emerge remains largely unexplored. This study, therefore, links rent and price dynamics to the evolving regulatory framework for improving building energy efficiency. By accounting for building conditions, spatial heterogeneity, market timing and differences between rents and prices, the research evaluates the effectiveness of energy policy measures and how policy interventions translate into investment signals.

4.5 Data

To minimize distortions, we focus on a homogeneous residential building type, specifically apartments, and select a consistent political region for analysis.[23] The EU's various political directives and climatic conditions make such differentiation appropriate (Dell'Anna et al., 2019; Sebi et al., 2019). According to the SDG Report 2023, Germany ranks fourth in sustainability measures, ahead of the United Kingdom (11th) and the United States (39th) (Sachs et al., 2023). Germany's relatively high rental prices, lower susceptibility to macroeconomic shocks (Voigtländer, 2014) and polycentric metropolitan structure underscore the importance of regional segmentation. Additionally, cross-market differences must also be considered within the scope of political intervention, such as rent control (Mense et al., 2023).

This study focuses on the Greater Munich region ("Oberbayern" at the NUTS-3 level). Munich is one of Germany's and Europe's most economically dynamic and fastest-growing cities, serving as a business, science and innovation hub. The city's population grew by 7.5% between 2013 and 2024, reaching 1.58 million, driven by substantial immigration and increased birth rates (Statistisches Amt der Landeshauptstadt München, 2024). However, this rapid population growth also poses challenges, such as increased demand, low vacancy rates and rising rental and property prices.

The dataset for this analysis is compiled from multiple sources, including socioeconomic data from GfK[24], spatial data from OpenStreetMap[25] and real estate data from VALUE market data[26], which aggregates building characteristics from more than 100 German multiple listing systems. Consequently, the analysis relies on asking prices and rents rather than transaction values, as in Baye and Dinger (2024) and Cajias (2019). In Germany, especially in densely populated areas, negotiations over listing prices are rare, so transaction values typically align with listed offers (Kolbe et al., 2021).

The analysis employs pooled cross-sectional data from separate rental and sales datasets because it is impractical to collect matched rental and sales data for the same property (since a property cannot be rented and sold simultaneously). Both datasets cover the same period of 38 quarters, from April 2014 to August 2023.

[23] This approach enables the exclusion of disruptive factors and ensures a consistent sample, allowing for a more precise depiction of marginal effects. Moreover, the procedure aligns with existing literature on green premiums (see Table 4.2).
[24] Growth from Knowledge (GfK) (https://www.gfk.com/home)
[25] OpenStreetMap (https://www.openstreetmap.org)
[26] VALUE market data (Value, 2023)

The time horizon is divided into four periods to reflect the changes in the regulatory framework and macroeconomic environment:

- **Period 1:** The time before the implementation of the Climate Action Plan, Germany's first restrictive regulation.
- **Period 2:** The years 2016 to 2019, during which the effects of the Climate Action Plan became visible in the market.
- **Period 3:** The period in which the impacts of the COVID-19 pandemic and the European Green Deal emerged.
- **Period 4:** The most recent phase (2022–2023) is characterized by the implementation of the German Building Energy Act (GEG) and the ongoing consequences of the COVID-19 pandemic. Rising interest rates, inflation reaching up to 8.7% and sharply increasing construction costs have contributed to a shift in the real estate market (Statistisches Bundesamt, 2023). Given the exceptional conditions, Period 4 will be examined separately.

All preprocessing techniques, assumptions, and adjustments for the independent variables are applied consistently to both datasets. The initial samples contain over 139 variables, encompassing hedonic property characteristics and geographical points of interest. Demographic variables at the ZIP code level are also included to derive findings based on population density and housing demand. Regions with over 21,459 inhabitants at the ZIP code level are classified as densely populated, while those below this threshold are considered sparsely populated.[27] Each dwelling's exact location is identified using longitude and latitude coordinates.

The energy efficiency of a building, a critical variable, is represented by categorical variables ranging from 'EPC AA' to 'EPC H' (see Appendix). Despite mandatory disclosure requirements, the data density for energy characteristics remains relatively sparse.[28] During the data cleaning process, observations missing relevant variables are excluded, and housing categories like student or public housing are removed, following a similar approach to Cajias (2019). Outliers in numerical variables are removed based on the 98th interquartile range (IQR).

To ensure that 'EPC H' is included in the model, the upper limit for the Energy Performance Value (EPV) is set at 300 kWh/m²/year, regardless of IQR results. These adjustments reduce the original sample from 433,000 rental and 211,000 sales disclosures to 114,758 and

[27] Based on the average median level per ZIP code.
[28] A crucial number of rental and sales listings are incomplete, particularly those missing energy efficiency information. This omission raises the possibility that listings without energy data may disproportionately exclude apartments with high EPV and poor EPC ratings, introducing potential bias in the dataset.

85,832, respectively, each comprising 33 variables. Removing outliers and transforming selected variables are critical to preventing multicollinearity and enabling meaningful data reduction (see Appendix).

Certain variables, including rent, price and size, undergo logarithmic transformations to address their positively skewed distribution and to mitigate heteroscedasticity. Tables 4.3 and 4.4 show that the structures of the two datasets are comparable, with only minimal differences in EPV characteristics. The rental market exhibits an average EPV of 105 kWh/m²/year, while the ownership market shows an average value of 108 kWh/m²/year.

Table 4.3 Descriptive Statistics of the Rent Dataset

	Mean	Std. Dev.	Q5.	Median	Q95.
Rent	1,006.631	429.155	450.000	920.000	1,860.000
Log(rent)	6.826	0.424	6.109	6.824	7.528
Size	70.544	24.84	32.000	69.000	115.000
Log(size)	4.189	0.378	3.466	4.234	4.745
Rooms	2.459	0.900	1.000	2.000	4.000
Age	38.717	27.365	4.000	35.000	88.000
EPV	105.057	49.940	27.100	103.100	190.000
Floors	1.704	1.402	0.000	1.000	4.000
Km to bus	0.196	0.156	0.042	0.161	0.448
Km to railway	2.000	2.166	0.238	1.205	7.044
Km to school	0.423	0.300	0.097	0.357	0.971
Km to restaurant	0.264	0.210	0.033	0.213	0.687
Km to supermarket	0.368	0.320	0.060	0.289	0.922
Km to kindergarten	0.356	0.293	0.072	0.291	0.823
Km to pharmacy	0.429	0.422	0.066	0.317	1.103
Km to park	0.471	0.564	0.077	0.314	1.423
Km to bakery	0.343	0.307	0.055	0.262	0.882
Km to playground	0.247	0.198	0.038	0.202	0.598
Km to biergarten	1.124	1.097	0.169	0.787	3.657
Km to motorway	3.091	3.258	0.470	2.018	10.125
Km to doctors	0.625	0.746	0.070	0.414	1.827
Km to hospital	2.304	2.452	0.285	1.361	7.950
Km to CBD	24.008	26.690	2.016	10.030	76.871
Longitude	11.643	0.341	11.266	11.568	12.523
Latitude	48.159	0.222	47.828	48.140	48.746
Population per ZIP	20,800.432	8,251.776	6,593.000	21,188.000	35,295.000
Income per household	57,936.545	7,694.357	45,110.890	57,983.400	71,233.390
Retrofitted	0.378	0.485			
Kitchen	0.626	0.484			
Parking	0.726	0.446			
Elevator	0.578	0.494			
Balcony or terrace	0.824	0.381			
EPC AA	0.058	0.233			
EPC A	0.079	0.27			
EPC B	0.165	0.371			
EPC C	0.17	0.376			
EPC D	0.224	0.417			
EPC E	0.172	0.377			
EPC F	0.095	0.293			
EPC G	0.03	0.17			
EPC H	0.007	0.085			

Note: Table 4.3 provides comprehensive descriptive statistics for both the rent dataset, showing the distribution and variability of the variables included in the study except for the spatial and fixed time effect variables. For each variable, the table contains the mean values, the standard deviation (SD), the 5th percentile (Q5), the median values and the 95th percentile (Q95).

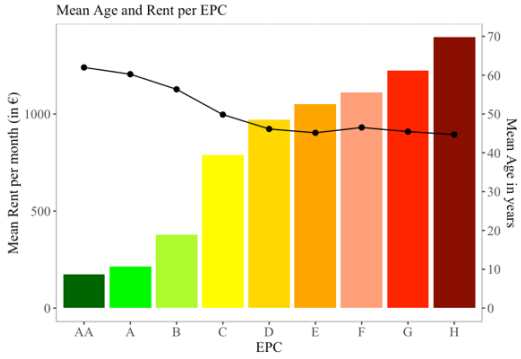
Table 4.4 Descriptive Statistics of the Price Dataset

	Mean	Std.Dev.	Q5	Median	Q95
Price	450,548.538	251,261.395	148,000.000	395,000.000	949,700.000
Log(price)	12.867	0.565	11.905	12.887	13.764
Size	73.917	27.530	31.996	72.475	125.000
Log(size)	4.228	0.401	3.466	4.283	4.828
Rooms	2.630	1.001	1.000	3.000	4.000
Age	38.387	23.322	5.000	40.000	68.000
EPV	108.896	48.093	30.000	109.000	190.000
Floors	1.849	1.690	0.000	2.000	5.000
Km to bus	0.192	0.130	0.043	0.164	0.430
Km to railway	1.977	2.105	0.233	1.188	6.657
Km to school	0.418	0.274	0.105	0.364	0.937
Km to restaurant	0.263	0.188	0.042	0.217	0.645
Km to supermarket	0.345	0.255	0.060	0.285	0.810
Km to kindergarten	0.352	0.266	0.072	0.294	0.795
Km to pharmacy	0.393	0.316	0.076	0.307	1.010
Km to park	0.426	0.453	0.078	0.306	1.209
Km to bakery	0.333	0.257	0.066	0.263	0.826
Km to playground	0.251	0.179	0.043	0.214	0.590
Km to biergarten	1.051	0.959	0.167	0.776	3.160
Km to motorway	3.041	3.301	0.530	1.986	9.860
Km to doctors	0.600	0.632	0.077	0.426	1.574
Km to hospital	2.156	2.162	0.298	1.374	7.394
Km to CBD	23.234	27.391	2.243	9.243	80.090
Longitude	11.640	0.354	11.256	11.563	12.555
Latitude	48.141	0.215	47.761	48.138	48.731
Population per ZIP	21,665.725	8,019.365	8,503.000	21,813.000	35,934.000
Income per household	56,794.065	7,397.804	44,963.984	56,829.110	68,874.670
Retrofitted	0.338	0.473			
Kitchen	0.597	0.491			
Parking	0.801	0.399			
Elevator	0.636	0.481			
Balcony or terrace	0.856	0.351			
EPC AA	0.050	0.218			
EPC A	0.072	0.258			
EPC B	0.129	0.336			
EPC C	0.173	0.378			
EPC D	0.254	0.435			
EPC E	0.183	0.387			
EPC F	0.101	0.302			
EPC G	0.032	0.175			
EPC H	0.006	0.074			

Note: Table 4.4 presents comprehensive overview of the descriptive statistics for both the price dataset, detailing the distribution and variability of the variables included in the study, excluding spatial and fixed time effect variables. For each variable, the table contains the mean values, the standard deviation (SD), the 5th percentile (Q5), the median values and the 95th percentile (Q95).

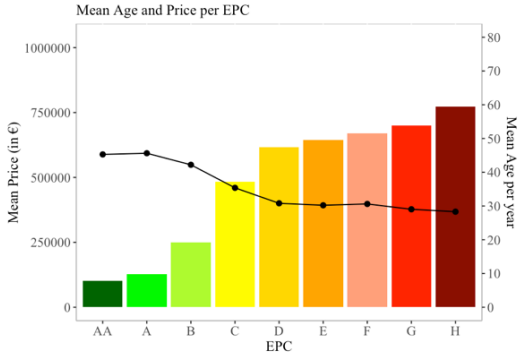
When considering correlations, the negative relationship between building age and rent (-0.06) indicates that older buildings tend to command lower rents. Consistent with this, EPV and age are positively correlated (0.63), meaning older buildings typically have higher energy consumption. These trends are also reflected in lower EPC ratings for older buildings (Figures 4.2 and 4.3).

Figure 4.2 Mean Rent and Age per EPC



Note: The line represents the mean rent (left-hand side (LHS)) for each EPC, while the bars indicate the mean age of properties (right-hand side (RHS)) within each EPC category.

Figure 4.3 Mean Price and Age per EPC



Note: The line represents the mean price (left-hand side (LHS)) for each EPC, while the bars indicate the mean age of properties (right-hand side (RHS)) within each EPC category.

A notable disparity arises for apartments rated 'EPC C' and below. Rental apartments tend to be older than those sold, suggesting a longer lifespan for rental apartments. Among all point of interest variables, proximity to Munich's central business district (CBD) shows the strongest correlation with rents and prices, highlighting the importance of metropolitan access. In contrast, the negative correlation with motorway distance underscores the continued importance of car accessibility in this regionally diverse dataset.

In both rental and sales datasets, apartments with better energy efficiency standards tend to be higher-priced and generally newer than those with lower energy efficiency standards. When comparing the datasets, the depreciation effect is more pronounced in sales prices than in rents, particularly for properties with EPC values below D. This suggests property prices are more sensitive to variations in energy efficiency than rental rates.

4.6 Methodology

The regressions are calculated independently for both the price and the rental data samples. Nevertheless, both models are estimated using the same fundamental criteria of building characteristics and geographical locations to determine the values for the same asset across the investment and rental markets. Comparing absolute values across locations can be problematic (Hattapoglu & Hoxha, 2014), the analysis includes variables that distinctly identify each property. All models are calculated using the statistical software R, version 4.3.1 (2022; R Core Team, 2023).

The ordinary least squares (OLS) linear regression approach is widely used in recent studies (Fuerst et al., 2015; Kholodilin et al., 2017; Olaussen et al., 2017; Taltavull et al., 2017; Taltavull De La Paz et al., 2019; Taruttis & Weber, 2022). However, as the OLS model falls

short in capturing complex relationships between variables, it is used primarily as a benchmark.

The generalized additive model (GAM), introduced by Hastie and Tibshirani (1986), addresses these by incorporating penalized smooth terms. This semi-parametric methodology is rooted in the Generalized Linear Model (GLM)[29] formulated by Nelder and Wedderburn (1972). While OLS aims to minimize inaccuracies in estimated coefficients, GAMs allow covariates to adopt a nonlinear functional structure (Eilers & Marx, 1996). This approach reduces the variance of errors and improves the model performance.

Pioneering research by Mason and Quigley (1996) was the first to apply the GAM within a real estate framework, demonstrating its advantages over OLS models. The enhanced flexibility and precision of GAMs have since led to their growing adoption in price prediction contexts (Cajias & Ertl, 2018). By using splines to integrate nonlinear relationships, the sample and a suitable model are precisely defined.

$$g(\hat{P}_{ijt}) = X_{ijt}^{\hat{P}}\beta^{\hat{P}} + Z_j^{\hat{P}}\delta^{\hat{P}} + \mu_t^{\hat{P}}\theta^{\hat{P}} + f(\tilde{x}_{ijt}^{\hat{P}}) + \varepsilon_{ijt} \quad (4.1)$$

$$g(\hat{R}_{ijt}) = X_{ijt}^{\hat{R}}\beta + Z_j^{\hat{R}}\delta^{\hat{R}} + \mu_t^{\hat{R}}\theta^{\hat{R}} + f(\tilde{x}_{ijt}^{\hat{R}}) + \epsilon_{ijt} \quad (4.2)$$

Equations (4.1) and (4.2) represent the models where P and R correspond to the prices and rents, respectively, of asset i, in ZIP code j and at time t. Each dwelling is characterized by the matrices $X_{ijt}^{\hat{P}}$ and $X_{ijt}^{\hat{R}}$, which include various continuous and binary hedonic characteristics. Within these vectors $X_{ijt}^{\hat{P}}$ and $X_{ijt}^{\hat{R}}$, the EPC rating is included using the most frequently occurring category as the reference level. Additionally, ZIP code-specific covariates are incorporated in $Z_j^{\hat{P},\hat{R}}$ to capture location effects. To control unobserved serial error components and fixed time effects, quarterly dummies ($\mu_t^{\hat{P}}$, $\mu_t^{\hat{R}}$) are included for the period when the dwelling was listed. These time-related vectors account for factors such as the economic situation, vacancy trends and the impact of the COVID-19 pandemic.

The GAM model also includes nonlinear variables via splines $f(\tilde{x}_{ijt}^{\hat{P}})$, $f(\tilde{x}_{ijt}^{\hat{R}})$, using a predefined set of nonlinear functions. The equations are calculated separately for each dwelling, with $\epsilon_{ijt}$and ε_{ijt} representing the error terms. The coefficients to be estimated include $\beta^{\hat{P}}$, $\beta^{\hat{R}}$ $\delta^{\hat{P}}$, $\delta^{\hat{R}}$ $\theta^{\hat{P}}$ and $\theta^{\hat{R}}$.

[29] The GLM offers flexibility, allowing the response to be distributed according to an exponential distribution family such as binomial, passion and gamma distributions (Nelder & Wedderburn, 1972).

Rent-to-Price Ratio

The rent-to-price ratio is used as a relative performance indicator, often referred to as the Net Initial Yield (NIY), as it relates the income generated by an asset (Net Operating Income (NOI)) to its market value (Rottke & Krautz, 2017). In a real estate context, annual rent (R) is considered NOI, while the gross purchase price (P) represents the property's market value (Cajias, 2019).

$$y = \frac{R}{P} \tag{4.3}$$

The P is determined by the sum of the defined price, transaction costs (TC) and property taxes (Cajias, 2019). Since TCs are not part of the database, they are assumed to be 4% of the price, covering brokerage fees and technical, legal and due diligence checks, following the assumptions made by Cajias (2019). Property taxes are also integrated, with the tax rate varying across German states, with Bavaria applying a rate of 3.5% (Grunderwerbsteuergesetz [GrEStG]). As net asking rents are tracked, no additional costs are incorporated in the numerator (Cajias, 2019).

The predicted purchase price and annual rent are used to evaluate the rent-to-price ratio, a proxy for the expected return and an indicator of investment incentives across the market (Baye & Dinger, 2024).

The estimated rent-to-price ratio for dwelling i at time t is denoted as $\hat{\imath}_{it}$ and calculated as follows:

$$\hat{\imath}_{it}^{pre\ retrofit} = 100 * \frac{12 * e^{\left(X_{ijt}^{\hat{R}}\beta^{\hat{R}} + Z_j^{\hat{R}}\delta^{\hat{R}} + \mu_t^{\hat{R}}\theta^{\hat{R}} + f\left(x_{ijt}^{\hat{R}}\right)\right)}}{e^{\left(X_{ijt}^{\hat{P}}\beta^{\hat{P}} + Z_j^{\hat{P}}\delta^{\hat{P}} + \mu_t^{\hat{P}}\theta^{\hat{P}} + f\left(x_{ijt}^{\hat{P}}\right)\right)} * (1 + Tax\ Rate) * (1 + TC)} \tag{4.4}$$

In the synthetic retrofit scenario, adjustments are applied simultaneously to both models, particularly to energy efficiency characteristics. Apartments with an EPV exceeding 130 kWh/m²/year are targeted for improvement. A retrofit that reduces EPV by 100 kWh/m²/year is defined as optimal, acting as a safeguard against stricter policy measures (Taruttis & Weber, 2022). The 'retrofit' dummy variable is adjusted accordingly.

A further critical adjustment involves the assumed building age. Following Fuerst et al. (2016), improving the EPC rating by one level corresponds to a six-year reduction in the building's age, reflecting an extended property lifespan. After applying these changes, new rents and property prices are re-estimated using the previously defined regression models,

holding all other variables constant. The effect of the synthetic retrofit is calculated as the difference between the pre- and post-retrofit rent-to-price ratio, denoted as $\Delta\hat{\imath}_{it}$,:

$$\Delta\hat{\imath}_{it} = \hat{\imath}_{it}^{pre\ retrofit} - \hat{\imath}_{it}^{post\ retrofit} \quad (4.5)$$

4.7 Results

The following section evaluates the effects of a synthetic retrofit across EPC ratings, regions and time to assess whether current energy policy measures create effective investment incentives. Before presenting the results, the performance of the applied models is compared. The semi-parametric GAM approach demonstrates superior estimation accuracy compared to the linear OLS benchmark, resulting in a more accurate depiction of how various characteristics influence the dependent variable (Table 4.5).

The evaluation of key performance indicators[30] and the adjusted coefficients of determination (adj. R^2) confirms that the more flexible GAM provides more precise estimation than OLS models. Therefore, the subsequent analysis is based on a GAM, which aligns with Cajias (2019).

Table 4.5 Model Comparison of OLS and GAM

		Rental market		Investment market	
	Model	**OLS (1)**	**GAM (2)**	**OLS (3)**	**GAM (4)**
Adj. R^2		0.862	0.900	0.854	0.908
MAE	Mean Absolute Error	119.740	10.220	70,353.650	56,369.900
RMSE	Root Mean Squared Error Loss	167.322	143.334	108,348.500	86,411.160
MAPE	Mean Absolute Percentage Error	0.122	0.102	0.168	0.129
MedAPE	Median Absolute Percentage Error	0.001	0.003	0.122	0.094
RRSE	Root Relative Squared Error Loss	0.390	0.334	0.433	0.344

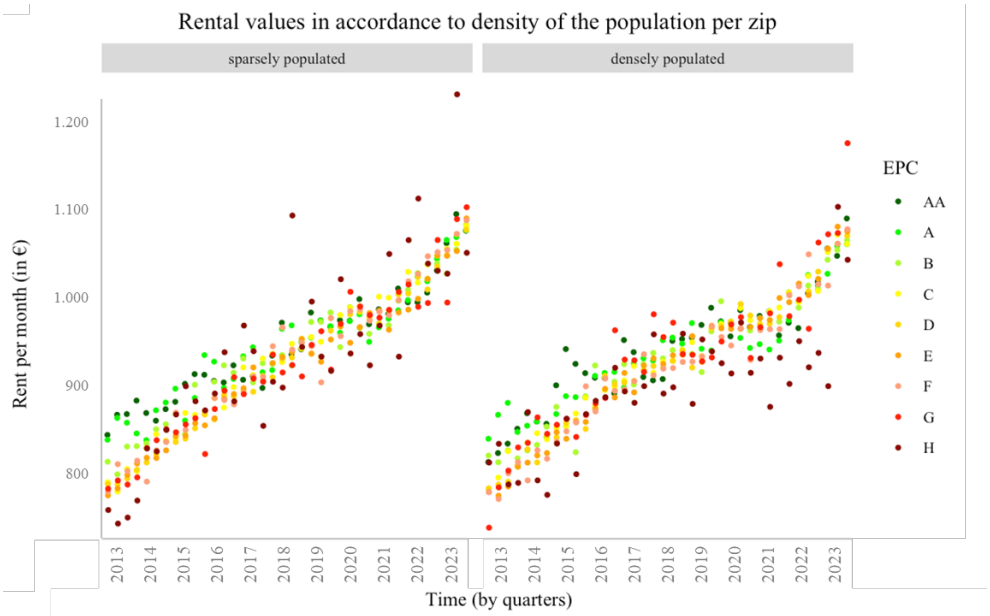
Note: The table presents a comparative analysis of the model performance between Ordinary Least Squares (OLS) and generalized additive models (GAM) across two market types: rental and price markets. Each model is evaluated using a range of statistical measures, including Adjusted R-squared (Adj. R2), Mean Absolute Error (MAE), Root Mean Squared Error Loss (RMSE), Mean Absolute Percentage Error (MAPE), Median Absolute Percentage Error (MedAPE) and Root Relative Squared Error Loss (RRSE), to assess model accuracy and error.

The estimated rents and prices are illustrated in Figures 4.4 and 4.5.[31] Rental values have steadily increased from around 800€ to 1,100€ despite shifts in market conditions over the past decade, reflecting the resilience of the rental market (Figure 4.4). However, rent growth stagnated during the COVID-19 pandemic (2020–2021), particularly in sparsely

[30] The formulas for the error terms MAE, MedAPE, MAPE, RMSE and RRSE are provided in the appendix.
[31] In both figures and the following analysis, a distinction is made between sparsely and densely populated areas to account for differences in market structures.

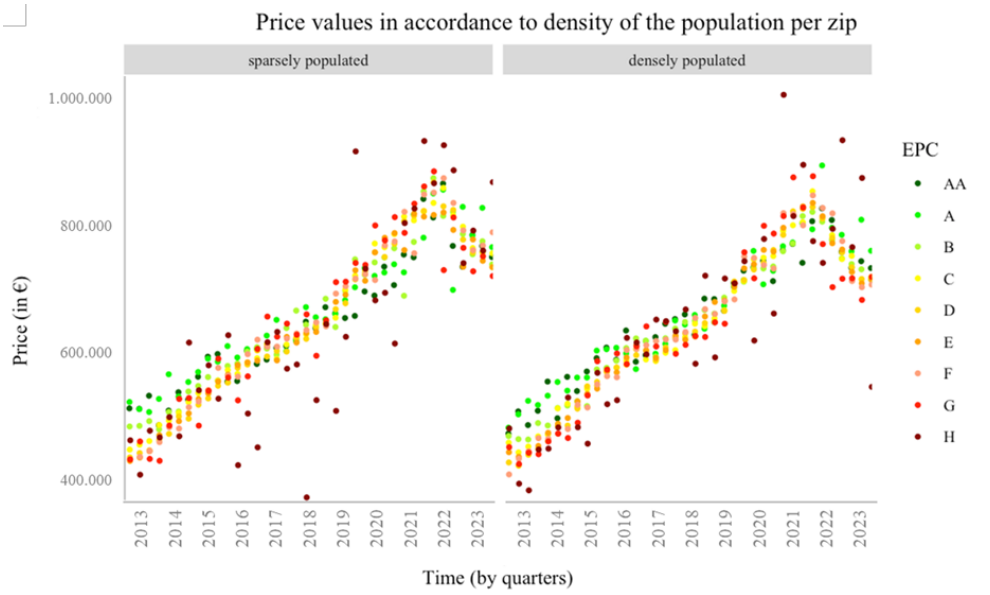
populated areas. Like rents, property prices have also shown a consistent upward trend (Figure 4.5). The pandemic's impact on prices was less pronounced, with stable value growth from 2020 to 2021. By 2022, however, marking the fourth period of analysis, prices declined across demographic conditions, suggesting a broader structural shift in the macroeconomic environment.

Figure 4.4 Rents by EPC and Population Density over Time (Pre-Retrofit)



Note: The figure depicts rental values over time, differentiated by population per ZIP code, ranging from sparsely to densely populated areas. The scatter plot features the x-axis representing time, divided into quarters, and the y-axis representing rental prices in Euros. EPC ratings, ranging from AA (most energy-efficient) to H (least energy-efficient), are indicated by different dot colors, with each color corresponding to a specific EPC rating.

Figure 4.5 Prices by EPC and Population Density over Time (Pre-Retrofit)



Note: The figure depicts price values over time, differentiated by population density per ZIP code, ranging from sparsely to densely populated areas. The scatter plot features the x-axis representing time, divided into quarters, and the y-axis indicating the rental price in Euros. EPC ratings, ranging from AA (most energy-efficient) to H (least energy-efficient), are indicated by different dot colors, with each color corresponding to a specific EPC rating.

Compared to rents, property prices display greater volatility under changing market conditions. This may be partly attributed to regulatory factors such as rental caps in Germany, which can constrain capitalization potential in the rental segment (Cajias et al., 2020). The perceived price and rent variations align with previous literature and reflect green premium effects, with a pronounced impact in rural regions (Cajias et al., 2019). This is most evident in fluctuations among extreme energy efficiency ratings (EPC AA, A, B, and G, H), which show the largest deviations. In contrast, properties with mid-range EPC ratings (C to F) exhibit more consistent and similar price patterns.

The observed dynamics become central when evaluating synthetic retrofits. Tables 4.6 and 4.7 present the rent and price effects after a synthetic retrofit according to demographic distribution. Thereby, the "worst-performing buildings" targeted by energy policy measures should exhibit the greatest price and rent effect following energy efficiency improvements.

Table 4.6 Average Percentage Change in Rents after Refurbishment

RENT	**Initial energy performance certificate before a synthetic refurbishment of 100 kWh/ m²/p.a.**			
EPC	**E**	**F**	**G**	**H**
Sparsely populated areas				
Period 1	10.088%	2.975%	2.604%	9.093%
Period 2	6.092%	3.498%	1.645%	1.461%
Period 3	4.126%	2.911%	2.077%	0.701%
Period 4	2.309%	1.656%	1.971%	1.067%
Densely populated areas				
Period 1	12.091%	6.174%	3.573%	-2.065%
Period 2	5.030%	3.658%	0.624%	3.262%
Period 3	2.683%	3.558%	2.352%	3.936%
Period 4	0.491%	2.660%	2.056%	8.172%

Note: Table 4.6 implicitly shows the average effect of a retrofit on the rental dataset, broken down by EPC rating, demographic region and time phase. The retrofit reduces the EPV by 100 kWh/ m²/year. The initial EPC classifications are provided, and the effect of the improvement in the energy standard on value is illustrated as a percentage change in value.

Table 4.7 Average Percentage Change in Prices after Refurbishment

PRICE	**Initial energy performance certificate before a synthetic refurbishment of 100 kWh/m²/p.a.**			
EPC	**E**	**F**	**G**	**H**
Sparsely populated areas				
Period 1	19.654%	10.740%	2.812%	3.266%
Period 2	8.784%	4.539%	1.260%	11.418%
Period 3	2.005%	2.829%	0.549%	12.741%
Period 4	3.576%	1.136%	3.056%	-0.344%
Densely populated areas				
Period 1	15.601%	10.356%	1.393%	8.953%
Period 2	7.898%	4.917%	2.741%	3.856%
Period 3	1.841%	2.003%	3.280%	5.914%
Period 4	3.808%	1.806%	3.951%	2.081%

Note: Table 4.7 implicitly shows the average effect of a retrofit on the rental dataset, broken down by EPC rating, demographic region and time phase. The retrofit involves reducing the EPV by 100 kWh/m²/year. The initial EPC classifications are provided, and the effect of the improvement in the energy standard on value is illustrated as a percentage change in value.

In the first period, the largest rental effect from a retrofit occurs in sparsely populated regions, with an average improvement of 10.088% for apartments initially rated as 'EPC E.' Other EPC ratings show significantly smaller rental gains. Overall, rental effects are generally higher in densely populated areas, where demand is stronger. By the final period, properties rated 'EPC H' exhibited the most substantial rental increase, indicating that policy measures successfully incentivized retrofits for the least energy-efficient buildings over time. However, in rural markets, policy objectives appear unmet. Properties with poor EPC ratings remain the least economically viable for retrofitting, even after multiple energy policy measures. In comparison, the investment market in low-density areas (Table 4.7) tends to align more closely with policy targets. In the third period, properties rated 'EPC H' show a 12.741% price increase. The trends remain consistent when comparing price effects across population densities, as retrofit incentives have increased, particularly for energy-inefficient buildings. However, spatial variations persist. Densely populated areas show moderate changes, ranging from 1.841% to 5.914%, while sparsely populated regions exhibit a wider spread, from 0.549% to 12.741%, in the third period. This suggests that the current policy framework has a more pronounced effect in low-density regions, with greater potential to generate significant investment incentives.

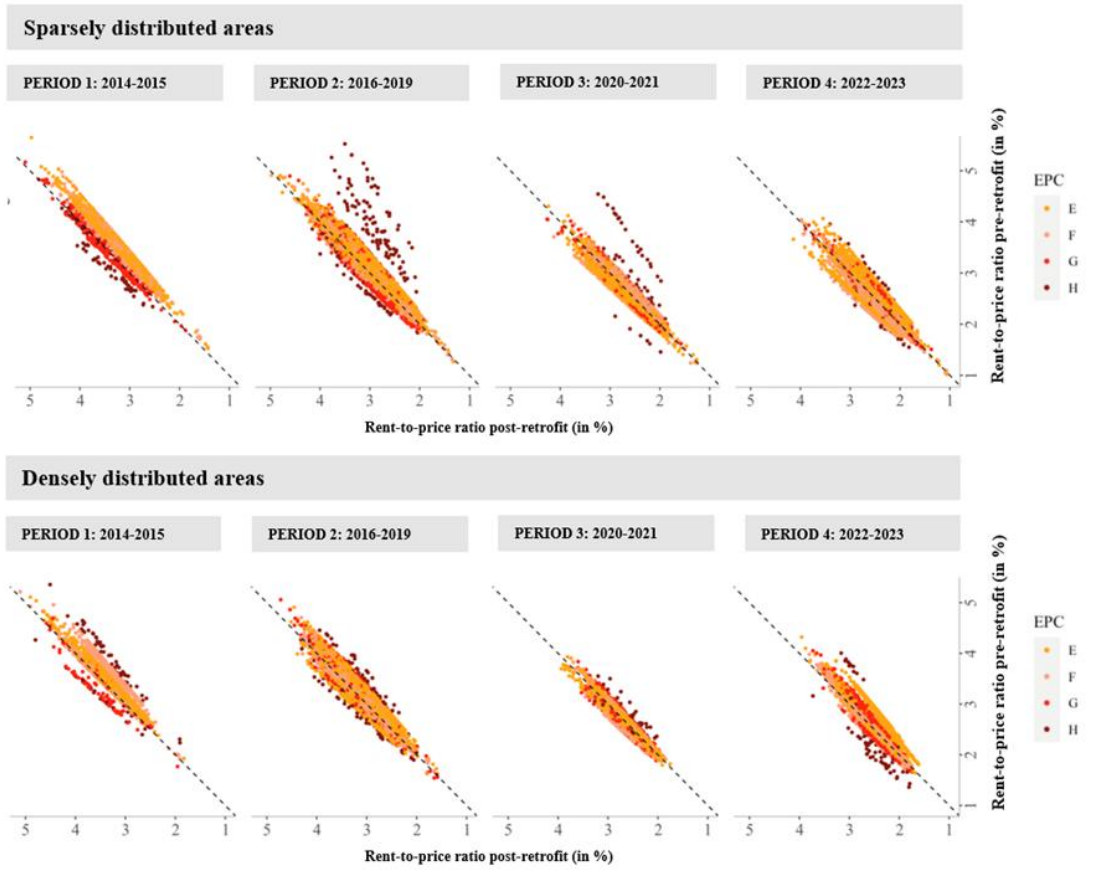
By combining rents and prices into the rent-to-price ratio, the results in Table 4.8 show that properties with lower energy standards exhibit higher ratios, as expected. The strongest effect is observed for apartments with the poorest EPC rating (EPC H), where a synthetic retrofit results in a reduction of up to 36.8 basis points (bp). This indicates substantial capitalization potential, suggesting that these properties are most economically viable for retrofitting. In addition, Table 4.8 highlights disparities that reflect the complexity of retrofit decisions under varying market conditions.

Firstly, differences in the effectiveness of energy policy measures are evident across regions. In the first period, rent-to-price ratios for properties rated 'EPC E' differed by up to 17.2 bp between areas. Initially, sparsely populated regions offered greater economic efficiency for retrofitting. As policies tighten, these disparities change, and densely populated urban areas show stronger financial advantages for retrofits. In contrast, energy-inefficient properties rated 'EPC H' show a significantly greater regional gap of 55.0 bp in the first period. Over time, this effect narrows, with sparsely populated regions exhibiting an increased retrofit potential of 28.7 bp. Figure 4.6 illustrates this trend for densely populated regions, as the proportion of dark red data points representing properties with the lowest EPC ratings is heavily concentrated along the diagonal. This suggests that regulatory measures have had a limited impact on making retrofits attractive in these areas. Overall, the findings imply that policy objectives aimed at incentivizing

retrofits of "worst-performing buildings" are more likely to be achieved in sparsely populated regions.

The second finding highlights variations across property conditions. Based on regional differences, properties with moderate EPC ratings exhibit lower regional price differences, indicating greater market stability. In sparsely populated areas, apartments with an EPC rating of E were the most profitable for retrofitting between 2014 and 2015, with a 27.3 bp improvement in the rent-to-price ratio. However, this effect drops to -0.54 bp in the third period, reducing the economic feasibility of retrofits over time as policy measures tighten. In contrast, apartments with the lowest EPC rating (EPC H) are becoming increasingly appealing for refurbishment. The average change in the rent-to-price ratio for 'EPC H' properties rises from -18.2 bp in the first period to 33 bp in the third period. A similar structural pattern emerges in densely populated areas.

Figure 4.6 Rent-to-Price Ratio Development by Regulations



Note: Figure 4.6 presents a series of scatter plots comparing rent-to-price ratios pre- and post-retrofitting across various periods, segmented by Energy Performance Certificate (EPC) ratings (E, F, G, H). Each plot represents a distinct period from 2014 to 2023, divided into segments. The X and Y-axes show the rent-to-price ratios before and after retrofitting, respectively, in percentage terms. The diagonal dashed line across each plot suggests where the rent-to-price ratio would be equal before and after retrofitting. The color-coded points represent properties with specific EPC ratings, where lighter colors (like orange) may represent a higher EPC rating, and darker colors (like red) indicate lower ratings. The spread of these points relative to the diagonal line indicates whether the rent-to-price ratios are higher, lower, or unchanged post-retrofitting. Observations above the diagonal indicate an improvement of the rent-to-price ratio following a retrofit (compression of the ratio).

Table 4.8 Mean Rent-to-Price Ratio Analysis Pre- and Post-Retrofit

		Sparsely populated					Densely populated				
		Mean rent-to-price ratio					Mean rent-to-price ratio				
EPC	Period	Pre-retrofit	Post-retrofit	Difference	SD pre-retrofit	SD post-retrofit	Pre-retrofit	Post-retrofit	Difference	SD pre-retrofit	SD post-retrofit
AA	1	2.913	2.913	0	0.306	0.306	2.823	2.823	0	0.188	0.188
	2	2.752	2.752	0	0.344	0.344	2.577	2.577	0	0.276	0.276
	3	2.532	2.532	0	0.296	0.296	2.374	2.374	0	0.223	0.223
	4	2.300	2.300	0	0.289	0.289	2.269	2.269	0	0.234	0.234
A	1	2.821	2.821	0	0.365	0.365	2.974	2.974	0	0.306	0.306
	2	2.591	2.591	0	0.341	0.341	2.646	2.646	0	0.287	0.287
	3	2.471	2.471	0	0.292	0.292	2.379	2.379	0	0.231	0.231
	4	2.267	2.267	0	0.311	0.311	2.172	2.172	0	0.24	0.24
B	1	2.932	2.932	0	0.372	0.372	3.039	3.039	0	0.274	0.274
	2	2.717	2.717	0	0.373	0.373	2.689	2.689	0	0.283	0.283
	3	2.436	2.436	0	0.327	0.327	2.418	2.418	0	0.254	0.254
	4	2.263	2.263	0	0.334	0.334	2.294	2.294	0	0.28	0.28
C	1	3.206	3.206	0	0.455	0.455	3.264	3.264	0	0.373	0.373
	2	2.864	2.864	0	0.423	0.423	2.882	2.882	0	0.339	0.339
	3	2.551	2.551	0	0.364	0.364	2.560	2.560	0	0.274	0.274
	4	2.383	2.383	0	0.357	0.357	2.420	2.420	0	0.309	0.309
D	1	3.428	3.428	0	0.483	0.483	3.517	3.517	0	0.375	0.375
	2	2.979	2.979	0	0.445	0.445	3.022	3.022	0	0.388	0.388
	3	2.606	2.606	0	0.367	0.367	2.672	2.672	0	0.279	0.279
	4	2.435	2.435	0	0.376	0.376	2.524	2.524	0	0.329	0.329
E	1	3.444	3.171	0.273	0.455	0.423	3.417	3.316	0.101	0.362	0.354
	2	2.978	2.905	0.073	0.421	0.408	3.019	2.940	0.079	0.362	0.335
	3	2.597	2.651	-0.054	0.364	0.353	2.656	2.680	-0.024	0.293	0.294
	4	2.482	2.456	0.026	0.381	0.368	2.524	2.442	0.082	0.334	0.285
F	1	3.416	3.178	0.238	0.439	0.41	3.525	3.394	0.131	0.391	0.371
	2	2.914	2.884	0.030	0.419	0.401	3.035	2.997	0.038	0.377	0.35
	3	2.578	2.581	-0.003	0.360	0.357	2.623	2.663	-0.040	0.279	0.277
	4	2.389	2.404	-0.015	0.357	0.356	2.517	2.535	-0.018	0.346	0.311
G	1	3.402	3.395	0.007	0.492	0.473	3.386	3.456	-0.070	0.442	0.436
	2	2.930	2.938	-0.008	0.458	0.404	3.117	3.048	0.069	0.454	0.397
	3	2.580	2.619	-0.039	0.399	0.386	2.708	2.681	0.027	0.346	0.313
	4	2.462	2.434	0.028	0.417	0.387	2.640	2.580	0.060	0.443	0.341
H	1	3.307	3.489	-0.182	0.513	0.455	3.724	3.356	0.368	0.631	0.501
	2	3.193	2.918	0.275	0.69	0.423	3.027	3.003	0.024	0.483	0.397
	3	2.865	2.535	0.330	0.651	0.35	2.609	2.566	0.043	0.351	0.313
	4	2.394	2.419	-0.025	0.444	0.356	2.394	2.511	-0.117	0.639	0.337

Note: Table 4.8 presents various statistics on energy efficiency changes before and after retrofitting, categorized by population density (densely vs. sparsely populated areas) and Energy Performance Certificate (EPC) ratings ranging from AA to H. The table includes several key metrics, such as the mean ratio pre-retrofit, the average ratio (likely related to energy usage or costs) before any retrofitting measures were applied, and the corresponding mean ratio post-retrofit, the average ratio after retrofitting measures have been implemented. Additionally, the table shows the difference in mean ratios, calculated as the post-retrofit mean ratio minus the pre-retrofit mean ratio, reflecting the change in the average ratio due to retrofitting. The table also includes the standard deviation of the pre-retrofit and post-retrofit ratios, indicating the variability of the data before and after retrofitting and reflecting the consistency or dispersion of the ratios within each category.

The fluctuating effects for "worst-performing buildings" imply a more volatile reaction to external factors. As energy policies become stricter, properties with lower EPC ratings offer greater profitability than those with better energy efficiency standards. In the first period, properties with 'EPC E' in urban areas showed an average improvement of 10.1 bp, which dropped to -2.4 bp by the third period. Surprisingly, in densely populated areas, "worst-

performing buildings" do not become more viable for retrofitting over time. The retrofit impact is lower in 2021 compared to 2014. However, while the feasibility of a retrofit for 'EPC H' buildings declines, it does not turn negative. Figure 4.6[32] displays the increased concentration of dark red data points, representing properties with the poorest EPC ratings, in the upper section of the graphs over the first three periods. This is evident within the spatial analysis, where properties with a lower EPC are more sensitive and attractive for retrofitting, particularly in sparsely populated regions when policies tighten. From an investment perspective, this change in the rent-to-price ratio represents a shift in the expected return, making assets with an 'EPC H' rating more attractive for retrofits within the regulatory framework and a rising market.

Third, changing market dynamics and falling prices produce different results. As the market evolves, renovating buildings with moderate EPCs becomes more feasible. In sparsely populated areas, properties with 'EPC E' show a more substantial retrofit effect (2.6 bp) than 'EPC H', which records a decline of -2.5 bp. The pattern mirrors trends observed before the implementation of policy measures, suggesting that market conditions have shifted the incentives for retrofitting back to the market environment of 2014. This indicates that energy policy measures fail to provide significant investment incentives in an environment of falling prices. The trend persists in densely populated regions, where retrofits of 'EPC E' properties lead to an average increase of 8.2 bp, while 'EPC H' properties declined by -11.7 bp. As shown in Figure 4.6, the concentration of 'EPC H' assets in the lower-left quadrant indicates the rising risk of stranded assets when prices fall. In contrast, properties with moderate EPC ratings are increasing in the upper half of the graph.

The negative trend for energy-inefficient assets underscores their vulnerability in declining markets, especially in high-demand markets, which tend to be less stable during downturns. These buildings face an increased risk of being classified as stranded assets. They lose value over time, resulting in negative rent-to-price performance, as the risk of asset devaluation and liquidity loss increases. The pattern generally suggests that current regulations fail to incentivize retrofits of the "worst-performing buildings".

[32] Observations above the diagonal imply attractive investment opportunities, as retrofitting leads to value improvements and a declining rent-to-price ratio. Conversely, apartments below the diagonal suggest less-profitable investments, as the rent-to-price ratio increases following retrofit, signaling diminished financial feasibility.

4.8 Conclusion

Given the operational lifespans of existing buildings and their prevailing energy inefficiency, retrofitting challenges are central to decarbonizing the real estate sector and meeting long-term climate objectives. The research provides evidence on the extent to which energy policy instruments effectively incentivize retrofits of residential properties, from a spatial and temporal perspectives. Using the rent-to-price ratio as a market-based indicator of investment profitability, our results show that energy retrofits are capitalized into both higher rental income and higher capital values, ceteris paribus. However, the strength and direction of the economic feasibility of energy efficiency retrofits vary across market phases and regional conditions. During periods of economic downturn and low economic growth, regulatory measures fail to incentivize retrofit activity. In other words, the risk of stranding increases despite supportive policy instruments, especially among the buildings with the highest energy consumption. Moreover, from a spatial perspective, we show that regulatory incentives are more effective in steering investment decisions in sparsely populated regions than in densely populated areas.

Our findings underscore the need for a stable, transparent and regionally adaptive regulatory framework that provides reliable investment signals. For policymakers and economists, this means energy policy must move beyond uniform regulations and align more closely with the heterogeneity of market dynamics and conditions. For investors, strategic alignment with local housing market dynamics and spatial conditions, alongside evolving regulatory developments, is also essential for mitigating the risk of stranded assets and capturing potential green premiums.

4.9 Appendix

4.9.1 Appendix I – Descriptive Statistics

Table 4.9 Variables in the Model

Variable	Source	Scale	Unit	Description
Rent	A	Numeric	€	Rent per month
Price	A	Numeric	€	Price of the asset
Size	A	Numeric	in m²	Leasable or Saleable floor area
Rooms	A	Numeric	Count	Number of rooms
Age	A	Numeric	in years	Relative to year 2023. Properties built before 1900 are assumed to be built in 1900.
EPV	A	Numeric	kWh/m²/year	Energy Performance Value
Floors	A	Numeric		Indication of the floor of the dwelling. Accessibility is assumed to be equivalent, whether the apartment is located on the first floor or an upper level.
Km to bus	B	Numeric	in kilometers (km)	Distance to closest bus stop
Km to railway	B	Numeric	in km	Distance to closest railway station
Km to school	B	Numeric	in km	Distance to closest school
Km to restaurant	B	Numeric	in km	Distance to closest restaurant
Km to supermarket	B	Numeric	in km	Distance to closest supermarket
Km to kindergarten	B	Numeric	in km	Distance to closest kindergarten
Km to pharmarcy	B	Numeric	In km	Distance to the closest pharmacy
Km to park	B	Numeric	in km	Distance to closest park
Km to bakery	B	Numeric	in km	Distance to closest bakery
Km to playground	B	Numeric	in km	Distance to closest playground
Km to biergarten	B	Numeric	in km	Distance to closest biergarten
Km to motorway	B	Numeric	in km	Distance to closest motorway to ensure the fundamental accessibility regardless of public transportation
Km to doctors	B	Numeric	in km	Distance to closest doctor
Km to hospital	B	Numeric	in km	Distance to closest hospital
Km to CBD	B	Numeric	in km	Distance to "Marienplatz" as the reference point to account for the centrality to the metropolitan region and incorporated spatial fixed effects.
Longitude	A	Numeric		
Latitude	A	Numeric		
Population per ZIP	C	Numeric		Inhabitants per ZIP in order to split the sample into densely and sparsely populated areas
Income per household	A	Numeric	in €	Average income per household by ZIP code
Retrofitted	A	Binary	1= yes	"Retrofitting" has taken place once the dwelling has had some sort of improvement measures in terms of renovation or refurbishment
Kitchen	A	Binary	1= yes	With kitchen included
Parking	A	Binary	1= yes	With parking included
Elevator	A	Binary	1= yes	With an elevator
Balcony or terrace	A	Binary	1= yes	With a balcony and/or terrace included
EPC	A	Factor	with 9 levels	Energy Performance Classification, Based on EPV according to German legislation (GEG, 2020).
Quarters	A	Factor	with 38 levels	Quarterly time dummies for the date of the disclosure are incorporated to assess the time frame and to include seasonal patterns.

Note: Table 4.9 provides a detailed summary of the variables used for the following analysis. The variables include numerical measurements such as the price and rent of the property (in Euros), the size in square meters, and the age of the property in relation to the year 2023. The distance to various amenities such as bus stops, train stations, schools, and restaurants is included. Additional binary variables indicate the presence of features such as kitchens, balconies or terraces, parking spaces, and elevators. The table includes the energy performance certificates (EPC) as a factor variable based on the energy performance value (EPV) according to German legislation. It is divided into nine levels to reflect the energy efficiency of the building. The status 'retrofitted' is recorded to indicate improvements or refurbishments. Population density by ZIP code and quarterly time dummies are included to capture demographic and temporal variations in the analysis.
A=VALUE market data, B=OpenStreetMap, C=Gfk

4.9.2 Appendix II – Regression Outputs

Table 4.10 Regression Output for Model 2

Parametric coefficients					
	Estimate	**Std. Error**	**t value**	**p-value**	
(Intercept)	6.6360787	0.0220976	300.308	< 0.001	***
Kitchen	0.0451885	0.0008616	52.447	< 0.001	***
Floors	0.0033122	0.0003078	10.762	< 0.001	***
Balcony or terrace	0.0251066	0.0011235	22.347	< 0.001	***
Parking	0.0139287	0.0010988	12.676	< 0.001	***
Elevator	0.0234792	0.0009065	25.900	< 0.001	***
Retrofitted	0.0465093	0.0009577	48.563	< 0.001	***
EPC A	-0.0066304	0.0269557	-0.246	0.805702	
EPC B	-0.0370210	0.0240167	-1.541	0.123206	
EPC C	-0.0663884	0.0233452	-2.844	0.004459	**
EPC D	-0.0690093	0.0229671	-3.005	0.002659	**
EPC E	-0.0855310	0.0230880	-3.705	< 0.001	***
EPC F	-0.0803408	0.0238415	-3.370	< 0.001	***
EPC G	-0.0757326	0.0276888	-2.735	0.006236	**
EPC H	-0.1074084	0.0366160	-2.933	0.003354	**
Density: densely populated	-0.0375686	0.0308803	-1.217	0.223764	
Time fixed effects	Yes				
Spatial fixed effects	Yes				
Approximate significance of smooth terms					
	edf	**Ref.df**	**F-Statitic**	**p-value**	
s(log(size))	8.122	8.797	14429.632	< 0.001	***
s(rooms)	5.732	6.524	91.613	< 0.001	***
s(km to bus)	5.162	5.929	15.687	< 0.001	***
s(km to CBD)	8.917	8.993	1109.254	< 0.001	***
s(km to school)	7.371	8.165	5.276	< 0.001	***
s(km to restaurant)	7.908	8.574	6.378	< 0.001	***
s(age)	30.020	33.295	440.308	< 0.001	***
te(latitude,longitude)	20.985	21.573	539.262	< 0.001	***
s(km to railway)	6.448	7.234	63.112	< 0.001	***
s(km to supermarket)	6.819	7.661	4.467	< 0.001	***
s(km to kindergarten)	4.471	5.179	4.989	< 0.001	***
s(km to pharmacy)	4.261	4.942	21.699	< 0.001	***
s(km to park)	8.194	8.738	14.757	< 0.001	***
s(km to bakery)	3.288	3.872	13.747	< 0.001	***
s(km to playground)	5.169	5.939	50.751	< 0.001	***
s(km to biergarten)	5.193	5.940	47.251	< 0.001	***
s(km to motorway)	8.536	8.905	57.662	< 0.001	***
s(km to doctors)	8.325	8.806	12.935	< 0.001	***
s(km to hospital)	8.611	8.927	73.942	< 0.001	***
s(population per ZIP)	8.463	8.843	44.407	< 0.001	***
s(income per household)	7.699	8.508	99.250	< 0.001	***

N = 114,758
R^2 (adj) = 0.9 R^2 = 90%

Signif. codes: 0 '***' 0.001 '**' 0.01 '*' 0.05 '.' 0.1 ' ' 1

Note: The table presents the output of the GAM regression, including both parametric and smooth terms. Parametric coefficients indicate the effects of categorical and continuous variables, while the smooth terms capture nonlinear relationships between rent and continuous predictors. Time and spatial fixed effects are included in the model, but not individually listed, and p-values and significance codes indicate statistical significance

Table 4.11 Regression Output for Model 4

Parametric coefficients					
	Estimate	**Std. Error**	**t value**	**p-value**	
(Intercept)	12.6063044	0.0209012	603.138	< 0.001	***
Kitchen	0.0314681	0.0013354	23.565	< 0.001	***
Floors	-0.0014028	0.0003726	-3.764	< 0.001	***
Balcony or terrace	0.0132826	0.0017383	7.641	< 0.001	***
Parking	0.0171522	0.0017141	10.006	< 0.001	***
Elevator	0.0066209	0.0013653	4.849	< 0.001	***
Retrofitted	0.0597445	0.0013995	42.691	< 0.001	***
EPC A	0.0190838	0.0259098	0.737	0.461399	
EPC B	-0.0567612	0.0248740	-2.282	0.022495	*
EPC C	-0.1341558	0.0239232	-5.608	< 0.001	***
EPC D	-0.1615726	0.0231401	-6.982	< 0.001	***
EPC E	-0.1742184	0.0232393	-7.497	< 0.001	***
EPC F	-0.1679325	0.0246556	-6.811	< 0.001	***
EPC G	-0.1690542	0.0318376	-5.310	< 0.001	***
EPC H	-0.1022416	0.0776560	-1.317	0.187977	
Density: densely populated	-0.0798318	0.0315457	-2.531	0.011386	*
Time fixed effects	Yes				
Spatial fixed effects	Yes				
Approximate significance of smooth terms					
	edf	**Ref.df**	**F-Statitic**	**p-value**	
s(log(size))	7.257	8.294	10241.273	< 0.001	***
s(rooms)	5.291	6.131	35.287	< 0.001	***
s(km to bus)	8.347	8.872	11.688	< 0.001	***
s(km to CBD)	8.685	8.960	974.998	< 0.001	***
s(km to school)	7.895	8.669	9.840	< 0.001	***
s(km to restaurant)	1.003	1.005	20.004	< 0.001	***
s(age)	20.682	24.178	727.841	< 0.001	***
te(latitude,longitude)	23.910	23.991	511.561	< 0.001	***
s(km to railway)	8.658	8.965	78.135	< 0.001	***
s(km to supermarket)	6.759	7.625	17.892	< 0.001	***
s(km to kindergarten)	7.975	8.624	7.366	< 0.001	***
s(km to pharmacy)	8.244	8.776	4.545	< 0.001	***
s(km to park)	7.318	8.299	4.545	< 0.001	***
s(km to bakery)	8.482	8.921	15.120	< 0.001	***
s(km to playground)	7.242	8.047	19.112	< 0.001	***
s(km to biergarten)	6.554	7.369	36.100	< 0.001	***
s(km to motorway)	7.631	8.346	62.304	< 0.001	***
s(km to doctors)	7.295	8.065	25.986	< 0.001	***
s(km to hospital)	8.695	8.953	76.094	< 0.001	***
s(population per ZIP)	8.679	8.944	45.541	< 0.001	***
s(income per household)	8.715	8.969	169.285	< 0.001	***
N=85,832					
R^2(adj.)= 0.908	R^2 = 90.8%				
Signif. codes:	0 '***' 0.001 '**' 0.01 '*' 0.05 '.' 0.1 '' 1				

Note: The table presents the output of the GAM regression, including both parametric and smooth terms. Parametric coefficients indicate the effects of categorical and continuous variables, while the smooth terms capture nonlinear relationships between rent and continuous predictors. Time and spatial fixed effects are included in the model but not individually listed, and p-values and significance codes indicate statistical significance

4.9.3 Appendix III – Energy Performance Certificate in Germany

Since 2014, it has been mandatory in Germany to submit an energy certificate with every contract, whether a property is rented or sold (GEG, § 80). Within that, Germany introduced two types of EPCs (GEG, §§82,83): Each property can be measured based on its calculated energy performance (Bedarfsausweis) or an EPC based on energy consumption of the last three years (Verbrauchsausweis). As Table 4.12 shows, the consumption-dependent EPC and demand-dependent EPC are included in different proportions in the rental and price data evaluation. In contrast to other studies (Taruttis & Weber, 2022), these types are relatively evenly distributed. Hence, they are summarized as energy performance values (EPV) for further applicability since each country and legislation has different rating scales.

Table 4.12 Distribution of Energy Performance Values

Energy performance certificate values	based on consumption	based on demand
Rental dataset	87,471	57,726
	60%	40%
Mean value	120.58	83.64
Price dataset	74,308	38,507
	66%	34%
Mean value	122.55	81.4

Note: The table displays the distribution of energy performance certificates, categorized by their assessment basis, which is either consumption or demand. This breakdown illustrates the differences in the certification criteria and their impact on the values shown in the individual datasets.

4.10 References

André, C., Bonga-Bonga, L., Gupta, R., & Muteba Mwamba, J. W. (2017). Economic policy uncertainty, U.S. real housing returns and their volatility: A nonparametric approach. *Journal of Real Estate Research*, 39(4), 493–514.

Baye, V., & Dinger, V. (2024). Investment incentives of rent controls and gentrification: Evidence from German micro data. *Real Estate Economics*, 52(3), 843–884.

Brändle, A., Füss, R., Schläpfer, J., & Weigand, A. (2025). The low-carbon rent premium of residential buildings. *Journal of Real Estate Research*. Advance online publication.

Brounen, D., & Kok, N. (2011). On the economics of energy labels in the housing market. *Journal of Environmental Economics and Management*, 62(2), 166–179.

Bundesverband energieeffiziente Gebäudehülle. (2024). *Sanierungsquote*. Accessed: 2025-08-12. URL: https://buveg.de/sanierungsquote/

Cajias, M. (2019). Understanding real estate investments through big data goggles: A granular approach on initial yields. *International Journal of Housing Markets and Analysis*, 12(4), 661–686.

Cajias, M., & Ertl, S. (2018). Spatial effects and non-linearity in hedonic modeling: Will large data sets change our assumptions? *Journal of Property Investment & Finance*, 36(1), 32–49.

Cajias, M., Freudenreich, P., Freudenreich, A., & Schäfers, W. (2020). Liquidity and prices: A cluster analysis of the German residential real estate market. *Journal of Business Economics*, 90(7), 1021–1056.

Cajias, M., Fuerst, F., & Bienert, S. (2019). Tearing down the information barrier: The price impacts of energy efficiency ratings for buildings in the German rental market. *Energy Research & Social Science*, 47, 177–191.

Cajias, M., & Piazolo, D. (2013). Green performs better: Energy efficiency and financial return on buildings. *Journal of Corporate Real Estate*, 15(1), 53–72.

Caloia, F. G., & Mastrogiacomo, M. (2022). The housing wealth effect: The role of renovations and home improvements. *Real Estate Economics*, 50(6), 1532–1547.

Cespedes-Lopez, M.-F., Mora-Garcia, R.-T., Perez-Sanchez, V. R., & Perez-Sanchez, J.-C. (2019). Meta-analysis of price premiums in housing with energy performance certificates (EPC). *Sustainability*, 11(22), 6303.

Chegut, A., Eichholtz, P., & Holtermans, R. (2016). Energy efficiency and economic value in affordable housing. *Energy Policy*, 97, 39–49.

Chinloy, P., Cho, M., & Song, I. (2018). House rent-price ratios: An international comparison. *Journal of Real Estate Research*, 40(3), 347–374.

de Ayala, A., Galarraga, I., & Spadaro, J. V. (2016). The price of energy efficiency in the Spanish housing market. *Energy Policy*, 94, 16–24.

Dell'Anna, F., Bravi, M., Marmolejo-Duarte, C., Bottero, M. C., & Chen, A. (2019). EPC green premium in two different European climate zones: A comparative study between Barcelona and Turin. *Sustainability*, 11(20), 5605.

Deng, Y., Han, C., Li, T., & Wang, Y. (2024). The effectiveness and consequences of the government's interventions for Hong Kong's residential housing markets. *Real Estate Economics*, 52(2), 324–365.

Deutsche Energie-Agentur. (2021). *Dena-Leitstudie Aufbruch Klimaneutralität*.

Dinan, T. M., & Miranowski, J. A. (1989). Estimating the implicit price of energy efficiency improvements in the residential housing market: A hedonic approach. *Journal of Urban Economics*, 25(1), 52–67.

Eilers, P. H. C., & Marx, B. D. (1996). Flexible smoothing with B-splines and penalties. *Statistical Science*, 11(2), 89–121.

Eurostat. (2026). *Distribution of population by tenure status, type of household and income group—EU SILC survey***.** Accessed: 2025-12-08. URL: https://ec.europa.eu/eurostat/databrowser/view/ILC_LVHO02__custom_3553007/bookmark/table?lang=en&bookmarkId=2457e44e-df35-4995-aacc-e79684402691

European Commission. (2020). *A renovation wave for Europe - Greening our buildings, creating jobs, improving lives (COM/2020/662)* [Communication].

European Commission. (2021). *Fit for 55- delivering the EU´s 2030 climate target on the way to climate neutrality (COM/2021/550)* [Communication].

European Parliament & Council of the European Union. (2024). *Directive (EU) 2024/1275 of the European Parliament and of the Council of 24 April 2024 on the energy performance of buildings (recast)* [Directive]. Official Journal of the European Union, L 2024/1275.

Fuerst, F., McAllister, P., Nanda, A., & Wyatt, P. (2015). Does energy efficiency matter to home-buyers? An investigation of EPC ratings and transaction prices in England. *Energy Economics*, 48, 145–156.

Fuerst, F., McAllister, P., Nanda, A., & Wyatt, P. (2016). Energy performance ratings and house prices in Wales: An empirical study. *Energy Policy*, 92, 20–32.

Ghosh, C., & Petrova, M. T. (2024). Building sustainability, certification, and price premiums: Evidence from Europe. *Journal of Real Estate Research*, 46(4), 514–537.

Gilbukh, S., Haughwout, A., Landau, R. J., & Tracy, J. (2023). The price-to-rent ratio: A macroprudential application. *Real Estate Economics*, 51(2), 503–532.

Government UK. (2023). *Buying or selling your home: Overview–GOV*. Accessed: 2025-12-08. URL: https://www.gov.uk/buy-sell-your-home/print

Hastie, T., & Tibshirani, R. (1986). Generalized additive models. *Statistical Science*, 1(3), 297–310.

Hattapoglu, M., & Hoxha, I. (2014). The dependency of rent-to-price ratio on appreciation expectations: An empirical approach. *The Journal of Real Estate Finance and Economics*, 49(2), 185–204.

Himmelberg, C., Mayer, C., & Sinai, T. (2005). Assessing high house prices: Bubbles, fundamentals and misperceptions. *Journal of Economic Perspectives*, 19(4), 67–92.

Hyland, M., Lyons, R. C., & Lyons, S. (2013). The value of domestic building energy efficiency - Evidence from Ireland. *Energy Economics*, 40, 943–952.

Kholodilin, K. A., Mense, A., & Michelsen, C. (2017). The market value of energy efficiency in buildings and the mode of tenure. *Urban Studies*, 54(14), 3218–3238.

Kolbe, J., Schulz, R., Wersing, M., & Werwatz, A. (2021). Real estate listings and their usefulness for hedonic regressions. *Empirical Economics,* 61, 3239–3269.

Lu, X., & Spaenjers, C. (2025). Energy labels, misreporting, and heuristic hedonic models. *Real Estate Economics*, 53(6), 1200–1222.

Marmolejo-Duarte, C., & Chen, A. (2019). The uneven price impact of energy efficiency ratings on housing segments and implications for public policy and private markets. *Sustainability*, 11(2), 372.

Mason, C., & Quigley, J. M. (1996). Non-parametric hedonic housing prices. *Housing Studies*, 11(3), 373–385.

McCord, M., Lo, D., Davis, P. T., Hemphill, L., McCord, J., & Haran, M. (2020). A spatial analysis of EPCs in the Belfast metropolitan area housing market. *Journal of Property Research*, 37(1), 25–61.

McCord, M., McCord, J., Davis, P., Haran, M., & Squires, G. (2024). Do private rental tenants pay for energy efficiency?: The dynamics of green premiums and brown discounts. *Journal of Property Research*, 41(3), 251–275.

Mense, A., Michelsen, C., & Kholodilin, K. A. (2023). Rent control, market segmentation, and misallocation: Causal evidence from a large-scale policy intervention. *Journal of Urban Economics*, 134, 103513.

Muzio, M. J., Niu, D., Steil, J., & Zheng, S. (2025). Understanding housing market responses to stringent energy codes. *Real Estate Economics*, 53(4), 676–700.

Nelder, J. A., & Wedderburn, R. W. M. (1972). Generalized linear models. *Journal of the Royal Statistical Society. Series A: General*, 135(3), 370–384.

Olaussen, J. O., Oust, A., & Solstad, J. T. (2017). Energy performance certificates – Informing the informed or the indifferent? *Energy Policy*, 111, 246–254.

Petrov, I., & Ryan, L. (2021). The landlord-tenant problem and energy efficiency in the residential rental market. *Energy Policy*, 157, 112458.

Pommeranz, C., & Steininger, B. I. (2021). What drives the premium for energy-efficient apartments – Green awareness or purchasing power? *The Journal of Real Estate Finance and Economics*, 62(2), 220–241.

R Core Team. (2023). *R: A language and environment for statistical computing*. The R Project for Statistical Computing.

Rottke, N. B., & Krautz, S. (2017). Investition in Wohnimmobilien. In D. Arnold, N. B. Rottke, & R. Winter (Eds.), *Wohnimmobilien: Lebenszyklus, Strategie, Transaktion* (pp. 775–832). Springer.

Sachs, J.D., Lafortune, G., Fuller, G., & Drumm, E. (2023). *Implementing the SDG Stimulus.* Sustainable Development Solutions Network.

Schuetz, J. (2024). How will US households adjust their housing behaviors in response to climate change? *Real Estate Economics*, 52(3), 596–617.

Sebi, C., Nadel, S., Schlomann, B., & Steinbach, J. (2019). Policy strategies for achieving large long-term savings from retrofitting existing buildings. *Energy Efficiency*, 12(1), 89–105.

Statistisches Amt der Landeshauptstadt München. (2024). *Statistische Daten zur Münchner Bevölkerung*. Accessed: 2025-12-08. URL: https://stadt.muenchen.de/infos/statistik-bevoelkerung.html

Statistisches Bundesamt. (2023). *Press release No. 022 of January 2023*.

Taltavull De La Paz, P., Perez-Sanchez, V., Mora-Garcia, R.-T., & Perez-Sanchez, J.-C. (2019). Green premium evidence from climatic areas: A case in southern Europe, Alicante (Spain). *Sustainability*, 11(3), 686.

Taltavull, P., Anghel, I., & Ciora, C. (2017). Impact of energy performance on transaction prices: Evidence from the apartment market in Bucharest. *Journal of European Real Estate Research*, 10(1), 57–72.

Taruttis, L., & Weber, C. (2022). Estimating the impact of energy efficiency on housing prices in Germany: Does regional disparity matter? *Energy Economics*, 105, 105750.

United Nations Environment Programme. (2022). *2022 global status report for buildings and construction: Towards a zero-emission, efficient and resilient buildings and construction sector*.

Value. (2023). *VALUE Marktdaten*. Accessed: 2025-12-08. URL: https://www.value-marktdaten.de

Voigtländer, M. (2014). The stability of the German housing market. *Journal of Housing and the Built Environment*, 29(4), 583–594.

5 Resilience through Energy Efficiency? Evidence from Price and Liquidity Dynamics across Market Regimes

5.1 Abstract

This study examines the capitalization of energy efficiency and whether it changes under adverse market conditions. We analyzed both expansionary market phases and periods characterized by rising energy prices, tighter financing conditions, increased construction costs, and regulatory pressure, using the German residential property market from 2017 to 2025 as an empirical setting. Although previous research has widely examined the price effects of energy efficiency in expanding markets, evidence on its role amid challenging market conditions remains limited. The evolution of price effects and liquidity dynamics was captured by combining semi-parametric pricing models and a survival analysis. The results show that the price and time on the market differ across regimes. During expansionary periods, price differentiation by energy efficiency remains limited, and liquidity is highest for properties with average energy performance, consistent with strong demand-absorbing quality differences. However, energy efficiency becomes more relevant to price and market absorption during downturns. Energy-efficient properties command larger premiums and shorter marketing periods, whereas energy-inefficient properties require larger discounts and longer time on market. These findings suggest that energy efficiency should be evaluated as a regime-dependent risk factor in pricing, marketability, and downside-risk assessments under changing market conditions.

Keywords: Energy Efficiency, Market Liquidity, Residential Property Market, Time on Market, Green Premium

5.2 Introduction

Recently, geopolitical tensions and supply constraints have increased the importance of energy security in the European Union. Russia's invasion of Ukraine led to a deterioration in energy relations between Russia and most European countries. Since Russia had been one of Europe's dominant natural gas suppliers (Bachmann et al., 2022, 2024), the abrupt reduction in supply caused a significant shock to energy availability, accompanied by rising energy prices and reduced consumption (Ruhnau et al., 2023).

Germany was highly exposed to reductions in natural gas supply and provides a relevant setting for studying these effects, as household gas prices increased from approximately 4 ct/kWh before the COVID-19 pandemic to peak levels of approximately 40 ct/kWh in the summer of 2022 (Hörz, 2025). This shock occurred in a broader macroeconomic and regulatory environment characterized by inflationary pressures, subsequent monetary tightening, higher interest rates, the lingering effects of the COVID-19 pandemic, and rising construction costs. Together, these developments increased pressure on housing markets and shifted attention to long-term operating costs and renovation risks. In addition, German sustainability policy and regulatory frameworks are comparatively advanced, reflected in Germany's fourth place ranking in the Sustainable Development Goals (SDG) Index (Sachs et al., 2025). These conditions provide relevant context for assessing how overlapping shocks and structural changes affect the property market with respect to energy efficiency.

In the context of the recent energy crisis in Germany, previous research has analyzed its effects on factors such as energy consumption, GDP changes, price elasticities, and household income (Bachmann et al., 2024; Ruhnau et al., 2023; Singhal et al., 2026). However, empirical evidence on the effects of the energy crisis on real estate markets remains limited. Existing studies on energy-efficiency pricing are restricted to linear frameworks or short-term analyses (Braakmann et al., 2026; Brolinson et al., 2026; Sagner, 2026). Research on long-term effects, temporal dynamics, and liquidity remains scarce. This research addresses this gap by analyzing both price and liquidity effects. The study examines how the valuation of energy efficiency evolves across changing market regimes and whether price and liquidity effects respond differently. This integrated perspective is relevant in the context of the energy crisis and the structural changes in real estate markets, which have recently been shaped by heightened uncertainty, shifting risk perceptions, and rapidly changing economic and regulatory conditions. The study aims to identify regime-dependent dynamics in the capitalization of energy efficiency and evaluate their

implications for prices and market absorption while accounting for temporal and spatial dimensions.

The following analysis provides a comprehensive picture of the German residential real estate market from 2017 to 2025 based on two key perspectives: price and time on market. Both are crucial for assessing market valuations and information dynamics in real estate markets (Zahirovic-Herbert & Turnbull, 2008), indicating whether energy efficiency is reflected in asset pricing and market absorption. Accordingly, the two outcome dimensions are modeled separately. Prices are estimated using a generalized additive model, whereas time on market is analyzed using a Cox proportional hazards model.

The results demonstrate that the price and liquidity effects follow different patterns over time. Strong demand under favorable market conditions partly offsets the differences in energy efficiency, resulting in comparatively weaker price differentiation during the low-interest-rate boom phase. Liquidity effects follow a different pattern, with the highest levels occurring around average and moderately lower energy-efficiency levels. Both patterns reverse under challenging market conditions. Price effects become more pronounced, leading to a widening spread. Inefficient properties experience larger price discounts, reflecting stronger pricing of operating cost risks, renovation requirements, and regulatory uncertainty. Liquidity dynamics reinforce the price discounts and indicate a dual penalty of weaker demand and longer market exposure. At the same time, energy-efficient properties tend to have shorter listing durations, indicating stronger demand for efficiency amid higher energy prices and increasing regulatory pressure. At the regional level, price effects are crucial in less densely populated areas, whereas liquidity reflects a more heterogeneous demand structure and segmentation, suggesting that local demand conditions strongly shape market absorption.

The remainder of the analysis is structured as follows. The first section outlines the background of the energy crisis and its significance for the European market and discusses how changing energy conditions affect the German real estate market. The subsequent data section presents the dataset and the key variables used in the empirical analysis. This is followed by the methodological section, which introduces the modeling framework for price and liquidity analyses. The results section proceeds in two steps: first, it presents the pricing results across the baseline, temporal, and spatial specifications; second, it examines the corresponding liquidity effects and reports robustness checks. The conclusion summarizes the main findings and discusses their practical implications, including their relevance beyond the German market.

5.3 Institutional and Market Background

A central objective of European climate policy is to improve the energy performance of the existing building stock over the long term, with an emphasis on the "worst-performing buildings". Several regulatory measures and policy objectives at European and national levels contributed to this goal. A key metric for measuring the energy efficiency of buildings is the energy performance value (EPV), which represents the annual energy consumption of a building per square meter in kilowatt-hours (kWh/m²/year). These values are converted into national rating scales that classify buildings according to their energy efficiency. In Germany, the disclosure of an energy performance certificate (EPC) and the corresponding energy efficiency class has been mandatory for properties offered for rent or sale since 2014 under Germany's Energy Saving Ordinance (Energieeinsparverordnung [EnEV]). The German classification is based on energy efficiency classes ranging from A+ to H (Table 5.1).

Table 5.1 EPC Nomenclature in Germany

Class	A+	A	B	C	D	E	F	G	H
EPV	≤ 30	≤ 50	≤ 75	≤ 100	≤ 130	≤ 160	≤ 200	≤ 250	> 250

Note: The EPC nomenclature is based on Annex 10 to Section 86 of the German Building Energy Act (Gebäudeenergiegesetz [GEG]). It defines EPC classes ranging from A+ to H and links them to continuous energy performance values expressed in kilowatt-hours per square meter per year (kWh/m²/year).

Several regulatory measures have been introduced in recent years to improve the energy efficiency of buildings. Overarching targets are defined at the European level, such as the European Energy Performance of Buildings Directive (EPBD), and are subsequently specified in national legislation. The EnEV played a particularly important role in the German residential real estate market until 2021, as it defined minimum energy requirements for new buildings and set energy-efficiency requirements for renovations. In 2020, the EnEV and related energy regulations were consolidated into the German Building Energy Act (Gebäudeenergiegesetz [GEG]). The GEG constitutes Germany's central national framework for implementing the EPBD, which aims to improve the energy efficiency of buildings across the European Union (EU). In 2021, another regulatory change was the introduction of a national CO_2 price on fossil fuels used in the building sector under the Fuel Emissions Trading Act (Brennstoffemissionshandelsgesetz [BEHG]). By increasing the cost of fossil energy sources, such as gas and heating oil, these charges raise operating costs, particularly for less energy-efficient buildings, and thereby strengthen the economic relevance of building energy efficiency.

In addition to these regulatory developments, the German property market has been shaped by an exceptional macroeconomic environment over the past few years. Expansive

monetary conditions by the European Central Bank, reflected in very low and partly negative policy rates, contributed to historically low financing costs in the real estate sector (Deutsche Bundesbank, 2026). This environment improved affordability, supported housing demand, and contributed to rising property prices. The situation changed substantially following several external shocks. Russia's invasion of Ukraine in 2022 led to disruptions in energy markets. Germany had been highly dependent on Russian gas imports. Hence, the resulting supply uncertainty led to a sharp increase in energy prices (Bachmann et al., 2022, 2024; Lutz & Becker, 2023). Previous studies indicate substantial macroeconomic effects caused by energy price shocks, with the extent of these effects being largely determined by the respective energy dependence and the diversification of energy sources (van de Ven & Fouquet, 2017). Energy price shocks affect macroeconomic outcomes, such as growth and inflation, and may generate welfare losses as their effects spread through value chains (Kilian, 2008). The resulting inflationary pressure triggered a monetary policy response by the European Central Bank, which raised its key interest rates (European Central Bank, 2026).

At the same time, construction costs rose due to supply chain disruptions and rising energy and material prices following the onset of the war in Ukraine (Deutsche Bundesbank, 2026; Statistisches Bundesamt, 2026b). Rising construction costs had already been observed between 2017 and 2020 due to the boom in the construction sector, but the strongest increase occurred in 2022 (Statistisches Bundesamt, 2026b). Together, these developments led to a deterioration in market conditions and contributed to declining construction activity (Statistisches Bundesamt, 2026a).

Rising financing and construction costs, along with greater regulatory requirements, contribute to increased uncertainty and reduced economic activity (Bernanke, 2018; Claessens & Kose, 2013). Ruhnau et al. (2023) found that households and small firms reduced energy consumption by 10–36% following the energy price shock. Against this backdrop, energy price shocks extend beyond immediate adjustments and provoke longer-term structural responses, as households shift from short-term reductions in consumption to investing in long-term energy-efficiency measures (Singhal et al., 2026). At the same time, rising energy prices exert a regressive effect because low-income households spend a disproportionately high share of their income on energy costs, which reduces purchasing power and thus indirectly influences housing demand (Bach & Knautz, 2022). More broadly, these developments reflect one of the central drivers of real estate market cycles, in which macroeconomic shocks affect real estate markets through credit conditions and expectations (Duca et al., 2021).

5.4 Related Literature

The empirical literature on green premiums originated in the commercial real estate sector, especially in office markets in the United States (US) (Eichholtz et al., 2010). Early studies provided evidence of a positive association between sustainability certifications and transaction prices, rents, and operational performance (Devine & Kok, 2015; Reichardt et al., 2012; Wiley et al., 2010). Certifications are understood as instruments that reduce information asymmetries regarding building quality and energy efficiency, thereby serving as market signals through which sustainability attributes are capitalized. Evidence beyond the US, especially in the United Kingdom (UK) and parts of continental Europe, broadly confirmed the existence of capitalization effects, although the magnitude of these effects differed across countries and market segments (Fuerst & van de Wetering, 2015; Ghosh & Petrova, 2024; Porumb et al., 2020; Surmann et al., 2015). These differences are partly explained by methodological choices, certification type, building quality, and location (Chegut et al., 2014; Porumb et al., 2020; Reichardt et al., 2012; Robinson et al., 2017). Moreover, several studies indicated that price premiums vary over time rather than being static, suggesting that capitalization depends on changing market conditions and policy regimes (Chegut et al., 2014; Eichholtz et al., 2026; Reichardt et al., 2012).

Price premiums for energy-efficient buildings, known as green premiums, are also evident in the residential real estate market. An extensive body of research indicates that energy efficiency and green-building features are reflected in housing prices (Brounen & Kok, 2011; Cadena & Thomson, 2021; Hyland et al., 2013; Kahn & Kok, 2014; Ou et al., 2025), whereas deviations are observed at both ends of the energy-efficiency spectrum (Copiello & Coletto, 2023).

A comparison of key studies across regions reinforces these findings. In the US, observed price premiums are predominantly in the lower- to moderate-single-digit percentage range (Aroul & Hansz, 2012; Aroul & Rodriguez, 2017; Cadena & Thomson, 2021; Kahn & Kok, 2014; Muzio et al., 2025). Higher premiums were reported in Asian markets (Dell'Anna & Bottero, 2021). For Europe, both earlier and more recent studies confirmed the positive effects, although the estimated premiums differ substantially across countries and specifications. In England, Fuerst et al. (2015) found price premiums of approximately 5% for energy-efficient buildings. For the Netherlands, Brounen and Kok (2011) showed a transaction premium of approximately 3.6% for A-rated properties. Studies for Spain reported price premiums of 5.4% to 9.8%, whereas for Finland, depending on the specification, premiums of up to 18.23% were found for the top efficiency classes (de Ayala et al., 2016; Fuerst et al., 2016). In Italian cities, Copiello and Coletto (2023) reported

premiums of approximately 20% for energy-efficient properties, whereas Micelli et al. (2024) showed differences of up to 30% between particularly efficient and inefficient properties.

These cross-country differences are partly attributable to the differences in rating systems and disclosure regimes. Cespedes-Lopez et al. (2019) emphasized that price effects differ across countries and rating systems, as mandatory and voluntary schemes yield diverse outcomes. Due to lower information asymmetry, premiums are lower within mandatory systems, as the label loses some of its signaling and scarcity functions (Amecke, 2012; Cespedes-Lopez et al., 2019; Chegut et al., 2020). The European EPC framework provides a more harmonized institutional setting for cross-country comparison. The literature reviews by Wilkinson and Sayce (2020) and Ou et al. (2025) indicated greater homogeneity in Europe than in most non-European markets. However, the estimated effects vary across regions, market segments, housing types, periods, and methodologies. Reported estimates typically range from approximately 3% to 21% for rents and approximately 10% to 26% for the prices of energy-efficient buildings, whereas discounts for inefficient buildings are partly even larger (Ou et al., 2025). [33]

Wilkinson and Sayce (2020) confirmed a positive capitalization effect in the European literature from an early stage, while also emphasizing that existing evidence is shaped by hedonic pricing approaches, data constraints, and limited explanatory power. Ou et al. (2025) further showed that the European literature expanded around 2020 and 2022, relies predominantly on price-based outcomes, uses EPC ratings as the primary benchmark, employs mostly linear hedonic models, and frequently omits explicit consideration of spatial dependencies. The review also suggested that the observed effects should be interpreted as the interplay between information quality, regional market structure, and bounded rationality.

Germany has a relatively broad body of literature (Ou et al., 2025). German evidence varies, depending on whether studies examine prices, rents, yields, or heating cost projections (Ou et al., 2025). The results show positive but heterogeneous capitalization effects. Cajias and Piazolo (2013) found that a 1% reduction in energy consumption increases market value by 0.45%, ceteris paribus. Taruttis and Weber (2022) showed that, for single-family homes, an efficiency gain of 100 kWh/m²/year is associated with an average price increase of 6.9%. Galvin (2023) noted that premiums may be distorted by prebound effects, as theoretical metrics overestimate actual consumption, leading buyers to misestimate future

[33] Although these findings point to broadly comparable capitalization patterns, EPC nomenclature and threshold definitions are not fully harmonized across EU countries, which limits the direct comparability of specific rating classes.

energy savings. However, the picture is more subdued for rents, where several studies found little or no green premiums (März et al., 2022; Sieger & Weber, 2023). Kholodilin et al. (2017) identified potential inefficiencies in the valuation of energy costs. Sieger (2024) indicated that the disclosure of total costs reduces these inefficiencies due to lower information asymmetry.

One source of variation in energy-efficiency capitalization lies in the hedonic characteristics of buildings. Real estate prices result from a combination of structural, qualitative, and locational attributes, including features such as structural condition, amenities, construction quality, size, type of use, and location (Copiello & Coletto, 2023). Thus, the effects of energy efficiency are context-dependent and shaped by property characteristics and local market conditions (Cadena & Thomson, 2021). Technical systems such as heating technologies are closely linked to energy efficiency (Mense, 2018).

Furthermore, the literature indicated that green premiums are spatially differentiated and depend on market conditions. Cadena and Thomson (2021) identified significant differences between neighborhood quintiles in the US, ranging from 1.2% to 6.9%. Comparable European markets exhibit a similar pattern, as documented by McCord et al. (2020), who found spatial variation in the capitalization of energy efficiency. Micelli et al. (2024) showed that value differences are greater in less dynamic markets, whereas they are relatively smaller in metropolitan regions. The importance of spatial and socioeconomic factors is also evident in Germany. Price effects in large urban markets are significantly weaker than those in rural regions because excess demand and high price levels overshadow the importance of energy efficiency (Taruttis & Weber, 2022). In addition, Pommeranz and Steininger (2021) highlighted the importance of purchasing power in housing markets, emphasizing its stronger role than environmental awareness in rent differentials. However, Ou et al. (2025) noted that spatial effects remain relatively underexplored because many studies are limited to specific submarkets and do not address broader regional structures.

The ownership structure, underlying financing, and incentive mechanisms provide another explanation for differences in capitalization. Particularly in the rental market, the so-called split-incentive problem indicates that investment costs and energy-efficiency savings are distributed among stakeholders, preventing full capitalization (Kholodilin et al., 2017; Sieger & Weber, 2023; von Platten et al., 2022). Energy efficiency premiums are insufficient in rental markets, whereas the price effects in owner-occupied markets are stronger (März et al., 2022; McCord et al., 2024; Sieger & Weber, 2023). Moreover, energy-efficient buildings are associated with reduced long-term risks and more stable cash flows,

potentially resulting in lower risk premia and more favorable financing conditions (Kempf & Syz, 2022).

Information systems hold a pivotal role. As illustrated by mandatory and voluntary systems, information asymmetries are crucial. Within the European system, EPCs are interpreted as signals because the market responds to label thresholds and price reactions appear discontinuous at rating boundaries, reinforced by the predominant use of discrete rating bands instead of continuous efficiency measures (Lu & Spaenjers, 2025; Ou et al., 2025). At the same time, nonlinear relationships between energy efficiency and prices were identified when continuous efficiency measures are used (Cajias & Piazolo, 2013; Copiello & Coletto, 2023). Additionally, enhanced information disclosure, such as heating costs, reduces market inefficiencies and strengthens market capitalization (Sieger, 2024). However, the expected heating cost savings are not fully considered in housing prices, indicating that market participants do not fully process the available information (Mense, 2018; Sieger & Weber, 2023).

Aydin et al. (2020) found that efficiency gains are driven by structural characteristics such as construction year, reflecting regulatory changes after the oil crisis, whereas EPC disclosure has limited effects. The findings suggest that the valuation of energy efficiency depends heavily on the market environment and its relevance to market participants' decision-making processes. Therefore, the assumption of constant capitalization over time is unreliable. Early research indicated that the level of the green premium changes over time (Brounen & Kok, 2011; Kahn & Kok, 2014). Cadena and Thomson (2021) confirmed variations in these effects between 2009 and 2019 and a strong dependence on market segments. Dell'Anna and Bottero (2021) found an unstable trend and fluctuations over time in the Singapore housing market. Similar evidence of time-varying green premiums is provided by Aroul and Rodriguez (2017) for the US, whereas Chegut et al. (2020) documented the gradual incorporation of energy efficiency into prices, indicating learning effects in the market. Nevertheless, most empirical studies implicitly modeled green premiums as static effects (Ou et al., 2025), without explicitly accounting for temporal dynamics (Chegut et al., 2014; de Ayala et al., 2016; Fuerst et al., 2016).

Price premiums are attributable not only to increased willingness to pay, but also to regulatory interventions and supply shortages (Muzio et al., 2025). Premiums are higher in the early phases of market introduction, subsequently decline, and then stabilize. Ou et al. (2025) confirmed this trend for the European market, whereas positive price premiums for energy-efficient buildings were more prevalent before 2016, and discounts for inefficient buildings have gained importance in more recent studies. Thus, brown discounts were

interpreted as a long-term trend, indicating that value differentiation increasingly reflects price discounts for inefficient buildings, rather than premiums for efficient ones (Wilkinson & Sayce, 2020). Besides market readjustment, economic fluctuations and exogenous shocks are key drivers of these dynamics. Evidence from the US housing market indicated that green premiums exhibit cyclical variation, tending to decline during economic downturns and increase during subsequent recovery periods (Kahn & Kok, 2014). Similar patterns in the EPC-based analyses suggested that the capitalization of energy labels is sensitive to market conditions (Brounen & Kok, 2011). In the commercial real estate sector, Reichardt et al. (2012) documented dynamic patterns for rental premiums, which increased prior to the financial crisis and declined in its aftermath. Energy price shocks are another important determinant of the observed heterogeneity in the price effects associated with energy efficiency. Conventional oil price shocks affect both the demand and supply channels, with effects that vary by region and are more pronounced in energy-dependent regions (Grossman et al., 2019). In this context, based on exogenous energy price shocks, Aydin et al. (2020) showed that actual energy efficiency gains are systematically reflected in prices, with a 10% increase in energy efficiency corresponding to price growth of approximately 2%. The latest energy crisis in Europe underscores these relationships. Brolinson et al. (2026) demonstrated, based on a difference-in-differences (DiD) analysis for 2020 to 2022 in Norway, that energy efficiency has limited relevance for prices under stable energy prices. As energy prices rise, the salience of operating costs increases, resulting in stronger capitalization and discounts of 1.2% to 3.6%. Energy-efficient buildings are less affected during the shock and thus exhibit greater resilience. These effects are delayed and take several months to fully unfold. In Norway, price premiums of 7.7% and discounts of approximately 25% were estimated using a linear model controlling for macroeconomic variables from 2011 to 2024 (Granum, 2025). Braakmann et al. (2026) identified discounts of less than 1% for inefficient properties in the UK from a short-term perspective. For the German market, Sagner (2026) found price drops of approximately 8% within a year after the energy price shock. Energy-inefficient buildings experienced the sharpest price declines, based on a DiD analysis. Furthermore, they showed that energy efficiency continues to gain importance and points to higher demand for more energy-efficient buildings within one year.

The existing literature has primarily examined the capitalization of energy efficiency based on prices and rents. Due to search and matching frictions, real estate markets are also shaped by the time it takes to complete a transaction (Williams, 1995). Consequently, the effects of capitalization are reflected in prices and liquidity (Zahirovic-Herbert & Turnbull, 2008). In this context, the marketing period is interpreted not only as a measure of

liquidity, but also as an informational-quality signal (Taylor, 1999), resulting in systematically distorted prices if liquidity is not considered (Fisher et al., 2003). Thus, time on market (TOM) is considered a key measure of market liquidity, capturing the duration required to absorb a property in the market and reflecting the trade-off induced by pricing decisions between the achievable price and time to sell (Anglin et al., 2003). Accordingly, examining both the price and TOM is crucial for deriving a consistent interpretation of market dynamics. For example, this is reflected in the development of TOM-based indices (Carrillo & Williams, 2019) and approaches that explicitly account for the bidirectional relationship between prices and TOM (Gerassimenko et al., 2025).

Haurin (1988) was the first to demonstrate that TOM can be modeled as an independent outcome variable and found that atypical properties remain on the market longer. Thus, pricing strategies, property characteristics, and prevailing market conditions are crucial factors (Jud et al., 1996; Kang & Gardner, 1989; Knight, 2002). Trippi (1977) highlighted the fundamental trade-off between price and marketing duration, as higher prices are associated with longer sales times. Furthermore, liquidity itself is strongly influenced by cyclical market conditions, with hot and cold markets resulting in considerable differences in TOM (Krainer, 1999).

Studies have found that liquidity is an independent adjustment mechanism influenced by a variety of factors. Similar to price effects, spatial heterogeneities are evident, and liquidity varies systematically across market segments (van de Meulen & Mitze, 2014; Cajias & Freudenreich, 2018; Cajias et al., 2020). The explanatory power of spatial variables depends on the degree to which they capture local market conditions (Cajias & Freudenreich, 2024; Cajias & Freudenreich, 2018; Gerassimenko et al., 2025). Housing market dynamics are shaped by both informational and behavioral factors. Enhanced price transparency improves market efficiency and leads to faster transactions (Aydin et al., 2020; Eerola & Lyytikäinen, 2015). Genesove and Mayer (2001) showed that behavioral factors matter because loss-averse sellers set higher asking prices and accept longer TOM.

Furthermore, liquidity is not solely determined by microeconomic factors. It also reacts to aggregate shocks over the business cycle, which affects prices, transaction volumes, and TOM (Díaz & Jerez, 2013). Exogenous shocks, such as the COVID-19 pandemic, further affect these dynamics, leading to significant changes in TOM (Gdakowicz & Putek-Szelg, 2025). Huang and Palmquist (2001) showed that environmental factors, such as noise, negatively affect pricing and TOM. In terms of energy efficiency, little is known about its direct link to liquidity. Aydin et al. (2020) showed that information on energy efficiency shortened TOM for both high and low EPC classes, as it reduces information asymmetries

between buyers and sellers. Once EPC information is published, liquidity effects are greater than for less informative or belatedly provided labels due to higher transparency. For the German rental market, Cajias et al. (2019) found that energy-inefficient buildings remain on the market significantly longer, providing evidence that energy efficiency is capitalized into both rents and market liquidity, whereas inefficient buildings face both price discounts and longer marketing periods. Gerassimenko et al. (2025) confirmed these patterns using a linear model to examine price, energy efficiency, and TOM in the Belgian market. The results indicated that energy-efficient buildings tend to have longer TOMs. By contrast, buildings with average EPC ratings (B/C) are associated with shorter TOM, whereas inefficient buildings respond differently across market segments, with shorter TOM in the sales market and longer TOM in the rental market. Furthermore, regional factors were found to have no significant impact, underscoring the importance of micro-local characteristics, as the immediate neighborhood appears to be more relevant than the broader geographic location (Aydin et al., 2020; Cajias & Freudenreich, 2024; Gerassimenko et al., 2025).

Overall, the existing literature provides compelling evidence that energy efficiency is capitalized not only in prices and rents but also, to a more limited extent, in market liquidity. Nevertheless, little is known about the long-term price and liquidity effects of energy efficiency across different market regimes. In particular, the literature on liquidity effects is limited to a small number of largely static cases, such as the Belgian market and the German rental market (Cajias et al., 2019; Gerassimenko et al., 2025). This approach defines energy efficiency as a market- and regime-dependent factor whose financial relevance may shift in response to changes in uncertainty, costs, and regulation. Therefore, this research aims to determine how energy efficiency is reflected in both pricing and market liquidity across multiple market phases and overlapping shocks, based on the German residential real estate market. By focusing on the post-2022 phase, characterized by the transition from a liquidity-driven to a more risk- and cost-driven market environment, the study contributes to a better understanding of regime dependence in green premiums and brown discounts, as well as their relevance for market liquidity and risk perception.

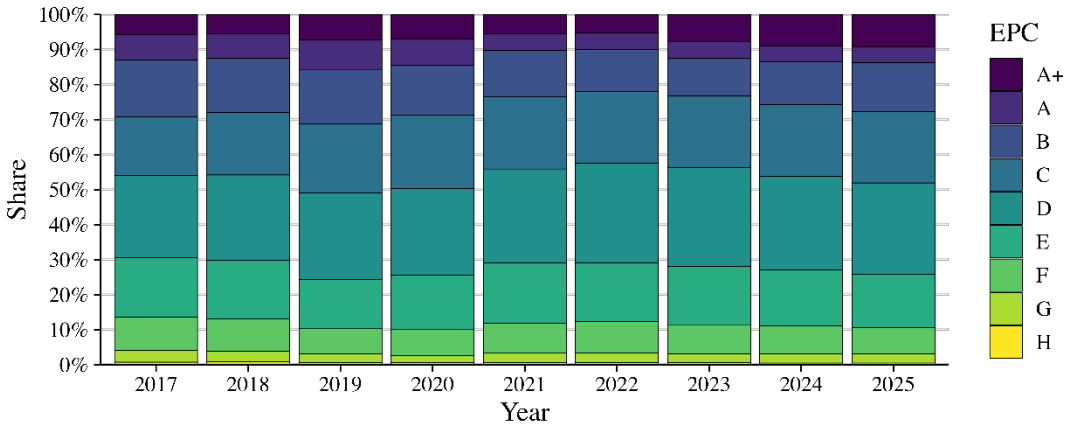
5.5 Data

The empirical analysis combines data from several sources to provide a comprehensive picture of the German residential real estate market. The main dataset is derived from Germany's largest online real estate platform (Leibniz-Institut für Wirtschaftsforschung, 2025). With a market share of over 50% of all residential property listings, the platform provides a high-frequency, geographically comprehensive dataset well-suited for analyzing regional residential real estate markets (Heuer & Thiel, 2025). The analysis focused exclusively on apartments, thereby improving comparability across observations and reducing structural heterogeneity across housing types. As the data are derived from online listings, the observed prices refer to the advertised asking prices. However, previous studies suggest that asking prices and actual transaction prices in the German real estate market are closely related and deviate only moderately (Kolbe et al., 2021; von Ahlefeldt-Dehn et al., 2023). Against this background, listing data provide an established basis for the empirical analyses of the German housing market (Cajias et al., 2019; Sagner, 2026). Within the analysis, the market is examined at the Nomenclature of Territorial Units for Statistics (NUTS)-3 level.[34] To account for spatial heterogeneity, the listed data are combined with the Eurostat typology of urban and rural areas provided by the Federal Institute for Research on Building, Urban Affairs, and Spatial Development (Bundesinstitut für Bau-, Stadt- und Raumforschung [BBSR], 2023; Eurostat, 2023). This classification distinguishes between three categories based on the proportion of the population living in urban agglomerations or rural grid cells within each NUTS-3 region. In addition, each property is georeferenced in a 1 km grid cell. This spatial reference captures fine-grained local variations beyond administrative boundaries and enables more precise control over spatial heterogeneity.

Energy efficiency is captured by the energy performance value (EPV), which reflects annual energy consumption per square meter and is expressed in kilowatt-hours per square meter per year (kWh/m^2/year) (Heuer & Thiel, 2025). Observations with missing energy-efficiency information were removed during the data cleaning process. A winsorization procedure is applied to the numerical variables (Huber, 1981) to reduce the influence of extreme outliers. The EPV variable is truncated at the 0.5th and 99.5th percentiles, resulting in an effective EPV range of 9.7 to 291 kWh/m^2/year. Figure 5.1 illustrates the distribution of listings across EPC classes over time, with EPC class D accounting for the largest share of observations.

[34] The NUTS-3 level corresponds to the district level and is based on the EU-wide NUTS classification (Statistisches Bundesamt, 2026c).

Figure 5.1 Distribution of EPC Classes over Time



Note: This figure provides an overview of the composition of the sample and shows the distribution of EPC classes over the period 2017 to 2025. The horizontal axis displays the years, while the vertical axis represents the share of observations. The stacked bars illustrate the proportion of each EPC class within the total sample for each year.

The final dataset comprises 656,649 observations from 2017 to 2025. An overview of the variables and their descriptive statistics is presented in Table 5.2. The analysis includes variables capturing property characteristics, as well as market- and location-specific factors. These include numerical variables, such as price and living area, binary indicators describing apartment features, and categorical variables representing building conditions and interior quality. Temporal control variables account for time-specific influences over the observation period, whereas spatial controls capture regional differences at the NUTS-3 level and fine-grained local variations at the 1 km grid-cell level. Continuous variables, such as price and living area, are log-transformed to account for right-skewed distributions.

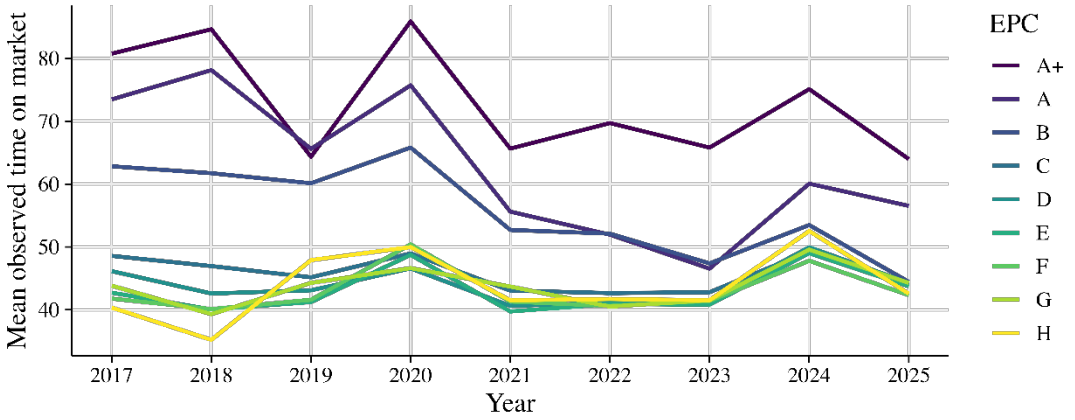
In addition to the price information, the dataset contains variables that provide insights into market liquidity and marketing dynamics. In particular, the TOM variable measures the time between the publication of a listing and its removal from the platform. Thus, TOM serves as an indicator of the marketing duration of a property and reflects the speed at which residential units are absorbed by the market (Cajias et al., 2019). The listing attention variable is provided by the data source as a duration-adjusted measure of listing attention and is therefore not mechanically driven by longer market exposure (Heuer & Thiel, 2025). Figure 5.2 illustrates the development of TOM over time across energy efficiency classes. The descriptive evidence indicates that listings for highly energy-efficient properties tend to remain on the market longer than listings for properties with lower energy efficiency. In particular, listings in EPC class A+ to B exhibit noticeably longer marketing durations than less energy-efficient properties.

Table 5.2 Descriptive Statistics

Variable	n	Share (%)	Mean	SD	Min	P25	P50	P75	Max
Price	656,649	100.00	321,204.46	217,682.71	30,000.00	168,000.00	268,000.00	410,000.00	1,288,000.00
log(Price)	656,649	100.00	12.46	0.69	10.31	12.03	12.50	12.92	14.07
Area	656,649	100.00	78.98	27.87	30.00	59.00	75.07	94.42	192.20
log(Area)	656,649	100.00	4.31	0.35	3.40	4.08	4.32	4.55	5.26
Rooms	656,649	100.00	2.78	0.93	1.00	2.00	3.00	3.00	5.50
EPV	656,649	100.00	105.54	47.98	9.70	73.00	105.00	134.30	291.00
TOM	656,649	100.00	48.87	55.97	1.00	13.00	30.00	62.00	916.00
Listing Views	656,649	100.00	63.81	74.58	2.71	19.74	37.49	74.36	484.00
log(Listing Views)	656,649	100.00	3.70	0.95	1.31	3.03	3.65	4.32	6.18
Elevator	656,649	100.00	0.39	0.49	0.00	0.00	0.00	1.00	1.00
Balcony	656,649	100.00	0.83	0.38	0.00	1.00	1.00	1.00	1.00
Guest Toilet	656,649	100.00	0.29	0.46	0.00	0.00	0.00	1.00	1.00
Rented-out	656,649	100.00	0.25	0.43	0.00	0.00	0.00	0.00	1.00
Kitchen	656,649	100.00	0.51	0.50	0.00	0.00	1.00	1.00	1.00
Renovated	656,649	100.00	0.28	0.45	0.00	0.00	0.00	1.00	1.00
Condition	656,649	100.00							
Maintained	439,761	66.97	0.67	0.47	0.00	1.00	1.00	1.00	1.00
New	97,285	14.82	0.15	0.36	0.00	0.00	0.00	0.00	1.00
Refurbished	86,817	13.22	0.13	0.34	0.00	0.00	0.00	0.00	1.00
Poor	32,786	4.99	0.05	0.22	0.00	0.00	0.00	0.00	1.00
Interior	656,649	100.00							
Standard	326,511	49.72	0.50	0.50	0.00	0.00	0.00	1.00	1.00
Low	25,794	3.93	0.04	0.19	0.00	0.00	0.00	0.00	1.00
High	276,224	42.07	0.42	0.49	0.00	0.00	0.00	1.00	1.00
Luxury	28,120	4.28	0.04	0.20	0.00	0.00	0.00	0.00	1.00
Urbanization	656,649	100.00							
Urban	431,431	65.70	0.66	0.47	0.00	0.00	1.00	1.00	1.00
Intermediate	181,193	27.59	0.28	0.45	0.00	0.00	0.00	1.00	1.00
Rural	44,025	6.70	0.07	0.25	0.00	0.00	0.00	0.00	1.00
Year	656,649	100.00							
2017	97,819	14.90	0.15	0.36	0.00	0.00	0.00	0.00	1.00
2018	72,687	11.07	0.11	0.31	0.00	0.00	0.00	0.00	1.00
2019	73,970	11.26	0.11	0.32	0.00	0.00	0.00	0.00	1.00
2020	35,617	5.42	0.05	0.23	0.00	0.00	0.00	0.00	1.00
2021	62,350	9.50	0.09	0.29	0.00	0.00	0.00	0.00	1.00
2022	75,916	11.56	0.12	0.32	0.00	0.00	0.00	0.00	1.00
2023	81,974	12.48	0.12	0.33	0.00	0.00	0.00	0.00	1.00
2024	102,870	15.67	0.16	0.36	0.00	0.00	0.00	0.00	1.00
2025	53,446	8.14	0.08	0.27	0.00	0.00	0.00	0.00	1.00

Note: This table summarizes descriptive statistics for the variables used in this analysis over the full sample period. For each variable, the number of observations (n), share (in %), mean, standard deviation (SD), minimum, the 25th percentile (P25), median(P50), the75th percentile (P75), and maximum values are reported.

Figure 5.2 Average TOM by EPC Class and Year



Note: This figure reports the annual mean TOM by EPC class over the period 2017 to 2025. The horizontal axis displays the years, while the vertical axis shows the average TOM, measured in days. Each line represents a specific EPC class. The figure does not control for hedonic property characteristics or market conditions.

The time series also reveals heterogeneity in TOM over the observation period across the energy efficiency classes. Observations in EPC classes A+, A, and B exhibited a gradual decline in mean observed TOM over time. By contrast, TOM in the lower EPC classes from C to H remains broadly stable, with only a slight tendency toward longer marketing durations in the later years of the sample. These descriptive patterns suggest that the evolution of listing durations differs systematically across EPC classes.

5.6 Methodology

The empirical approach is twofold, examining both price effects and TOM dynamics. Analyzing both outcomes reflects the close relationship between price and marketing duration because both jointly shape market outcomes (Kalra et al., 1997). Prices and TOM are evaluated in separate models, whereas specific effects, such as temporal variation and spatial heterogeneity, are assessed consistently across both approaches.

In the first step, price effects are estimated. For this analysis, energy efficiency is incorporated in two ways. First, the EPC categories are used to capture potential threshold and classification effects. Second, continuous EPV is included, enabling a fine-grained assessment of the variation in energy efficiency (Copiello & Coletto, 2023). For the continuous EPV specification, the reference value is set to the sample mean (106 kWh/m²/year), whereas for the categorical EPC specification, the reference category is EPC class D.[35]

[35] The reference specifications are closely related, but not identical. EPC class D serves as the reference category in the categorical specification and corresponds to values above 100 and up to 130 kWh/m²/year, whereas the

Most studies evaluate the price premium for energy efficiency in a linear price model (Fuerst & van de Wetering, 2015; Kholodilin et al., 2017; Taruttis & Weber, 2022). Hence, ordinary least squares (OLS) models based on Rosen (1974) are used as benchmark specifications in Models (1) and (2) to estimate baseline price effects. The OLS specification includes the variables presented in Table 5.2, with the exception of TOM and listing views.[36]

Generalized additive models (GAMs) are estimated, as introduced by Hastie and Tibshirani (1987), to go beyond this linear benchmark. GAMs allow for the identification of nonlinear sensitivities and threshold effects that are not apparent in OLS specifications, by relaxing the linearity assumption, and may improve model fit and predictive power. The corresponding Models (3) to (8) are based on the same set of covariates as the benchmark OLS Models (1) and (2). Accordingly, the interpretation of nonlinear terms relies more on smooth effect plots than on single-point estimates. The analysis proceeds in three parts. In each part, both EPC- and EPV-based GAM specifications are estimated. In the first part (baseline setting), the EPC based Model (3) captures class-specific price differentials, whereas the EPV-based Model (4) examines nonlinear associations between energy efficiency and prices. The EPV-based GAM specification corresponding to Model (4) is shown in Equation 5.1.

$$log(P_{ijt}) = \alpha + X_{ijt}\beta + f(S_{ijt}) + f(EPV_{ijt}) + \mu_t + \gamma_j + \varepsilon_{ijt} \quad (5.1)$$

in which P_{ijt} denotes the price of property i at location j at time t. The vector $X_{ijt}\beta$ contains the covariates entering the model linearly, implying constant marginal effects that remain interpretable in line with the benchmark OLS specification. The smooth term $f(EPV_{ijt})$ represents the nonlinear price gradient of energy efficiency and $f(S_{ijt})$ captures the nonlinear spatial effects using penalized smooth functions of the property location. The terms μ_t and γ_j denote the fixed effects for each month and each district, respectively, accounting for temporal heterogeneity through common time shocks and spatial heterogeneity through persistent district-level differences.

The baseline Models (3) and (4) are extended by year-specific interaction effects in the second part to assess the temporal heterogeneity in responses to regulatory tightening, energy price fluctuations, and regime changes. Therefore, Models (5) and (6) capture whether the price effects of energy efficiency vary over time, building on the short-term

continuous specification uses the sample mean of 106 kWh/m²/year as the reference value. Results may vary between the two approaches.

[36] TOM is excluded, as it represents a post-listing outcome realized after market entry and jointly determined by pricing decisions and market responses. Conditioning on this variable would introduce post-treatment bias.

pricing effects (Sagner, 2026). Finally, spatial heterogeneity is assessed across market environments to reflect the differences in regional structures, local market conditions, and market segments (McCord et al., 2020; Sagner, 2026; Taruttis & Weber, 2022). Models (7) and (8) include urbanization-specific effects and evaluate whether the price effects of energy efficiency differ across the urban, intermediate, and rural markets.[37]

The second step moves beyond prices and examines TOM as a measure of housing market liquidity (Carrillo & Williams, 2019; Kluger & Miller, 1990). In this setting, TOM is defined as the duration until a listing exits the platform. The event of interest is delisting, which proxies market absorption, rather than a verified sale. Listings that remain active at the end of the observation window do not experience the event and are therefore treated as right-censored observations. Accordingly, TOM constitutes a positive duration variable subject to right-censoring (Collett, 2014; Kalbfleisch & Prentice, 2011).

A semi-parametric Cox proportional hazards model is estimated to account for this duration and censoring structure following Cox (1972). In real estate research, Cox models have been widely used to analyze residential liquidity and TOM dynamics (Cajias & Freudenreich, 2018; Cajias et al., 2019; Carrillo & Williams, 2019; Gerassimenko et al., 2025; Kluger & Miller, 1990). In this framework, the survival function describes the probability that a listing remains in the market up to duration τ, whereas the hazard function specifies the instantaneous delisting rate, conditional on survival up to that point (Cox, 1972; Kalbfleisch & Prentice, 2011). Cox models assume that the covariate effects are proportional to the observed TOM duration, whereas the baseline hazard remains unspecified and may vary freely over time (Collett, 2014; Cox, 1972). Hazard ratios above one indicate faster delisting and thus a shorter TOM, whereas ratios below one signal slower delisting and thus longer TOM. The semi-parametric baseline specification for Cox Model (9) is given by

$$h_i\left(\tau\middle|Z_{ijt}, u_t, \gamma_j\right) = h_0(\tau)\exp\left(Z_{ijt}\beta + f\left(EPV_{ijt}\right) + \mu_t + \gamma_j\right) \tag{5.2}$$

in which $h_i\left(\tau\middle|Z_{ijt}, u_t, \gamma_j\right)$ denotes the hazard that listing i exits the market at duration τ, conditional on the covariates Z_{ijt}, the energy performance value EPV_{ijt}, and the temporal and spatial fixed effects μ_t and γ_j, respectively, whereas $h_0(\tau)$ denotes the baseline hazard. The vector Z_{ijt} contains the same structural control variables as vector $X_{ijt}\beta$ in the price models, but is extended by the initial asking price and listing attention. This reflects

[37] In the specifications based on EPV, interaction effects between EPV and the respective grouping variable Z are incorporated through group-specific smooth functions ($f_{Z(i)}\left(EPV_{ijt}\right)$. These allow the nonlinear effects of energy efficiency to vary flexibly across categories, such as year or urbanization level.

the different conditioning structures of the two outcomes: the asking price is determined at listing entry and may influence subsequent market absorption, whereas TOM and the listing views are realized only ex post and are therefore excluded from the price specification (Anglin et al., 2003; Cajias et al., 2019). The smooth term $f(EPV_{ijt})$ captures the nonlinear association between EPV and the delisting hazard. The survival analysis is only based on continuous EPV specification.

In line with the price analysis, the Cox analysis proceeds in three parts. First, the Cox Model (9) estimates the baseline association between EPV and the delisting hazard. Second, the Cox Model (10) extends the baseline specification by including an interaction term between EPV and the listing year, capturing year-specific EPV effects. Third, the Cox Model (11) includes a term that captures variation in EPV effects across urbanization levels, accounting for spatial heterogeneity. Together, these specifications capture variation in the relationship between EPV and delisting hazards over time and urbanization contexts.

5.7 Results

5.7.1 Price Effects

We first apply the baseline OLS specifications as a parametric benchmark to estimate the price effects of energy efficiency. Models (1) and (2), reported in Appendix Table 5.9, estimate the baseline associations using EPC classes and continuous EPV, respectively. The results indicate that energy efficiency is significantly associated with housing prices under both specifications. Building on the OLS benchmark, the GAM specifications account for potential nonlinearities in the relationship between energy efficiency and prices. As shown in Table 5.3, they outperform the OLS benchmark in terms of model fit and prediction error, indicating that price effects are better represented in a semi-parametric framework. This is in line with previous studies documenting the nonlinear pricing effects of energy efficiency (Cajias & Piazolo, 2013; Copiello & Coletto, 2023; Perez et al., 2025).

Table 5.4 reports the GAM results for the baseline specifications, Models (3) and (4), and the extended specifications, Models (5) to (8). Part 1 presents the parametric coefficients with standard errors, whereas Part 2 reports the effective degrees of freedom (EDF) and corresponding approximate F-statistics for smooth terms. Across the EPV specifications (Models (4), (6) and (8)), the reported EDF values are consistently greater than one and highly significant, indicating that the relationship between energy efficiency and prices is nonlinear. The adjusted R^2 remains similar across all models, suggesting that the interaction

terms capture heterogeneity in the pricing of energy efficiency over time and by urbanization level, rather than altering overall model fit. This is further reflected in the variation in EPV smooths across years and urbanization categories, where the magnitude and shape of the energy-efficiency effect depend on the market context.

Table 5.3 Model Performance

Model	OLS		GAM	
	Baseline		Baseline	
	(1)	(2)	(3)	(4)
	EPC	EPV	EPC	EPV
n	656,649	656,649	656,649	656,649
Adj. R^2	0.8770	0.8766	0.8985	0.8986
MAE (EUR)	57,237.95	57,379.04	52,079.62	52,019.31
RMSE (EUR)	87,617.91	87,769.35	80,142.16	80,062.01
MAPE (%)	19.13	19.17	17.27	17.26
MdAPE (%)	14.88	14.90	13.61	13.60
RRSE	0.40	0.40	0.37	0.37

Model	GAM			
	Year		Urbanization	
	(5)	(6)	(7)	(8)
	EPC	EPV	EPC	EPV
n	656,649	656,649	656,649	656,649
Adj. R^2	0.8988	0.8990	0.8986	0.8988
MAE (EUR)	51,909.50	51,861.17	52,048.84	51,985.22
RMSE (EUR)	79,989.30	79,910.29	80,066.71	79,980.28
MAPE (%)	17.23	17.22	17.26	17.24
MdAPE (%)	13.56	13.55	13.61	13.60
RRSE	0.37	0.37	0.37	0.37

Note: This table reports model performance metrics for OLS and GAM specifications of the price model. All models are estimated based on the same sample. Fitted values are back-transformed prior to computing error metrics. The Mean Absolute Error (MAE) indicates the average magnitude of prediction errors, the Mean Absolute Percentage Error (MAPE) and the Median Absolute Percentage Error (MdAPE) reflect errors in relative terms (in %). The Root Mean Squared Error (RMSE) reports the quadratic mean of residuals, emphasizing larger deviations, and the Relative Root Squared Error (RRSE) shows model performance relative to a mean-only benchmark.

Table 5.4 GAM Results

Models	Baseline		Year		Urbanization	
	(3)	(4)	(5)	(6)	(7)	(8)
	EPC	EPV	EPC	EPV	EPC	EPV
Dependent variable	log(Price)	log(Price)	log(Price)	log(Price)	log(Price)	log(Price)
Part 1: Parametric coefficients						
Intercept	8.0116***	8.0458***	7.7183***	8.0394***	8.0562***	8.0465***
	(0.0218)	(0.0218)	(0.0171)	(0.0218)	(0.0253)	(0.0218)
log(Area)	1.0000***	0.9997***	1.0014***	1.0012***	0.9996***	0.9992***
	(0.0015)	(0.0015)	(0.0015)	(0.0015)	(0.0015)	(0.0015)
Rooms	-0.0143***	-0.0144***	-0.0147***	-0.0148***	-0.0140***	-0.0141***
	(0.0005)	(0.0005)	(0.0005)	(0.0005)	(0.0005)	(0.0005)
Elevator	0.0328***	0.0313***	0.0325***	0.0310***	0.0328***	0.0313***
	(0.0007)	(0.0007)	(0.0007)	(0.0007)	(0.0007)	(0.0007)
Balcony	0.0413***	0.0411***	0.0413***	0.0411***	0.0412***	0.0411***
	(0.0008)	(0.0008)	(0.0008)	(0.0008)	(0.0008)	(0.0008)
Guest Toilet	0.0280***	0.0281***	0.0280***	0.0281***	0.0280***	0.0282***
	(0.0007)	(0.0007)	(0.0007)	(0.0007)	(0.0007)	(0.0007)
Rented-out	-0.0569***	-0.0570***	-0.0570***	-0.0571***	-0.0569***	-0.0570***
	(0.0007)	(0.0007)	(0.0007)	(0.0007)	(0.0007)	(0.0007)
Kitchen	0.0255***	0.0255***	0.0256***	0.0256***	0.0255***	0.0255***
	(0.0006)	(0.0006)	(0.0006)	(0.0006)	(0.0006)	(0.0006)
Renovated	0.0482***	0.0475***	0.0475***	0.0468***	0.0481***	0.0473***
	(0.0009)	(0.0009)	(0.0009)	(0.0009)	(0.0009)	(0.0009)
Condition: New	0.1495***	0.1472***	0.1527***	0.1503***	0.1493***	0.1470***
	(0.0013)	(0.0013)	(0.0013)	(0.0013)	(0.0013)	(0.0013)
Condition: Refurbished	0.0183***	0.0193***	0.0180***	0.0190***	0.0184***	0.0193***
	(0.0009)	(0.0009)	(0.0009)	(0.0009)	(0.0009)	(0.0009)
Condition: Poor	-0.0889***	-0.0885***	-0.0889***	-0.0886***	-0.0888***	-0.0886***
	(0.0014)	(0.0014)	(0.0014)	(0.0014)	(0.0014)	(0.0014)
Interior: Low	-0.1016***	-0.1012***	-0.1012***	-0.1007***	-0.1013***	-0.1010***
	(0.0016)	(0.0016)	(0.0016)	(0.0016)	(0.0016)	(0.0016)
Interior: High	0.1764***	0.1754***	0.1758***	0.1748***	0.1764***	0.1753***
	(0.0007)	(0.0007)	(0.0007)	(0.0007)	(0.0007)	(0.0007)
Interior: Luxury	0.3170***	0.3149***	0.3172***	0.3151***	0.3173***	0.3149***
	(0.0015)	(0.0015)	(0.0015)	(0.0015)	(0.0015)	(0.0015)
EPC	Yes		Yes		Yes	
EPC × Year			Yes			
EPC × Urbanization					Yes	
Part 2: Smooth terms						
s(EPV)	---	6.950 19,593.8***	---	---	---	---
s(EPV) in 2017	---	---	---	6.593 3,111.1***	---	---
s(EPV) in 2018	---	---	---	6.459 1,857.5***	---	---
s(EPV) in 2019	---	---	---	6.744 2,849.7***	---	---
s(EPV) in 2020	---	---	---	6.602 1,405.0***	---	---
s(EPV) in 2021	---	---	---	6.660 1,618.3***	---	---
s(EPV) in 2022	---	---	---	6.856 3,188.5***	---	---
s(EPV) in 2023	---	---	---	6.885 7,096.8***	---	---
s(EPV) in 2024	---	---	---	6.846 6,849.1***	---	---
s(EPV) in 2025	---	---	---	6.602 5,852.2***	---	---

continued on next page

Table 5.4 GAM Results - **continued**

s(EPV) in urban areas	---	---	---	---	---	6.927 13,954.3***
s(EPV) in intermediate areas	---	---	---	---	---	6.908 7,241.5***
s(EPV) in rural areas	---	---	---	---	---	6.320 3,039.4***
Spatial smooth	Yes	Yes	Yes	Yes	Yes	Yes
Fixed effects & fit						
Temporal fixed effects	Yes	Yes	Yes	Yes	Yes	Yes
Spatial fixed effects	Yes	Yes	Yes	Yes	Yes	Yes
Observations	656,649	656,649	656,649	656,649	656,649	656,649
Adjusted R^2	0.8985	0.8986	0.8988	0.8990	0.8986	0.8988

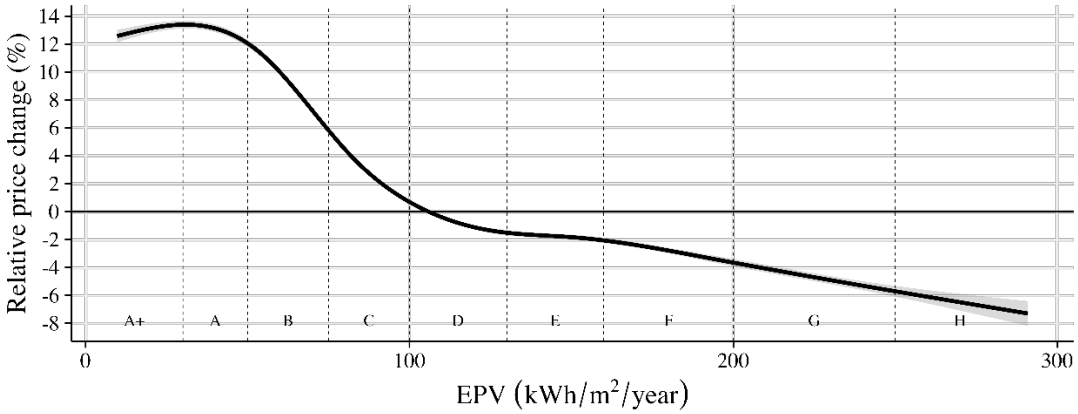
Note: This table reports the parametric coefficients, smooth terms, fixed effects, and model fit statistics from the GAM specifications for log(Price). Energy efficiency is measured either by discrete EPC classes or by continuous EPV in kWh/m²/year. Parametric coefficients are reported with standard errors in parentheses. For smooth terms, the first row reports the effective degrees of freedom (EDF), while the second row reports the corresponding approximate F-statistic and significance level. Models (3) and (4) present the baseline specifications, Models (5) and (6) the year-specific specifications, and Models (7) and (8) the urbanization-specific specifications, each estimated using either EPC or EPV. In the EPV specifications (6) and (8), smooth terms are estimated separately by year or urbanization category. The bottom panel reports temporal fixed effects, spatial fixed effects, spatial smooths, the number of observations, and adjusted R^2. Significance levels are: *** p < 0.001, ** p < 0.01, * p < 0.05, . p < 0.1.

Figure 5.3 illustrates the nonlinear relationship between EPV and prices for Model (4), while controlling for structural characteristics and common spatial and temporal effects. Relative to the sample mean of 106 kWh/m²/year, the results reveal a green premium of approximately 13% for highly efficient buildings, while less efficient buildings exhibit price discounts of up to 8%. This pattern points to nonlinear, heterogeneous price effects across the EPV spectrum. Moreover, the estimated curve displays flat segments in certain EPV ranges, where price effects remain stable. Highly efficient buildings, corresponding to EPC classes A+ and A, exhibit a constant premium, whereas moderately inefficient buildings around EPC class E are associated with discounts of about 2%. Outside these flat ranges, price effects change between highly efficient and average EPV levels and toward the highly inefficient end of the distribution. This interpretation aligns with evidence on discrete pricing effects at EPC class thresholds (Lu & Spaenjers, 2025).[38]

A static illustration does not show whether the market pricing of energy efficiency remains stable over time and across market phases (Chegut et al., 2014; Eichholtz et al., 2026; Reichardt et al., 2012). Therefore, Model (6) allows the price gradient of EPV to vary through the interaction between the EPV and year. Figure 5.4 presents the resulting yearly price effects across the EPV range, and Table 5.5 reports the corresponding premiums and discounts from Model (5) based on categorical EPC specifications. Over time, both the green premium and brown discount change in magnitude.

[38] The price effects for EPC bands are estimated in Model (3). Figure 5.10, reported in the Appendix, provides the corresponding discrete estimates for each EPC class.

Figure 5.3 Relative Price Effects by EPV



Note: This figure presents the estimated partial effects of EPV over the full sample period 2017 to 2025, based on Model (4). Energy efficiency is captured using continuous EPV (kWh/m²/year). The horizontal axis displays the EPV, while the vertical axis shows the estimated partial effects expressed as percentage changes relative to the reference value of 106 kWh/m²/year (sample mean).

At the beginning of the observation period in 2017, the green premium reached approximately 16%, whereas the brown discount amounted to approximately 8%.[39] This implies a spread of approximately 24%. Table 5.5 reflects this pattern in the EPC-based specification. The estimated curve suggests that highly energy-efficient buildings commanded substantial price premiums, whereas energy-inefficient buildings were moderately discounted. By contrast, price differentials remained small across the middle and lower parts of the efficiency scale. This may reflect a market environment characterized by low interest rates and strong demand, in which buyers were less selective regarding energy efficiency (Taruttis & Weber, 2022).

The following year, price differentiation by energy efficiency was weaker than in 2017. Both premiums and discounts declined, while the estimated price effects remained flat across the middle of the EPV distribution. This pattern is reflected in the EPC-based results in Table 5.5 with stable price effects for mid-ranging EPC classes from B to F. In 2018 and 2019, rising construction costs added to supply-side pressure. The year 2019 also marked a period of intensifying climate-policy debate. In Germany, the Climate Action Program 2030 and the related discussion on CO_2 pricing in the building sector increased the salience of energy efficiency in housing markets. Despite these political signals, the estimated price effects exhibited limited adjustment in 2019, with the brown discount remaining moderate at approximately 1% to 6%. This suggests that price adjustments occurred gradually in 2019, and that policy signals and expectations might be reflected in prices only over time (Cadena & Thomson, 2021). A stronger repricing became apparent from 2020 onward.

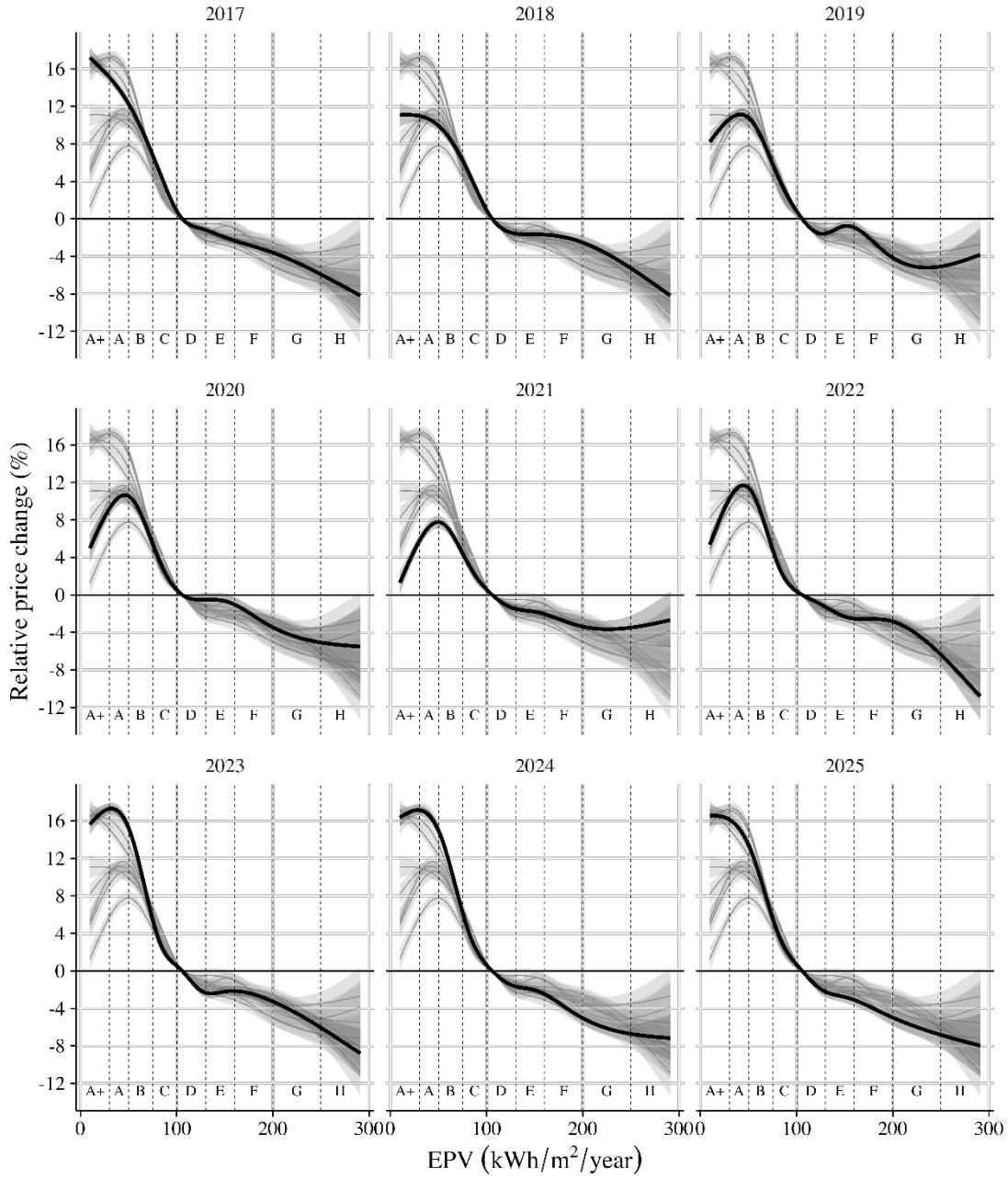
[39] For comparison, price effects in 2015 and 2016 are also examined in the robustness check.

For 2020, the estimated curve shows a steeper discount at the inefficient end of the EPV distribution, whereas the price gradient levels off around EPC classes D and E before declining further. Compared to 2019, this points to a modest increase in the penalization of energy-inefficient buildings rather than a broad-based repricing across the entire market. However, 2020 was shaped by the COVID-19 pandemic. Despite heightened economic uncertainty, interest rates remained very low, reinforcing housing demand and prices. In this context, the price effect associated with energy efficiency evolved gradually. This is in line with research from the US, showing that residential markets remained comparatively resilient during the pandemic period (Wang, 2021).

During the second year of the pandemic, the pricing of energy efficiency remained stable. Both the green premium and brown discount were small, relative to earlier years, revealing limited differentiation by energy efficiency. As shown in Figure 5.4, the spread between premiums and discounts narrowed further. Housing demand remained strong despite ongoing pandemic-related uncertainty, thereby compressing energy-efficiency-related price differentials. This is consistent with previous evidence suggesting that, in expansionary market phases with strong demand, differences in energy efficiency are less strongly capitalized because buoyant market conditions partially offset quality differentials across properties (Reichardt et al., 2012). Although the first signs of rising energy costs were emerging, these changes were not yet materially reflected in housing prices.

The market environment changed in 2022, when the Russian invasion of Ukraine triggered an increase in energy prices (Bachmann et al., 2024; Lutz & Becker, 2023). At the same time, changes in monetary policy of the European Central Bank caused financing costs to rise. As borrowing became more expensive, market participants had stronger incentives to consider long-term cost structures (Duca et al., 2021). Property prices responded gradually in 2022, with a broader market correction becoming apparent toward the end of the year. The results suggest that energy efficiency became more relevant for price formation during this period. Brown discounts widened relative to preceding years, whereas green premiums increased. This pattern is reflected in the EPC-based results in Table 5.5. The energy price shock and the shift in financing conditions increased the salience of future operating costs and renovation risks, leading the market to differentiate more strongly between efficient and inefficient properties (Brolinson et al., 2026).

Figure 5.4 Time-Varying Price Effects by EPV



Note: This figure presents the estimated effects of energy efficiency over the full sample period 2017 to 2025, based on Model (6). The model is specified with an interaction term between year and EPV, where energy efficiency is measured using continuous EPV (kWh/m^2/year). Each panel represents a separate year. The horizontal axis displays the EPV, while the vertical axis shows the estimated effects expressed as percentage changes relative to the reference value of 106 kWh/m^2/year (sample mean). EPC classes are indicated along the EPV scale for reference. The black line highlights the respective year, while the grey lines represent the effects estimated for the other years. Shaded areas show the associated confidence intervals.

The repricing became more visible in 2023, particularly at the high-efficiency end of the EPV distribution. The green premium rose to as much as 17%, reaching its highest level of the observation period, whereas the brown discount remained elevated. Accordingly, the gap between energy-efficient and energy-inefficient buildings widened relative to previous years. Based on Table 5.5, the EPC-based specification reveals a clear spread in price effects. This suggests a delayed capitalization of higher energy prices in property values.

In addition, construction costs and financing costs peaked, contributing to market uncertainty (Bernanke, 2018; Claessens & Kose, 2013). In this environment, energy-efficient buildings may be perceived as more attractive due to lower operating costs, reduced renovation risks, and potentially more favorable financing conditions (Singhal et al., 2026).

In 2024, the green premium persisted at a high level, whereas the brown discount widened further. This increased the pricing spread between energy-efficient and energy-inefficient properties. The pattern points to the growing importance of energy efficiency, suggesting that high financing and construction costs, along with tightening regulatory requirements, amplified the devaluation of inefficient buildings. This suggests that risk and regulatory pressure were gradually incorporated into housing prices over time.

The adjustment of green premiums and brown discounts to the energy crisis and the changing regulatory environment stabilized by 2025. At the same time, interest rates remained higher than before the crisis, meaning that market participants may have continued to pay close attention to long-term operating costs, expected renovation needs, and broader holding costs (Taruttis & Weber, 2022).

Table 5.5 EPC Class Price Premiums and Discounts over Time

EPC	Overall	2017	2018	2019	2020	2021	2022	2023	2024	2025
A+	13.65	16.80	12.98	10.31	6.95	3.46	7.51	17.10	17.52	17.77
A	13.76	13.88	10.04	11.52	10.52	8.95	14.19	19.28	18.00	16.76
B	9.16	9.67	8.95	8.91	7.74	6.73	7.90	10.05	10.53	9.72
C	3.49	4.13	4.19	3.02	2.16	2.81	2.79	3.36	3.85	4.39
D	0.00	0.00	0.00	0.00	0.00	0.00	0.00	0.00	0.00	0.00
E	-0.84	-0.97	-0.33	0.04	-0.81	-1.15	-0.87	-1.23	-0.89	-1.22
F	-1.96	-3.21	-0.73	-1.60	-1.36	-1.84	-1.79	-1.45	-2.21	-2.81
G	-3.33	-1.15	-2.95	-3.27	-3.97	-2.71	-3.73	-3.59	-5.66	-3.63
H	-6.10	-9.03	-6.35	-5.07	-6.23	-1.90	-6.11	-5.39	-6.01	-5.69

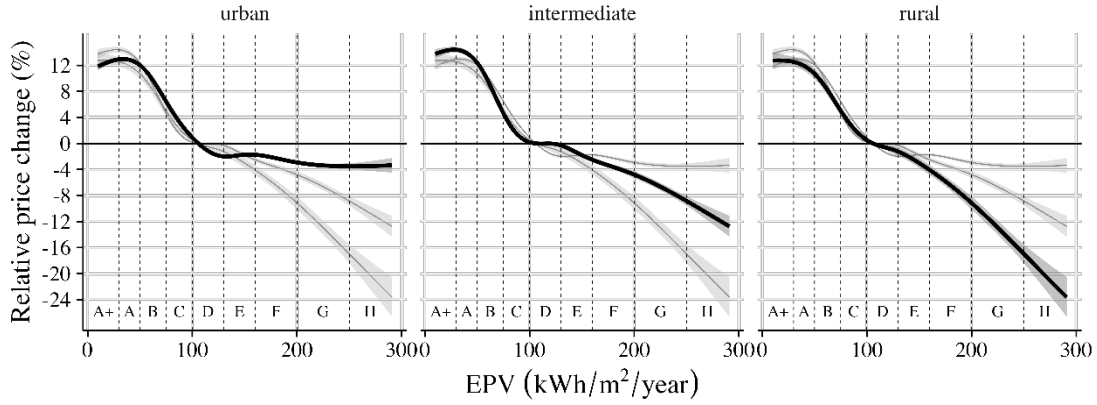
Note: This table reports estimated price premiums (positive values) and discounts (negative values) in percent relative to EPC class D. EPC class D is normalized to zero in all specifications by construction. The year-specific columns are based on Model (5), and values are expressed as percentage changes derived from the estimated coefficients. The Overall column reports the average premium across all years, based on Model (3).

Comparing the complete observation period from 2017 to 2025, green premiums did not follow a monotonic trend; instead fluctuated over time. Although the green premium was high at the beginning of the observation period, the overall spread between efficient and inefficient properties narrowed during the low-interest-rate phase and widened again after the onset of the energy crisis. However, a more persistent pattern appeared at the inefficient end of the distribution. Brown discounts were slightly larger at the end of the sample than at the beginning. This suggests that the market increasingly penalizes energy-inefficient assets over time, reflecting greater sensitivity to energy costs, renovation needs, and regulatory risks. The repricing of energy efficiency was driven not only by an increase

in green premiums but also by a stronger capitalization of downside risks for inefficient buildings.

With regard to regional heterogeneity, Figure 5.5 shows that prices vary not only over time but also by degrees of urbanization. In urbanized areas, where housing demand tends to be high (Taruttis & Weber, 2022), differences in energy efficiency have only a limited price effect and brown discounts remain small. By contrast, rural regions, typically characterized by weaker demand, exhibit greater differentiation by energy efficiency. Properties with high EPV face larger discounts, suggesting that energy inefficiency is more strongly capitalized in lower-demand markets. Intermediate markets fall between urban and rural areas in terms of the extent to which energy efficiency is reflected in prices. This pattern is also reflected in the EPC-based results for Model (7) in Table 5.6, in which the differentiation is greatest at the inefficient end of the distribution. According to Model (7), for the worst EPC class, the discount is -3.01% in urban markets, -10.51% in intermediate markets, and -19.22% in rural markets. Differences across urbanization levels emerge mainly from EPC class F onward, with the strongest spatial heterogeneity among the "worst-performing buildings". By contrast, green premiums vary less across urbanization levels, suggesting that locational differences mainly reflect stronger penalties for inefficient buildings.

Figure 5.5 Spatial Variation in Price Effects by EPV



Note: This figure presents the estimated effects of energy efficiency over the full sample period 2017 to 2025, based on Model (8). The model is specified with an interaction term between EPV and the level of urbanization. Energy efficiency is measured as a continuous value (kWh/m²/year). EPCs are indicated along the EPV scale for reference. The horizontal axis displays the EPV, and the vertical axis shows the estimated effects expressed as percentage changes relative to the reference value of 106 kWh/m²/year (sample mean). The three panels represent the urbanization categories urban, intermediate, and rural. The black line highlights the respective urbanization category, and the grey lines represent the effects estimated for the other categories. Shaded areas show the associated confidence intervals.

Table 5.6 EPC Class Price Premiums and Discounts by Urbanization Levels

EPC	Urban	Intermediate	Rural
A+	13.22	13.97	14.06
A	13.98	13.57	12.52
B	9.81	8.02	7.66
C	4.22	1.53	4.55
D	0.00	0.00	0.00
E	-0.66	-1.14	-1.08
F	-1.29	-3.34	-4.21
G	-1.54	-6.80	-11.12
H	-3.01	-10.51	-19.22

Note: This table reports estimated price premiums (positive values) and discounts (negative values) in percent relative to EPC class D across different urbanization levels. Values are expressed as percentage changes derived from the estimated coefficients. EPC class D is normalized to zero in each urbanization category by construction. The columns report price effects within urban, intermediate, and rural markets based on Model (7).

5.7.2 Liquidity Effects

The analysis of market liquidity examines how quickly a property exits the market after listing and thus focuses on the delisting hazard. The results of the corresponding Cox Models (9) to (11) are reported in Table 5.7. Most covariates are statistically significant and therefore contribute to explaining variation in market liquidity. In addition, the concordance, which measures the model's ability to correctly rank listings by their relative delisting risk, indicates high accuracy. Model (10), accounting for temporal differences, performs slightly better than the baseline and urbanization-specific specifications, although the differences are small.

The model specifications isolate the association between energy efficiency and the delisting hazard and express it relative to the reference value.[40] The baseline specification, shown in Figure 5.6, indicates that market liquidity is highest around average energy efficiencies and decreases toward both tails of the EPV distribution. Properties with high EPV values exhibit a lower delisting hazard, signaling longer marketing periods for less energy-efficient buildings. A smaller decline is also visible among highly efficient properties, which may reflect selective demand or higher asking prices in this segment.

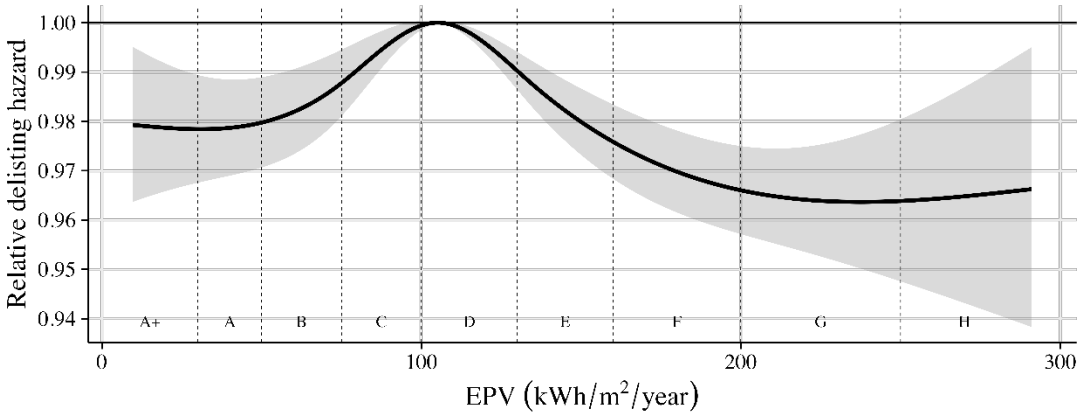
[40] The reference value, analogous to the price analysis, refers to the mean EPV of 106 kWh/m²/year, which corresponds to EPC class D.

Table 5.7 Cox Survival Model Results

	Baseline	Year	Urbanization
Models	(9)	(10)	(11)
Dependent variable	TOM	TOM	TOM
Parametric coefficients: Hazard ratios			
log(Price)	0.933***	0.931***	0.934***
	(0.0052)	(0.0052)	(0.0052)
log(Area)	0.864***	0.871***	0.864***
	(0.0087)	(0.0087)	(0.0087)
Rooms	1.001	0.999	1.001
	(0.0025)	(0.0025)	(0.0025)
Elevator	0.948***	0.946***	0.947***
	(0.0030)	(0.0030)	(0.0030)
Balcony	1.021***	1.022***	1.021***
	(0.0035)	(0.0035)	(0.0035)
Guest Toilet	1.009**	1.010**	1.008*
	(0.0033)	(0.0033)	(0.0033)
Rented-out	0.846***	0.844***	0.846***
	(0.0032)	(0.0032)	(0.0032)
Kitchen	1.053***	1.052***	1.052***
	(0.0029)	(0.0029)	(0.0029)
Renovated	1.047***	1.035***	1.047***
	(0.0041)	(0.0041)	(0.0041)
Condition: New	0.817***	0.851***	0.817***
	(0.0061)	(0.0062)	(0.0061)
Condition: Refurbished	0.980***	0.980***	0.980***
	(0.0040)	(0.0040)	(0.0040)
Condition: Poor	0.993	0.991	0.993
	(0.0065)	(0.0065)	(0.0065)
Interior: Low	1.035***	1.039***	1.035***
	(0.0073)	(0.0073)	(0.0073)
Interior: High	1.025***	1.023***	1.026***
	(0.0034)	(0.0034)	(0.0034)
Interior: Luxury	1.094***	1.091***	1.094***
	(0.0072)	(0.0072)	(0.0072)
log(Listing views)	1.651***	1.656***	1.651***
	(0.0017)	(0.0017)	(0.0017)
Nonlinear terms			
ns(EPV)	Yes	Yes	Yes
ns(EPV) × Year		Yes	
ns(EPV) × Urbanization			Yes
Fixed effects & fit			
Temporal fixed effects	Yes	Yes	Yes
Spatial fixed effects	Yes	Yes	Yes
Observations	656,649	656,649	656,649
Concordance	0.6778	0.6780	0.6778

Notes: This table reports estimation results from Cox proportional hazards models of TOM. Energy efficiency is measured by continuous EPV in kWh/m2/year. Coefficients are reported as hazard ratios, with standard errors of the underlying coefficients shown in parentheses. Values above one indicate a higher delisting hazard and thus shorter TOM, while values below one indicate a lower delisting hazard and thus longer TOM. Models (9) to (11) present the baseline, year-specific, and urbanization-specific specifications, respectively. All specifications include temporal and spatial fixed effects. Nonlinear effects of EPV are modeled using natural cubic splines. Interaction rows indicate whether the respective term is included. In Models (10) and (11), interaction terms allow the association between EPV and the delisting hazard to vary across years and urbanization levels. The bottom panel reports the number of observations and the concordance statistic. Significance levels are: ∗∗∗p < 0.001, ∗∗p < 0.01, ∗p < 0.05, .p < 0.1.

Figure 5.6 Relative Delisting Hazard by EPV



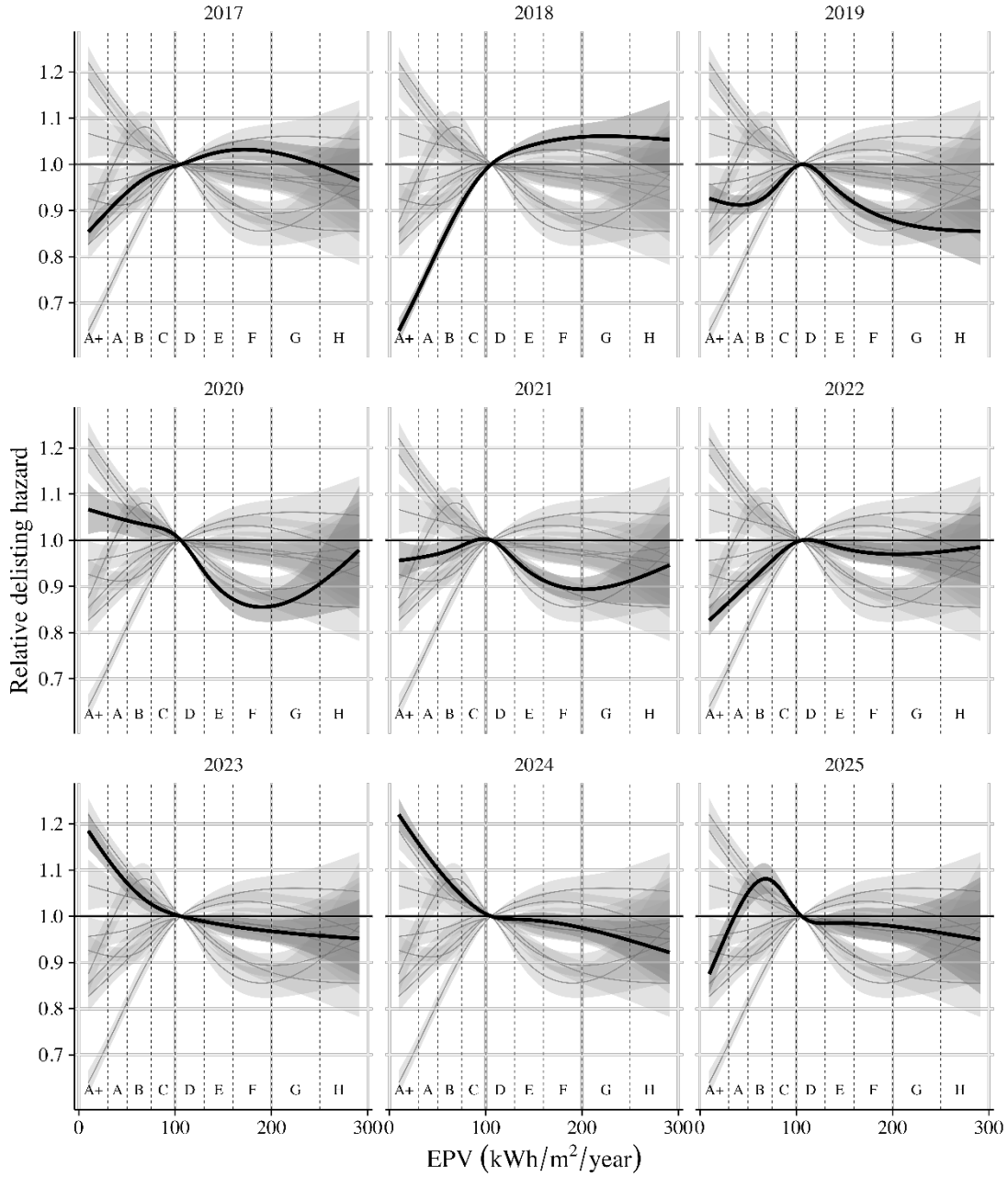
Note: This figure presents the estimated association between energy efficiency and the delisting hazard based on the Cox Model (9). Energy efficiency is measured using continuous EPV in kWh/m²/year. The horizontal axis displays EPV, and the vertical axis shows the estimated hazard ratios relative to the reference value of 106 kWh/m²/year (sample mean). Values above one indicate a higher delisting hazard and thus shorter TOM, and values below one indicate a lower delisting hazard and thus longer TOM. All other covariates are held constant. Shaded areas show the associated confidence intervals. EPC classes are shown along the EPV scale for reference.

Figure 5.7 illustrates the year-specific delisting hazards across the EPV range. It shows that the relationship between energy efficiency and market liquidity varies over time. In the early years of the observation period, the relationship between energy efficiency and market liquidity was not monotonic. In 2017, energy-efficient properties did not appear to sell faster than listings with a reference EPV of 106 kWh/m²/year. Their lower delisting hazards imply longer TOM. By contrast, delisting hazards increased toward the middle of the EPV distribution and remained elevated for moderately inefficient properties, suggesting higher market liquidity in this segment. The pattern weakened again at the least efficient end of the distribution. In 2018, this pattern became more pronounced. Highly efficient properties again showed relatively low delisting hazards, while listings around the reference EPV and in the moderately inefficient range exhibited higher delisting hazards. This suggests that market liquidity was highest for average to moderately inefficient properties, rather than for the most energy-efficient listings.

From 2019 onward, the pattern changed. The year-specific curves peaked around the reference value, suggesting that listings with average EPVs exhibited the highest delisting hazard and thus the shortest TOM, whereas both efficient and inefficient properties remained on the market somewhat longer. During the low-interest-rate phase and under strong demand conditions, properties with extreme EPV profiles were associated with slightly lower liquidity. This contrasts with the price results, in which differentiation across energy efficiency levels remained visible, albeit weaker. A similar pattern persisted from 2020 to 2022, with delisting hazards peaking around the reference category and liquidity differences across the EPV distribution remaining modest. The COVID-19 pandemic

increased economic uncertainty, but low interest rates and robust housing demand might dampen differences in market liquidity across the EPV distribution.

Figure 5.7 Relative Delisting Hazard by EPV over Time



Note: This figure presents the estimated delisting hazard across the EPV range over time, based on the year-specific Cox specification of Model (10). Energy efficiency is measured using continuous EPV in kWh/m²/year. The horizontal axis displays EPV, while the vertical axis shows the estimated hazard ratios relative to the reference value of 106 kWh/m²/year (sample mean), holding all other covariates constant. Values above one indicate a higher delisting hazard and thus shorter TOM, while values below one indicate a lower delisting hazard and thus longer TOM. Each panel represents a specific year. The black line highlights the respective year, while the grey lines show the estimated effects for the other years. Shaded areas show the associated confidence intervals. EPC classes are shown along the EPV scale for reference.

A clearer shift emerged in 2023, when the effects of the energy crisis and tightening regulatory requirements became apparent. Properties with lower EPV tended to exhibit higher delisting hazards and thus shorter TOM, suggesting that energy efficiency was associated with stronger marketability during periods of increased uncertainty. The price

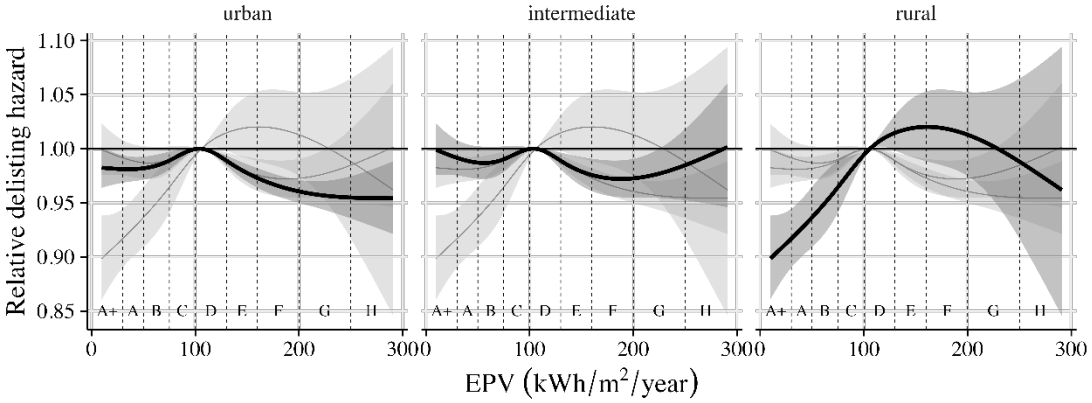
results also pointed to stronger differentiation by energy efficiency. In this sense, inefficient properties faced a joint disadvantage in both price and marketability. These adjustments appear with a temporal lag relative to rising energy prices and regulatory pressure, suggesting that TOM responses materialize gradually as market participants revise expectations and market frictions delay transaction processes (Cajias & Freudenreich, 2018; Díaz & Jerez, 2013). In 2024, the liquidity advantage of energy efficiency became evident, as delisting hazards remained above the reference level at the efficient end and below it at the inefficient end.

Market liquidity stabilized further in 2025. Energy-efficient properties exhibited a relative liquidity advantage, although the pattern was less pronounced than during the immediate post-crisis adjustment phase. At the same time, the peak of market liquidity shifted from approximately 106 kWh/m^2/year in 2019 to approximately 60 kWh/m^2/year in 2025. This suggests that the liquidity advantage of energy-efficient properties has become more firmly embedded in market absorption dynamics amid the energy crisis and tightening regulations. Overall, the liquidity effect of energy efficiency is not constant over time but depends on changing market conditions. The liquidity patterns suggest that price and marketability do not necessarily evolve in parallel.

Regarding the spatial dimension, Figure 5.8 shows that the liquidity effects are broadly similar in urban and intermediate markets, with only modest differences across the EPV range. In both urban and intermediate markets, the peak in market liquidity is close to the reference value, and the hazard-rate profiles are relatively compressed. This indicates that differences in energy efficiency translate only weakly into differences in TOM. In these markets, strong demand appears to reduce the extent to which energy efficiency affects market liquidity. However, this pattern differs in rural markets. Here, the spread in hazard ratios is substantially larger, suggesting that energy efficiency becomes more relevant for TOM when overall demand is weaker. Market liquidity peaks among moderately inefficient properties, roughly in the EPC class E–F range, whereas both highly efficient and highly inefficient properties remain on the market longer. This pattern is partly consistent with the price effects. In the liquidity analysis, however, the larger spread in rural markets suggests that buyers also differentiate more strongly by energy performance when demand pressure is lower. By contrast, liquidity appears to reflect demand-side frictions more directly (Clayton et al., 2008). In less competitive markets, buyers may be more price-sensitive, shifting demand toward properties in the middle of the energy-efficiency distribution rather than toward the most efficient segment. Although efficient buildings offer lower operating costs, they may appeal to a narrower pool of buyers due to higher acquisition costs. At the same time, highly inefficient properties face weaker market

demand due to expected renovation costs and regulatory risks. Consequently, price and liquidity differentiation are related but not identical: price effects reflect the capitalization of energy efficiency, whereas liquidity also reflects heterogeneous demand and market frictions.

Figure 5.8 Relative Delisting Hazard by EPV and Urbanization Levels

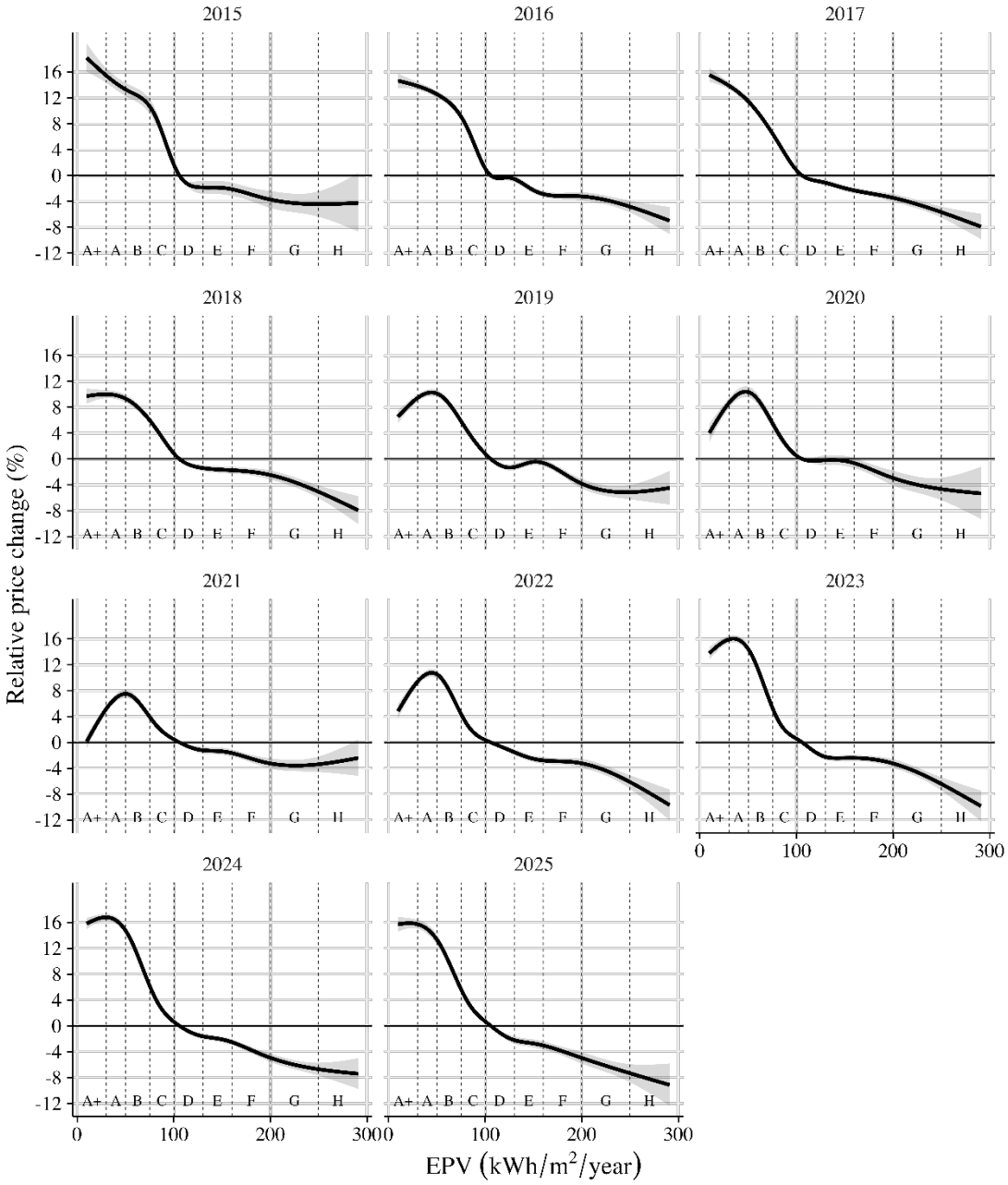


Note: This figure presents the estimated delisting hazard across the EPV range by urbanization level, based on the urbanization-specific Cox specification (Model (11)). Energy efficiency is measured using continuous EPV in kWh/m²/year. The horizontal axis displays EPV, and the vertical axis shows the estimated hazard ratios relative to the reference value of 106 kWh/m²/year (sample mean), holding all other covariates constant. Values above one indicate a higher delisting hazard and thus shorter TOM, and values below one indicate a lower delisting hazard and thus longer TOM. Each panel represents one urbanization category (urban, intermediate, rural). The black line highlights the respective category, and the grey lines show the estimated effects for the other categories. Shaded areas show the associated confidence intervals. EPC classes are shown along the EPV scale for reference.

5.7.3 Robustness Check

We extend the observation period to include 2015 and 2016 and contextualize our findings on green premiums and brown discounts. Extending the sample further back would add limited value, since mandatory EPC and EPV disclosure in Germany began in 2014. The robustness check is conducted for the GAM Models (5) and (6), which form the basis of the year-specific price analysis. Including 2015 and 2016, the sample size increases to 878,199 observations. Figure 5.9 shows that the estimated price effects for 2015 and 2016 do not differ markedly from those observed in 2017. The slopes of the curves are broadly similar, and the upper end of the distribution exhibits premiums of more than 13%. This suggests that such premiums can be regarded as a persistent feature rather than as a short-lived anomaly. By contrast, brown discounts are smaller in the earlier years, indicating that the larger discounts for energy-inefficient buildings are more likely a longer-term development (Wilkinson & Sayce, 2020). Overall, the extended sample supports the main findings, as the estimated patterns remain highly consistent with the main specifications.

Figure 5.9 Extended Sample for Year-Specific Price Effects by EPV



Note: This figure presents the estimated effects of energy efficiency over the extended sample period 2015 to 2025, based on Model (6). The model is specified with an interaction term between year and EPV. Energy efficiency is measured using continuous EPVs (kWh/m²/year). EPC classes are indicated along the EPV scale for reference. The horizontal axis displays the EPV, and the vertical axis shows the estimated effects expressed as percentage changes relative to the reference value of 106 kWh/m²/year (sample mean). Each panel represents a separate year. The black line highlights the respective year, and the grey lines represent the effects estimated for the other years.

In order to assess the stability of the liquidity findings, the following robustness check examines whether the results persist under a parametric duration model that does not rely on the Cox proportional hazards framework. The Cox model assumes proportional covariate effects on the hazard over listing duration, and the baseline hazard remains unspecified and may vary freely over time (Cox, 1972). However, in real estate markets, changing market conditions and other exogenous influences may cause effects to vary

over the duration time, potentially violating the proportional hazards assumption. To determine the robustness of the results to alternative model assumptions, we additionally estimate accelerated failure time (AFT) models. In contrast to the Cox models, which focus on the delisting hazard, AFT models directly specify the time until the event occurs and therefore provide a useful alternative in survival analysis (Kalbfleisch & Prentice, 2011; Wei, 1992). This formulation links the covariates directly to listing duration rather than to the hazard rate (Caamaño-Carrillo et al., 2025; Collett, 2014). Accordingly, the coefficients can be interpreted as multiplicative changes in listing duration. We adopt a Weibull specification because it provides a flexible parametric framework for modeling survival times and is suitable for the observed distribution of listing durations (Collett, 2014; Kalbfleisch & Prentice, 2011). The results of AFT Models (12), (13), and (14) are reported in Table 5.10 and in Figures 5.11 to 5.13 in the Appendix. Relative to the Cox models, the interpretation of the plots in terms of TOM is reversed since longer durations correspond to lower hazards. Nevertheless, the substantive patterns remain similar across both specifications. The main turning points occur at comparable times, including the shift from around 2018 to 2019, the market adjustment from around 2022 to 2023, and the subsequent period toward 2025. The overall curve shapes and spatial patterns are reproduced in the AFT specification, indicating that the results are robust to alternative model assumptions.

5.8 Conclusion

The importance of energy efficiency is widely recognized in research, policy debates, and market practice, particularly in the transition toward a more sustainable building stock. However, most existing evidence was generated under market conditions characterized by rising prices, low interest rates, and economic stability. By contrast, far less is known about how energy efficiency is capitalized under adverse conditions marked by geopolitical uncertainty, tighter monetary policy, and escalating energy costs. Germany was strongly affected by the energy crisis because of its former dependence on Russian natural gas, while simultaneously representing an advanced regulatory setting. Covering the period from 2017 to 2025, which includes both expansion phases and the recent market regime change in Germany, the study enables a direct comparison of how external shocks affect pricing and liquidity patterns in residential markets. Considering price and liquidity dynamics over time extends the existing literature and captures an additional dimension of market adjustment and capitalization effects. This combination allows an assessment of how regime changes jointly shape pricing and liquidity patterns.

Building on this context, the results reveal that the pricing of energy efficiency is neither static nor monotonic but follows a cyclical pattern shaped by macroeconomic and regulatory shifts. The widening price spread suggests stronger differentiation during periods of rising energy costs and higher interest rates. Energy-inefficient buildings appear more exposed to adverse market conditions and experience pronounced price discounts, whereas energy-efficient buildings maintain price premiums, indicating greater resilience to market shocks. However, price effects alone do not fully capture market dynamics. The analysis shows that price and time on market effects follow different patterns over time, although both become more sensitive to energy efficiency under adverse market conditions. During the low-interest-rate phase, market liquidity was highest for properties with average energy performance and, in some years, even for moderately inefficient EPVs, suggesting that strong demand partly absorbed quality differences. In contrast, during downturns and periods of increased uncertainty, energy-efficient properties tend to exhibit higher liquidity, whereas inefficient assets face a double burden of steeper price declines and longer time on the market. This dynamic is also reflected at the regional level. Although price effects are more pronounced in rural markets, liquidity effects appear to reflect the interplay of affordability, expected operating costs, and demand-side preferences.

Overall, these findings suggest that market adjustments follow different patterns over time, but that both price and liquidity effects become more strongly shaped by energy efficiency under adverse market conditions and uncertainty. Prices appear to reflect downside risks more strongly than upside potential, implying that crises widen the gap between green premiums and brown discounts during periods of market uncertainty and weak demand. Crucially, these reactions emerge with a time lag due to lingering effects of policy measures and market adjustment frictions.

The results have implications for investors and asset managers, as energy efficiency should not be treated as a static value, but as a regime-dependent factor that affects both pricing and marketability. During expansionary periods, strong demand partly absorbs differences in energy efficiency. However, during downturns, inefficient assets face a double burden of larger discounts and longer marketing periods, whereas efficient properties show greater resilience in terms of value preservation and market absorption. This points to cyclical inefficiencies and reinforces the importance of active portfolio adjustments. Therefore, strategies should consider both potential green premiums and the downside risk associated with inefficient assets. As price and liquidity effects differ across urban and rural markets, uniform policy approaches appear to be only partially effective. Stronger

alignment of regulatory measures with regional market structures could improve policy efficiency and support more targeted retrofit incentives.

The analysis relies on listing data rather than transaction data. Thus, TOM cannot be interpreted as a direct measure of completed transactions. Although this limitation is common in the German context due to limited data availability, the analysis treats delisting as a proxy for a successful transaction, thereby overlooking alternative outcomes such as withdrawal or platform switching. Although such cases may be infrequent and non-systematic, they cannot be fully excluded. Future research could address these limitations by incorporating transaction prices and verified transaction outcomes, extending the analysis to other markets, and accounting for financing conditions as an additional transmission channel.

5.9 Appendix

5.9.1 Appendix I – Descriptive Statistics

Table 5.8 Pearson Correlation

	(1)	(2)	(3)	(4)	(5)	(6)	(7)	(8)	(9)	(10)	(11)	(12)	(13)	(14)	(15)	(16)
(1) Price	1.000															
(2) log(Price)	0.913	1.000														
(3) EPV	-0.278	-0.283	1.000													
(4) Area	0.589	0.579	-0.174	1.000												
(5) log(Area)	0.563	0.581	-0.177	0.973	1.000											
(6) Rooms	0.404	0.420	-0.089	0.795	0.821	1.000										
(7) TOM	0.033	0.021	-0.126	0.049	0.049	0.017	1.000									
(8) Listing Views	0.013	0.035	0.100	0.031	0.031	0.062	-0.239	1.000								
(9) log(Listing Views)	-0.001	0.030	0.175	0.045	0.044	0.085	-0.345	0.851	1.000							
(10) Elevator	0.301	0.292	-0.363	0.112	0.098	-0.012	0.095	-0.036	-0.080	1.000						
(11) Balcony	0.169	0.208	-0.161	0.185	0.208	0.140	0.013	0.026	0.031	0.163	1.000					
(12) Guest Toilet	0.343	0.350	-0.159	0.512	0.508	0.435	0.027	0.034	0.040	0.151	0.162	1.000				
(13) Rented-out	-0.235	-0.259	0.140	-0.205	-0.209	-0.165	0.033	-0.027	-0.032	-0.104	-0.070	-0.146	1.000			
(14) Kitchen	0.037	0.068	0.178	-0.018	-0.028	-0.016	-0.123	0.093	0.155	-0.075	0.018	0.007	-0.071	1.000		
(15) Renovated	0.235	0.240	-0.418	0.184	0.183	0.108	0.127	-0.049	-0.107	0.310	0.120	0.163	-0.215	-0.207	1.000	
(16) Condition: Maintained	-0.188	-0.184	0.256	-0.100	-0.098	-0.051	-0.118	0.073	0.141	-0.209	-0.039	-0.072	0.220	0.287	-0.400	1.000
(17) Condition: New	0.295	0.306	-0.528	0.191	0.190	0.100	0.204	-0.132	-0.238	0.381	0.129	0.173	-0.231	-0.350	0.652	-0.594
(18) Condition: Refurbished	0.014	0.005	0.110	-0.032	-0.036	-0.028	-0.027	0.009	0.015	-0.069	-0.052	-0.055	-0.040	0.016	-0.051	-0.556
(19) Condition: Poor	-0.098	-0.111	0.138	-0.045	-0.043	-0.010	-0.036	0.043	0.060	-0.061	-0.043	-0.041	-0.037	-0.074	-0.119	-0.326
(20) Interior: Standard	-0.410	-0.422	0.339	-0.272	-0.262	-0.151	-0.058	0.017	0.046	-0.271	-0.132	-0.205	0.237	0.041	-0.378	0.347
(21) Interior: Low	-0.107	-0.122	0.122	-0.083	-0.085	-0.043	-0.030	0.023	0.036	-0.061	-0.073	-0.061	0.022	-0.055	-0.103	-0.086
(22) Interior: High	0.344	0.382	-0.343	0.240	0.241	0.143	0.069	-0.024	-0.056	0.246	0.145	0.183	-0.213	-0.034	0.370	-0.273
(23) Interior: Luxury	0.278	0.229	-0.118	0.164	0.143	0.066	0.004	-0.006	-0.013	0.128	0.043	0.117	-0.086	0.034	0.131	-0.108
(24) Urbanization: Urban	0.198	0.210	0.084	-0.003	-0.010	-0.027	-0.081	0.094	0.129	0.059	-0.038	0.007	0.003	-0.029	-0.048	-0.018
(25) Urbanization: Intermediate	-0.150	-0.159	-0.064	0.014	0.020	0.029	0.059	-0.066	-0.088	-0.044	0.034	0.008	0.005	0.021	0.035	0.012
(26) Urbanization: Rural	-0.107	-0.114	-0.045	-0.019	-0.018	-0.001	0.049	-0.060	-0.089	-0.035	0.011	-0.028	-0.015	0.018	0.029	0.013
(27) Year: 2017	-0.133	-0.166	0.012	0.025	0.021	0.008	0.024	-0.082	-0.055	0.020	0.022	0.027	0.004	-0.061	0.176	-0.056
(28) Year: 2018	-0.066	-0.078	0.011	0.020	0.018	0.008	0.009	-0.010	0.042	0.010	0.015	0.012	-0.007	-0.018	0.138	-0.024
(29) Year: 2019	-0.040	-0.054	-0.037	0.009	0.008	-0.007	0.003	0.276	0.253	0.036	0.006	0.006	0.012	-0.041	0.105	-0.046
(30) Year: 2020	0.011	0.010	-0.017	0.016	0.013	0.005	0.028	0.114	0.109	0.011	-0.008	0.002	-0.007	-0.012	0.021	-0.017
(31) Year: 2021	0.061	0.069	0.017	0.007	0.006	0.011	-0.024	0.064	0.075	-0.011	-0.010	-0.004	-0.011	0.019	-0.037	0.013
(32) Year: 2022	0.059	0.071	0.027	-0.037	-0.035	-0.019	-0.027	-0.017	-0.028	-0.023	-0.029	-0.018	0.014	0.037	-0.088	0.042
(33) Year: 2023	0.037	0.050	0.009	-0.026	-0.023	-0.011	-0.030	-0.052	-0.048	-0.024	-0.013	-0.020	-0.007	0.024	-0.100	0.032
(34) Year: 2024	0.046	0.063	-0.010	-0.005	-0.001	0.006	0.029	-0.144	-0.179	-0.018	0.006	-0.005	-0.003	0.033	-0.130	0.032
(35) Year: 2025	0.046	0.058	-0.017	-0.005	-0.003	0.002	-0.013	-0.090	-0.111	0.004	0.006	0.000	0.003	0.021	-0.088	0.024

continued on next page

Table 5.8 Pearson Correlation – **continued**

	(17)	(18)	(19)	(20)	(21)	(22)	(23)	(24)	(25)	(26)	(27)	(28)	(29)	(30)	(31)	(32)	(33)	(34)	(35)
(18)	-0.163	1.000																	
(19)	-0.096	-0.089	1.000																
(20)	-0.387	-0.099	0.035	1.000															
(21)	-0.082	-0.066	0.422	-0.201	1.000														
(22)	0.378	0.100	-0.182	-0.847	-0.172	1.000													
(23)	0.112	0.063	-0.047	-0.210	-0.043	-0.180	1.000												
(24)	-0.046	0.058	0.025	-0.041	0.014	0.017	0.047	1.000											
(25)	0.036	-0.044	-0.017	0.031	-0.010	-0.012	-0.036	-0.854	1.000										
(26)	0.024	-0.032	-0.016	0.023	-0.010	-0.010	-0.024	-0.371	-0.165	1.000									
(27)	0.086	0.003	-0.024	-0.036	-0.033	0.049	-0.001	-0.001	-0.003	0.006	1.000								
(28)	0.036	0.003	-0.011	-0.025	-0.021	0.028	0.013	-0.020	0.015	0.011	-0.148	1.000							
(29)	0.071	-0.001	-0.016	-0.026	-0.022	0.030	0.013	-0.021	0.019	0.004	-0.149	-0.126	1.000						
(30)	0.018	0.010	-0.008	-0.010	-0.011	0.012	0.006	0.005	-0.001	-0.008	-0.100	-0.084	-0.085	1.000					
(31)	-0.031	0.009	0.008	0.005	0.008	-0.011	0.005	0.020	-0.014	-0.013	-0.136	-0.114	-0.115	-0.078	1.000				
(32)	-0.062	0.001	0.007	0.029	0.018	-0.032	-0.012	0.014	-0.012	-0.005	-0.151	-0.128	-0.129	-0.087	-0.117	1.000			
(33)	-0.045	-0.008	0.017	0.027	0.025	-0.034	-0.009	0.008	-0.006	-0.004	-0.158	-0.133	-0.135	-0.090	-0.122	-0.137	1.000		
(34)	-0.045	-0.008	0.017	0.025	0.021	-0.030	-0.008	-0.002	0.000	0.003	-0.180	-0.152	-0.154	-0.103	-0.140	-0.156	-0.163	1.000	
(35)	-0.033	-0.004	0.008	0.008	0.014	-0.012	-0.004	-0.002	0.000	0.004	-0.125	-0.105	-0.106	-0.071	-0.096	-0.108	-0.112	-0.128	1.000

Note: Entries report Pearson correlation coefficients computed on the estimation sample using pairwise complete observations. Factor variables are represented via dummy-coded level indicators. The table is reported to document bivariate dependence and potential multicollinearity among covariates used in the empirical specifications.

5.9.2 Appendix II – Price Analysis

Table 5.9 OLS and GAM Model Results for Prices

	OLS				GAM					
	(1)	(2)	(3)	(4)	(5)	(6)	(7)	(8)		
	Baseline		Baseline		Year		Urbanization			
	EPC	EPV	EPC	EPV	EPC	EPV	EPC	EPV		
Dependent variable	log(Price)	log(Price)	log(Price)	log(Price)	log(Price)	log(Price)	log(Price)	log(Price)		
Parametric coefficients										
Intercept	---	---	8.0116***	8.0458***	7.7183***	8.0394***	8.0562***	8.0465***		
			(0.0218)	(0.0218)	(0.0171)	(0.0218)	(0.0253)	(0.0218)		
log(Area)	0.9985***	0.9997***	1.0000***	0.9997***	1.0014***	1.0012***	0.9996***	0.9992***		
	(0.0207)	(0.0207)	(0.0015)	(0.0015)	(0.0015)	(0.0015)	(0.0015)	(0.0015)		
Rooms	-0.0173***	-0.0172***	-0.0143***	-0.0144***	-0.0147***	-0.0148***	-0.0140***	-0.0141***		
	(0.0032)	(0.0033)	(0.0005)	(0.0005)	(0.0005)	(0.0005)	(0.0005)	(0.0005)		
Elevator	0.0486***	0.0510***	0.0328***	0.0313***	0.0325***	0.0310***	0.0328***	0.0313***		
	(0.0118)	(0.0115)	(0.0007)	(0.0007)	(0.0007)	(0.0007)	(0.0007)	(0.0007)		
Balcony	0.0404**	0.0390**	0.0413***	0.0411***	0.0413***	0.0411***	0.0412***	0.0411***		
	(0.0123)	(0.0120)	(0.0008)	(0.0008)	(0.0008)	(0.0008)	(0.0008)	(0.0008)		
Guest Toilet	0.0302***	0.0302***	0.0280***	0.0281***	0.0280***	0.0281***	0.0280***	0.0282***		
	(0.0028)	(0.0028)	(0.0007)	(0.0007)	(0.0007)	(0.0007)	(0.0007)	(0.0007)		
Rented-out	-0.0570***	-0.0576***	-0.0569***	-0.0570***	-0.0570***	-0.0571***	-0.0569***	-0.0570***		
	(0.0167)	(0.0166)	(0.0007)	(0.0007)	(0.0007)	(0.0007)	(0.0007)	(0.0007)		
Kitchen	0.0253***	0.0248***	0.0255***	0.0255***	0.0256***	0.0256***	0.0255***	0.0255***		
	(0.0068)	(0.0067)	(0.0006)	(0.0006)	(0.0006)	(0.0006)	(0.0006)	(0.0006)		
Renovated	0.0430***	0.0480***	0.0482***	0.0475***	0.0475***	0.0468***	0.0481***	0.0473***		
	(0.0058)	(0.0062)	(0.0009)	(0.0009)	(0.0009)	(0.0009)	(0.0009)	(0.0009)		
Condition: New	0.1472***	0.1607***	0.1495***	0.1472***	0.1527***	0.1503***	0.1493***	0.1470***		
	(0.0149)	(0.0175)	(0.0013)	(0.0013)	(0.0013)	(0.0013)	(0.0013)	(0.0013)		
Condition: Refurbished	0.0238**	0.0213*	0.0183***	0.0193***	0.0180***	0.0190***	0.0184***	0.0193***		
	(0.0079)	(0.0082)	(0.0009)	(0.0009)	(0.0009)	(0.0009)	(0.0009)	(0.0009)		
Condition: Poor	-0.0871***	-0.0864***	-0.0889***	-0.0885***	-0.0889***	-0.0886***	-0.0888***	-0.0886***		
	(0.0107)	(0.0107)	(0.0014)	(0.0014)	(0.0014)	(0.0014)	(0.0014)	(0.0014)		
Interior: Low	-0.1020***	-0.1009***	-0.1016***	-0.1012***	-0.1012***	-0.1007***	-0.1013***	-0.1010***		
	(0.0051)	(0.0050)	(0.0016)	(0.0016)	(0.0016)	(0.0016)	(0.0016)	(0.0016)		
Interior: High	0.1874***	0.1914***	0.1764***	0.1754***	0.1758***	0.1748***	0.1764***	0.1753***		
	(0.0052)	(0.0056)	(0.0007)	(0.0007)	(0.0007)	(0.0007)	(0.0007)	(0.0007)		
Interior: Luxury	0.3438***	0.3504***	0.3170***	0.3149***	0.3172***	0.3151***	0.3173***	0.3149***		
	(0.0116)	(0.0113)	(0.0015)	(0.0015)	(0.0015)	(0.0015)	(0.0015)	(0.0015)		
EPC	Yes		Yes		Yes		Yes			
EPC × Year					Yes					
EPC × Urbanization							Yes			
EPV		Yes								

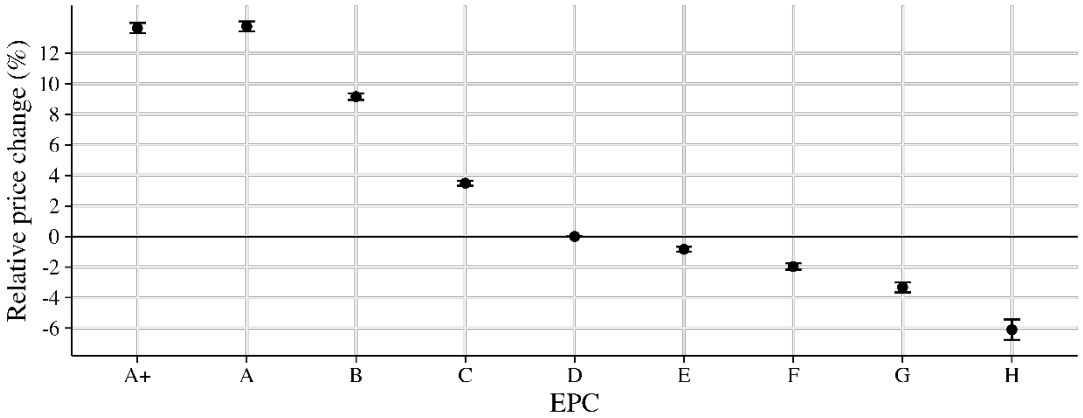
continued on next page

Table 5.9 Price Analysis Output – **continued**

	OLS		GAM					
	(1)	(2)	(3)	(4)	(5)	(6)	(7)	(8)
	Baseline		Baseline		Year		Urbanization	
	EPC	EPV	EPC	EPV	EPC	EPV	EPC	EPV
Smooth terms and model specification								
s(EPV)	---	---	---	6.950 19,593.8***	---	---	---	---
s(EPV) in 2017	---	---	---	---	---	6.593 3,111.1***	---	---
s(EPV) in 2018	---	---	---	---	---	6.459 1,857.5***	---	---
s(EPV) in 2019	---	---	---	---	---	6.744 2,849.7***	---	---
s(EPV) in 2020	---	---	---	---	---	6.602 1,405.0***	---	---
s(EPV) in 2021	---	---	---	---	---	6.660 1,618.3***	---	---
s(EPV) in 2022	---	---	---	---	---	6.856 3,188.5***	---	---
s(EPV) in 2023	---	---	---	---	---	6.885 7,096.8***	---	---
s(EPV) in 2024	---	---	---	---	---	6.846 6,849.1***	---	---
s(EPV) in 2025	---	---	---	---	---	6.602 5,852.2***	---	---
s(EPV) in urban areas	---	---	---	---	---	---	---	6.927 13,954.3***
s(EPV) in intermediate areas	---	---	---	---	---	---	---	6.908 7,241.5***
s(EPV) in rural areas	---	---	---	---	---	---	---	6.320 3,039.4***
Spatial smooth			Yes	Yes	Yes	Yes	Yes	Yes
Fixed effects & fit								
Temporal fixed effects	Yes	Yes	Yes	Yes	Yes	Yes	Yes	Yes
Spatial fixed effects	Yes	Yes	Yes	Yes	Yes	Yes	Yes	Yes
Observations	656,649	656,649	656,649	656,649	656,649	656,649	656,649	656,649
Adjusted R^2	0.8770	0.8766	0.8985	0.8986	0.8988	0.8990	0.8986	0.8988

Note: This table reports the smooth terms, model components, and fit statistics for the global price analysis across OLS and GAM specifications. OLS Models (1) and (2) do not include smooth terms or spatial smooths. For GAM models, smooth terms report effective degrees of freedom (EDF) in the first row and approximate F-statistics with significance levels in the second row.
Significance levels are: *** p < 0.001, ** p < 0.01, * p < 0.05, . p < 0.1.

Figure 5.10 Relative Price Effects by EPC



*Note: T*his figure presents the estimated partial effects of EPC classes over the full sample period 2017 to 2025, based on Model (3). Energy efficiency is captured using discrete EPC classes (A+ to H). The horizontal axis displays the EPC classes, and the vertical axis shows the estimated partial effects expressed as percentage changes relative to the reference category EPC class D (sample mean).

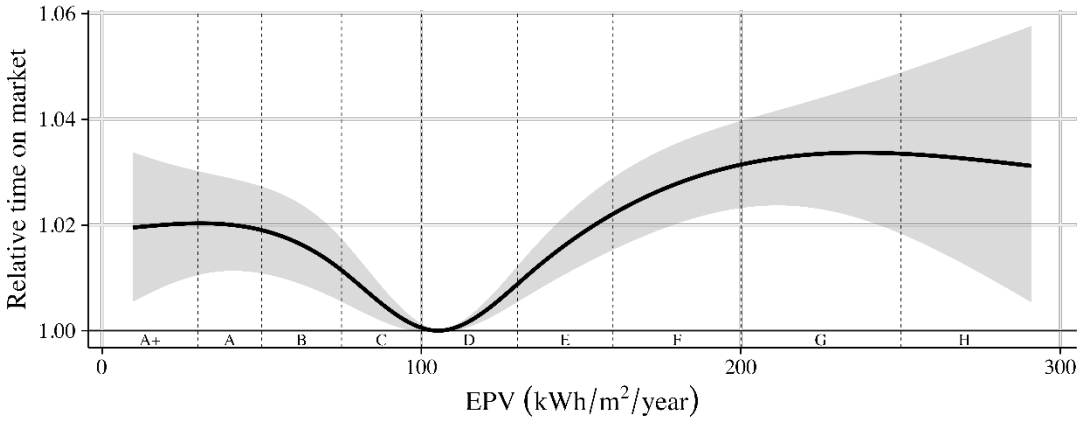
5.9.3 Appendix III – Robustness Check

Table 5.10 TOM Results: Cox and AFT Models

	COX			AFT		
	Baseline	Year	Urbanization	Baseline	Year	Urbanization
Models	(9)	(10)	(11)	(12)	(13)	(14)
Dependent variable	TOM	TOM	TOM	TOM	TOM	TOM
Parametric coefficients						
log(Price)	0.933***	0.931***	0.934***	1.062***	1.063***	1.061***
	(0.0052)	(0.0052)	(0.0052)	(0.0045)	(0.0045)	(0.0045)
log(Area)	0.864***	0.871***	0.864***	1.138***	1.130***	1.138***
	(0.0087)	(0.0087)	(0.0087)	(0.0075)	(0.0075)	(0.0075)
Rooms	1.001	0.999	1.001	0.998	1.000	0.998
	(0.0025)	(0.0025)	(0.0025)	(0.0021)	(0.0021)	(0.0021)
Elevator	0.948***	0.946***	0.947***	1.049***	1.050***	1.049***
	(0.0030)	(0.0030)	(0.0030)	(0.0026)	(0.0026)	(0.0026)
Balcony	1.021***	1.022***	1.021***	0.980***	0.980***	0.980***
	(0.0035)	(0.0035)	(0.0035)	(0.0030)	(0.0030)	(0.0030)
Guest Toilet	1.009**	1.010**	1.008*	0.993**	0.992**	0.993*
	(0.0033)	(0.0033)	(0.0033)	(0.0028)	(0.0028)	(0.0028)
Rented-out	0.846***	0.844***	0.846***	1.161***	1.162***	1.160***
	(0.0032)	(0.0032)	(0.0032)	(0.0028)	(0.0028)	(0.0028)
Kitchen	1.053***	1.052***	1.052***	0.954***	0.955***	0.954***
	(0.0029)	(0.0029)	(0.0029)	(0.0025)	(0.0025)	(0.0025)
Renovated	1.047***	1.035***	1.047***	0.961***	0.970***	0.961***
	(0.0041)	(0.0041)	(0.0041)	(0.0035)	(0.0035)	(0.0035)
Condition: New	0.817***	0.851***	0.817***	1.204***	1.160***	1.204***
	(0.0061)	(0.0062)	(0.0061)	(0.0052)	(0.0054)	(0.0052)
Condition:	0.980***	0.980***	0.980***	1.017***	1.016***	1.017***
Refurbished	(0.0040)	(0.0040)	(0.0040)	(0.0034)	(0.0034)	(0.0034)
Condition: Poor	0.993	0.991	0.993	1.006	1.007	1.005
	(0.0065)	(0.0065)	(0.0065)	(0.0056)	(0.0056)	(0.0056)
Interior: Low	1.035***	1.039***	1.035***	0.971***	0.967***	0.971***
	(0.0073)	(0.0073)	(0.0073)	(0.0063)	(0.0063)	(0.0063)
Interior: High	1.025***	1.023***	1.026***	0.978***	0.980***	0.978***
	(0.0034)	(0.0034)	(0.0034)	(0.0029)	(0.0029)	(0.0029)
Interior: Luxury	1.094***	1.091***	1.094***	0.924***	0.926***	0.924***
	(0.0072)	(0.0072)	(0.0072)	(0.0062)	(0.0062)	(0.0062)
log(Listing views)	1.651***	1.656***	1.651***	0.644***	0.643***	0.644***
	(0.0017)	(0.0017)	(0.0017)	(0.0015)	(0.0015)	(0.0015)
Nonlinear terms						
ns(EPV)	Yes	Yes	Yes	Yes	Yes	Yes
ns(EPV) × Year		Yes			Yes	
ns(EPV) × Urbanization			Yes			Yes
Fixed effects & fit						
Temporal fixed effects	Yes	Yes	Yes	Yes	Yes	Yes
Spatial fixed effects	Yes	Yes	Yes	Yes	Yes	Yes
Observations	656,649	656,649	656,649	656,639	656,639	656,639
Concordance	0.6778	0.6780	0.6778			
AIC				6,047,309	6,045,191	6,047,265

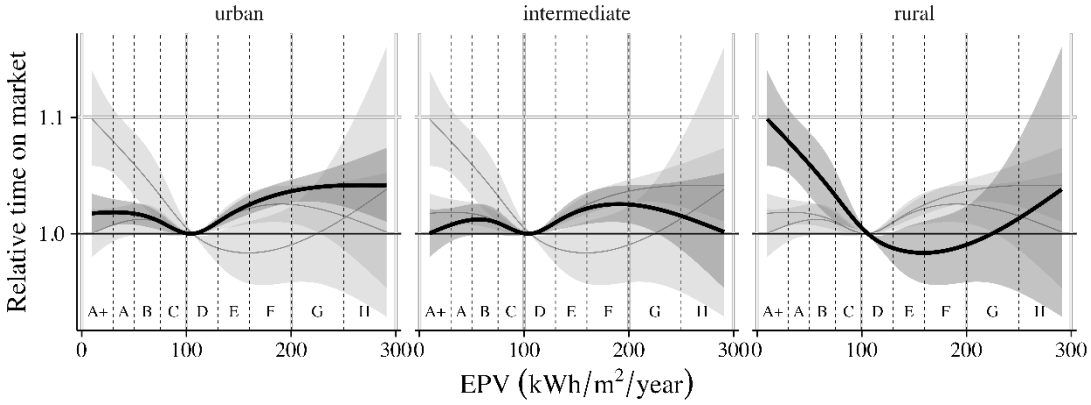
Note: This table reports estimation results for the global TOM analysis across Cox proportional hazards and Weibull accelerated failure time (AFT) models. Cox Models (9) to (11) report hazard ratios, whereas AFT Models (12) to (14) report time ratios. Standard errors of the underlying model coefficients are shown in parentheses in the second row. Cox hazard ratios above one indicate a higher delisting hazard and thus shorter TOM, while values below one indicate longer TOM. AFT values above one indicate longer TOM, while values below one indicate shorter TOM. All models use continuous EPV. Year- and urbanization- specific interaction rows indicate whether the respective nonlinear term is included. Nonlinear effects of EPV are modeled using natural cubic splines. All specifications include temporal and spatial fixed effects. The bottom panel reports the number of observations and the model-specific fit statistics.
Significance levels are: *** $p < 0.001$, ** $p < 0.01$, * $p < 0.05$, . $p < 0.1$

Figure 5.11 Relative TOM by EPV (AFT Specification)



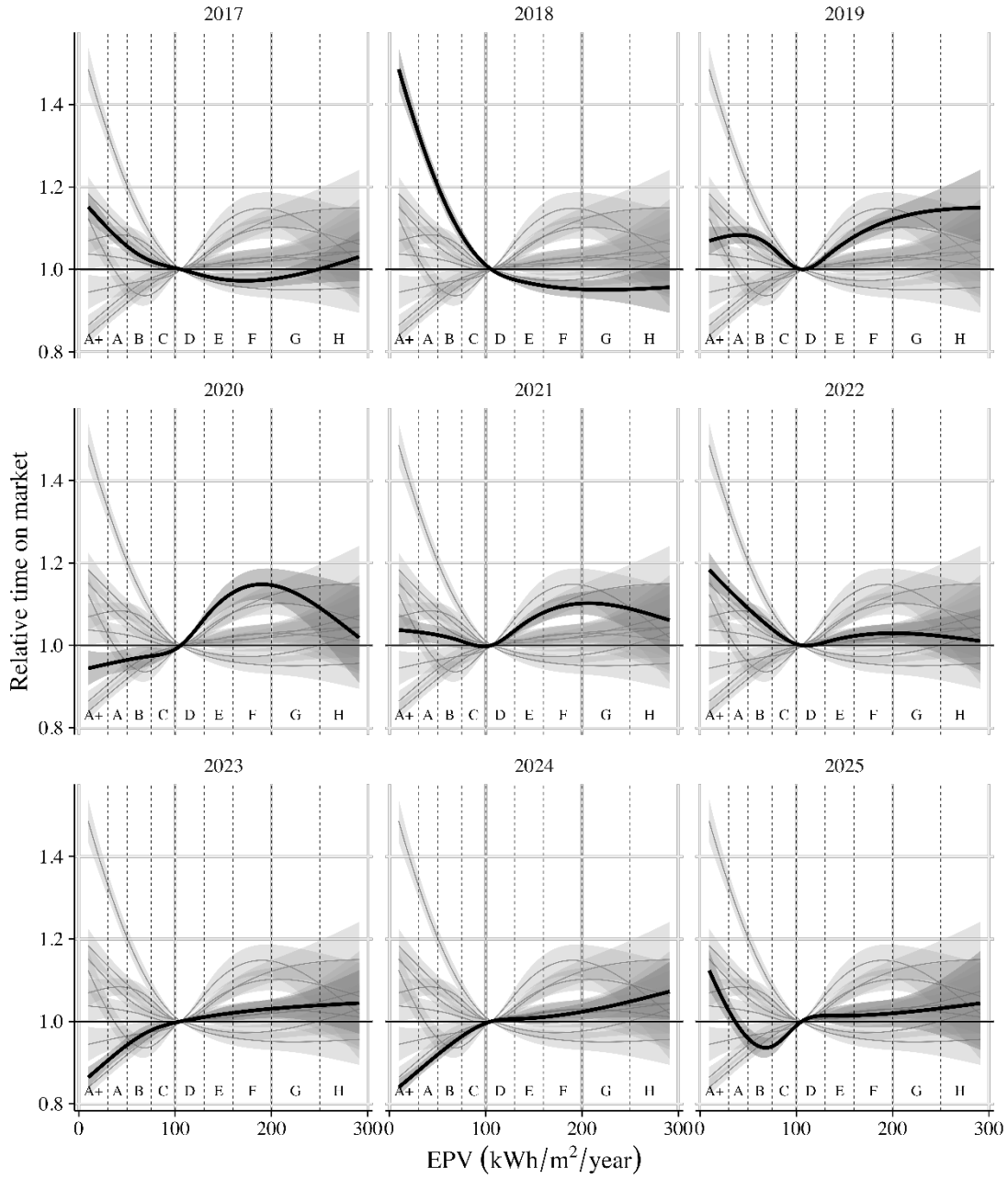
*Note: T*his figure presents the estimated effects of energy efficiency on time on market, based on the Weibull AFT Model (12). Energy efficiency is measured using continuous EPV in kWh/m²/year. The horizontal axis displays EPV, and the vertical axis shows the predicted relative time on market, expressed with respect to the reference value of 106 kWh/m2/year (sample mean). Values above one indicate a longer expected time on market, while values below one indicate a shorter one. All other covariates are held constant. Shaded areas show the associated confidence intervals. EPC are indicated along the EPV scale for reference.

Figure 5.12 Relative TOM by EPV and Urbanization Levels (AFT Specification)



Note: This figure presents the estimated effects of energy efficiency on TOM across different urbanization levels, based on the Weibull AFT (Model (14)). The model includes an interaction term between EPV and the level of urbanization. Each panel represents a specific urbanization category (urban, intermediate, rural). The year is fixed at 2022, and all other covariates are held constant. Energy efficiency is measured using continuous EPV in kWh/m²/year. The horizontal axis displays EPV, and the vertical axis shows the predicted relative TOM, expressed with respect to the reference value of 106 kWh/m²/year. Values above one indicate a longer expected TOM, while values below one indicate a shorter one. The black line highlights the respective category, while the grey lines represent the effects estimated for the other categories. Shaded areas show the associated confidence intervals. EPC are indicated along the EPV scale for reference.

Figure 5.13 Relative TOM by EPV over Time (AFT Specification)



Note: This figure presents the estimated effects of energy efficiency on TOM over time, based on the Weibull AFT Model (13). The model includes an interaction term between EPV and year. Energy efficiency is measured using continuous EPV in kWh/m²/year. The horizontal axis displays EPV, and the vertical axis shows the predicted relative TOM, expressed with respect to the reference value of 106 kWh/m²/year (sample mean). Values above one indicate a longer expected TOM, while values below one indicate a shorter one. Each panel represents a specific year. The black line highlights the respective year, while the grey lines represent the effects estimated for the other years. All other covariates are held constant. Shaded areas show the associated confidence intervals. EPC classes are indicated along the EPV scale for reference.

5.10 References

Amecke, H. (2012). The impact of energy performance certificates: A survey of German home owners. *Energy Policy*, 46, 4–14.

Anglin, P. M., Rutherford, R., & Springer, T. M. (2003). The trade-off between the selling price of residential properties and time-on-the-market: The impact of price setting. *Journal of Real Estate Finance and Economics*, 26(1), 95–111.

Aroul, R., & Hansz, J. A. (2012). The value of "green:" Evidence from the first mandatory residential green building program. *Journal of Real Estate Research*, 34(1), 27–50.

Aroul, R. R., & Rodriguez, M. (2017). The increasing value of green for residential real estate. *Journal of Sustainable Real Estate*, 9(1), 112–130.

Aydin, E., Brounen, D., & Kok, N. (2020). The capitalization of energy efficiency: Evidence from the housing market. *Journal of Urban Economics*, 117, 103243.

Bach, S., & Knautz, J. (2022). Hohe Energiepreise: Ärmere Haushalte werden trotz Entlastungspaketen stärker belastet als reichere Haushalte. *DIW Wochenbericht*, 89(17), 244–251.

Bachmann, R., Baqaee, D., Bayer, C., Kuhn, M., Löschel, A., McWilliams, B., Moll, B., Peichl, A., Pittel, K., Schularick, M., & Zachmann, G. (2022). *How it can be done* (Policy Brief No. 034). ECONtribute.

Bachmann, R., Baqaee, D., Bayer, C., Kuhn, M., Löschel, A., Moll, B., Peichl, A., Pittel, K., & Schularick, M. (2024). What if? The macroeconomic and distributional effects for Germany of a stop of energy imports from Russia. *Economica*, 91(364), 1157–1200.

Bernanke, B. S. (2018). The real effects of disrupted credit: Evidence from the global financial crisis. *Brookings Papers on Economic Activity*, 49(2), 251–322.

Braakmann, N., Dursun, B., & Pickard, H. (2026). Energy price shocks and the demand for energy-efficient housing: Evidence from Russia's invasion of Ukraine. *Economica*, 93(369), 30–51.

Brolinson, B., Doerner, W. M., Pollestad, A. J., & Seiler, M. J. (2026). European energy crisis: Did electricity prices shock real estate markets? *Journal of Environmental Economics and Management*, 137, 103283.

Brounen, D., & Kok, N. (2011). On the economics of energy labels in the housing market. *Journal of Environmental Economics and Management*, 62(2), 166–179.

Bundesinstitut für Bau-, Stadt- und Raumforschung. (2023). *Raumbeobachtung–Raumgliederungen des BBSR.* Accessed: 2026-03-02. URL: https://www.bbsr.bund.de/BBSR/DE/forschung/raumbeobachtung/Raumabgrenzungen/raumabgrenzungen-uebersicht.html

Caamaño-Carrillo, C., Bevilacqua, M., & Gallardo, D. I. (2025). Spatial survival models based on Weibull random fields. *Spatial Statistic*s, 70, 100943.

Cadena, A., & Thomson, T. A. (2021). The value of "green" in resale residential real estate: Premium by neighborhood value quintile, homestead status and year. *Journal of Sustainable Real Estate*, 13(1), 12–29.

Cajias, M., & Freudenreich, A. (2024). What are tenants demanding the most? A machine learning approach for the prediction of time on market. *Journal of Property Investment & Finance*, 42(2), 151–165.

Cajias, M., & Freudenreich, P. (2018). Exploring the determinants of liquidity with big data – market heterogeneity in German markets. *Journal of Property Investment & Finance*, 36(1), 3–18.

Cajias, M., Freudenreich, P., Schäfers, W., & Freudenreich, A. (2020). Liquidity and prices: A cluster analysis of the German residential real estate market. *Journal of Business Economics*, 90(7), 1021–1056.

Cajias, M., Fuerst, F., & Bienert, S. (2019). Tearing down the information barrier: The price impacts of energy efficiency ratings for buildings in the German rental market. *Energy Research & Social Science*, 47, 177–191.

Cajias, M., & Piazolo, D. (2013). Green performs better: Energy efficiency and financial return on buildings. *Journal of Corporate Real Estate*, 15(1), 53–72.

Carrillo, P. E., & Williams, B. (2019). The repeat time-on-the-market index. *Journal of Urban Economics*, 112, 33–49.

Cespedes-Lopez, M.-F., Mora-Garcia, R.-T., Perez-Sanchez, V. R., & Perez-Sanchez, J.-C. (2019). Meta-analysis of price premiums in housing with energy performance certificates (EPC). *Sustainability*, 11(22), 6303.

Chegut, A., Eichholtz, P., Holtermans, R., & Palacios, J. (2020). Energy efficiency information and valuation practices in rental housing. *Journal of Real Estate Finance and Economics*, 60, 181–204.

Chegut, A., Eichholtz, P., & Kok, N. (2014). Supply, demand and the value of green buildings. *Urban Studies*, 51(1), 22–43.

Claessens, S., & Kose, M. A. (2013). *Financial crises: Explanations, types and implications* (Working Paper WP/13/28). International Monetary Fund.

Clayton, J., MacKinnon, G., & Peng, L. (2008). Time variation of liquidity in the private real estate market: An empirical investigation. *Journal of Real Estate Research*, 30(2), 125–160.

Collett, D. (2014). *Modelling survival data in medical research* (3rd ed.). Chapman & Hall/CRC.

Copiello, S., & Coletto, S. (2023). The price premium in green buildings: A spatial autoregressive model and a multi-criteria optimization approach. *Buildings*, 13(2), 276.

Cox, D. R. (1972). Regression models and life-tables. *Journal of the Royal Statistical Society: Series B (Methodological)*, 34(2), 187–220.

de Ayala, A., Galarraga, I., & Spadaro, J. V. (2016). The price of energy efficiency in the Spanish housing market. *Energy Policy*, 94, 16–24.

de Meulen, P., & Mitze, T. (2014). Exploring the spatial variation in quality-adjusted rental prices and identifying hot spots in Berlin's residential property market. *Regional Science*, 1(1), 310–328.

Dell'Anna, F., & Bottero, M. (2021). Green premium in buildings: Evidence from the real estate market of Singapore. *Journal of Cleaner Production*, 286, 125327.

Deutsche Bundesbank. (2026). *Housing loans to households / mortgage loans secured by residential real estate.* Accessed: 2026-05-05. URL: https://www.bundesbank.de/en/statistics/money-and-capital-markets/interest-rates-and-yields/housing-loans-to-householdsmortgage-loans-secured-by-residential-real-estate-621950

Devine, A., & Kok, N. (2015). Green certification and building performance: Implications for tangibles and intangibles. *The Journal of Portfolio Management*, 41(6), 151–163.

Díaz, A., & Jerez, B. (2013). House prices, sales, and time on the market: A search-theoretic framework. *International Economic Review*, 54(3), 837–872.

Duca, J. V., Muellbauer, J., & Murphy, A. (2021). What drives house price cycles? International experience and policy issues. *Journal of Economic Literature*, 59(3), 773–864.

Eerola, E., & Lyytikäinen, T. (2015). On the role of public price information in housing markets. *Regional Science and Urban Economics*, 53, 74–84.

Eichholtz, P., Kok, N., & Quigley, J. M. (2010). Doing well by doing good? Green office buildings. *American Economic Review*, 100(5), 2492–2509.

Eichholtz, P., Kok, N., & Sun, X. (2026). The impact of minimum energy performance standards on the commercial real estate market. *Nature Communications*, 17, 4038.

European Central Bank. (2026). *Key ECB interest rates*. Accessed: 2026-05-05. URL: https://www.ecb.europa.eu/stats/policy_and_exchange_rates/key_ecb_interest_rates/html/index.en.html

Eurostat. (2023). *Territorial typologies manual – urban-rural typology*. Accessed: 2026-03-02. URL: https://ec.europa.eu/eurostat/statistics-explained/index.php?title=Territorial_typologies_manual_-_urban-rural_typology

Fisher, J., Gatzlaff, D., Geltner, D., & Haurin, D. (2003). Controlling for the impact of variable liquidity in commercial real estate price indices. *Real Estate Economics*, 31(2), 269–303.

Fuerst, F., McAllister, P., Nanda, A., & Wyatt, P. (2015). Does energy efficiency matter to home-buyers? An investigation of EPC ratings and transaction prices in England. *Energy Economics*, 48, 145–156.

Fuerst, F., Oikarinen, E., & Harjunen, O. (2016). Green signalling effects in the market for energy-efficient residential buildings. *Applied Energy*, 180, 560–571.

Fuerst, F., & van de Wetering, J. (2015). How does environmental efficiency impact on the rents of commercial offices in the UK? *Journal of Property Research*, 32(3), 193–216.

Galvin, R. (2023). How prebound effects compromise the market premium for energy efficiency in German house sales. *Building Research & Information*, 51(5), 501–517.

Gdakowicz, A., & Putek-Szelag, E. (2025). Analyzing rental time and pricing trends before, during, and after the COVID-19 pandemic. *International Journal of Strategic Property Management*, 29(6), 409–420.

Genesove, D., & Mayer, C. (2001). Loss aversion and seller behavior: Evidence from the housing market. *The Quarterly Journal of Economics*, 116(4), 1233–1260.

Gerassimenko, A., De Moor, L., & Defau, L. (2025). Do energy performance certificates influence time on market? An exploratory research of the residential housing market in Flanders. *International Journal of Housing Markets and Analysis*, 18(6), 1447–1474.

Ghosh, C., & Petrova, M. T. (2024). Building sustainability, certification, and price premiums: Evidence from Europe. *Journal of Real Estate Research*, 46(4), 514–537.

Granum, M. E. (2025). *Rising energy costs and the premium for energy-efficient homes*. SSRN.

Grossman, V., Martínez-García, E., Torres, L. B., & Sun, Y. (2019). Drilling down: The impact of oil price shocks on housing prices. *The Energy Journal*, 40(SI2), 59–84.

Hastie, T., & Tibshirani, R. (1986). Generalized additive models. *Statistical Science,* 1(3), 297–310.

Haurin, D. (1988). The duration of marketing time of residential housing. *Real Estate Economics*, 16(4), 396–410.

Heuer, F., & Thiel, P. (2025). *FDZ data description: Real-estate data for Germany (RWI-GEO-RED v13): Advertisements on the internet platform ImmobilienScout24, 2007–06/2025*. RWI – Leibniz-Institut für Wirtschaftsforschung.

Hörz, M. (2025). *Gaspreis aktuell: So viel kostet die Kilowattstunde.* NDR. Accessed: 2026-05-05. URL: https://www.ndr.de/nachrichten/info/Gaspreis-aktuell-wie-viel-kostet-Kilowattstunde,gaspreis142.html

Huang, J.-C., & Palmquist, R. B. (2001). Environmental conditions, reservation prices, and time on the market for housing. *Journal of Real Estate Finance and Economics*, 22(2/3), 203–219.

Huber, P. J. (1981). Robust statistics. John Wiley & Sons.

Hyland, M., Lyons, R. C., & Lyons, S. (2013). The value of domestic building energy efficiency – Evidence from Ireland. *Energy Economics*, 40, 943–952.

Jud, D., Seaks, T., & Winkler, D. (1996). Time on the market: The impact of residential brokerage. *Journal of Real Estate Research*, 12(2), 447–458.

Kahn, M. E., & Kok, N. (2014). The capitalization of green labels in the California housing market. *Regional Science and Urban Economics*, 47, 25–34.

Kalbfleisch, J. D., & Prentice, R. L. (2011). *The statistical analysis of failure time data* (2nd ed.). John Wiley & Sons.

Kalra, R., Chan, K. C., & Lai, P. (1997). Time on market and sales price of residential housing: A note. *Journal of Economics and Finance*, 21(2), 63–66.

Kang, H. B., & Gardner, M. J. (1989). Selling price and marketing time in the residential real estate market. *Journal of Real Estate Research*, 4(1), 21–35.

Kempf, C., & Syz, J. (2022). Why pay for sustainable housing? Decomposing the green premium of the residential property market in the canton of Zurich, Switzerland. *SN Business & Economics*, 2, 170.

Kholodilin, K. A., Mense, A., & Michelsen, C. (2017). The market value of energy efficiency in buildings and the mode of tenure. *Urban Studies*, 54(14), 3218–3238.

Kilian, L. (2008). The economic effects of energy price shocks. *Journal of Economic Literature*, 46(4), 871–909.

Kluger, B. D., & Miller, N. G. (1990). Measuring residential real estate liquidity. *Real Estate Economics*, 18(2), 145–159.

Knight, J. R. (2002). Listing price, time on market, and ultimate selling price: Causes and effects of listing price changes. *Real Estate Economics*, 30(2), 213–237.

Kolbe, J., Schulz, R., Wersing, M., & Werwatz, A. (2021). Real estate listings and their usefulness for hedonic regressions. *Empirical Economics*, 61, 3239–3269.

Krainer, J. (1999). Real estate liquidity. *Economic Review - Federal Reserve Bank of San Francisco*, (3), 14–26.

Leibniz-Institut für Wirtschaftsforschung. (2025). *Wohnungskaufdaten: Scientific use file (SUF), RWI-GEO-RED v13 (Version 13)* [Dataset].

Lu, X., & Spaenjers, C. (2025). Energy labels, misreporting, and heuristic hedonic models. *Real Estate Economics*, 53(6), 1200–1222.

Lutz, C., & Becker, L. (2023). Effects of energy price shocks on Germany's economy and private households. In R. Bardazzi & M. G. Pazienza (Eds.), *Vulnerable households in the energy transition: Energy poverty, demographics and policies* (pp. 11–28). Springer.

März, S., Stelk, I., & Stelzer, F. (2022). Are tenants willing to pay for energy efficiency? Evidence from a small-scale spatial analysis in Germany. *Energy Policy*, 161, 112753.

McCord, M., Lo, D., Davis, P. T., Hemphill, L., McCord, J., & Haran, M. (2020). A spatial analysis of EPCs in the Belfast metropolitan area housing market. *Journal of Property Research*, 37(1), 25–61.

McCord, M., McCord, J., Davis, P., Haran, M., & Squires, G. (2024). Do private rental tenants pay for energy efficiency?: The dynamics of green premiums and brown discounts. *Journal of Property Research*, 41(3), 251–275.

Mense, A. (2018). The value of energy efficiency and the role of expected heating costs. *Environmental and Resource Economics*, 71, 671–701.

Micelli, E., Giliberto, G., Righetto, E., & Tafuri, G. (2024). Urban disparities in energy performance premium prices: Towards an unjust transition? *Land*, 13(2), 224.

Muzio, M. J., Niu, D., Steil, J., & Zheng, S. (2025). Understanding housing market responses to stringent energy codes. *Real Estate Economics*, 53(4), 676–700.

Ou, Y., Bailey, N., McArthur, D. P., & Zhao, Q. (2025). The price premium of residential energy performance certificates: A scoping review of the European literature. *Energy & Buildings*, 332, 115377.

Perez, H., Amoudi, O., Famuyiwa, F., & Tah, J. H. M. (2025). An investigation of the impact of energy performance certificate (EPC) ratings on residential property prices in Oxfordshire: A hedonic study. *Advances in Building Energy Research*, 19(1), 66–86.

Pommeranz, C., & Steininger, B. I. (2021). What drives the premium for energy-efficient apartments – Green awareness or purchasing power? *Journal of Real Estate Finance and Economics*, 62(2), 220–241.

Porumb, V.-A., Maier, G., & Anghel, I. (2020). The impact of building location on green certification price premiums: Evidence from three European countries. *Journal of Cleaner Production*, 272, 122080.

Reichardt, A., Fuerst, F., Rottke, N., & Zietz, J. (2012). Sustainable building certification and the rent premium: A panel data approach. *Journal of Real Estate Research*, 34(1), 99–126.

Robinson, S., Simons, R., & Lee, E. (2017). Which green office building features do tenants pay for? A study of observed rental effects. *Journal of Real Estate Research*, 39(4), 467–492.

Rosen, S. (1974). Hedonic prices and implicit markets: Product differentiation in pure competition. *Journal of Political Economy*, 82(1), 34–55.

Ruhnau, O., Stiewe, C., Muessel, J., & Hirth, L. (2023). Natural gas savings in Germany during the 2022 energy crisis. *Nature Energy*, 8, 621–628.

Sachs, J.D., Lafortune, G., Fuller, G., & Iablonovski, G. (2025). *Sustainable development report 2025: Financing sustainable development to 2030 and mid-century*. Sustainable Development Solutions Network.

Sagner, P. (2026). Energy price shock and housing market dynamics: Evidence from Germany. *Journal of Housing Economics*, 71, 102119.

Sieger, L. (2024). Investigating inefficiencies in the German rental housing market: The impact of disclosing total costs on energy efficiency appreciation. *Energy & Buildings*, 312, 114183.

Sieger, L., & Weber, C. (2023). Inefficient markets for energy efficiency? – The efficiency premium puzzle in the German rental housing market. *Energy Policy*, 183, 113819.

Singhal, P., Kaestner, K., Schwarz, A., & Pahle, M. (2026). How do households react to a real cost shock? Evidence from the energy price crisis in Germany. *Energy Economics*, 155, 109142.

Statistisches Bundesamt. (2026a). *Bauinvestitionen*. Accessed: 2026-05-05. URL: https://www.destatis.de/DE/Themen/Wirtschaft/Konjunkturindikatoren/Volkswirtschaftliche-Gesamtrechnungen/kvgr119.html

Statistisches Bundesamt. (2026b). *Construction price indices for residential buildings and non-residential buildings*. Accessed: 2026-05-05. URL: https://www.destatis.de/EN/Themes/Economy/Short-Term-Indicators/Prices/bpr110.html

Statistisches Bundesamt. (2026c). *NUTS-Klassifikation*. Accessed: 2026-05-05. URL: https://www.destatis.de/Europa/DE/Methoden-Metadaten/Klassifikationen/UebersichtKlassifikationen_NUTS.html

Surmann, M., Brunauer, W., & Bienert, S. (2015). How does energy efficiency influence the market value of office buildings in Germany and does this effect increase over time? *Journal of European Real Estate Research*, 8(3), 243–266.

Taruttis, L., & Weber, C. (2022). Estimating the impact of energy efficiency on housing prices in Germany: Does regional disparity matter? *Energy Economics*, 105, 105750.

Taylor, C. R. (1999). Time-on-the-market as a sign of quality. *The Review of Economic Studies*, 66(3), 555–578.

Trippi, R. R. (1977). Estimating the relationship between price and time to sale for investment property. *Management Science*, 23(8), 838–842.

van de Ven, D. J., & Fouquet, R. (2017). Historical energy price shocks and their changing effects on the economy. *Energy Economics*, 62, 204–216.

von Ahlefeldt-Dehn, B., Cajias, M., & Schäfers, W. (2023). Forecasting office rents with ensemble models – the case for European real estate markets. *Journal of Property Investment & Finance*, 41(2), 182–207.

von Platten, J., Mangold, M., Johansson, T., & Mjörnell, K. (2022). Energy efficiency at what cost? Unjust burden-sharing of rent increases in extensive energy retrofitting projects in Sweden. *Energy Research & Social Science*, 92, 102791.

Wang, B. (2021). How does COVID-19 affect house prices? A cross-city analysis. *Journal of Risk and Financial Management*, 14(2), 47.

Wei, L. J. (1992). The accelerated failure time model: A useful alternative to the Cox regression model in survival analysis. *Statistics in Medicine*, 11(14–15), 1871–1879.

Wiley, J. A., Benefield, J. D., & Johnson, K. H. (2010). Green design and the market for commercial office space. *Journal of Real Estate Finance and Economics*, 41, 228–243.

Wilkinson, S. J., & Sayce, S. (2020). Decarbonising real estate: The evolving relationship between energy efficiency and housing in Europe. *Journal of European Real Estate Research*, 13(3), 387–408.

Williams, J. T. (1995). Pricing real assets with costly search. *The Review of Financial Studies*, 8(1), 55–90.

Zahirovic-Herbert, V., & Turnbull, G. K. (2008). School quality, house prices and liquidity. *Journal of Real Estate Finance and Economics*, 37, 113–130.

6 Conclusion

6.1 Executive Summary

The following section summarizes the content of all four articles and presents them in terms of their relevance and objectives. It further describes the underlying data and the methodological approaches used in each study, followed by the presentation of the key findings and their scientific and practical implications.

Paper 1: The Price of Clean Air - Quantifying Air Pollution Exposure in Real Estate Decisions

Problem and Objective

Air pollution negatively impacts health and is particularly relevant to urban development and densely populated property markets. Its importance is expected to grow, as 68% of the world's population is projected to live in cities by 2050 (United Nations Environment Programme, 2011). Major sources of air pollution include fuel combustion in transportation and industrial processes, which contribute substantially to nitrogen dioxide (NO_2) emissions. Particulate matter (PM), such as PM_{10}, refers to coarser particles with diameters of up to 10 µm and originates from sources including road traffic, industrial activity, and agricultural erosion (Umweltbundesamt, 2022).

Previous research examined the relationship between these pollutants and property values using hedonic regression approaches and identified a negative association between pollution concentrations and real estate prices (Borja-Urbano et al., 2021; Le Boennec & Salladarré, 2017; Ridker & Henning, 1967). However, the body of research remains geographically concentrated, focusing on American and Asian property markets (Borja-Urbano et al., 2021; Sun & Yang, 2020). The European and German markets have received little attention in this regard. To improve the assessment in Germany, this paper investigates the effect of air quality on residential rents in Berlin, the capital of Germany. Therefore, the study aims to operationalize the assessment of air quality and examines the relationship between pollutants and property rents.

Methodology and Data

The analysis draws on two data sources to examine the relationship between air quality and residential rents in Berlin. Air pollution data are collected from 150 publicly accessible sensors and cover daily measurements for PM_{10} and NO_2 for 2018 and 2021. Rental market data are derived from VALUE market data and comprise asking rents for more than 80,000 dwellings in Berlin, including both continuous and categorical property characteristics. The dataset is further enriched with socioeconomic indicators at the ZIP code level, including purchasing power, resulting in a total of 24 variables used to characterize individual properties.

The integration of these datasets requires a combination of geostatistical, geographical, and econometric methods. In the first step, three interpolation techniques are tested to generate seasonal pollution maps for summer and winter in each observation year: Inverse distance weighting (IDW), ordinary Kriging accounting for anisotropy (OK-wind), and empirical Bayesian Kriging (EBK). Among these methods, EBK performs best, yielding the lowest error values. In a second step, the resulting pollution surfaces are merged with the property dataset and analyzed within a semi-parametric regression framework, a generalized additive model (GAM).

Results and Their Contribution to Science and Practice

The findings show that even with limited monitoring infrastructure, geostatistical interpolation techniques can estimate spatial pollution patterns and generate economically meaningful exposure measures. The results further reveal a significant association between air quality and residential rents, with lower PM_{10} concentrations corresponding to higher rental values. However, these effects cannot be generalized to all pollutants, as the effects of NO_2 are inconclusive, potentially due to its lower perceptibility. Overall, the extent of areas with high pollutant concentrations decreased over time as air quality improved.

These findings have several practical implications. The results suggest that measures that improve local environmental quality, such as clean heating technologies, traffic reduction, or urban greening, may contribute to residential attractiveness and rental performance. Air pollution exposure, therefore, provides relevant information for location assessment and rental portfolio optimization. For policymakers, the study underscores the need for denser pollution sensor networks, greater transparency in environmental data, and stronger integration of air-quality considerations into urban planning.

Paper 2: Quantifying the Impact of Urban Heat Islands on Residential Property Prices

Problem and Objective

Globally, rising temperatures associated with climate change are intensifying climate hazards such as heat waves, droughts, and heavy rainfall, with far-reaching implications for quality of life, biodiversity, and environmental stability (United Nations Environment Programme Finance Initiative, 2023). Urbanization amplifies these challenges, as cities account for 75% of global energy consumption and 70% of global greenhouse gas emissions (International Energy Agency, 2024). Cities are therefore not only drivers of climate change but also highly exposed to its consequences. They face growing thermal stress, rising energy demand, increasing pressure on infrastructure, and deepening social and spatial inequalities, particularly where access to climate-resilient environments is unevenly distributed (Dodoo & Gustavsson, 2016; Sinha & Cropper, 2013).

In this context, urban heat islands (UHIs) are particularly relevant, as they refer to the phenomenon in which urban areas exhibit higher temperatures than surrounding suburbs or rural areas (Oke, 1982). However, the magnitude of the UHI effect is spatially heterogeneous, varying across neighborhoods and individual buildings due to differences in urban morphology, construction density, and the thermal characteristics of building materials (Offermann et al., 2022). Previous research relies on cross-regional comparisons and spatially or temporally aggregated temperature measures, limiting the identification of intra-urban economic effects and building-level heterogeneity (Albouy et al., 2016; Cvijanović & Van de Minne, 2024; Klaiber et al., 2017). This study contributes to the literature by using granular, building-level temperature data to examine how persistent UHI exposure is reflected in residential prices within a city. Accordingly, the paper aims to analyze the relationship between UHI intensity and housing prices in Berlin, focusing on localized pricing patterns, spatial heterogeneity, and the distinction between daytime heat exposure and nighttime heat retention.

Methodology and Data

This analysis is based on two datasets: surface temperature data and residential property price data. The temperature data, provided by Meteoblue on a 30 m × 30 m grid, capture temperatures daily at 4 a.m. and 1 p.m. Property price information is sourced from VALUE market data and serves as the basis for assessing the value of residential real estate across Berlin. Both datasets share the same spatial and temporal scope, covering Berlin over the 2014–2023 period.

The UHI intensity is derived by calculating the relative temperature difference between each property's location and the lowest temperature recorded across the entire sample. This variable is subsequently linked to the property dataset to assess how UHI conditions affect price developments during periods of elevated thermal stress. The resulting data are examined using a generalized additive model (GAM), which enables flexible, non-parametric estimation of the effects on the dependent variable (Wood, 2017).

Results and Their Contribution to Science and Practice

The empirical results reveal economically relevant intra-city temperature differences, with higher UHI exposure associated with lower residential property prices. The effect is particularly pronounced for nighttime UHI intensity, suggesting that a location's cooling potential exerts a greater impact on property values than daytime heat exposure. Financial performance indicators support this finding, indicating that thermally more favorable locations are associated with lower risk levels. Moreover, the results indicate spatial variation, with stronger price effects at locations farther from the city center and near a park. In socioeconomic terms, households with higher incomes exhibit greater price sensitivity to temperature deviations.

Gradual intensification and spatial redistribution of UHI effects suggest that urban areas will continue to face persistent thermal stress, with practical implications for urban planning, energy demand, and real estate markets. For investors, UHI exposure is a location-specific risk, as persistent heat stress can reduce climate amenity values, undermine thermal comfort, and impair long-term marketability. Accounting for daytime heat exposure and nighttime heat retention in due diligence, pricing, and asset management enables a more precise assessment of location-specific heat risk and potential future value losses. For policymakers and urban planners, the findings underline the importance of integrating UHI resilience into urban development through heat-resilient building materials, green spaces, and targeted adaptation measures in vulnerable neighborhoods.

Paper 3: The Impact of Energy Policies in Residential Markets: Quantifying Retrofit Incentives and Asset Performance

Problem and Objective

With 75% of the existing European building stock not meeting current or future energy efficiency requirements (European Parliament & Council of the European Union, 2024), the need for large-scale renovation is evident. Germany's retrofit rate of just 0.69% highlights the gap between current renovation activity and the pace required to achieve decarbonization targets (Bundesverband energieeffiziente Gebäudehülle, 2026). In response, several regulatory measures have been introduced at the EU level to incentivize refurbishment and accelerate improvements in the energy performance of the existing building stock. These measures primarily focus on "worst-performing buildings", as improving their energy performance offers some of the highest potential to achieve climate protection targets (Deutsche Energie-Agentur, 2021). In addition, improved energy efficiency positively affects property values, as premiums can be achieved for buildings with higher energy standards and are seen as a hedge against market risks (Kempf & Syz, 2022). Limited evidence exists on whether regulatory interventions effectively incentivize energy-efficiency retrofits that improve building energy performance across changing market regimes. Prior research has largely been conducted under favorable market conditions (Cajias et al., 2019; Pommeranz & Steininger, 2021; Taruttis & Weber, 2022). To assess the extent to which these price premiums create measurable investment incentives, the rent-to-price ratio is used as a key indicator, capturing the relationship between rental income and prices (Kurzrock, 2017). Cajias (2019) found lower rent-to-price ratios in markets with lower investment risk, greater appreciation potential, and higher liquidity.

This paper aims to assess the effectiveness of energy policies by evaluating whether they establish economic incentives for retrofitting residential properties and improving their energy efficiency. Alongside temporal variation, spatial factors are considered to examine how regional market disparities influence the impact of these measures.

Methodology and Data

The empirical approach covers both the rental and investment segments of the residential property market in the Munich metropolitan area over a ten-year period characterized by notable market volatility. The observation period extends from April 2014 to August 2023 and is subdivided into four phases, each reflecting shifts in regulatory frameworks and economic conditions. To provide a comprehensive perspective, the analysis draws on multiple data sources, namely GfK, OpenStreetMap, and VALUE market data.

Methodologically, the study proceeds in two steps. First, rents and prices are estimated within a semi-parametric framework for both the existing property state and a scenario with improved energy efficiency. Second, the resulting estimates are used to calculate the rent-to-price ratio before and after the assumed retrofit. Changes in this ratio indicate whether energy-efficiency improvements may generate financial benefits.

Results and Their Contribution to Science and Practice

The findings show that greater energy efficiency is generally associated with higher property values. The magnitude of this effect varies with market conditions and demographics and is more pronounced in sparsely populated areas. The results further suggest that regulatory changes strengthen incentives to retrofit "worst-performing buildings", as properties with poor energy performance values (EPV) exhibit the lowest rent-to-price ratios after a synthetic retrofit. However, rental and price segments do not adjust uniformly. Rents respond less strongly to changes in economic conditions than prices do, as reflected in the rent-to-price ratio. During downturn phases, the pattern changes. Mid-range EPVs generate the highest returns, particularly in urban areas. Overall, despite market changes, the rent-to-price ratio declines over time.

The study expands knowledge of the impact of regulatory interventions by indicating that their effectiveness depends on macroeconomic factors. During economic downturns, the incentives for retrofitting energy-inefficient buildings are lower, and properties with moderate energy efficiency perform better. For investors, this highlights the importance of integrating macroeconomic scenario analysis into retrofit strategies. Investment decisions should consider not only the potential for technical improvements but also capital market sensitivities, rent-price elasticities, and regional supply dynamics. For urban planners and policymakers, the results show that uniform retrofit incentives lead to suboptimal capital allocation. Targeted measures are needed to account for local markets and the heterogeneity in the existing building stock.

Paper 4: Resilience through Energy Efficiency? Evidence from Price and Liquidity Dynamics across Market Regimes

Problem and Objective

Energy supply has evolved in recent years from a cost-related factor into a central economic and geopolitical issue. In Europe, Russia's invasion of Ukraine heightened international tensions and exacerbated supply shortages, as Russia had been one of Europe's most important natural gas suppliers (Bachmann et al., 2024). The abrupt reduction in supply caused a significant shock to energy availability. This translated directly into higher energy costs for households and firms, affecting both operating expenses and consumption behavior (Ruhnau et al., 2023) and triggering pronounced market adjustments. In addition to the energy shock, the recent period has been characterized by other developments, including the COVID-19 pandemic, rising construction costs and regulatory changes. This economically challenging environment underscores the importance of examining how the role of energy efficiency as a pricing and liquidity factor evolves under changing market conditions. While a large body of literature documents the capitalization of energy performance in real estate markets, most studies focus primarily on price effects and rely on static linear models, neglecting temporal dynamics and broader market conditions (Ou et al., 2025). Recent studies addressing the energy crisis extended this perspective but remained limited to linear frameworks and short observation windows (Braakmann et al., 2026; Brolinson et al., 2026; Sagner, 2026). Moreover, price effects provide only a partial view of adjustment processes. Market absorption dynamics offer a broader perspective, revealing how energy efficiency shapes demand behavior and asset marketability. Yet, no study has jointly examined price and liquidity responses to energy efficiency across extended market cycles.

The research aims to examine how the valuation of energy efficiency evolves across different market phases and assess whether price and liquidity effects respond differently to changing economic conditions. By analyzing price and time on market (TOM) dynamics, the study identifies regime-dependent effects in the capitalization of energy efficiency and evaluates their implications by accounting for temporal variation and spatial heterogeneity.

Methodology and Data

The analysis is based on residential property listings across Germany from 2017 to 2025. The dataset comprises 656,649 apartment listings, including property characteristics, EPVs, and market- and location-specific variables. In addition, the dataset includes TOM, measured as the duration between listing and delisting, as a proxy for market absorption (Cajias et al., 2019), and listing attention (clicks), reflecting the intensity of user interaction.

Given the dual focus on price and liquidity, the empirical strategy follows a two-step approach. Prices and TOM are evaluated in separate models, both incorporating temporal and spatial heterogeneity. Price effects are estimated using a GAM, allowing for a flexible, nonlinear relationship between EPVs and prices. In the next step, liquidity dynamics are evaluated in a Cox proportional hazards model. Its hazard ratio reflects the probability that a listing will be absorbed at a given point in time (Cox, 1972; Kluger & Miller, 1990; Cajias et al., 2019). In line with the price analysis, the models are extended by year-specific effects to account for temporal variation and urbanization-specific interaction terms to capture spatial heterogeneity.

Results and Their Contribution to Science and Practice

The results show that energy performance is capitalized in residential prices, with the magnitude varying across market phases. During expansionary phases, price differentials between energy-efficient and inefficient buildings remain comparatively low. Liquidity dynamics, however, do not follow this attenuating pattern. Demand is highest for buildings with mid-range efficiency levels, suggesting that strong market conditions absorb energy-related price disparities while redistributing demand toward average energy performance. Under changing market regimes, energy efficiency becomes a stronger determinant of pricing and demand patterns. This shift is reflected in a widening price spread and weaker market absorption of energy-inefficient properties. Spatially, effects differ across urbanization levels: Price effects are more pronounced in less densely populated areas, while liquidity differences become stronger in less urbanized regions.

From a practical perspective, the results underscore the need to strategically integrate building energy performance into investment analysis. Under deteriorating market environments, energy-inefficient buildings may be particularly vulnerable, as they face both lower valuations and slower market absorption. This calls for earlier portfolio screening, targeted retrofit planning, and a cautious assessment of exit timing. At the policy level, the findings suggest that transition measures should be tailored to regional conditions, as the spatial effects of energy-efficiency pricing and liquidity vary.

6.2 Final Remarks

The real estate market contributes to climate change through its significant share of global emissions, material extraction, and energy consumption (Umweltbundesamt, 2024; United Nations Environment Programme, 2026). At the same time, it is increasingly vulnerable to these dynamics, including both physical climate risks and transition-related pressures (Contat et al., 2024; Duca et al., 2021). Both dimensions are central to real estate market dynamics and remain relevant despite shifting economic conditions.

In recent years, the real estate sector has been shaped by rising financing costs, falling prices, stricter regulatory requirements, and growing exposure to physical climate risks. Nevertheless, environmental sustainability continues to shape policy and investment decisions, as climate and retrofit targets remain difficult to achieve (Umweltbundesamt, 2024). The way environmental risks are perceived, priced, and translated into market responses depends on a complex interplay of regulatory, macroeconomic, and asset-specific factors. A context-specific perspective is therefore essential to account for varying economic conditions.

This dissertation approaches residential real estate markets through several dimensions of environmental sustainability. The first two articles examine the direct effects of physical risks on prices and rents. They evaluate the extent to which air pollution and heat stress in German cities are reflected in prices and rents. The results indicate that their market impact depends on the perceptibility of the respective exposure, with capitalization effects being more evident for coarser particulate matter and elevated nighttime temperatures. The subsequent articles address transition risks and examine the role of rising energy standards and the resilience of energy-efficient properties across economic cycles. These risk types require a comprehensive analytical perspective, as they are often reflected through institutional, financial, and market-based channels rather than through direct physical exposure. The findings suggest that the relevance of energy efficiency and retrofit measures depends not only on their capitalization in prices or rents, but also on investment conditions, spatial context, and timing. Policy measures support retrofit activity when economic environments are favorable, whereas adverse market conditions increase market participants' risk sensitivity to energy performance. Together, these papers provide an integrated perspective on how environmental risk factors affect performance indicators in the residential real estate sector across various channels.

Although this dissertation contributes to the literature, it has several limitations. Due to the limited availability of data in the German real estate market, the analysis is based on asking prices, which primarily reflect sellers’ expectations. The liquidity measures provide

only an indirect approximation of market absorption and cannot fully capture realized transaction outcome. Nevertheless, asking prices and transaction prices are closely aligned in high-demand markets. Furthermore, cost components such as renovation, operating, and adaptation costs are not included, limiting the extent to which the economic viability of energy efficiency and adaptation measures can be assessed from a cost-benefit perspective. Moreover, due to differences in market structures, regulatory frameworks, and climatic conditions across countries and regions, the external validity of the findings depends on the comparability of market contexts and is therefore somewhat limited. However, the results provide indicative evidence and underscore the importance of a market-based analysis.

These limitations point to several avenues for future research. Expanding the approach to comparable regions and countries could provide comparative evidence across market structures, climate conditions, and stages of policy implementation. In addition, incorporating transaction prices or comparing asking and transaction prices could clarify how climate-related risks are reflected in actual market outcomes. Future studies could integrate cost components, including renovation expenditures and ongoing operating and adaptation expenses, to assess energy efficiency measures more comprehensively. Such analyses could account for initial investment outlays, payback periods, and long-term income effects. Since the market will continue to evolve, future research should also adopt more dynamic designs that capture adjustment processes, evolving risk perceptions, and the gradual incorporation of sustainability-related information into market indicators.

The four papers illustrate that climate risks not only influence long-term performance but also shape the conditions under which residential properties are valued, marketed, and held as investments. In this sense, physical risks affect market outcomes not only through objective exposure levels but also through market participants' perceptions of their implications for everyday use, location quality, and marketability. For investors, this implies that these risks must also be understood as structural factors that alter the economic functioning of assets, even when their effects materialize only indirectly. In the context of transition risks, regulation-induced changes in value can affect refinancing decisions and portfolio strategies before they are fully reflected in observed market outcomes. The findings also point to broader strategic and policy implications, making early risk recognition a critical component of investment management. For climate-related policy, the results suggest that uniform regulatory approaches are limited in their ability to address heterogeneous markets. The effectiveness of policy measures depends on regional differences, economic conditions, and socioeconomic contexts. At the same time, this evidence underlines their social dimension. While environmental and climate risks affect

the residential building stock broadly, the capacity to adapt is unevenly distributed. Consequently, climate-related regulation in the housing sector should account not only for ecological effectiveness but also for distributional effects, affordability constraints, and differences in adaptive capacity.

Overall, this dissertation shows that climate risks affect residential real estate markets through heterogeneous and interrelated mechanisms. A holistic and methodologically adaptable approach is therefore essential for assessing sustainability-related real estate processes and for developing responses that reflect both market dynamics and societal implications.

6.3 References

Albouy, D., Graf, W., Kellogg, R., & Wolff, H. (2016). Climate amenities, climate change, and American quality of life. *Journal of the Association of Environmental and Resource Economists*, 3(1), 205–246.

Bachmann, R., Baqaee, D., Bayer, C., Kuhn, M., Löschel, A., Moll, B., Peichl, A., Pittel, K., & Schularick, M. (2024). What if? The macroeconomic and distributional effects for Germany of a stop of energy imports from Russia. *Economica*, 91(364), 1157–1200.

Borja-Urbano, S., Rodríguez-Espinosa, F., Luna-Ludeña, M., & Toulkeridis, T. (2021). Valuing the impact of air pollution in urban residence using hedonic pricing and geospatial analysis, evidence from Quito, Ecuador. *Air, Soil and Water Research*, 14, 117862212110532.

Braakmann, N., Dursun, B., & Pickard, H. (2026). Energy price shocks and the demand for energy-efficient housing: Evidence from Russia's invasion of Ukraine. *Economica*, 93(369), 30–51.

Brolinson, B., Doerner, W. M., Pollestad, A. J., & Seiler, M. J. (2026). European energy crisis: Did electricity prices shock real estate markets? *Journal of Environmental Economics and Management*, 137, 103283.

Bundesverband energieeffiziente Gebäudehülle. (2026). *Sanierungsquote*. Accessed: 2026-05-16. URL: https://buveg.de/sanierungsquote/.

Cajias, M. (2019). Understanding real estate investments through big data goggles: A granular approach on initial yields. Int*ernational Journal of Housing Markets and Analysis*, 12(4), 661–686.

Cajias, M., Fuerst, F., & Bienert, S. (2019). Tearing down the information barrier: The price impacts of energy efficiency ratings for buildings in the German rental market. *Energy Research & Social Science*, 47, 177–191.

Contat, J., Hopkins, C., Mejia, L., & Suandi, M. (2024). When climate meets real estate: A survey of the literature. *Real Estate Economics*, 52(3), 618–659.

Cox, D. R. (1972). Regression models and life-tables. *Journal of the Royal Statistical Society: Series B (Methodological)*, 34(2), 187–220.

Cvijanović, D., & Van de Minne, A. (2024). *Temperature extremes and commercial real estate*. SSRN.

Deutsche Energie-Agentur. (2021). *Dena-Leitstudie Aufbruch Klimaneutralität*.

Dodoo, A., & Gustavsson, L. (2016). Energy use and overheating risk of Swedish multi-storey residential buildings under different climate scenarios. *Energy*, 97, 534–548.

Duca, J. V., Muellbauer, J., & Murphy, A. (2021). What drives house price cycles? International experience and policy issues. *Journal of Economic Literature*, 59(3), 773–864.

European Parliament & Council of the European Union. (2024). *Directive (EU) 2024/1275 of the European Parliament and of the Council of 24 April 2024 on the energy performance of buildings (recast)* [Directive]. Official Journal of the European Union, L 2024/1275.

International Energy Agency. (2024). *Empowering urban energy transitions: Smart cities and smart grids*.

Kempf, C., & Syz, J. (2022). Why pay for sustainable housing? Decomposing the green premium of the residential property market in the canton of Zurich, Switzerland. *SN Business & Economics*, 2, 170.

Klaiber, H. A., Abbott, J. K., & Smith, V. K. (2017). Some like it (less) hot: extracting trade-off measures for physically coupled amenities. *Journal of the Association of Environmental and Resource Economists*, 4(4), 1053–1079.

Kluger, B. D., & Miller, N. G. (1990). Measuring residential real estate liquidity. *Real Estate Economics*, 18(2), 145–159.

Kurzrock, B. M. (2017). Immobilienanalyse. In N. B. Rottke & M. Thomas (Eds.), *Immobilienwirtschaftslehre – Management* (pp. 717–762). Springer.

Le Boennec, R., & Salladarré, F. (2017). The impact of air pollution and noise on the real estate market. The case of the 2013 European Green Capital: Nantes, France. *Ecological Economics*, 138, 82–89.

Oke, T. R. (1982). The energetic basis of the urban heat island. *Quarterly Journal of the Royal Meteorological Society,* 108(455), 1–24.

Offermann, M., Lindner, S., Reiser, M., Braungardt, S., Bürger, V., Kocher, D., Bruse, M., & Cramer, L. (2022). *Nachhaltige Gebäudeklimatisierung in Europa: Konzepte zur Vermeidung von Hitzeinseln und für ein behagliches Raumklima* [Climate Change 30/2022]. Umweltbundesamt.

Ou, Y., Bailey, N., McArthur, D. P., & Zhao, Q. (2025). The price premium of residential energy performance certificates: A scoping review of the European literature. *Energy & Buildings*, 332, 115377.

Pommeranz, C., & Steininger, B. I. (2021). What drives the premium for energy-efficient apartments– green awareness or purchasing power? *Journal of Real Estate Finance and Economics*, 62(2), 220–241.

Ridker, R. G., & Henning, J. A. (1967). The determinants of residential property values with special reference to air pollution. *The Review of Economics and Statistics*, 49(2), 246–257.

Ruhnau, O., Stiewe, C., Muessel, J., & Hirth, L. (2023). Natural gas savings in Germany during the 2022 energy crisis. *Nature Energy*, 8, 621–628.

Sagner, P. (2026). Energy price shock and housing market dynamics: Evidence from Germany. *Journal of Housing Economics*, 71, 102119.

Sinha, P., & Cropper, M. L. (2013). *The value of climate amenities: Evidence from US migration decisions* (Working Paper No. 18756). National Bureau of Economic Research.

Sun, B., & Yang, S. (2020). Asymmetric and spatial non-stationary effects of particulate air pollution on urban housing prices in Chinese cities. *International Journal of Environmental Research and Public Health*, 17(20), 7443.

Taruttis, L., & Weber, C. (2022). Estimating the impact of energy efficiency on housing prices in Germany: Does regional disparity matter? *Energy Economics*, 105, 105750.

Umweltbundesamt. (2022). *Natürliche Quellen der Luftschadstoffe*. Accessed: 2023-05-18. URL: https://www.uba.de/n94500de

Umweltbundesamt. (2024). Emissionsübersichten KSG-Sektoren 1990–2023. Accessed: 2026-05-15. URL: https://www.umweltbundesamt.de/system/files/medien/361/dokumente/2024_03_13_em_entwicklung_in_d_ksg-sektoren_thg_v1.0.xlsx

United Nations Environment Programme. (2011). *Cities: investing in energy and resource efficiency–Towards a green economy pathways to sustainable development and poverty eradication*.

United Nations Environment Programme. (2026). *Global status report for buildings and construction 2025–2026: As climate risks rise and cities grow, we must rethink how we build to create better lives for all.*

United Nations Environment Programme Finance Initiative. (2023). *Climate Risks in the Real Estate Sector*.

Wood, S. N. (2017). Generalized additive models. An introduction with R (2nd ed.). CRC Press.

Universität Regensburg
IRE|BS Institut für Immobilienwirtschaft
Fakultät für Wirtschaftswissenschaften